Inhibition of HDAC7 Using RNAi As an Epigenetic-Based Therapy in Targeting Malignancies

Ola Hassan

Bachelor of Pharmacy, Cairo University 2009

Master of Pharmaceutical Science, Cairo University 2016

A Dissertation Submitted in Partial Fulfillment of the Requirements for Degree of Doctor of Philosophy in the Division of Biology and Medicine at Brown University

Providence, RI, May 2024

Signature Page

This dissertation by Ola M. Hassan is accepted in its present form by the Division of Biology and Medicine as satisfying the dissertation requirement for the degree of Doctor of Philosophy.

Date: _____ _____

Dr. Nikos Tapinos (Advisor)

Recommended to the Graduate Council

Date_____ _____

Dr. Paul Bertone (Reader)

Date: _____ _____

Dr. Wafik El-Deiry (Reader)

Date: _____ _____

Dr. Jennifer Sanders (Reader)

Date: _____ _____

Dr. Andras Fiser (Outside Reader)

Approved by the Graduate Council

Date: _____ _____

Dr. Thomas A. Lewis, Dean of the Graduate School

CURRICULUM VITAE

OLA HASSAN

EDUCATION

Ph.D. in Pathobiology, **2024**
Brown University, Providence, RI

Master of Pharmaceutical Sciences **2016**
Cairo University, Cairo, Egypt

Bachelor of Pharmacy degree **2009**
Pharmacy School, Cairo University, Cairo, Egypt

PROFESSIONAL EXPERIENCE

Doctoral Candidate, Brown University **2019- 2024**
Graduate researcher- Dr Nikos Tapinos, MD, PhD

- **Project:** Led a cutting-edge project that aims to develop a novel innovative epigenetic therapeutic for human glioblastoma
- **Highlights:**
    - Awarded the best poster award for thesis work from the Pathobiology program at Brown University
    - Awarded WLF Young Scholar honor award: one of the two distinguished graduate students in a pool of highly accomplished candidates at Brown University graduate school to be recipient for the World Laureates Forum honor award.
- **Analytics:** In addition to conventional wet lab expertise, I have acquired expertise in applying advanced analytics to biological systems. This includes proficiency in computational bioinformatics, interpretation of theory-based discoveries, analysis of publicly available genomic data, and utilization of computationally predictive models. I have also mastered the integration of clinical data with various outputs from Next-Generation Sequencing (NGS).
- **Mentorship:** Peer mentored other fellow graduate students and Peer mentored other graduate students and was responsible for training and mentoring undergraduate students.

Research associate, UMass Chen Medical School **2017-2018**
Research associate- Gyongi Szabo, MD, Ph.D.

- **Project:** Led and significantly contributed to projects studying the role of important signaling pathways in steatohepatitis and hepatic cancer.

Pharmacy Master Candidate, Cairo University **2010-2016**
Graduate researcher for a collaborative project between Cairo University and Aswan Heart Center Prof. Sir. Magdi Yacoub, OM, FRS, Ahmed Attia, Ph.D., and Dr. Ossama ElTayeb, Ph.D.

- **Project:** Led a high-scale grant-funded research project at Aswan Heart Center (60 beds) aimed at tracking hospital-acquired infections with the objective of mitigating antibiotic misuse within the hospital.
- **Highlights:** The thesis findings helped the revisit of the infection control plan for Aswan Heart Center, one of the biggest cardiac centers in Egypt and the findings was presented in one of the major conferences in the country.
  Ranked 2nd within my Master's degree cohort.

Genomics Research fellow, United States Naval Medical Research Unit-3 (NAMRU-3), Cairo, Egypt **2013-2014**
Research fellow- Dr Rania Nada
The Genomics Fellowship focused on integrating genomic tools into epidemiological studies. Its goal was to proficiently merge clinical data with epidemiological data using bioinformatic techniques and to draw critical conclusions through analytical thinking based on global datasets.

Molecular Biology Research fellow, Pharmacy School, Helwan University, Cairo, Egypt **2012**
55-hour training for post pharmacy graduates – Molecular biology

University of Toronto, Toronto, Canada **2010**
36-hour training for post pharmacy graduates - Therapeutics

Sherif Pharmacy, Cairo, Egypt **2009**
Community Licensed Pharmacist

Marketeers Medical Research Group, Cairo, Egypt **2007-2009**
Research fellow in cardiovascular diseases and Diabetes.

PATENTS AND INNOVATION

Tapinos N, Hassan O, Karambezi, D
"HDAC7 as an epigenetic based therapy in Cancer"

- Tech ID 3125J (0312021.01017)
- *US Patent Application International*
  Bearing Serial No. 63/254,826 **2021**
- *International Patent Application*
  Bearing Serial No. PCT/US2022/077910 **2022**

PUBLICATIONS

Ola Hassan, Mattia Pizzagalli, Laura Jinxuan Wu, David Karambizi, John P. Zepecki, Eduardo Fajardo, Andras Fiser, Nikos Tapinos "Heterochromatin spreading in cancer cells through HDAC7 mediated histone H3.3 landscape reprogramming." BioRxiv preprint. DOI: **10.1101/2024.03.12.584656**

John Zapecki, David Karambizi, Lauren Sugamann, Mattia Pizzagalli, **Ola Hassan,** Jorge Eduardo, Andras Fischer, and Nikos Tapinos. "Targeting of FTO rewires the cancer epitranscriptome and induces ferroptosis in cancer cells." under submission.

Ola Hassan, David Karambizi, and Nikos Tapinos."Targeting Histone Deacetylase-7 as a Novel Therapeutic Strategy for Glioblastoma Multiforme". **The FASEB Journal 36(S1).** DOI: **10.1096/fasebj.2022.36.S1.R3259. May 2022**

Ola M. Hassan, Magdi H. Yacoub, Ossama M. ElTayeb, Ahmed S. Attia. "Phenotypic and molecular characterization of gram-negative isolates causing perioperative infections following open heart surgeries in Aswan Heart Center". **The FUE international conference of pharmaceutical sciences,** Cairo, Egypt. Feb 2015

SELECTED HONORS

- **Pathobiology Graduate Program** **Aug 2022**
  Brown University
  Best Poster Presentation Award on the Thesis work
- **Travel Award for academic excellence and poster presentation** **April 2022**
  Experimental Biology 2022 meeting, Philadelphia
- **4th World's Laureates Forum** **Nov 2021**
  Young scholar award at the 4th WLF, Shanghai
  Nominated to represent Brown University at the foremost scientific gathering for prize winners including laureates of the Nobel prize.
- **FUE 3rd international conference of pharmaceutical sciences,** **Feb 2015**
  Future University, Cairo, Egypt
  Best Poster Presentation Award
- **Aswan Heart Center Research Annual Meeting,** **Jan 2014**
  Oral Presentation award

- **Pharmaceutical Entrepreneurship and Innovation Program (EIP),** **Nov 2013**
  American University at Cairo, Egypt
  Best Team award
  Developing an innovative drug targeting idea among competing teams.
- ***Pfizer* Model of Pharmaceutical Marketing,** **Apr 2013**
  Cairo University, Cairo, Egypt.
  Best Team developing and presenting a launching plan for a pharmaceutical product (Zithromax® of *Pfizer*®)

TEACHING AND MENTORING

- **Brown University,** RI, USA **2022**
  Peer mentor in the Pathobiology graduate program

- **Brown University,** RI, USA **2020 - Now**
  Cofounder and a group leader in the Community STEM at Brown University project
  Key Responsibilities
  -Inspired and mentored middle school students from severely under-resourced educational backgrounds in RI, MA, and NY. The program's mission is to expand access to resources with a collaboration with 100 mentors' platform in the form of science mentorship and a real-world bench and keep mentoring those students from middle school and through high school. **Website:** Webpage to Community STEM

- **Brown University,** RI, USA **2021**
  Teaching Assistant for a Biochemistry undergraduate BIO0285 class
  Key Responsibilities
  - Served on leading discussions among undergraduate students.
  - Assisted in lectures, exams, internal auditing, strategic planning, and upgrading of the practical courses.

- **Ahram Canadian University (ACU)**, Giza, Egypt
  Instructor of Microbiology and Immunology **2015 – 2016**
  Teaching Assistant of Microbiology & Immunology undergraduate courses **2009–2015**
  Key Responsibilities
  - Delivery of the practical and theoretical components to the Pharmacy and Dentistry students.
    Led and assisted in lectures, exams, courses registration, quality assurance, academic control unit, internal auditing, strategic planning, academic advising, and upgrading of the practical courses.

SELECTED LEADERSHIP & COMMUNITY SERVICE

Pathobiology Graduate Program, Brown University. RI, USA — **2021/2022**
Admission committee member
Served on the admission committee for selecting the new qualifying cohort for graduate students for the Pathobiology graduate program

Community STEM, Brown University, RI, USA — **2020 - Now**
Cofounder and a group leader in the Community STEM at Brown University
- As a team, we provided inspiration and guidance to middle school students from severely under-resourced educational backgrounds in RI, MA, and NY. The program's objective is to enhance access to resources through collaboration with 100 mentors' platform. This initiative takes the form of science mentorship and real-world bench experiences, with ongoing mentorship extending from middle school through high school.
- **Website:** Webpage to Community STEM

Alhuda Middle School, Worcester, MA, USA — **2020 - Now**
Founder of STEM tutoring program
- Aimed to expose young girls from underprivileged backgrounds to STEM

Magdi Yacoub Foundation, Aswan, Egypt. — **2015**
Led arranging monthly seminars.
The seminars aimed to increase the awareness of infection control parameters amongst healthcare settings at Aswan Heart Center

International Education and Resource Network iEARN, Cairo, Egypt. — **2008-2012**
Group leader
A non-profit organization aimed to empower the youth to work together using communications technologies for cultural exchange purposes

SELECTED INVITED SCIENTIFIC PRESENTATIONS

- **Hassan, O.** *Novel Epigenetic Therapeutic for Human Glioblastoma Multiforme.* Poster presentation at Legorreta Cancer Center Membership Retreat. August 31, 2023; Providence, RI.

- **Hassan, O.** *Novel approaches in targeting cancers at the epigenome level.* Oral presentation at Pathobiology Program Annual Retreat. August 2023; Providence, RI.

- **Hassan, O.,** Pizzagalli, M., David Karambizi, and Nikos Tapinos. *More than a histone deacetylase, targeting Histone Deacetylase-7 as a Novel Therapeutic Strategy for Glioblastoma Multiforme.* Poster presentation at Pathobiology Program Annual Retreat. August 2023; Providence, RI.

- **Hassan, O.** *Epigenetics-based therapy in treating malignancies*. Invited speaker for oral presentation at Summer at Brown epigenetics class. July 2023; Providence, RI.

- **Ola Hassan**, David Karambizi, and Nikos Tapinos. *Targeting Histone Deacetylase-7 as a Novel Therapeutic Strategy for Glioblastoma Multiforme*. The FASEB Journal 36(S1). DOI: 10.1096/fasebj.2022.36.S1.R3259. May 2022

- **Ola Hassan**, and Nikos Tapinos. *HDAC7 and the epigenomic alterations in cancers*. Poster presentation at the 4th World Laureates forum. Nov 2021. Shanghai, China (Virtual)

- **Ola Hassan**. *Women in STEM.* Invited speaker for oral presentation at Alhuda Middle School. December 2021; Providence, RI.

- **Ola Hassan** and Nikos Tapinos. *Thesis Research update.* Pathobiology graduate program Journal Club. October 2021; Providence, RI.

- **Ola Hassan** and Nikos Tapinos. *New findings for HDAC class IIa implications in Glioblastoma Multiforme.* Albert Einstein Medical school. Feb 2021 (Virtual)

- **Ola Hassan**. *Master's Degree Research presentation.* Pathobiology graduate program Journal Club. March 2020; Providence, RI.

SKILLS

- **Programming Languages & Bioinformatics tools:** R Studio, SAMtools, BEDtools, Bioconductor, GSEA, PYMOL, ImagJ, FlowJo, PEAKS Studio, GraphPad Prism, Adobe Illustrator

- **Dry Laboratory:**
  - Integrating clinical data with multiple Next-Generation Sequencing (NGS) output data
  - Extended Experience working with publicly available NGS datasets, such as TCGA, CGGA, and various genomic signature data sets.
  - Experience with biological statistics.
  - Experience with bioinformatics.

- **WET Laboratory:** Sterile Tissue/Cell Culture Techniques, Transformation, RNAi Transfection, qPCR, DNA/RNA Preparation, Coimmunoprecipitation, Agarose Gel Electrophoresis, SDS-PAGE, Spectrophotometry, ELISA, Flow Cytometer, High-Resolution Melting Analysis, Western Blot Analysis, Microscopy, Immunofluorescence, Immunocytochemistry, histone and nuclear extraction and purification, preparations for NGS sequencing.

- **Natural Languages**: English (Fluent), Arabic (Native), French (beginner)

ACKNOWLEDGMENTS

In the name of God, the Most Gracious, the Most Merciful.

"Are those who have knowledge and those who have no knowledge alike? Only the men of understanding are mindful. " Surah Az Zumar __(Quran, 39:9)."

I am profoundly grateful to the ultimate author of all things, God, to whom I attribute my knowledge and for guiding me on this remarkable journey. Representing a highly underrepresented minority in STEM—as a woman, a mother, a hijabi, and an international student pursuing graduate studies—has been both a dream and a significant challenge. Despite encountering numerous tests, challenges, and instances of prejudice along the way, I've remained steadfast in my resolve, thanks to the grace of Allah and the unconditional support of my mother, Dr. Seham El Massah. Her constant encouragement and belief in me, even flying from the Middle East to the US every year to offer months of support, have been invaluable. She has been my rock, backing me every turn of the way, instilling in me a passion for science and a thirst for knowledge that I inherited from her.

To my father, entire family, extended family, and friends in the US and Egypt, I extend my heartfelt thanks for your devoted support and encouragement throughout this journey. Your love and support have been indispensable to me.

I express my deepest gratitude to my husband, Amr Elmeligy, who has been my best friend and guiding light. His passion for Brown University, instilled in me after completing his medical training there, has been a driving force. I am truly blessed to have embarked on our life journey together, sharing a common pursuit of knowledge to better ourselves. His unwavering companionship, love, and perseverance have been my constant source of strength and motivation. To my daughters, Malak, and Maryam, you both inspire me daily, and I am endlessly grateful for your presence in my life. I strive to set an example for you both.

To all members, past and present, of the Tapinos lab, I express my gratitude for the cherished memories, laughter, and support you have provided. Special thanks to Mattia Pizzagalli for his outstanding friendship and support. I also want to express my appreciation to my committee members—Dr. Paul Bertone, Dr. Wafik El-Deiry, Dr. Jennifer Sanders, and the external reader, Dr. Andras Fiser—for their consistent commitment and valuable assistance.

I owe a debt of gratitude to my previous mentor and staunch advocate, Sir Magdi Yacoub, the globally renowned cardiothoracic surgeon who laid the groundwork for my early career.

I extend my sincerest appreciation to the remarkable "Difference Maker," Dr. Nikos Tapinos. Your influence on me as both a scientist and a person has been profound in countless ways. Your perseverance and dedication to excellence set a standard I will refuse to compromise on. Your compassionate and distinctive mentorship and teaching were instrumental in sustaining me throughout this groundbreaking project. I am incredibly thankful for your belief in my autonomy and leadership and for being the exemplary leader that I have always looked up to.

PREFACE

The work presented in this thesis was performed by me, Ola Hassan, at Rhode Island Hospital in Dr. Nikos Tapinos' laboratory. I performed all the experiments reported and singularly wrote and put together all figures within the manuscript with the following exceptions:

Chapter 2: The colony formation assay was done by John Zepecki (Figure 2.7D)

Chapter 3: We got help from Dr. Andras Fiser and his team at Albert Einstein University regarding conducting the small molecule inhibitor library screening and the small molecule inhibitor design.

Chapter 4: The immunofluorescence experiment for H3.3 and H3K9me3 was done by John Zepecki (Figures 4.5A and 4.55C). Dr. David Karambizi helped redesign Figures 4.2C, 4.2D, and 4.3, and enhance Figures 4.6B, and 4.6D.

TABLE OF CONTENTS

Chapter 3: Drug design pipeline to identify novel specific isoform-selective HDAC inhibitor.

Chapter 4: Heterochromatin Spreading in Cancer Cells Through HDAC7-Mediated Histone H3.3 Landscape Reprogramming

LIST OF TABLES

LIST OF FIGURES

Chapter 1: Introduction

Chapter 2: Targeting HDAC7 as a novel therapeutic approach in GBM

CHAPTER 1:

Introduction

I. Epigenetic Implications in Biology and Disease

a) Introduction to the Epigenome

By definition, the epigenome is derived from the Greek word epi, which means "above" the genome. The epigenome includes all chemical compounds that change or mark the genome to direct it to a specific fate in terms of time and space. The diversity among cell types is also reflected in the diversity of the epigenetic marks. Although these epigenetic marks are not considered a part of the DNA, they are still passed from cell to cell during division and across generations. Thus, in eukaryotes, each cell type will be entailed by the same genome, along with as many epigenomes as there are various cell types.

Epigenetics comprises heritable changes in gene expression not attributable to nucleotide sequence modifications [1]. Epigenetic mechanisms entail modifications to genomic DNA, which can be either inherited or acquired. These modifications influence cellular characteristics that may contribute to disease development and outcomes.

The term epigenomics is the study of epigenetic changes on a genome-wide basis with the cross-talking influences from the chromatin architecture, chromatin folding and proximity to the nuclear matrix, packaging of DNA around nucleosomes, covalent modifications of histone tails, and DNA methylation. Chromatin comprises proteins called histones and the tightly packed DNA to fit into the nucleus. The Chromatin complex can be modified by enzymes and some forms of RNA, such as microRNAs and small interfering RNAs. These modifications regulate chromatin structure to affect genetic expression. In general, tightly folded chromatin tends to be "turned off" or transcriptionally repressed, while open chromatin is "turned on" or transcriptionally active. It has been studied that heterochromatin is a region of the epigenome characterized by low gene

density, contains satellite repeat elements, and has later replication [2]. Thereupon, it was established that heterochromatin and euchromatin are marked with unique DNA methylation and histone modification patterns that associate with distinct genetic states, creating what is called an 'epigenetic code' that determines the chromatin state and gene expression [3]. It was shown that an epigenetic memory system is mediated by polycomb (PcG) and trithorax group (TrxG) proteins to maintain silent heterochromatin states [4, 5]. Moreover, short hairpin RNAs have been shown to mediate heterochromatin formation via an RNAi pathway [6], setting heterochromatin as the base of epigenetic silencing.

The epigenome is largely more dynamic than the genome, which is reflected in the various diverse functional states. The reversible epigenetic modifications of DNA methylation and histone tail modifications partly govern the epigenome dynamics [7, 8]. Other noncovalent modifications, such as microRNAs and chromatin-remodeling complexes, can also modulate the epigenome, but they cannot be regarded as epigenetic marks. The epigenome can be defined as the complete set of chemical modifications of chromatin components [7, 8].

b) Introduction to the role of epigenetics in biology and disease

The rigorous studies that have been made on the human genome and the identification of all human genes have created gaps in our understanding of genetic regulation. Epigenetics further explains the hierarchical regulation of gene expression during cell division, with exposure to environmental cues and with aging [9, 10]. For instance, studies have shown that monozygotic twins may have different disease susceptibility. Intriguingly, they may carry the same disease mutation but display different clinical outcomes [11]. Epigenetic silencing explains why genetic twins can exhibit phenotypic differences [12]. Another example is X-chromosome inactivation in

female mammals, protecting females from having double the number of X-chromosome gene products as males [13].

Epigenetics plays a crucial role in the majority of key cellular processes, enabling the diversity of cell types within the human body. Epigenetics regulates the cellular differentiation of various cell types, all of which have the same DNA but differentiate into diverse cells from neurons, blood cells, kidney cells, inflammatory cells, and others. Thus, epigenetics functions as a higher level of regulation to activate specific sets of genes while suppressing others.

Our understanding of gene expression now extends beyond the notion that genetics alone primarily regulate developmental biology and human diseases. This paradigm fails to explain the plasticity to quickly respond to environmental cues, nor does it justify aberrant development and pathologies without genetic mutations. By asking epigenetic questions alongside genetic ones, we gain a complementary understanding of how dysregulation occurs during the development of human diseases. Thus, the current paradigm shift highlights that hierarchical genetic and epigenetic regulation generates a dynamic cascade of events involved in developmental biology as well as human disease [14].

The myriad epigenetic factors are diverse during development. DNA methylation is thought to begin the epigenetic programming role. The chromatin structure and histone modifications follow to modify the expression of many genes needed during the different stages of growth and development. For example, DNA methylation is implicated in early development to help designate early cell lineages (e.g., stem cells); it also regulates the activity of promoters and repeat elements [15]. Whereas histone modifications are localized in the promoter and genomic regions, modulating the genetic expression [16]. The chromatin structure can also regulate gene expression at a distant region in the genome through processes of looping, nuclear matrix

association, and nucleosome positioning [17]. Moreover, the noncoding RNAs can regulate promoters that modulate gene expression at a distance [18].

Epigenetic abnormalities have been reported and linked to many human diseases through anomalous DNA methylation, histone modifications, or RNA silencing. DNA accessibility is epigenetically regulated throughout the human course of life. During the embryonic stages, histone modifications and demethylation occur in the paternal genome [19]. On the other hand, the maternal genome initiates embryonic re-methylation followed by another demethylation, setting up the epigenetic profile of the developing embryo, which must be rigorously maintained for efficient gene regulation. Any deviation in maintenance may contribute to congenital disorders or predispose humans to various life-term pathologies [1, 20]. Prenatal and postnatal exposure to environmental factors from nutrition, xenobiotic chemicals, and even social behavior can cause epigenome dysregulation in somatic cell lineages [21]. Studies showed knocking out epigenetic genes results in embryo lethality or developmental defects [21]. Thus, our clear understanding is that mammals undergo developmental periods of genome-wide epigenetic reprogramming patterns in the embryonic phase of life. Such reprogramming silences after fetal development.

Epigenetic anomalies were reported in many pathologies. Disparities among monozygotic twins for developing systemic lupus erythematosus (SLE) suggest that environmental factors are pivotal drivers for the disease pathology. Epigenetic abnormalities such as histone modifications and DNA methylation were shown to be able to modulate gene expression in mature T cells. Numerous genes in T lymphocytes of SLE patients were found to have gone through hypomethylations, such as CD11a (ITGAL), perforin (PRF1), CD70 (TNFSF7), and CD40LG (TNFSF5) [22]. In rheumatoid arthritis (RA), Kawabata *et al*. reported an increased HDAC1 expression by TNF-α supplementation in RA synovial fibroblasts [23]. Further, HDAC inhibitors

(HDACi) presented anti-inflammatory properties in RA animal models. Also, givinostat, an HDACi, showed therapeutic activity with an extensive safety profile in treating juvenile idiopathic arthritis [24]. It was shown that reduced H3K27me3 levels and the accumulation of the Jumanji demethylase JMJD3 were implicated with the anomalies of CD4+ cells in systemic sclerosis (SSc) [25]. Interestingly, HDAC7 was found to be a specific target for the treatment of SSc because it does not up-regulate the expression of profibrotic molecules such as ICAM-1 and CTGF while showing anti-tumorigenic properties through reducing the cytokine TGF-β expression by inducing the constitutive expression of the extracellular matrix proteins type I and type III collagen [26]. Moreover, Patel *et al*. showed that the chromatin remodeling via HDACi resets the immune system and induces the anti-tumor chemokine IFN-γ production [27] and the transcription activity of Tbx21 in T lymphocytes, alleviating the inflammatory damage in cancer [27] and in the autoimmune type I diabetes [28]. Hence, various pathologies have the potential to be corrected by epigenetic-based therapies.

c) Epigenetics and cancer

The heritable changes during cellular biological processes require proper genetic and epigenetic regulation. Any mistakes during epigenetic maintenance could result in the inhibition or activation of gene expressions and pathways that could be associated with malignancies [13]. Cancer is considered an outcome of cross-talking genetic mutations with epigenetic dysregulation that could be attributed to environmental and/or hereditary factors. Many studies have shown that global epigenetic aberrations, together with genetic mutations, are found in human cancer cells [29-31]. These genetic and epigenetic abnormalities crosstalk at all stages of cancer growth, synergistically mediating cancer progression. In addition,

epigenetic modifications influence the progression of cancers by regulating the interaction between the tumor cell and its specific microenvironment by regulating mechanisms known to support the tumor cells with various stromal factors [32]. Recent studies agree that epigenetics plays the cornerstone in initiating events in some types of cancers [33]. Luckily, epigenetic dysregulations are potentially reversible, unlike genetic mutations. Epigenetic-based therapy holds great potential in treating many malignancies by restoring normal epigenetic modifications [34].

In cancer, the changes in the chromatin architecture were shown to be both localized and global. For instance, early studies have proposed an overall decrease in DNA methylation, in cancer epigenomes [35]. However, more recent studies found that the abrupt distribution of DNA methylation is more likely than the overall increase [36]. Also, genome-wide histone modifications of specific marks are now seen as hallmarks of cancers. For instance, loss of acetylation at lysine 16 and trimethylation at lysine 20 of histone H4 is a common hallmark of human cancer [37], and specific histone modification patterns or “epigenetic code” are now seen as the risk prediction of cancer recurrence [38].

Gene silencing at the chromatin level is crucial for the life of eukaryotic organisms and is particularly important in regulating fundamental biological processes, including differentiation, imprinting, silencing of large chromosomal domains like the X chromosome in female mammals, and silencing of developmental genes in the postnatal life [39-41]. The disruption of gene-silencing machinery is implicated heavily in cancers. Abnormal gene silencing was shown to mediate the early clonal expansion of cancer cells, providing the snowball for a cascade of genetic and epigenetic abnormalities allowing tumor progression

[33]. Silencing can be initiated and maintained by various epigenetic processes, including noncoding RNAs, covalent modifications of chromatin, physical alterations in nucleosome positioning, and DNA methylation. For instance, the histone methylation and deacetylation of lysine residues like lysine 9 in histone H3 or lysine 27 in histone H3 were proven to maintain gene silencing [42]. Also, a set of genes known to have DNA hypermethylation in preinvasive stages of cancers are known as "epigenetic gatekeepers"; these genes are rarely mutated in these cancers [43]. By epigenetic silencing, these gatekeepers prevent stem/progenitor cells from becoming immortalized and gaining indefinite cell renewal capability during chronic stress [43]. In contrast, gene silencing is balanced by activating specific sets of genes when stem/precursor cells need to differentiate physiologically. The improper silencing of these genes thwarts their crucial roles, allows for indefinite survival and clonal expansion, and stops differentiation. For example, mutations mediate abnormal activation of the Wnt pathway, the canonical pathway in driving colon cancer, which was shown to take place during the imbalance of the epigenetic gatekeeper, β-catenin [44]. It was shown that cancer cells undergo "addiction" to Wnt pathway activation, resulting in a tumor made up of a subpopulation of cancer stem cells and neoplastic progeny in the absence of genomic silencing [44].

d) Epigenetics modifications: writers, erasers, and readers

The identification of the enzymes that direct posttranslational modification (PTM) to the histones and the DNA has been studied rigorously over the last two decades; such modifications were found to be dynamic, where PTM can be added, erased, or additionally regulated.

The DNA in eucaryotes is packed in the highly organized chromatin structure with wrapping around nucleosomes. The nucleosome is composed of eight core histones, two copies of each histone, H2A, H2B, H3, and H4, wrapped by 147 DNA base pairs. PTM occurs mostly at the N-terminal tails, as well as globular domains of each histone. The PTM includes methylation, acetylation, phosphorylation, ubiquitylation, and others (**Table 1.1**) [45-47]. These histone modifications regulate the structure of the chromatin by acting as binding hubs for transcription factors, chromatin remodelers, histone chaperones, and DNA/histone-modifying enzymes [45]. Hence, chromatin modifications regulate many cellular events, including gene expression, DNA replication and repair, chromatin condensation, cell-cycle processes, and cell division [48]. Chromatin exists in two structurally and functionally distinct states: a closed "silent" form (heterochromatin), which is known to maintain transcriptional repression. The other form is the open chromatin (euchromatin), which sustains transcriptional activation. Which chromatin state will take place is entailed by the PTM of core histone proteins and the covalent modifications of DNA. The PTM precise modifications make up the “epigenetic code”. A characteristic feature of this code is its ability to respond to environmental cues, as what happens during the developmental changes of an organism from a zygote to an adult, as well as in cancer [49].

Chromatin modifications	**Amino acid residue modified**	**Epigenetic regulation**
Acetylation	Lysine **K**-ac	Transcription, DNA repair, condensation, DNA replication
Methylation	Lysine **K**-me1, **K**-me2, **K**-me3 Arginine **R**-me1 **R**me2a **R**-me2s	Transcription, DNA repair

Phosphorylation	Serine **S**-ph Threonine **T**-ph	Transcription, condensation DNA repair
Ubiquitylation	Lysine **K**-ub	Transcription, DNA repair
Sumoylation	Lysine **K**-su	Transcription
ADP ribosylation	Glutamic acid **E**-ar	Transcription
Deimiation	**R > Cit**	Transcription
Proline Isomerization	**P-cis > P-trans**	Transcription

Table1.1 Various classes of modifications identified on histones . Classification overview for different histone modifications with their main epigenetic function studied in literature, reprinted after approved permission from the publisher [45]**.**

The "Writers" are a group of enzymes that covalently add PTM groups, such as histone acetyltransferases (HATs) and histone methyltransferases (HMTs)[50]. The "Writers" epigenetic function is counteracted by the "erasers", which are enzymes that remove the covalent histone modifications, such as histone deacetylases (HDACs), and histone demethylases (HDMs) [51]. The readers are regulatory proteins that recognize either specific PTM or a combination of PTMs "histone code" to direct a particular transcriptional outcome [50]. Thus, one could think of the "readers" as the regulators of the regulators for modulating the epigenetic regulator.

The epigenetic writers, erasers, and readers usually function within multiprotein complexes that target promoters and enhancers to regulate various transcriptional activities. The combination of PTMs occurring on the same histone tail (in cis) or on another tail (in trans) constitutes the histone signature that is specific to the time, space, location, and context of the epigenome [52]. The "reader" exerts a very crucial function by translating this code, creating the right interactome

for downstream pathways. For example, the reader function of chromodomains is through recognizing methylated histones, while bromodomains exert their function after binding to acetylated histones [53]. It has been proposed that recognizing PTMs by reader-containing complexes is the way to decode the epigenetic signature, consequently directing the relevant chromatin remodeling and changing the gene transcription [54]. For instance, the PcG proteins (the polycomb repressive complex 2 (PRC2) complex that catalyzes H3K27 trimethylation were reported to exert their function through specific DNA-binding transcription factors that signal the PRC2 complex [53, 54]. Thus, the mechanism and the dynamics by which histone-modifying enzymes are recruited to particular histone targets are crucial to the chromatin state and the subsequent genomic regulation [55]

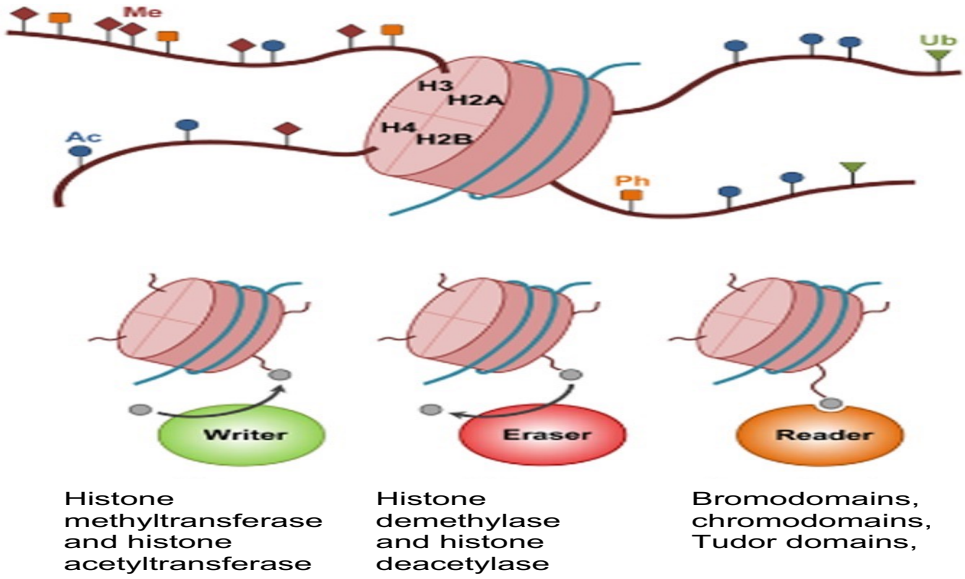

Figure 1.1
Epigenetic writers, erasers, and readers.
Epigenetic writers, erasers, and readers. The foundational building unit of chromatin is the nucleosome, which comprises DNA wrapped around histones (H2A, H2B, H3, and H4). Core histone tails are extended from nucleosomes and are subject to PTMs. PTMs include methylation (Me), acetylation (Ac), phosphorylation (Ph), and ubiquitination (Ub). The epigenetic modifiers are classed as writers, erasers, and readers of PTMs. Epigenetic writers add chemical modifications. Epigenetic erasers mediate the displacement of the chromatin modifications. Epigenetic readers are proteins with specific domains that recognize and recognize regulators. Figure edited and reprinted after permission granted from the publisher [50]

e) DNA methylation

DNA methylation compromises the epigenetic transfer of a methyl group by DNA methyltransferases (DNMTs) to the C-5 position of the cytosine ring of the DNA, which mostly occurs in the CpG dinucleotide regions in somatic cells [56]. A quarter of all DNA methylations in a non-CpG region occur in the embryonic stem cells (ESCs) [10]. It was reported that the maintenance methyltransferase, DNMT1, localization at the replication foci during the S phase is responsible for copying DNA methylation patterns to the daughter strands during the DNA replication [57].

DNA methylation is known to exert its crucial role in the configuration of chromatin via interactions with other epigenetic modifications such as the histone PTM, polycomb complexes, nucleosome positioning, noncoding RNA, and ATP-dependent chromatin remodeling proteins [58]. The majority of the CG dinucleotides are methylated in eukaryotes, whereas CG dinucleotides at promoter regions are protected from methylation [59]. Flaws in DNA methylation have malignant outcomes [56]. Epigenetic hallmarks of cancer show global alterations in DNA methylation and site-specific hypermethylation of CpG islands [58]. Site-specific hypermethylation of DNA was reported at promoter CpG islands of tumor suppressor genes, inducing transcriptional dysregulation and further oncogenic development [60]. In addition, it was shown that DNA methylation might physically hinder the binding of transcriptional regulators to the gene causing flaws in gene expression [61]. During development and in cancer, DNA methylation works hand in hand with distinct histone modifications to regulate each other in the deposition over the chromatin. It was shown that histone methylation and DNA methylation can regulate one another [60]. For instance, the

trimethylation of histone H3 lysine 9 (H3K9), histone H3 lysine 27 (H3K27), and histone H4 lysine 20 (H4K20) has been proposed to be a requirement for proper DNA methylation [59]. Also, SUV39H1/2 and EZH2, the histone methyltransferases responsible for H3K9 and H3K27 methylation, respectively, have been shown to directly interact with DNMT1, DNMT3A, and DNMT3B [59]. Furthermore, the pericentromeric localization of DNMT3B was reported to be regulated by SUV39H1/ 2-mediated H3K9 dimethylation or trimethylation [62].

f) Histone modifications

Most histone modifications are dynamic and promptly respond to environmental cues. More than 80 histone marks were identified, and a lot is yet to be discovered [48, 63, 64]. In addition, the complexity of PTM mechanisms of action is still not fully understood [65, 66]. Nevertheless, it is widely established that histone modifications play fundamental roles in numerous biological processes, regulating and influencing DNA expression across various life stages and disease states [45]. There are two identified mechanisms for the function of histone modifications. The first involves widening spaces between nucleosomes to open or expose the chromatin and gain accessibility to the DNA. The second is the recruitment of regulatory proteins that regulate gene expression [43]. Some of these recruited proteins possess enzymatic activities (e.g., remodeling ATPases) that additionally modify chromatin. The dynamics of the recruitment of these proteins are determined by the cellular processes that require specific functions, such as transcription, replication, and repair. Each cellular activity requires a distinct set of histone modifications

to recruit the relevant regulatory proteins [45]. Therefore, the precise combination of histone modifications is the dynamic regulatory mechanism to orchestrate various downstream cellular activities.

I. Histone Acetylation

The first acetylation of histone was reported in 1964 [67]. The dynamic histone acetylation is mediated by the two regulatory family enzymes, histone acetyltransferases (HATs) and histone deacetylases (HDACs). HATs transfer an acetyl group to the N-lysine tail, which works as a neutralization for the N-lysine residue. Such neutralization weakens the interactions between histones and DNA, making the DNA more transcriptionally accessible. Thus, it has been established that histone acetylation mediates the unfolding of the chromatin and the subsequent transcriptional activation [16]. Thus, any change in histone charge is known to have effects on the chromatin configuration [45].

There are two main classes of HATs: class (A) and class (B). Class (A) HATs acetylate free histones but not those already deposited into chromatin. Class (B) HATs acetylate newly synthesized histones of H3 and H4 at specific sites needed for the deposition of the histones. On the other hand, HAT enzymes are further classified into three families entailed by their amino-acid sequence homology and conformational structure: GNAT, MYST, and CBP/p300 families [68]. Every HAT enzyme acetylates specific sites within the histone N-terminal tails. The neutralization of HATs' enzymes to the lysine residues disrupts the nucleosome electrostatic interactions and creates the platform for transcriptional activity [69]. In addition to the histone tails, additional acetylation sites are present within the globular histone core, such as H3K56, which is acetylated in mammals

by hGCN5 [70]. It has been shown that the H3K56 side chain points towards the DNA major groove, facilitating more DNA accessibility by affecting histone-DNA interaction in addition to the acetylation the histone N-terminal tail lysine [71].

Like other histone-modifying enzymes, HATs are often present within large multi-protein complexes [69]. Such proteome is crucial in regulating substrate specificity. For example, invitro purified scGCN5 acetylates free histones but not those existing within a nucleosome [72]. However, when scGCN5 exists within a multi-protein complex like the SAGA complex, it efficiently acetylates nucleosomal histones [72]. Furthermore, it has been shown that by chemically ligating modified tail peptides onto recombinant histone core proteins in vitro, the acetylation of H4K16 negatively affected the forming of a 30-nanometer chromatin fiber and the build-up of higher-order configurations [73].

II. Histone Deacetylation

HDAC enzymes are natural antagonists to HATs, reversing lysine acetylation and restoring the lysine's positive charge at the N-terminal tails of histones [74]. There are 18 HDAC enzymes; each HDAC belongs to either the histone deacetylase family or the Sir2 regulator family. HDACs are divided into separate classes based on protein domain homology **(Table 1.2**, illustrated in **Figure 1.3**) [51]. They are divided into four classes: Class I, II, III, and IV HDACs. Class II HDACs are further subdivided into Class IIa HDACs. Class I HDACs have sequence homology to the yeast Rpd3 protein. Class II HDACs have sequence homology to the yeast Hda1 protein. Class I and II HDACs also relate to the *Saccharomyces cerevisiae* Hos proteins. Class III proteins have sequence

homology to the yeast Sir2 protein. Class IV proteins share homology with Class I and II proteins. Similar to HATs, some HDACs exhibit substrate specificity [51].

Superfamily	**Family**	**Class**	**Yeast Protein homology**	**Subclass**	**Human protein analogue**
Arginase/deacetylase superfamily	Histone deacetylase family	Class I	Rpd3, Hos1, Hos2, Hos3		HDAC1, HDAC2, HDAC3, HDAC8
		Class II	Hda1	Class IIa	HDAC4, HDAC5, HDAC7, HDAC9
				Class IIb	HDAC6, HDAC10,
		Class IV			HDAC11
NAD/FAD-binding domain superfamily	Sir2 regulator family	Class III	Sir2, Hst1,	I II III IV	SIRT1, SIRT2, SIRT3 SIRT4 SIRT5 SIRT6, SIRT7

Table 1.2. HDAC superfamily classification and subdivision. Adapted after approved permission for reprinting from the publisher [51]

Figure 1.2 HDAC superfamily with their protein domain differences. Reprinted from [75] (open to use without prior permissions)

Class I, II, and IV HDACs belong to the arginase/deacetylase superfamily of proteins (**Table 1.3**). This superfamily contains the arginase-like amidino hydrolases and the histone

deacetylases [51]. The functional and structural homology viewed that classical HDACs include the three structurally related classes: Class I, II, and IV HDACs [76]. Individual HDACs within each class have related three-dimensional structures, and sequence homology. Interestingly, evolution studies found that all Class I, II, and IV HDACs precede the evolution of histones, suggesting that it could be that the primary substrates for the HDAC family are nonhistone proteins in the first place [76].

a. Class I HDACs

Class I HDACs were shown to mediate transcriptional repression by recruiting transcription factors and corepressors [77]. Homology studies showed that the deacetylase domains of Class I HDACs are highly conserved and have 45%–94% amino acid sequence similarity [51]. Class I HDACs have been implicated in cancers [78]. HDACs 1, 2, and 3 were shown to regulate crucial cell cycle genes such as p21 [78]. Some studies showed that HDAC3 works with SMRT and NCoR, regulating gene expression and causing repression of gene expression [79]. In addition, the over-expression of HDAC3 was reported in hematopoietic progenitor cells and was shown to be implicated in cell cycle progression and stem cell self-renewal [80]. HDAC8, the last member of Class I HDAC, was found to regulate telomerase activity inducing tumorigeneses, and its inhibition was shown to have antitumor effects [81].

b. Class II HDACs

Class IIa HDACs (HDAC 4, 5, 7, and 9) are characterized by tissue-specific expression [82]. They shuttle between the nucleus and the cytoplasm according to various regulatory signals [82]. What characterizes Class IIa HDACs is that they have an extended N-terminus that acts as a

binding site for the recruitment of the regulatory proteins. For instance, it was reported that the DNA-binding transcription factor MEF2 interacts with the regulatory domain of class IIa HDACs [83].

Another distinct feature of class IIa HDACs is their limited enzymatic activity. The catalytic activity of class II HDACs is significantly lower than class I HDACs by approximately 1/1000-fold [82]. In addition, most classical HDACs have tyrosine and two histidine residues in the active site for enzymatic activity. In contrast, class IIa HDACs have histidine instead of tyrosine [82]. It has been found that the tyrosine residue in the catalytic site is what increases the catalytic activity of the carboxyl domain of HDACs [84]. It was demonstrated that by substituting histidine with tyrosine through a point mutation in HDAC4, a 1000-fold increase in deacetylase activity was obtained compared to the wild-type [85]. However, it is controversial whether class IIa HDACs exhibit any deacetylation activity on histones at all. This raises the question of whether class IIa HDACs fit into the "eraser" category in the first place.

HDAC7 is a member of the Class IIa HDAC, which encodes a polypeptide of 912 amino acids. It was reported to be shuttling between the nucleus and cytoplasm of human muscle, neuroblastoma, and embryonic cell lines where it’s overexpressed [86]. HDAC7’s deacetylase enzymatic activity was shown to rely on its binding to HDAC3 in the nucleus, whereas it is found in the cytoplasm in an enzymatically inactive form. Crystalizing HDAC7 showed a distinction of HDAC7 compared to other Class IIa members, which was shown to have an enlarged active site pocket and a zinc-binding structural motif distant from its catalytic active site [87]. In addition, HDAC7 has been reported to be the only class IIa HDAC enzyme that gets activated in macrophages, mediating reprogramming for glycolysis and metabolism [88].

Although the scaffolding function of class IIa HDAC proteins is well documented [89], the function of the inactive catalytic domain is not well understood. One hypothesis proposes that class IIa HDACs act as "reader" proteins, analogous to bromodomain proteins where acetyl-lysine binding spin-offs downstream effects [90]. A recent study reported that class IIa HDAC proteins act as readers to acetylated lysine androgen and estrogen receptors to promote NCOR-HDAC3 dissociation and the subsequent transcriptional activation [89]. The same group showed that the unacetylated androgen receptor binds to the HDAC7- NCoR-HDAC3 complex to exert a transcriptionally repressed state [89]. Conversely, when the complex dissociates in the presence of the androgen receptor, it causes a transcriptional activation where the acetylated lysine residue binds to the active site of HDAC7 to break up the NCoR-HDAC3 complex from the androgen receptor [89].

Advancements in proteomics and peptidomimetic approaches have provided great insights into ways to target class IIa HDACs. This could enable the development of class IIa-specific inhibitors, which focus on disrupting their peptide-peptide interactions based on complex structures with other protein partners. This approach was demonstrated for HDAC4, where researchers were able to disrupt the protein interaction between the SMRT corepressor and HDAC4, [91].

Class IIb HDACs (HDAC6 and 10) have a unique long extra extension at the C-terminus, known as a tail domain. HDAC6 contains two deacetylase domains and a C-terminal zinc finger ubiquitin-binding domain, whereas HDAC10 has only one deacetylase domain and a leucine-rich repeat domain at its C-terminus. It was shown before that HDAC6 is implicated in the

deacetylation of α-tubulin, cortactin, chaperones, and IFNαR, regulating cell proliferation, metastasis, invasion, and mitosis in tumors [92].

c. Class IV HDACs

HDAC class IV comprises exclusively HDAC11, which shares a catalytic domain with class I and class II HDACs [93]. HDAC11 has been reported to have a role in modulating the DNA replication factor CDT1 and interleukin-10 expression, affecting gene expression [94].

d. Class III HDACs

Class III HDACs are the least related to the other HDACs because of their deoxyhypusine synthase-like NAD/FAD-binding domain, a distinct characteristic among HDACs [51]. They are required for gene silencing and are conserved in many species, from bacteria to humans [95]. There are seven different Sir2-like proteins (SIRT1-7) in humans. A remarkable feature of these sirtuins is that they display the most histone deacetylase enzymatic activity [96].

e. Histone Methylation

The methylation of histones is through the addition of methyl group(s) on its basic residues: arginines, lysines, and histidines. The methylation of lysines can be in the form of monomethylation (me1), dimethylation (me2), or trimethylation (me3) on their ε-amine group [49]. The most rigorously studied histone methylation sites are histone H3 lysine 9 (H3K9), H3K27, H3K36, H3K79, H3K4, and H4K20 [55]. Also, arginine (R) methylation sites were studied, including H3R2, H3R8, H3R17, H3R26, and H4R3 [49]. A summary of some of the most studied histone methylated marks and the methylating enzymes are shown in (**Table 1.4**)

Nonetheless, epigenetics and histone modification are an ongoing field of research and growing exponentially, and many other basic residues throughout the histone proteins are yet to be identified and studied.

Methylation is generally considered to change relatively slower compared to many other PTMs [97]. Some methylation processes may need to be more stably maintained, for instance, methylation involved in the developmental mitosis of a silenced heterochromatin [98]. In contrast, other methylation is relatively faster when cells have to respond to environmental cues promptly. Methylated histones are targets for epigenetic 'readers,' generating the environment for recruiting other regulatory molecules to modify the chromatin and gene transcription [53].

Histone methyltransferases comprise three family enzymes that catalyze the addition of methyl groups from S-adenosylmethionine to histones. The lysines are methylated by the SET-domain- proteins [99] and the DOT1-like protein families [100], while members of the PRMT family have been shown to methylate arginines [46]. Also, calmodulin-lysine *N*-methyltransferase, a non-SET-domain family protein, has been shown to methylate calmodulin and histones as well [101].

Histone mark substrate	**Methyltransferase enzyme**		
	Me3	Me2	Me1
H3K9	SUV39H1; SUV39H2; SETDB1; PRDM2	SUV39H1; SUV39H2; SETDB1; G9a; EHMT1; PRDM2	SETDB1; G9a; EHMT1; PRDM2

H3K27	EZH2; EZH1	EZH2; EZH1	
H3K4	SETD1A; SETD1B; ASH1L; MLL; MLL2; MLL3; MLL4; SMYD3; PRMD9	SETD1A; SETD1B; MLL; MLL2; MLL3; MLL4; SMYD3	SETD1A; SETD1B; ASH1L§; MLL; MLL2; MLL3: MLL4; SETD7
H3K36	SETD2	NSD3; NSD2; NSD1; SMYD2; SETD2	SETD2; NSD3; NSD2; NSD1
H3R2		CARM1(a); PRMT6(a); PRMT5(s); PRMT7(s)	CARM1; PRMT6*; PRMT5; PRMT7
H3R26		CARM1(a)	CARM1
H3R17		CARM1(a)	CARM1

Table 1.3 Histone methyltransferases. Adapted from Adapted after granted approved for reprinting form the publisher [55]

III. Histone Demethylation

Two main histone demethylase families have been reported to remove the methyl group(s) from lysines: amine oxidases and Jumonji C (JmjC)-domain-containing, iron-dependent dioxygenases [102].

The mechanism and the dynamics by which methyltransferases, or their counter antagonists, demethylases, are recruited to specific histone targets are crucial to the chromatin state and genomic regulation. Some characteristic DNA sequences were reported to have a role in recruiting several methyltransferase and demethylase enzymes. For instance, the Trithorax group (TrxG) response elements (TREs) and polycomb group (PcG) response elements (PREs) direct recruitment of some methyltransferases [103].

Histone mark substrate	**Demethylase enzyme**		
	Me3	Me2	Me1
H3K9	KDM3B; KDM4A; KDM4B; KDM4C; KDM4D	KDM3A; KDM3B; KDM4A; KDM4B; KDM4C; KDM4D; PHF8; KDM1A; JHDM1D	KDM3A; KDM3B; PHF8; JHDM1D
H3K27	KDM6A; KDM6B;	KDM6A; KDM6B; JHDM1D	JHDM1D
H3K4	KDM2B; KDM5A; KDM5B; KDM5C; KDM5D; NO66	KDM1A; KDM1B; KDM5A; KDM5B; KDM5C; KDM5D; NO66	KDM1A; KDM1B; KDM5B; NO66
H3K36	NO66; KDM4A; KDM4B; KDM4C	KDM2A; NO66; KDM2B; KDM4A; KDM4B; KDM4C	KDM2A; KDM2B

Table 1.4 Histone demethylases. Adapted after granted approval for reprinting from the publisher [55]

g) Chromatin remodeling

Chromatin remodelers provide the machinery needed for modifying chromatin, subsequently driving transcription signals to reach their motif targets on the DNA. Chromatin remodelers are large, multiprotein complexes that use the energy of ATP hydrolysis to move and restructure nucleosomes [104]. With the nucleosomes wrapping 146 base pairs of DNA in roughly 1.7 turns around an octamer histone, the DNA inside each nucleosome is generally inaccessible to the regulatory factors. Here, the chromatin remodellers intervene to provide access to the underlying DNA to enable transcription, chromatin assembly, DNA repair, DNA replication, and other cellular processes by actively shaping the packaging of the DNA [105]. The abundant arrays of uniformly spaced nucleosomes are reflected in the nonrandom positioning of the nucleosome across the genome [106]. The nucleosomes are uniform in distances between nucleosomes and arrayed or phased relative to a reference barrier like the promoter. The nucleosome organization is exemplified at the 5′ ends of transcriptionally active genes, illustrated in (**Figure 1.4**) [107]. The promoter region does not have nucleosomes and is thus termed a nucleosome-free or nucleosome-depleted region (NFR or NDR, respectively); it is followed by the foremost nucleosome downstream of the transcription start site (TSS), termed as +1 nucleosome. Nucleosomes that follow take an array of +2, +3, and so on, uniformly arrayed over the gene body [108].

Nucleosomes are highly structured, and their organization may be either activational or inhibitory for DNA-templated reactions. For example, nucleosomes may impede transcription-factor binding sites and thus repress transcription [107]. Contrarily, active DNA replication requires a particular structure of nucleosomes around replication origins [109].

The leading remodeller families are SWI/SNF, INO80, ISWI, and CHD, which share the features of having Snf2-type motor ATPases. Snf2-type ATPases utilize chemomechanical cycles of ATP binding and hydrolysis to mobilize DNA[107]. On nucleosomes, this translocation breaks histone–DNA physical interaction, which drives DNA mobilization around histones, with the subsequent histone exposure and exchange of histone variants or (un)modified histones. However, it is still elusive how remodelers transform the energy of ATP hydrolysis into mechanical power to mobilize the nucleosome, nor do we know why different (un)modified histones remodeler complexes select specific nucleosomes to mobilize and reposition [108].

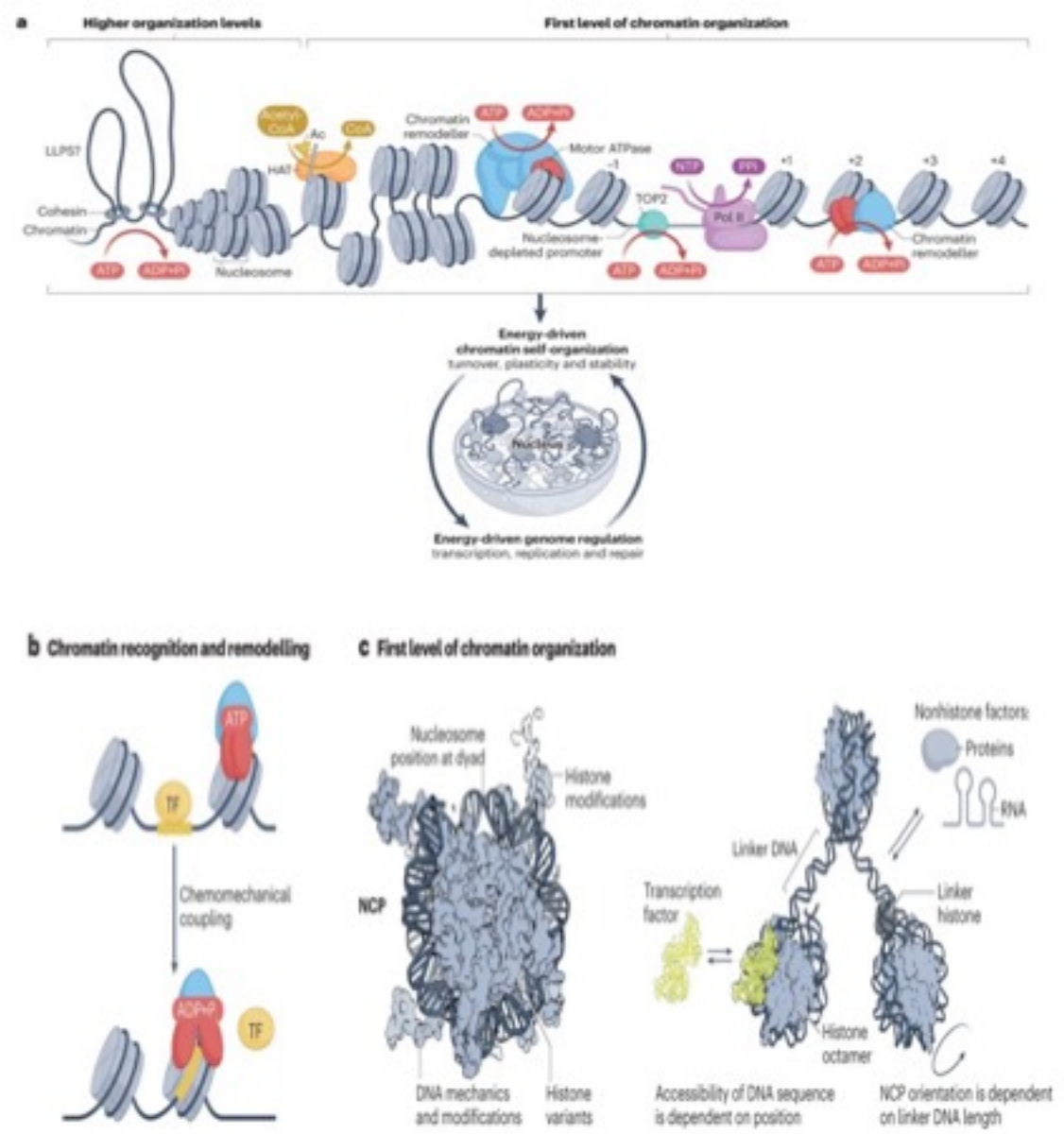

Figure (1.3) Chromatin self-organization and regulation of genomic activities. A. *Schematic diagram demonstrating the self-organization of chromatin and its interaction with genome regulation to maintain cellular maintenance and plasticity. a-Energy-driven machinery orchestrates multilevel self-organization of chromatin within the nucleus of a eukaryotic cell. Initially, chromatin remodelers utilize ATP to restructure nucleosomes at specific DNA loci. This phase involves the recruitment of DNA topoisomerase 2 (TOP2), DNA methyltransferases, and histone posttranslational modifiers such as acetyl coenzyme A (acetyl-CoA)-dependent histone acetyltransferases (HAT). Chromatin-loop extrusion mediated by cohesin and related complexes, along with liquid-liquid phase separation (LLPS), further contribute to higher levels of chromatin organization facilitated by ATP-dependent systems. The organized chromatin subsequently modulates various genomic processes, including active transcription, DNA replication, and DNA repair. Nucleosome arrays are positioned relative to nucleosome-depleted promoters, akin to the regulation of transcription by RNA polymerase II (Pol II).*

***B**. Illustration demonstrating how remodelers can impede transcription through ATP hydrolysis-driven mobilization of nucleosomes, thereby concealing a transcription factor binding site within the histone octamer, making it inaccessible to the transcription factor (TF).*
***C.** Schematics depicting how remodelers facilitate transcriptional access by restructuring nucleosome core particles (NCPs), thereby regulating the accessibility of transcription factors to their target motifs (highlighted in yellow). Additionally, bidirectional regulation occurs between nucleosome repositioning and linker DNA, contributing to higher-order chromatin fiber organization. Reprinted with approved permission from the publisher* [108].

h) The interplay between the dynamics of chromatin accessibility and gene regulation

The physical accessibility to the DNA is highly dynamic and tightly regulated through the plasticity-driven modulation of the chromatin structure with its diverse components, thus establishing and maintaining cellular identity. The highly structured chromatin reflects a network of coworking and physical interacting regulators from active enhancers, promoters, insulators, and chromatin-binding factors, which cooperatively regulate gene expression. Such accessibility topography shifts dynamically in response to environmental and developmental cues.

Arising evidence proposes that homeostatic maintenance of chromatin accessibility is dynamically regulated through a competitive cross-talk between chromatin-binding factors and nucleosomes [110]. The chromatin structure and its compaction into the nucleus were found to be tuned by four non-mutually exclusive mechanisms. These comprise (1) The fuel through the ATP-dependent remodeling complexes that use the energy of ATP hydrolysis to move the nucleosomes, exposing histones from the tight chromatin fiber. (2) PTMs of histones that precisely entail and modify the histone-DNA interactions and the recruitment of specific regulatory elements to the chromatin. (3) The existence of the histone chaperones that, together with chromatin remodelers, regulate the deposition of free histones. (4) The presence of the histone variants with their distinct binding domains, distinguishable from the canonical histones in their structure and function in the chromatin fiber [53].

The complexity, self-organizing stability, and plasticity of chromatin states provide a foundation for epigenetic regulation, which is maintained without sustained signaling and promotes different functions to unfold from the same genome [20]. Active gene transcription requires the *cis* arrangement *of* regulatory elements and gene promoters for the RNA polymerase and its regulatory factors to access the motif gene body [111]. Thus, transcriptional activity mandates coordination between chromatin architecture designed by the histone modifying writer, eraser, reader proteins, and chromatin remodelers, which generate the machinery to mobilize the nucleosomes [112].

Another complex interplay between chromatin state and function is seen between the transcriptional impact of enhancer and promoter accessibility; even though both are required for transcription [113], enhancers and promoters of transcriptionally silent genes are often open, suggesting that chromatin accessibility is essential, but not sufficient, for enhancer or promoter to orchestrate transcriptional activity [113]. Another contrasting crosstalk model between accessibility and transcriptional activity is displayed during embryonic development, where the chromatin is open, yet many accessible genes are transcriptionally inactive until later developmental stages [110]. All these findings establish multilayered regulation crosstalk between chromatin accessibility and genomic regulation.

The network structure of open chromatin across enhancers, insulators, promoters, and gene bodies provides a dynamic, biophysical environment through which constituents of the chromatin epigenome interact. The presence of constraints yet dynamic physical interaction rules within the chromatin landscape shapes the genomic transcription and cellular decisions. Understanding how these regulatory systems are dynamically designated when cells transition between the different

developmental stages or during tumor growth and the biophysical rules licensing how regulatory elements determine gene expression profiles remain an ongoing focal point in epigenetic research.

i) Canonical and Non-Canonical Histones

Histones represent about half of the eukaryotic chromosome mass, with 73 histone genes already identified in humans [114]. Two types of histones have been established: canonical histones and variant histones. Expression of canonical histones is regulated by promoters, which guide transcription during the cell cycle S-phase, concurrent with new DNA synthesis [115]. Canonical histone genes lack introns as well as are not polyadenylated; instead, they carry a stem-loop sequence and a histone downstream element in the 3′UTR that confine its expression to the S phase to match only the demand for newly synthesized DNA [116].

In contrast, genes encoding histone variants often have introns, thus generating various alternative isoforms that may contribute to nucleosomal diversity [114]. Moreover, histone variants are expressed throughout the cell cycle, independent of replication or DNA synthesis [117]. Histone variants may substitute canonical histones in the nucleosome positioning, resulting in distinct organizational shifts and influencing gene expression, DNA replication, and DNA repair [118]. Another distinguishing feature is that while the newly assembled nucleosomes having the canonical histones are inserted in the gaps within earlier assembled nucleosomes, histone variants have a distinct feature of replacing existing previously assembled nucleosomal subunits. This feature is rigorously regulated by a complex machinery of histone chaperones and ATP-dependent chromatin remodelers [114]. Thus far, more than 50 histone variants have already been identified in mammals [119].

While histone variants have been associated with all four histones, most of them were identified for histone H2A and histone H3 [114]. The deposition of histone variants can directly affect the configuration of nucleosomes, which could impact the accessibility of DNA and the regulation of transcription, replication, and DNA repair [120]. Such deposition is correlated with the nucleosomes containing the histone variants being distributed over specific locations on the chromatin rather than being regularly distributed [120]. For instance the H3 variant H3.3, which is enriched at promoters of transcriptionally active genes [121]. Moreover, CENP-A, the histone H3-like centromeric protein A, is deposited into specific nucleosomes to form a functional centromere, making the role of this protein fundamental for kinetochore assembly and integrity [122].

Like the core histone proteins being a target for an extensive number of PTMs at their N-terminal tails, the deposition of histone variants in nucleosomes has the same PTM susceptibility. That adds more complexity and diversity to the epigenetic cellular profile, impacting the "open" versus "closed" state of chromatin and subsequent gene expression of crucial cellular processes like during embryonic development, cell differentiation, and in cancer [107, 120, 123].

The presence of mutations in canonical and variant histone mutations has introduced a new class of epigenetic mutations in cancer [124]. Genes encoding histone proteins were found to be mutated in many tumors, impacting nucleosome stability, histone PTMs, and overall chromatin dynamics [125]. It has been proposed that the high frequency of histone mutations observed across diverse cancers validates the notion that the typical chromatin configuration acts as a shield against tumors.

Oncohistone mutations were found to rattle chromatin organization and transcriptional regulation, predisposing to cancer development. Oncohistones include the histone H3K27M mutation found in deadly pediatric gliomas, diffuse midline glioma (DMG), and diffuse intrinsic pontine glioma (DIPG). H3K27M mutation can occur in both canonical (H3.1, H3.2) and variant (H3.3) histone H3 genes. Recent studies have validated that, despite constituting few proportions of the H3 pool, H3K27M mutant histones were shown to be the primary inhibitor for the PRC2 in DIPG. H3K27M was found to be responsible for the global reduction of the heterochromatin marks H3K27me2 and H3K27me3 levels with concomitant increases of the transcriptionally active mark, H3K27ac [126, 127].

Histone mutations have also been identified in diffuse large B cell lymphoma, head and neck squamous cell carcinoma, acute myeloid leukemia, and uterine and ovarian carcinosarcoma [128]. Other solid cancers showed the histone H2BE76K mutation that impacts nucleosome organization and stability [129]. Many of these histone gene mutations occur with a frequency similar to that of somatic mutations in known oncogenes, such as BRCA2, TET2, SMAD4, and NOTCH1. Nevertheless, whether oncohistone gene mutations are the drivers for these oncogenes in early tumor development still needs to be better understood [130]. The better we understand the mechanisms of operations for oncohistone mutations, we will gain further insights into how the dysregulation of nucleosomal-mediated gene repression drives tumorigenesis and whether it could be corrected therapeutically.

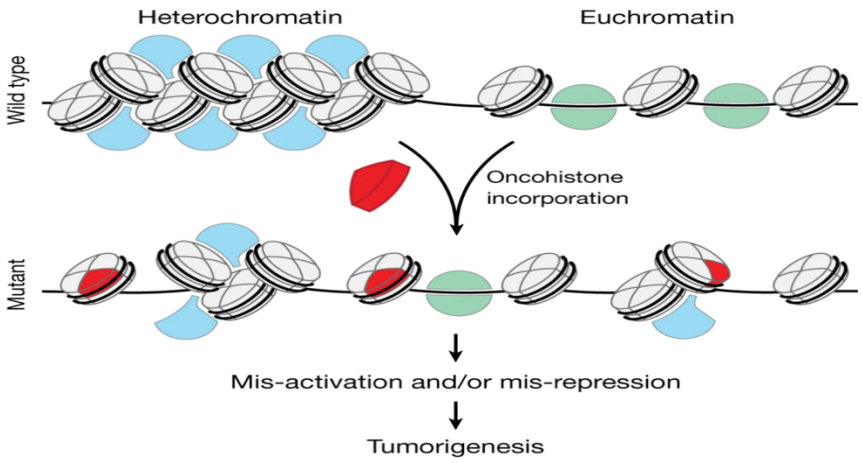

Figure (1.4) The effect of oncohistones on the chromatin configuration. *Oncohistones (in red) deposition within the chromatin polymer may cause significant shifts in the epigenomic organization by transforming the biophysical properties between the two states of the chromatin, heterochromatin, where chromatin remodelers (blue) bind regulating transcription versus euchromatin, where TFs (green) bind and activate transcription. Reprinted after approved permission from the publisher* [131].

j) Chromatin dynamics during tumorigenesis

With different cancers varying, possibly in their origins and the implicated pathways, all cancers share specific hallmarks such as uncontrolled proliferation, evasion of apoptosis, lack of response to tumor suppressors, high expression of growth factors, invasive metastatic potential, and supported angiogenesis [7, 43]. The features unifying all these cancer hallmarks are genomic instability and epigenetic disorganization. The multi-level chromatin organization provides the required degree of condensation to regulate the entire genome within the nucleus. The self-correcting machinery of chromatin enables the maintenance of cellular processes like transcription and replication events and DNA repair in response to environmental cues. The link between oncogenesis and chromatin dysregulation is multidimensional, involving dysregulation occurring at different levels from chromosomal rearrangements, chimeric transcription factors, or modified epigenetic marks. Interestingly, the epigenetic marks on

cancer cells tend to differ within the same tumor. Such epigenetic heterogeneity indicated that these could be the cancer drivers and the reason behind the tumor heterogeneity and therapeutic resistance. Strikingly, whole genome omics techniques showed that around half of the oncogenic mutations for many cancers are chromatin regulators [132].

The established understanding of cancer development is the eruption of oncogenes or repression of tumor-suppressor genes, either provoked by driver mutations or by the global alteration of epigenetic marks. Nevertheless, heterochromatin disorganization could be an oncogenic driver itself. This disbalance in heterochromatin/ euchromatin proportion can promote tumorigenesis and the heterogeneity of cancer [133]. It was established in 1928 by the epigenetic pioneer Emil Heitz that heterochromatin/euchromatin comprise the fundamental architecture of eukaryotic chromosomes and that the euchromatin is genetically active and the heterochromatin is genetically passive [134]. Still, later, the hypothesis about inert heterochromatin was challenged by the discovery of developmental genes in heterochromatin regions. Heitz then noted that heterochromatin is often found in the sex chromosomes, but later, it was established that heterochromatin could be facultative heterochromatin (fHet) compared to constitutive heterochromatin (cHet) [135].

The mutual exclusivity between heterochromatin and euchromatin is foundational for the genome to fold into separate regulatory domains correctly. There is a significant correlation between the chromatin state and the three-dimensional (3D) folding of the genome, a relationship validated by the recently developed chromosome conformation capture method known as the Hi-C method. Hi-C revealed genomic regions distant in the genome but adjacent

in the 3D space [136]. It allowed the quantification of the frequency of such genomic interactions by the numbers of normalized read pairs that span the interaction regions.

At the omics scale, the chromosomes are segregated into two types of compartments that have a bias towards long-range interactions within the regions of the same compartment; the more loose and open "A" compartment refers to euchromatin, and the "B" compartment refers to heterochromatin that has a higher frequency of interactions to configure a more condensed chromatin structure at a more defined scale [137]. The compartments can be additionally segregated into topologically associated domains (TADs) that span up to hundreds of kilobases of genomic regions, where TAD boundaries are strictly defined by the enrichment of cohesion and CTCF insulator proteins that securely maintain the TAD boundaries respect [138]. This displays that in addition to self-assembly, there is a chromatin looping (loop extrusion), where chromatin extrudes by the cohesion complex until it finds the TAD boundary, which adds more complexity to the genomic organization [139]. Thus, disrupting the boundary rules by removing CTCF/cohesion proteins between TADs shifts the boundaries that can alter gene expression and drive the tumorigenesis [140].

Moreover, the change in the chromatin structure may modify the accessibility of enclosed DNAs to replication or repair complexes predisposing to cancer. A multi-omics study of the cancer genome characterizing more than 40 genomic instability features found that the change in the histone heterochromatin mark H3K9me3 binding level is accountable for more than 40% of the mutation rate variation in the cancer genome [40].

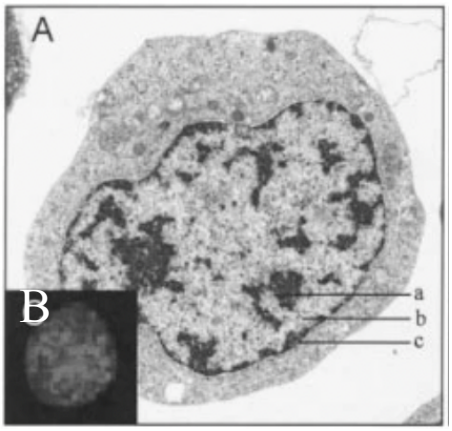

Figure (1.5) Electron microscopy of A- Condensed Jurkat cell *showing condensation displaying condensed heterochromatic regions **A**. versus euchromatic regions **B.** with the condensation appearing to line the nuclear envelope; Scale bar: 1 µm. Heterochromatin is usually distributed close to the nuclear periphery and tethered to the lamina or around the nucleoli, while euchromatin is located in the nuclear interior. Picture reprinted after approved permission from the publisher* [141]

Phenotypically, electron microscopy studies were able to capture the morphology of the chromatin that revealed that condensed heterochromatin tends to line the nuclear membrane, and it can be broken by clear areas at the nuclear pores so that transport is allowed; distinct form euchromatin that tends to be instead dispensed and not readily stained [142]. With the paramount impact on genomic stability, there was a pressing need to understand how the chromatin transitions from the euchromatin to the heterochromatin state and what rules should be governed during this transition.

Three models have been proposed for the chromatin state transition, illustrated in **(Figure 1.7)** [143]. The first model involves de novo establishment of the heterochromatin domain in an euchromatin background mediated by Transposable element (TE) insertion into the euchromatic region that triggers heterochromatin formation with new domains mediated by small RNA pathways [144]. This model has been shown in the mouse embryonic stem cell lines carrying polymorphic retroposon insertions, and H3K9me3 and H4K20me3 marks have been observed in some retroposon insertions [145]. Such interactions may impact the nearby genes or genes on a different chromosome by reshaping the genome-wide folding [144, 145].

The second model doesn't include element insertion; instead, it displays the change in euchromatin/heterochromatin balance. Such disbalance could be forced by the expansion of heterochromatin driven by the upregulation of heterochromatin-associated proteins or the downregulation of euchromatin-associated proteins [39, 146]. It has been proposed that such chromatin-boundaries-crossing form without the participation of boundary elements, such as CTCF proteins, and are thus called negotiable borders [143].

The third model of the chromatin state shift is through mutations of TAD boundary sequences between euchromatin and heterochromatin domains. As described earlier, the TAD boundary sequences are usually CTCF binding sites, transcriptionally active genes, or large genomic rearrangements, such as inversions, deletions, or duplications [147]. Removal or inversion of TAD boundary sequences may expand heterochromatin domains into euchromatin regions [143].

The major genomic instability driven by the chromatin phenotypic shift and euchromatin/heterochromatin disbalance makes it highly likely that altered chromatin structure drives tumorigenesis.

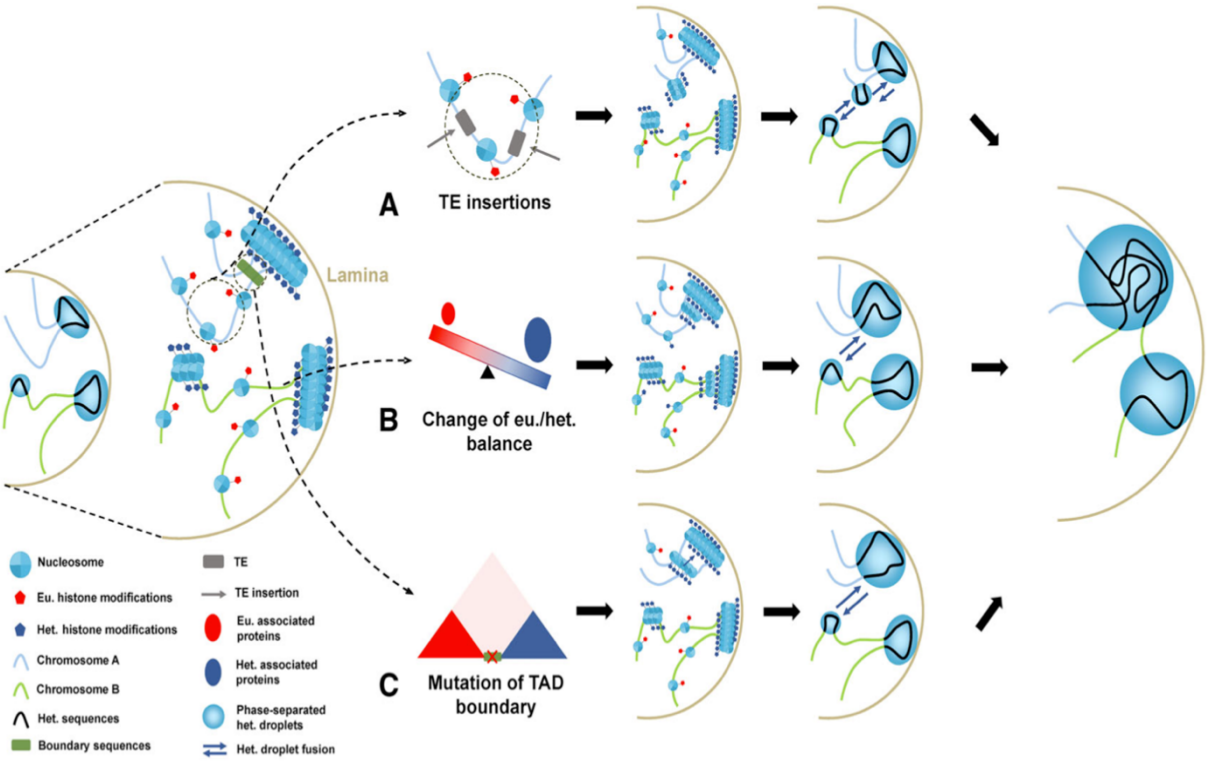

Figure (1.6). Chromatin Phenotype transition from euchromatin to heterochromatin state. *Three proposed models of euchromatin to heterochromatin transition.* ***A****. The* de novo *formation of heterochromatin regions by TE insertions may impact proximal genes' expression by the expansion effect of newly formed heterochromatin regions.* ***B.*** *Balance shift in euchromatin/heterochromatin ratio. The spreading of heterochromatin can be promoted by upregulating heterochromatin-associated marks (e.g., H3K9me3 and H3K27me3, shown as dark blue dots) or downregulating euchromatin-associated marks (e.g., H3K9ac and H3K4me3, appear as red dots), the disbalance created what is named "negotiable borders" where chromatin boundaries form without the influence of boundary elements, such as CTCF proteins.* ***C****. Mutations of TAD boundary sequences between euchromatin and heterochromatin domains (appear as green lines between the two TADs). The alterations in boundary sequences may lead to the heterochromatin spreading into euchromatin. The newly formed heterochromatin domains from the three proposed models, A, B, or C, will interact with other preexisting heterochromatin domains at the lamina through phase-separated droplet fusion. Such chromatin dynamic changes may impact adjacent or distant genes by reshaping the chromatin folding. Het, heterochromatin; Eu, euchromatin; TE, transposable element. Reprinted after approved permission from the publisher* [143]

The high-throughput chromatin sequencing technologies (ChIA-PET, HiChIP, AQuA-HiCHIP, TrAC-looping, Capture-HiC) significantly changed our understanding of the chromatin

organization for the cancer genome, which was shown to be vastly different from human reference genomes [148-150]. All these mechanistic studies demonstrated that chromatin looping, topologically associating domains (TADs), and the chromatin-defined "A" compartment (euchromatin regions) and "B" compartment (heterochromatin region) are implicated with the chromosome structural variation in malignancies.

Cancer cells also undergo transitions in this compartmentalization to evade the expression of tumor-suppressor genes or promote the expression of proto-oncogenes. Recent studies showed that cervical cancer, triple-negative breast cancer, and neoplastic B-cells have around a quarter of this compartmentalization altered during cancer transformations, and cancer-specific TADs were reported in the prostate as well as breast cancer cells [151-154]. Heterochromatin markdown was shown to coincide with the acquisition of a transformed cancerous phenotype concurrent with the increase of the KDM4B and KDM6A demethylase enzymes that were found to be essential for the cancerous cells' survival [155]. Also, the reduced levels of Heterochromatin Protein 1α isoform or loss of its dimerization have been shown to induce the metastatic ability of breast cancer by disrupting the tethering of peripheral heterochromatin to the nuclear lamina, making the nuclei more avail, resulting in subnormal nuclear morphology and segregation errors that are common in cancers [156]. Furthermore, the accumulation of the euchromatin-regulating enzyme, KDM4C histone demethylase, was shown to be essential for the Wnt- β-catenin-TC4 signaling pathway needed for the regulation of glioblastoma tumorigenesis [157]. Reduced chromatin condensation causes a loss of nuclear rigidity, increased nuclear malleability, and more chromatin abnormality and destabilization [158].

All these supported data validate that chromatin assembly is fundamental not only for the compaction of the genome in a confined nuclear space but equally crucial for regulated gene expression, repair mechanisms, and response to environmental cues. The hallmark features of aberrant gene expression and immortality of cancer cells observed at the onset of malignancy are now seen as outcomes of chromatin disorganization. Cancer establishment and progression show chromatin dynamics changes at multi-levels, alone or in conjunction with other tumorigenic events. Ultimately, there is a shift in the cancer genomics field, putting chromatin disorganization in cancer as a primary driver for cancer aggressiveness and therapy failure instead of being seen as an outcome of the oncogenic expression.

II. Epigenetic-based therapy for human malignancies

a. Introduction to the epigenetic-based therapy for human diseases.

Despite the expansive growth in the therapeutic industry and the array of treatment modalities available, cancer remains the leading cause of death. Effective therapeutic responses are typically achievable during the early stages of cancer by employing combinations of chemotherapy, radiotherapy, immunotherapy, surgical resection, and targeted cancer therapies. [159]. Nevertheless, drug resistance and aggressive secondary relapses of the malignancy are widespread, leading to treatment failure and cancer recurrence [160].

The past decade has witnessed an outburst of discoveries regarding the significant impact of epigenetic mechanisms in changing cellular regulation and cancer phenotypes. These remarkable interventions aim to correct the DNA packaging without changing the primary DNA base sequence

in the genome. As referenced earlier, many aspects of epigenome disorganization serve as defensive mechanisms for tumor cells to maintain immortality and self-renewal at the cost of a normal cellular state. Thus, there has been a growing emphasis on designing epigenetic-based therapies to reprogram cancer cells to retrieve normalcy. Many agents with different targeting epigenetic mechanisms are indeed under development or in clinical trials [161, 162]. Epigenetic-based therapies have great potential because, in contrast to genetic abnormalities, epigenetic changes are reversible, allowing recovery of function for implicated oncogenes without changing DNA sequences [163].

During embryonic development, the plasticity of the epigenome enables changes in cellular phenotypes from an embryonic to a terminal differentiated state. However, in cancer, epigenetic abnormalities emerge, trapping the cell in self-renewing machinery and impeding normal differentiation. Such cellular reprogramming phases usually evolve over years of neoplasm initiation and progression, leading to late cancer prognosis and posing significant challenges for successful therapeutic intervention. [164].

It wasn't until the 1990s that drugs targeting epigenetic mechanisms started to gain access to clinical trials; however, reversing epigenetic alterations was initiated as early as the 1970s when agents targeting DNA methylation introduced [165]. DNA demethylating epigenetic therapies are now approved by the US Food and Drug Administration (FDA) as a chemotherapeutic [166].

The global incidence of multiple cancers has been steadily increasing each year [160]. However, rapid advancements in our comprehension of epigenome regulation have enabled significant strides in the development of novel epigenetic therapeutic drugs. These drugs hold immense promise in reducing therapy-related side effects, improving survival rates, and potentially

offering long-term cures for certain cancers. Consequently, it is imperative to elucidate resistance mechanisms across different types of cancers, develop prediction models, and devise various strategies with combinational therapies to overcome resistance early in the treatment process.

b. Targeting epigenetics regulators as anti-cancer to overcome cancer resistance.

Drug resistance is mainly responsible for cancer recurrence and poor prognosis [159]. With the rising evidence regarding aberrant epigenetic regulations as a significant contributor to tumor therapy resistance, targeting epigenetic modifiers is an effective strategy to reverse drug resistance.

Multiple identified drug resistance mechanisms exist through which cancer cells develop considerable tolerance to the therapy. Among the principal resistant mechanisms is the P-glycoprotein (P-gp), which promotes the efflux of drugs, where inhibition of P-gp was shown to reverse drug resistance significantly [167]. Also, the built-in protective cellular autophagic response often counteracts the apoptotic mechanisms of some anticancer drugs, contributing to the development of drug resistance [168]. However, most therapeutic resistance has been attributed to the intra-tumoral heterogeneity of the cancer cells. After starting a chemotherapeutic treatment, heterogenous or genetically diverse cell clones induce the development of clones of drug-resistant cancer cells, including cancer stem cells (CSCs). Notably, CSCs have additional unique mechanisms to evade the corrective immune system attacks. The mechanisms used by the immune checkpoint to mediate immunosuppression and facilitate CSC stemness are well established [169]. Remarkably, reversing the stemness phenotype that CSCs develop throughout the tumorigenesis journey has been among the top focuses as an effective means to overcome chemotherapeutic resistance [170].

Furthermore, gene mutations are well known to contribute to drug resistance, like building resistance to tyrosine kinase inhibitors by the EGFR mutation [171]. A striking question is whether the epigenetics abnormality is one of the mechanisms for mediating chemotherapeutic resistance or is instead the primary drive under which the other resistance mechanisms are downstream. Notably, the overlapping between the modifications of DNA and histone affects the function of transcription factors during tumor development and regulates other epigenetic regulators, such as chromatin remodeling and non-coding RNAs, to secure the neoplastic environment [172]. The development of epigenetic therapies that aim to counteract drug resistance has provided hope to cancers with drug-resistant tumors [173]. Ongoing efforts to identify additional resistance mechanisms will continue to grow parallel with the development of novel treatments for drug-resistant cancer. The discovery of these "bench-to-bedside" targeted epigenetic therapeutics will be achieved by tirelessly working on uncovering novel mechanisms and drivers that initiate, aggravate cancers, or activate drug resistance pathways.

c. Histone modifications and chemotherapeutic resistance

. Histone modifications play a crucial role in fostering chemotherapeutic resistance in cancer cells through various mechanisms. They drive changes in gene expression profiles associated with resistance and contribute to increased heterogeneity among cancer cells, promoting the preferential selection of resistant phenotypes. Additionally, histone modifications have been associated with the enrichment of stemness markers in cancer stem cells (CSCs). In addition, histone modifications have been linked to the suppression of essential tumor-associated antigens in cancer cells, a tool in evading the immune system's detection [174]. Furthermore, histone-modifying enzymes were found to reduce the expression of the anti-tumorigenic chemokines [175]. It resulted in creating

the immunosuppressive tumor microenvironment that contributed to the immune evasion of CSCs [175].

Histone methylation has been shown to play a major role in chemotherapeutic resistance. For instance, the increased expression of EZH2 was shown to activate cell survival pathways that drive the drug resistance of ovarian cancer cells to the chemotherapeutic cisplatin [176]. In addition, EZH2 was found to activate the PI3K/AKT pathway, which rendered Non-Small Cell Lung Cancer (NSCLC) [177] resistant to induced chemo resistant to gefitinib. In contrast, the combination therapy of EZH2 with the chemotherapeutic oxaliplatin showed a positive outcome in colorectal cancer cells [178]. Moreover, SETDB1 can interact with PELP1 and activate AKT, driving breast cancer resistance to tamoxifen [179]. Also, repressing the histone methyltransferase G9A increased the expression of tumor suppressor gene SOX6, significantly inhibiting the survival and self-renewal ability of leukemia stem cells [180]. Furthermore, the methyl transferase SETDB1 was shown to be involved in stem cell maintenance driving therapy resistance [181]. On the contrary, knocking down SETDB1 significantly increases KRAS-mutant colorectal cancer's sensitivity to cetuximab treatment [182].

Histone acetylation has also been implicated in chemotherapeutic resistance. Generally, high deacetylation of histones was linked to chemotherapy resistance [159]. It was shown that HDAC6 increased drug resistance in NSCLC and melanoma by stimulating the stability of EGFR and tubulin β3 and inhibiting apoptosis, [183]. HDAC1, 2, and 6 were demonstrated to induce cancer stemness and resistance of GBM to temozolomide [184]. Notably, the overexpression of HDAC1 and HDAC7 increased the stemness phenotype markers miR-34a, CD44, and CD166, which induced chemotherapy resistance, metastasis, and induced recurrence in breast cancer and

ovarian cancer [185]. Furthermore, uncontrolled expression of HDAC7 has been linked to less response to chemotherapy [186]. HDAC11 was also shown to interact with the transcription factor GLI1 to activate the expression of SOX2, which induces drug resistance in NSCLC [93, 187].

The central role of HDACs in tumor regulation and drug resistance underscores the high potential of HDAC inhibitors as a class of epigenetic-based therapy. Indeed, extensive trials of HDAC inhibitor monotherapy or combination therapy with other drugs have been initiated for various drug-resistant tumors with some showing promising results [90, 188-192]. The earlier pan HDAC inhibitors, such as vorinostat and panobinostat, displayed more positive outcomes than anticipated when administered in combinational therapy in preclinical models of various drug-resistant cancers. [85]. Vorinostat was shown to reverse cisplatin resistance and reduce the stemness phenotype of CSCs by repressing NOTCH signaling in solid tumors like head and neck and pancreatic cancer cells [169].

Nevertheless, pan-HDAC inhibition remains complicated due to the interaction with the vast array of HDACs with their diverse mechanisms and regulation. Therefore, initiatives have been encouraged to conduct in-depth studies of each HDAC's differential mechanisms of action in different cancers. Such in-depth studies will enable the development of more targeted therapies for treating chemo-resistant cancers.

III. HDAC class IIA inhibitors as epigenetic-based therapy for tumorigenesis.

a) HDAC inhibition drug targeting opportunities

The different classes of HDACs were primarily grouped based on their structural semi-homology. However, on the functional and mechanistic level, members of the HDAC family

are diverse, and some of them act as tumor promotors or suppressors and dually regulate cancer progression by influencing cellular activities such as stemness, proliferation, apoptosis, differentiation, angiogenesis, migration, and invasion [85]. A comprehensive understanding of the structural disparities among HDACs and their corresponding mechanistic roles in binding and interacting with various cellular regulators is crucial. Such understanding will significantly enhance our comprehension of the involvement of HDACs in tumorigenesis. Moreover, it will aid in the development of isoform-specific HDAC inhibitors tailored to specific malignancies.

Class I, II, and IV HDACs are zinc-dependent. The active sites of all the zinc-dependent HDACs consist of a curved tubular pocket with a wide cavity. The enzymatic mechanism is mediated by a charge-relay system of two adjacent histidine residues, two aspartate residues, and one tyrosine residue [51, 69]. The Zn^{2+} ion stabilizes the acetylated substrate in the enzyme's catalytic pocket and polarizes the carbonyl group, making the carbon a target for neutralizing water molecules via hydrogen bonding [51, 69]. The HDAC inhibitors' mechanism of action is through interacting with the zinc ion and the charge-relay system. The tyrosine residue may undergo a conformational transition in or out to adjust substrate binding. In class IIa, the tyrosine residue is substituted by a histidine, which proved crucial for forming the tetrahedral intermediate [51, 69, 77]. Such conformational differences justify the diminished enzymatic activity of the members of class IIa compared with that of other HDACs.

Figure (1.7) An illustration of the Zn-dependent HDAC interaction with an acetylated substrate. *Enzyme-substrate complex showing the binding interaction between HDAC and an acetyllysine-bearing protein substrate that potentially blocks the active site and inhibits the deacetylation enzymatic activity. Picture adapted and reprinted after permission granted from the publisher* [193]

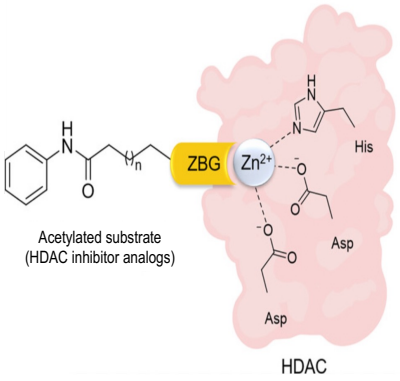

A characteristic structural feature of HDAC IIa is that in addition to the Zn binding regions, the catalytic domains of class II HDACs exhibit another zinc ion-binding site known as the structural zinc ion-binding subdomain. Class IIa-specific residues are attracted to this structural zinc ion-binding site and at the entry site to the catalytic site [51, 69, 77].

Because of the substrate binding through the catalytic carboxyl domain, HDAC targeting by HDAC inhibitors was predominantly through the targeting catalytic pocket of HDAC. Thus, many competitive HDAC inhibitors targeting the catalytic pocket have been designed. Many of these HDAC inhibitors were indeed examined in many preclinical and clinical settings [90, 188-192, 194-199]. Pan HDAC inhibitors such as SAHA (Vorinostat, Zolinza™, Merck & Co, Inc., USA) and FK228 (Romidepsin, Istodax™, Celgene Corp., USA) are FDA-approved drugs and were introduced in the treatment of cutaneous T-cell lymphoma. The FDA recently approved Belinostat (PXD101, BELEODAQ™, Spectrum Pharmaceuticals, Inc.) against peripheral T-cell lymphoma. Moreover, panobinostat (Farydak, Novartis Pharmaceuticals) was approved for treating multiple myeloma in 2015 [84].

Nonetheless, like other anticancer therapeutics, pan-HDAC inhibitors have generated toxicity and unwanted effects [90]. The side effects reported include thrombocytopenia,

neutropenia, nausea, vomiting, diarrhea, and fatigue [84]. The most problematic adverse effect is cardiac toxicity with ventricular arrhythmia [84]. The major problem with the currently available HDAC inhibitors is their lack of HDAC target specificity. The pan inhibition for all classes of HDACs does not proportionate with the significant differential tumor suppression mechanism of action and capability. Therefore, there has been a pressing call for the design of isoform-specific HDAC that would be relevant for the appropriate tumor, thereby minimizing off-target toxicity and unwanted effects. A thorough understanding of the mechanistic roles of each HDAC in tumorigenesis is essential for maximizing the efficacy of this promising class of epigenetic drugs in combating malignancies.

b) Modulation of cell cycle regulators by HDAC inhibitors

The mechanisms by which different HDACs regulate the cell cycle during cancer growth and development are diverse. HDACs can induce a range of cellular and molecular regulations through their deacetylating domains (in most HDACs) or their regulatory domain (in HDAC class IIa) [77, 200, 201]. Studies have shown that HDACs can suppress tumor suppressor gene expression and modulate various oncogenic cell-signaling pathways [77, 84, 90, 202].

On the contrary, HDACi was shown to induce cell-cycle arrest in G1 through the up-regulation of cyclin-dependent kinase (CDK) inhibitors or down-regulation of cyclins and CDKs [77, 203]. HDAC inhibition was also demonstrated to disrupt the G1/S cell cycle transition by reactivating the Rb function and inhibiting the transcription factor E2F, blocking the gene transcription needed for the G1 progression [77, 204]. Furthermore, it was shown that treating leukemia cells with the

HDACi Vorinostat stimulated apoptosis in G0, G1, and S phases in the cell cycle [205]. HDACi FR901228 induced G1 and G2/M arrest in multiple cancer cell lines [206]. In addition, the role of HDACi in the cell cycle was shown to be dose-dependent, where a study showed that low doses of HDACi caused G1 arrest, whereas high doses stimulated G1 and G2/M arrests [207].

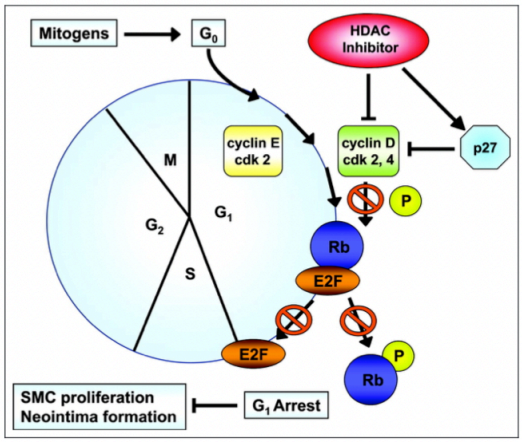

Figure (1.8) HDAC inhibition targets cell cycle progression. *HDAC inhibition thwarts cell cycle progression by directly inhibiting cyclin D1 or indirectly by stimulating p27. Disrupted activation of cyclin-CDK complexes inhibits mitogen-induced Rb phosphorylation and the subsequent activation of E2F-regulated genes, resulting in G1 arrest and diminished SMC proliferation. The image was reprinted after the publisher approved permission* [208].

c) HDAC inhibitors' effect on cancer stemness

A characteristic feature of tumors is their composition of a highly heterogeneous cell population, of which only a tiny subset of stem-like cells, known as CSCs, can self-renew and recapitulate tumors in vivo [170]. These CSCs are a significant clinical challenge as they are resistant to established cancer therapies and play central roles in chemotherapy resistance, metastasis, and tumor relapse [162]. Despite the significant evolution in cancer therapeutics, it has been challenging to develop CSC-targeted treatments. Such a challenge can be attributed to our limited understanding of CSC biology and its uniqueness. Each tumor comprises a hierarchy of cells, of which CSCs form the royal subset with the ability to self-renew indefinitely and recapitulate tumors in vivo [162]. The rest of the tumor bulk is mainly comprised of differentiated non-stem tumor cells that descend from CSCs but lack any stemness capability to regenerate

tumors; they are capable only of transient proliferation and, therefore, do not contribute to long-term tumor growth [209].

The hierarchical differentiation of CSCs to differentiated cells takes a long time and many cell cycles, yet interestingly, it is also reversible, which indicates the implication of the epigenomic factors, including histone modifications, to be involved in the regulation of the CSC phenotype transition. The past few years saw a whole new perspective in our understanding of the CSC model, which showed tremendous plasticity, where they have a high potential to move up and down the hierarchy of phenotypic differentiation regulated by the environmental niche rather than the older terminal differentiation notion [209, 210].

The classical CSC model established that the outcome of asymmetric cell divisions is another CSC or differentiated cell (transient amplifying cell). The more advanced CSC model has now established that there are neutral competition dynamics, where environmental niche signals determine the fate of the division process of CSCs to daughters [209]. Hence, CSCs can descend to one, two, or no daughter CSCs, depending on the available niche cues. More intriguingly, the number of CSC progeny is determined by the niche dimension, where daughter CSCs compete to colonize such niche that defines the number of the CSC progeny. Only cells loyal to the niche (remain in the niche) are specified as CSCs, whereas those that are hesitant (linger outside the niche) undergo differentiation [211, 212]. Additional features of the new CSC model include the observation that, in solid tumors, tumor progression occurs through the acquisition of more genetic alterations in the same signaling pathways that sustain the self-renewal of normal stem cells. This process has two outcomes. First, these mutations shift the CSCs to grow independently of niche signals, so more differentiated cells as the tumor evolves [209]. The second option is that the

liberated CSC phenotype inhibits differentiation, giving rise to a hierarchy with numerous CSCs and few non-CSCs [209].

The dysregulation of two classes of enzymes, HATs, and HDACs, is involved in the regulation of the CSC stemness properties by regulating vital signaling pathways essential in the maintenance of CSCs' niche fate [213]. It was shown that HDAC1 and HDAC7 are notably overexpressed in CSCs compared to non-stem tumor cells [185]. In addition, it was demonstrated that HDAC1 and HDAC7 are essential to sustain CSC properties and that overexpression of HDAC7 is sufficient to enrich the CSC phenotype [185]. Furthermore, HDAC7 overexpression in MCF7 cells was shown to upregulate 334 pro-metastatic or cancer stemness genes and was found to be responsible for driving gene alterations of CSC-related metabolic pathways [214]. Another study showed that HDAC1 and HDAC7 are targets for miR-34a, where HDAC1 and HDAC7 overexpression was implicated with increased cancer cell survival and therapy resistance via augmentation of stemness and inhibition of autophagic cell death in breast cancer [215]. It was also reported that the overexpression of HDAC 1, 7, and 8 in pancreatic ductal adenocarcinoma compared to non-tumor tissues and that patients with high HDAC 1, 7, or 8 expression levels showed significantly worse overall survival related to increased stemness phenotype [216].

Conversely, it was demonstrated that HDACi could induce selective death of the CSC subpopulation in NSCLC and colorectal cancer models [183, 217]. Similarly, HDACi abexinostat decreased the tumorphere formation ability and increased CSC differentiation in 16 genotypically different breast cancer cell lines [218]. In addition, downregulating HDACs 1, 7, and 8 was demonstrated to suppress EMT and inhibit CSC phenotypes, decrease therapy resistance, and inhibit the likelihood of metastasis in the pancreatic ductal adenocarcinoma [216].

Nevertheless, the mechanism by which HDACi influences cancer stemness is still poorly understood. The last few years have shown increased attempts to unravel these mechanisms owing to the tremendous effect HDACi has displayed in clinical and preclinical settings. For example, a class I- II HDAC inhibitor was reported to influence CSC by inhibiting TGF-β, Yap, and Notch signaling by double inhibiting cancer stemness genes SMAD4 and SMAD3 [219]. Another proposed mechanism is the depletion of nuclear depletion of YAP/TAZ, which are fundamental for inducing stemness, proliferation, and chemoresistance [220]. Furthermore, downregulating the transcription factor Notch1 downstream of TGF- β1 inhibition was reported as an outcome of HDACi treatment [221]. HDAC inhibition was also shown to inhibit Wnt pathway activation by induction of APCL, a negative regulator of β−catenin, after which the stemness genes *c-Jun*, *c-Myc*, *Cyclin D1*, and *CD44* were downregulated [222]. Despite that, the direct role and interactions governing HDACi activity remain obscure. Hence, further investigations are crucial for understanding the mechanisms by which each HDAC is involved in CSCs across different types of cancer. Such efforts will also necessitate the search for isoform-specific HDACi tailored to match the diverse pathways and conditions present in various malignancies.

d) HDAC inhibitor compounds

The extensive investigations that have been made on HDACs and their pivotal role in cancer accelerated the development of a promising new class for cancer therapeutics. Numerous synthetic and natural molecules that target classes I, II, and IV enzymes have already been developed and characterized; some have licensed FDA approval, and others are in clinical and subclinical trials.

HDACi recognition of HDACs is through binding to the Zn2+ ion located within the active site of HDACs, disrupting their enzymatic activity and thereby inhibiting their function. However, newer HDAC inhibitors have been designed to block not only the Zn2+ binding site but also the N-terminal binding site, as observed in class IIa HDAC inhibitors [90, 202, 223]. Based on chemical structures, HDACi are categorized into four groups: hydroxamates, benzamides, short-chain fatty acids, and cyclic peptides, illustrated by a table showing HDACi already under clinical investigation **(Table 1.5)**. Most of these molecules have been developed as cancer therapeutics with variable specificity, efficiency, pharmacokinetic and pharmacodynamic properties.

i. Hydroxamates

Hydroxamates comprise the first class to be introduced as HDACi. They are organic compounds containing the active group C(O)-N(R)-OH. Their carbonyl and *N*-hydroxy groups can interact with metals, including zinc. The hydroxamate group was called the zinc-binding group (ZBG). All Zn-dependent HDAC inhibitors share three standard features: First, a large hydrophobic moiety, a surface binding or cap group (cap), that binds near the HDAC enzyme's hydrophobic active site. Second is an aliphatic chain, typically consisting of five to six carbons (linker). Third, a functional zinc binding group that interacts with the zinc ion and disrupts the enzymatic activity of the HDAC enzyme. Many hydroxamate derivatives have been investigated in clinical trials; however, most were not licensed for inadequate trial design, low metabolic instability, poor bioavailability, and toxicity [224]. However, three pan HDACi from the hydroxamate class have been FDA-approved as drugs: vorinostat, panobinostat, and belinostat, even though they showed poor pharmacokinetics and unwanted effects [77]. Vorinostat (SAHA)

was the first HDAC approved by the FDA to treat patients with cutaneous T-cell lymphoma (CTCL). Preclinical studies have demonstrated that SAHA stimulates apoptosis and cell-cycle arrest and inhibits the CSC stemness and metastatic potential of cancer cells [200]. Also, belinostat (Beleodaq/PXD101) and panobinostat (LBH-589) were granted FDA approval to treat peripheral T-cell lymphomas (PTCL) [225]and multiple myeloma [226], respectively. These drugs are also under study in combination therapies for solid tumors [227].

ii. Cyclic tetrapeptides

This is a natural class of HDACi with selective preferential towards class I HDAC selective, specifically HDAC1 and 2. The only clinically investigated and approved is Romidepsin, which is a prodrug; upon uptake by the cell, it is reduced by glutathione into a monocyclic dithiol. Reduced disulfide bond enables a free thiol group to bind to the zinc ion in the HDACs, blocking the active site. Romidepsin showed antitumor efficacy in multiple cancer models and was approved for treating CTCL and PTCL [77, 228].

iii. Benzamides

This class of HDACs is structurally different from other HDACi; the aminobenzamide ring chelates the zinc ion to render more specificity towards Class I HDAC. An example of this class is Mocetinostat, currently in phase II clinical trial for relapsed classical Hodgkin's lymphoma (NCT00358982) [229]. Also, other drugs of the same class showed antiproliferative activity at micromolar concentrations against A549 and SF268 cancer cell lines by interacting with EGFR mRNA and protein expression [230].

iv. Short-chain fatty acids

Valproic acid is a known example of the short-chain fatty acids class of HDACs. They show selectivity towards Class I and II HDACs. However, they are relatively weak HDACi compared to hydroxamic acid or cyclic peptide-based agents. Studies on Valproic acid showed that it induces differentiation of CSCs in acute myeloid leukemia patients [231]. In addition, it demonstrated efficacy in inhibiting the overall tumor growth and metastasis formation in animal models [231].

HDAC INHIBITOR	SPECIFICITY	CANCER TYPES	CLINICAL TRIAL	REFERENCES
		HYDROXAMIC ACID		
VORINOSTAT (SAHA)	Classes I, II, and IV	CTCL	FDA approved in 2006	[232]
BELINOSTAT (BELEODAQ/PXD101)	Classes I, II, and IV	PTCL	FDA approved in 2014	[225]
PANOBINOSTAT (LBH-589)	Classes I, II, and IV	MM	FDA approved in 2015	[226]
RESMINOSTAT (4SC-201)	Classes I and II	Advanced colorectal and hepatocellular carcinoma; HL	Phase II trial	[233, 234]
GIVINOSTAT (ITF2357)	Classes I and II	CLL; MM; HL	Phase II trial	[235, 236]
PRACINOSTAT (SB939)	Classes I, II, and IV	AML	Phase II trial	[237]

ABEXINOSTAT (PCI-24781)	Classes I and II	Metastatic solid tumors; HL; non-HL; CLL	Phase I trial	[192, 238]
QUISINOSTAT (JNJ-26481585)	Class I and II HDACs	Advanced solid tumor; lymphoma; CTCL	Phase I and II trial	[239]
MPT0E028	HDAC1, 2, 6	Advanced solid tumor	Phase I trial	[191]
CHR-3996	Class I	Solid tumor	Phase I trial	[240]
CUDC-101	Classes I and II HDAC, EGFR, HER2	Solid tumor	Phase I trial	[241]
CUDC-907	Classes I and II HDAC, PI3K	MM; lymphoma; solid tumor	Phase I trial	[242]
	BENZAMIDES			
ENTINOSTAT (MS-275)	Class I	Solid and hematological malignancies	Phase I and II trial	[199]
MOCETINOSTAT (MGCD0103)	Class I and IV	Solid and hematological malignancies	Phase I and II trial	[229]
TACEDINALINE (CI-994)	Class I	MM; lung and pancreatic cancer	Phase II and III trial	[198]
RICOLINOSTAT (ACY-1215)	HDAC6	MM; lymphoma	Phase I and II trial	[189]
CHIDAMIDE (CS055/HBI-8000)	HDAC1, 2, 3, and 10	Breast cancer; NSCLC	Phase II and III trial	[196, 197]

CYCLIC PEPTIDES				
ROMIDEPSIN (DEPSIPEPTIDE/FK228)	Class I	CTCL; PTCL	FDA approved in 2009 and 2011	[190]
ALIPHATIC FATTY ACIDS				
VALPROIC ACID (VPA)	Class I and II	Solid and hematological malignancies	Phase I and II trial	[195]
PHENYLBUTYRATE	Classes I and II	Solid and hematological malignancies	Phase I and II trial	[243]
AR-42	Class I and IIb	AML	Phase I trial	[194]
PIVANEX (AN-9)	Classes I and II	NSCLC; myeloma; CLL	Phase II trial	[188]

Table 1.5. HDACi currently approved or under clinical phase trials. *Adapted and reprinted after the publisher approved permission [77]*

e) Class IIa-specific HDACi

The unique regulatory domain for class IIa HDAC and its specific epigenetic "reader" function made it an appealing target for HDACi, specifically for class IIa HDACs. A high-throughput screen discovered the trifluoromethyl oxadiazole (TMFO) derivatives as inhibitors selective for class IIa HDACs [244]. TMP269, a TMFO derivative, was shown to stimulate apoptosis by activating ER stress signaling and enhance the tumor response to the chemotherapeutics, tunicamycin or carfilzomib in multiple myeloma [244] More recently, it was shown that TMP269 treatment showed anti-tumor proliferative effects and induced additive apoptotic effects when used

in combination with the chemotherapy Venetoclax in Acute myeloid leukemia [245]. Besides TMP269, another class IIa HDAC that gained interest is MC1568, which significantly enhanced apoptosis and drove G2/M arrest in pancreatic cancer cells [246]. It was also shown that the combination treatment of MC1568 with simvastatin led to synergistic induction of p27 expression and increased the antiproliferative effect in colorectal cancer cells [247]. Furthermore, MC1568 potentiated the cytotoxicity in gastric cancer cells when combined with docetaxel [248].

f) Novel approaches: HDAC-specific PROTAC

With the established role HDACs play in regulating cancer and the high number of HDAC small molecule inhibitors in clinical trials, new innovative therapies using advanced approaches have also been investigated to give additional hope in combatting cancer with this promising class of therapeutics. In the last few years, the proteolysis-targeting chimera (PROTAC) technology has gained attention as its unique mechanism of action extends hope for innovation in targeted cancer therapeutics. PROTAC protein degraders add additional specificity owing to their potential to therapeutically modulate proteins that are challenging to target with conventional small molecules [249].

PROTACs are heterobifunctional small molecules comprised of two ligands joined by a linker; one ligand recruits and binds the targeting protein of interest, while the other recruits and binds an E3 ubiquitin ligase. The double protein binding of the target protein and ligase by the PROTAC stimulates ubiquitylation of the targeting protein and its subsequent degradation by the ubiquitin-proteasome complex; after the degradation of the targeted protein, the PROTAC complex is recycled to target another copy of the targeted protein [249].

Compared to the classical small molecule HDACi, HDAC-PROTAC offers several advantages. The enhanced specificity of HDAC-PROTAC for a specific HDAC isoform overcomes the broad spectrum pan inhibition notion for the HDACi already in clinical trials. All HDACi under clinical investigation inhibit several HDAC isoforms and are, at best, class-selective [250]. HDAC-PROTAC usually copies the HDAC isoform inhibition profile of its parent HDACi [251]. The added benefits for HDAC-PROTACs above their parent HDACi include their mode of action, where they act catalytically [249]. Accordingly, a much lower drug load is needed. In addition, via targeted degradation,

HDAC-PROTAC exhibits a more sustained inhibition than their parent HDACi [251]. While an HDAC-PROTAC targeting class IIa HDACs induces the degradation of the HDAC enzyme and interrupts their downstream signal pathways [252], HDAC-PROTAC can additionally be designed in a way to target the regulatory function which is independent of the deacetylase activity of these HDAC, which are poor deacetylating agents [74]. Taken together, the HDAC-PROTAC technology enables tremendous therapeutic benefits, which have great potential as a therapeutic approach to malignancies. The first group that reported this innovative strategy observed collateral loss of HDAC proteome complexes using the HDAC-PROTAC [251].

g) Novel approaches: RNAi-dependent-HDACi

Gene therapy has paved its way as a promising therapeutic strategy. It presents high selectivity for its specific targeting of disease-causing genes in a sequence-specific manner, which enables a more personalized approach to combatting life-threatening diseases, including cancer [253]. Via orienting a specific nucleic acid change in the targeted gene, gene expression can be downregulated, upregulated, or fixed. Gene therapy molecules clinically investigated for inhibiting

gene expression include small interfering RNA (siRNA), microRNA (miRNA), and inhibitory antisense oligonucleotides (ASOs) [254]. Conversely, molecules aimed at inducing increased or corrected gene expression include plasmid DNA, messenger RNA (mRNA), small activating RNA (saRNA), and CRISPR/Cas. [255].

RNA interference (RNAi) is a known biological protective mechanism by which the genome guards against outward invasion. Since their outstanding discovery, it has been proposed that they can silence any disease-related genes in a sequence-specific fashion, which puts small interfering RNA (siRNA) on the promising therapeutic horizon. More than two decades after its discovery by the Nobel Prize winner Craig Mellow [256], four FDA-approved siRNA therapeutics exist and demonstrate safety and efficacy in inhibiting their disease targets. GIVLAARI™ (givosiran) and ONPATTRO® (patisiran) are two siRNA therapeutics for Alnylam Pharmaceuticals that patients safely and effectively use. From the pharmaceutical standpoint, siRNA therapy has set up an unprecedented milestone among valid therapeutics, as it has indeed paved the road to a novel approach to treating and managing human diseases.

Despite the high potential, RNAi therapeutics face some challenges in the systemic administration [257]. For example, the nuclease degradation and short-lived circulation of the siRNA. Stability against degradation was successfully circumvented by incorporating chemical modifications in the siRNA sequence [258]. Utilizing the enhanced stabilization chemistry approach (ESC) introduced four chemical modifications at the 5′-end of the antisense strand and the 3′-end of the sense strand. These changes significantly improved siRNA potency and pharmacodynamics in the circulation by evading degradation by nucleases [259].

Adequate accumulation in target tissue is another problem that faces the siRNA therapeutics. In blood circulation, unspecific binding and glomerular filtration inhibit siRNA accumulation in target tissues. In addition, the relatively small size of the siRNA molecule (~7-8 nm in length and 2-3 nm in diameter) makes it easily filtered into the urine and excreted out from the body quickly, within a few minutes to half an hour, which prevents them from accumulating in targeted tissues or cells [257]. However, adequate accumulation in the liver was the fastest to achieve by the siRNA-loaded nano-formulations using ionizable lipid nanoparticles (iLNPs) that predominantly accumulate in the liver by interacting with serum lipoproteins [260]. Furthermore, the innovation of the ligand–siRNA conjugation strategy introduced tissue specificity and accumulation in target tissues, hampered undesired side effects and toxicity, and achieved potent gene silencing at a low dosage [261]. The ligand–siRNA conjugation strategy's specific recognition was achieved by several ligands, including carbohydrates, peptides, antibodies, aptamers, and small molecules, that can recognize and bind to the surface receptor of the target tissue [261].

Another challenge for the siRNA therapeutic is the adequate transmembrane trafficking [257]. The relatively high molecular weight (~14 kD) and the total negative charge constrain siRNA from crossing the cell membrane [257]. Then, the idea of utilizing carriers to achieve efficient transmembrane delivery was introduced. Cationic cell-penetrating peptides can facilitate the interaction between the siRNA guanidinium groups and the negative phosphates, sulfates, and carboxylates on the cell membrane surface [254]. This interaction showed cell membrane pore formation, resulting in the cellular uptake of siRNA. Another approach was also introduced by using positively charged lipids or polymers that can neutralize the negative charge of the siRNA and facilitate its membrane uptake via an adsorptive pinocytosis [254].

Achieving intracellular trafficking of siRNA in vivo requires escaping endosomes and lysosomes for cytoplasmic release and loading into RISC. Ideally, the siRNA delivery complex should release its contents from the acidic endosomal compartment, avoiding lysosomal degradation [261, 262]. Proper delivery ensures uptake via endocytosis, confining the siRNA complex within endosomes for recycling or degradation. pH adaptation is crucial for preventing siRNA degradation, with many systems employing pH-responsive mechanisms. These systems utilize a positively charged delivery complex to increase endosomal or lysosomal osmotic pressure, facilitating membrane disruption and siRNA release into the cytoplasm [261, 262]. Increasing the efficiency of the cytoplasmic release is still under rigorous investigation. Recently, a novel approach has been innovated to enhance liposomal evasion and cytosolic release [263]. Qui *et al*. developed novel endoplasmic reticulum (ER) membrane-modified hybrid nanoplexes (EhCv/siRNA NPs) that showed much improved RNAi activity systemically [263]. They employ the endosome–Golgi–ER pathway instead of the endosome–lysosome pathway for trafficking, thereby avoiding the lysosomal degradation of siRNA. In addition, electroporation was offered as an alternative to enable siRNA to cross the cell membrane directly, presenting an effective strategy to bypass liposomal evasion [264].

Thus far, four RNAi therapeutics, GIVLAARI™ (givosiran), ONPATTRO® (patisiran), OXLUMO® (lumasiran), and LEQVIO® (inclisiran), have been sanctioned for commercial therapeutic usage. Furthermore, at least seven siRNA-dependent therapeutics are undergoing phase-3 clinical studies, with more candidates in preclinical settings targeting various diseases, including cancer, utilizing multiple delivery systems and ample drug pipelines [254].

The development of new drugs and the pipeline of therapeutics is undeniably challenging. However, the discovery of RNAi has revolutionized cancer drug design, offering relatively rapid approaches. Moreover, the array of FDA-approved nanoparticles made from polymers and lipids designed for RNAi drug delivery provides promising prospects for the efficacy and safety of small interfering RNA (siRNA) therapeutics in cancer treatment. Combining an HDAC inhibitor with an RNAi targeting strategy to yield long-sought isoform-specific HDAC inhibitors may herald a new era in treating numerous cancers where individual HDACs play a significant role. While the potential of HDAC inhibitors is remarkable, translating these advancements to clinical use will necessitate the innovative design of novel, potent, and isoform-specific HDAC inhibitors that maximize efficacy while minimizing side effects.

IV. Glioblastoma Multiform as a disease model.

a. Introduction to GBM

Glioblastoma (GBM) is the most common and aggressive high-grade malignant primary brain tumor with an abysmal prognosis. It most commonly erupts in the frontal lobe, followed by the temporal, parietal, and occipital lobes, as reported by the American Brain Tumor Association®. The tumor comprises various cell types (including abnormal astrocytic cells and blood vessels) and areas of dead cells (necrosis). GBM is inherently invasive to different regions of the brain. It can also sometimes disseminate to the other half of the brain through the corpus callosum or the ventricular system [265].

There has been a significant expansion for GBM genotyping in the new WHO classification. The expansion of multi-omics techniques and machine learning strategies are creating milestones toward more accurate determination of GBM prognoses and predictive responses to treatments [266]. In 2017, the formation of cIMPACT-NOW (Consortium to Inform Molecular and Practical Approaches to Central Nervous System (CNS) Tumor Taxonomy) was announced to evaluate and recommend changes to the WHO classification of brain tumors [267]. Also, the rigorous GBM research and the discovery of new mutations and targets in GBM opens the prospect of creating unexplored drugs with new potential for such a deadly disease.

GBM is now defined as Astrocytoma IDH-wildtype tumors with one or more of the following: microvascular proliferation, necrosis, *EGFR* gene amplification, *TERT* promoter mutation, or combined copy number variations of gain of chromosome 7 and loss of chromosome 10 [268]. Currently, there are no curative treatment options for GBM. Despite the revolutionary advancement in cancer research and the innovation of novel cancer therapies, the outcome for patients remains almost universally lethal. Median overall survival is 15 months after diagnosis, and the 5-year survival is 5%, which is the lowest long-term survival rate for brain tumors [268].

There is a significant challenge in treating GBM. The failure of GBM treatment can be attributed to several factors, but on top of them is the presence of a population of stem-like cells known as glioblastoma stem cells (GSCs) [269]. These cells have the ability to self-renew, indefinitely proliferate, and differentiate into various cell types, thereby recapitulating the entire tumor invivo [270]. GSCs tend to migrate into the adjacent normal brain tissues and along the vasculature, which causes failure of complete surgical resection and limits the success of radiotherapy [271]. The treatment failure is also attributed to the blood-brain barrier (BBB) that

prevents many treatments from locally approaching the tumor. Furthermore, GBM is heterogeneous among patients (inter-tumoral heterogeneity). It can also change over time within the same patient (intra-tumoral heterogeneity), adding a poorer prognosis of the disease and making it more resistant to the treatment [272].

GBM has been subdivided into different subtypes to categorize its diverse phenotypes, predict the treatment response, and offer a more reliable prognosis [273]. Initial genomic and transcriptomic profiling for the GBM landscape established from bulk RNA sequencing experiments has classified GBM into four subtypes (classical, mesenchymal, proneural, and neural) [274]. These subtypes are mainly distinguished by the expression levels of specific gene sets and known GBM mutations, and these subtypes showed different sensitivity to drug treatment [274]. The recent update for GBM classification helped narrow down the formerly designated profiles into only three main subtypes (proneural, classical, and mesenchymal), excluding the neuronal subtype for the more likely neuronal lineage contamination [275].

The plasticity and intra-conversion among different GBM subtypes during GBM progression and recurrence were reported [275]. In addition, single-cell RNA- seq (scRNA-seq) experiments revealed that the GBM tumor exhibits substantial gene expression profile differences among the different cell states within the same tumor regarding the cell cycle, hypoxia, the immune response, and oligodendrocyte function [276]. Intriguingly, the three cell states' genomic profiles were also reported in diffuse midline gliomas (pediatric gliomas), underscoring their importance [277].

GBM cell identity is highly dynamic, and reversible plasticity between the various cell states is ubiquitous and tends to be patient-specific. Current therapeutic intervention options result in complex transformations in the GBM landscape, further adding to its heterogeneity [276]. A

single oncogene does not drive GBM but can result from many different mutations. The most commonly mutated genes in GBM patients include TP*53*, *EGFR*, *ATRX*, *TERT*, *IDH1-wild type*, *PTEN*, and *MDM2* [278].

GBM inherently lacks immune support, and that returns to the brain being regarded as an immune-quiescent site with limited access; that is why the T cells' immunogenic functions are lacking in the brain. The immune deficiency of the brain returns to the safeguard BBB, lack of dedicated lymphatic channels, the low expression level of Major Histocompatibility Complex (MHC) class II molecules, lack of antigen-presenting cells (APC), and the inherent expression of immunosuppressive cytokines such as TGF-β [279]. That explains the high level of TGF-β in intracranial gliomas in in-vivo models, causing the accumulation of Tregs and immature dendritic cells, making an immunosuppressive feedback loop. This environment counters the priming of T cells and ultimately impairs the anti-tumor immune response [280].

However, advanced research has improved our understanding of immune reactions in the CNS. A classical lymphatic system exists in the CNS through a circulation across the cerebrospinal fluid [280]. Accordingly, antigen-presentation cells and T and B lymphocyte priming happen at the deep cervical lymph nodes, indicating the existence of adequate immune responses in the CNS [280]. However, these immune mechanisms shift in the GBM, consistent with low CD4+ T cell counts, correlate with poor outcomes in GBM patients receiving the standard therapy [281]. In addition, the infiltration of CD8+ T cells in newly diagnosed GBM patients is linked to enhanced patient survival [282]. The GBM micro-environment adds more intertumoral heterogeneity, especially regarding the distinct populations of immune cells. Significant differences were found in the overall number of T cells and the contribution to different T cell states per patient. In

addition, the number of CD8+ T cells and Natural Killer (NK) cells differ significantly between patient subsets [283].

Typically, microglia comprise ~ 10% of CNS cells, which regulates the normal quiescent phenotype in the healthy CNS, expressing low levels of MHC molecules and the priming conditions [284]. However, in the presence of an immunogen, the peripheral immune cells access the CNS and orchestrate immune responses; functioning microglia stimulate MHC II molecules and costimulatory molecules and present antigens to activated T cells [280, 284]. These findings support the notion that the CNS should be regarded as a unique immune environment rather than an immune-deficient site and provide the foundation for opportunities to develop targeting immunotherapy for GBM [285].

b. Molecular basis of GBM

Recent advancements in genomic techniques have enhanced our knowledge of the critical molecular changes that trigger or aggravate GBM. Some molecular markers were shown to carry prognostic and predictive information, increase tumor progression, and present a new hope for targeted therapies. For instance, *ATRX* gene mutation (a-thalassemia/mental-retardation-syndrome-X-linked) is a biomarker for GBM[286]. The *ATRX* gene encodes the ATRX chromatin-remodeling protein, which works with DAXX to chaperone histone H3.3 to the heterochromatin [287, 288]. *ATRX* mutations exist in more than half of the relapsed GBM [268]. In a prospective study, losing ATRX expression was linked to a better prognosis than those with higher ATRX expression [289]. Another crucial biomarker is *TP53* (Tumor protein P53) gene mutation. The functional p53 protein regulates proliferation, survival, genome integrity, and other cellular functions. The presence of *TP53* inactivation mutations is linked with the progression of GBM, as

well as increased invasiveness, decreased cell apoptosis, increased proliferation, worse overall patient survival, and chemotherapy resistance, including temozolomide by increasing MGMT expression [290, 291]. Also, the GBM biomarker *EGFR* (epidermal growth factor receptor) gene mutation encodes a receptor with tyrosine kinase activity activated by EGF (epidermal growth factor) [292]. EGFR protein promotes cell proliferation by activating the MAPK and PI3K-Akt pathways [292]. The *EGFR* gene amplification was reported in 50-60% of GBM cases and has been associated with poor prognoses [293]. Also, *MGMT* (O6-methylguanine DNA methyltransferase) mutation indicates a GBM prognosis. The *MGMT* gene encodes the MGMT protein responsible for DNA repair, removing an alkyl group from the DNA alkylation site O6 position of guanine. MGMT promoter methylation positively predicts a better overall survival [294, 295]. The standard of care chemotherapeutic, Temozolomide, works by mimicking MGMT function and methylates DNA at the N7 and O6 atoms for guanine and N3 for adenine. Identifying the MGMT promoter methylation status is crucial to identify patients who might benefit and who might not from Temozolomide in the combinational therapy of newly diagnosed GBM, which would pave the way towards more tailored therapies, overcoming drug resistance and refractory GBM [294, 296].

Furthermore, *TERT* (Telomerase Reverse Transcriptase) promoter mutation has been excessively reported in GBM tumor tissues. The *TERT* gene encodes telomerase enzyme protein, an enzyme that adds the missing 3′ end of a DNA strand during replication. After serial cell divisions, once telomere length has reached a specific size (the Hayflick limit), normal cells should undergo irreversible cell cycle arrest, referred to as senescence [297]. Senescence physically prevents additional cell proliferation and DNA replication, safeguarding cells from genetic mutations and chromosome rearrangements, which could result in oncogenesis [298]. Telomerase

prevents telomere loss by stabilizing and elongating telomeres by adding the telomere repeat of TTAGGG to the 3′ ends of human chromosomes [299]. The mutation of the *TERT* gene promoter results in increased telomerase activity and telomere elongation, increasing TERT expression to a fourfold increase [300]. Although *pTERT* mutations are present in up to 80% of GBM [301], the role of p*TERT* mutation as a prognostic factor is still being studied under the heterogeneous co-occurring factors from other mutation biomarkers of *IDH*, *EGFR* mutations, and *MGMT* methylation status [302].

c. Glioblastoma stem cells as the main drive of GBM pathology.

While the exact origin of GBM remains controversial, the expansion in genomic sequencing, particularly scRNA-seq data, expanded our knowledge of specific niches, cellular hierarchies, and transcriptional programs in GBM tumors [303]. The presence of GSCs as the central seed for GBM tumors is now a matter of fact; however, their evolution and plasticity during tumor development remain an active research area. GSCs have been linked to therapy tolerance, and their role in building and communicating with the tumor microenvironment has direct implications for the relevance and success of any targeting therapy [276]. The cell of origin for a tumor refers to the normal cell that receives the initial cancer-promoting genetic hit(s) and responds by initiating a transformation. Thus, which normal brain cell received the first transforming hit requires understanding the hierarchy of cell lineages in the CNS.

The primary progenitor stem cells in the brain are the neural stem cells (NSC), which are quiescent cells that exhibit indefinite self-renewal capability and multipotentiality to proliferate into a hierarchy of progenitor cells that have the less self-renewal capability and are fated to differentiate into various cell types. NSCs give rise to multipotent progenitors (MPPs) that give rise to all CNS cell types [211, 304, 305]. NSCs can differentiate into bipotential progenitors

(BPP), such as *Ascl1* progenitors, that give rise to both adult oligodendrocyte progenitor cells (OPCs) and neural progenitor cells (NPCs). Unipotent progenitors (UPP) differentiate into oligodendrocytes, neurons, or astrocytes [211, 304, 305]. However, the hierarchical relationship between these progenitors still needs to be clarified. Experiments using conditional inducible mutations and known GBM driver mutations showed that all these progenitors can transform to GSC and give rise to GBM **(Figure 1.9)**. Whether each cell of origin is susceptible to specific mutations is still being investigated.

Many studies suggest that stem cells and progenitors are widely vulnerable to various mutations [306]. It was proposed that specific cell types may display preferential susceptibility to certain mutations and that particular cell of origin-mutation assortments lead to specific genetic and epigenetic signatures, which might shape the various GBM genotypes and the inter-tumoral heterogeneity [304]. Indeed, the relentless pursuit of global research continues each day, bringing us closer to understanding the precise origin of GBM tumors. This ongoing effort holds the promise of unlocking new avenues for targeted therapies, offering hope for improved treatment outcomes, and ultimately enhancing the quality of life for patients affected by this devastating disease.

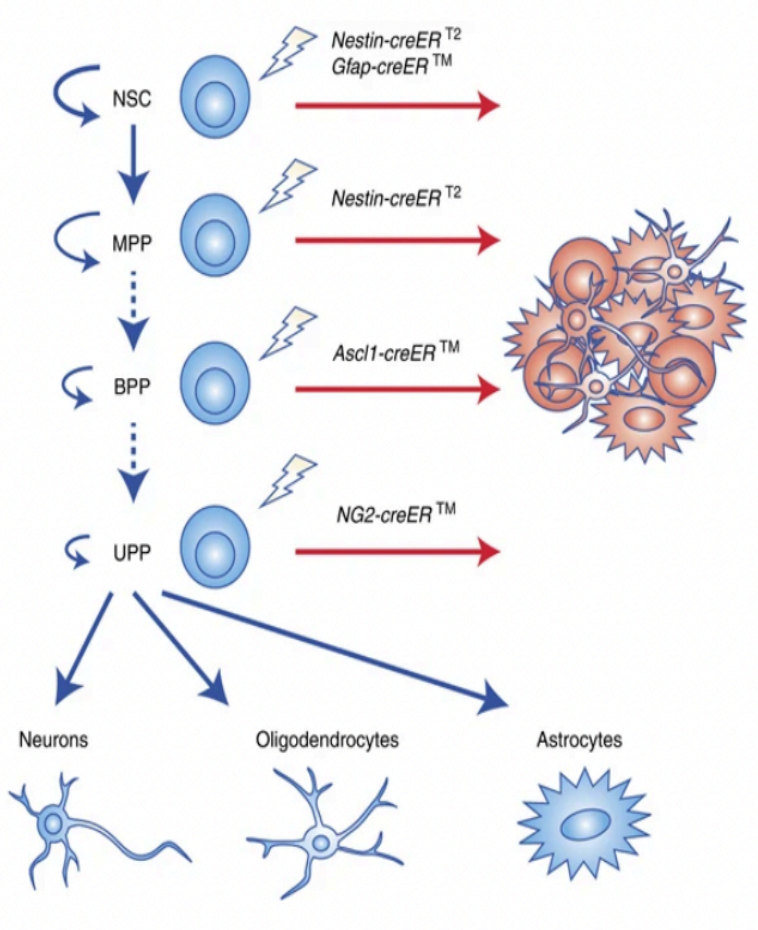

Figure 1.9 Lineage hierarchy of GBM-cell of origination.

The multipotentiality of NSCs gives rise to multiple cell progenitors with the likelihood of transforming any cell populations to GSCs to recapitulate the GBM tumor with exposure to conditional inducible mutations and known GBM driver mutations. Multipotent progenitors (MPPs) give rise to all CNS cell types. NSCs differentiate into bipotential progenitors (BPP) that give rise to both adult oligodendrocyte progenitor cells (OPCs) and neural progenitor cells (NPCs). Unipotent progenitors (UPP) differentiate into oligodendrocytes, neurons, or astrocytes. Dashed lines denote that the hierarchical relationship between different progenitors is still undefined. Picture reprinted from [304] *(reprinting was allowed without additional permission from the publisher)*

d. Inter- and Intra-tumoral heterogeneity of GSCs

The recent comprehensive understanding of inter-tumoral heterogeneity in GBM is seen as an outcome of genetic and epigenetic alterations, along with gene signature profiles resulting from variances in the cell of origin [304]. Such intertumoral heterogeneity needs to be crucially considered when making therapeutic decisions. Subgroup-specific therapeutic designs must be enforced based on the final biological phenotype, which takes in consideration the GBM heterogeneity. For instance, treatment of IDH mutant glioma with an epigenetic modifier was shown to restore insulator function and downregulate the prominent glioma oncogene, the receptor tyrosine kinase gene *PDGFRA* [307]. In contrast, using DNA alkylating temozolomide in such

IDH wild-type GBM may require revision, as it generates a relapsed hypermutated phenotype [269].

Heterogeneous tumor marker gene expression patterns and uneven cellular distribution of genetic alterations were seen in genomic studies and even in earlier immunohistochemistry and pathological studies [276, 308]. Advancements in genomic sequencing techniques have revealed how multiple clones harboring various genetic alterations coexist within the same tumor. Moreover, segregating clones based on genetic signature has unraveled a side of the tumor development process [275]. The paradigm for clonal evolution posits that tumor formation is initiated in a cell of origin and is followed by the accumulation of single or multiple somatic genetic alterations, driving more complex heterogeneity and providing the tumor with survival mechanisms [304]. Cells harboring similar genetic alterations tend to aggregate, yet their invasive nature results in clonal mixing and brain infiltration. Invading tumor cells penetrate the normal brain parenchyma, contributing to further heterogeneity; these infiltrated cells are the clones likely to evade surgical removal. Referred to as the "invasive niche" or "surgery-flee clones", they migrate along vasculature and white matter tracts, utilizing cadherins and integrins to navigate the extracellular matrix [304].

Two further environmental niches add further heterogeneity at the cellular level within the same tumor. Hypoxic and necrotic niches are a hallmark of GBM and provide GSCs with mechanisms for maintenance, proliferation, as well as drug resistance. Clones residing in the hypoxic niche develop survival mechanisms under nutrient-deficient conditions, promoting shifts towards aerobic glycolysis and glutamine-mediated fatty acid production [305, 309]. This leads to the enrichment of therapy-resistant cell populations. [305, 309].

The perivascular niche serves as the third reported niche, facilitating paracrine signaling among tumor clone cells (inter-clonal communication) or between tumor clone cells and immune cells (inflammatory niche). Within this niche, crucial cues are provided for maintaining GSCs' stemness and inducing the enrichment of pathways necessary for migration and DNA repair [310]. For instance, proximity to the endothelial cells supports GSCs' stemness phenotype through NOTCH and nitric oxide signaling pathways, among many others. In contrast, tumor cell clones, such as tumor-associated macrophages, reside in the perivascular and secrete pro-tumorigenic chemokines that induce GSCs' growth and proliferation [310, 311]. A schematic representation of all these cross-talking niches is illustrated in (**Figure 1.10**).

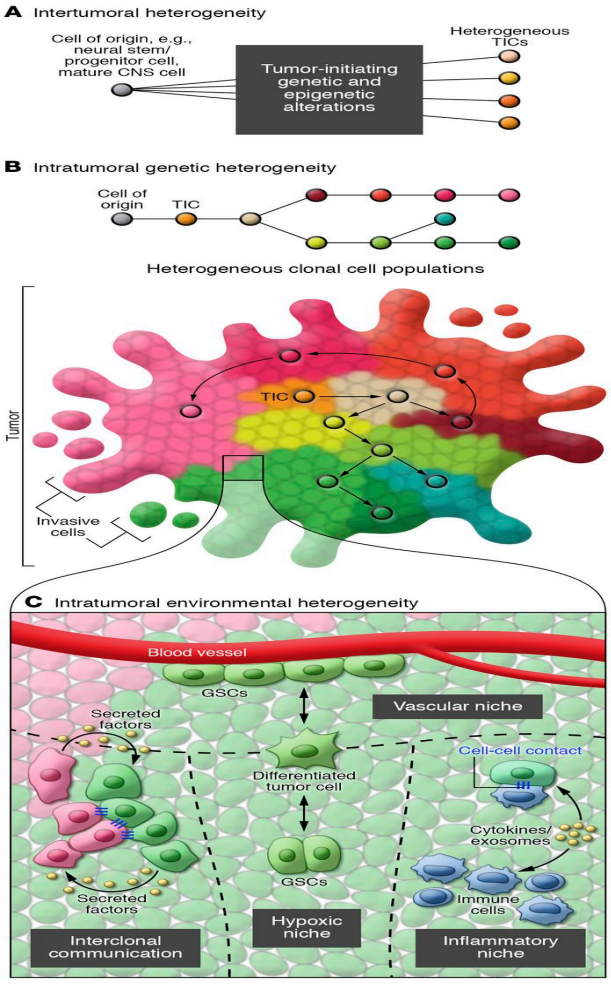

Figure 1.10 The complexity of inter- and intra-tumoral heterogeneity in GBM.

Inter- and intra-heterogeneity between different patient populations arises from the cell of origin and the subsequent significant epigenetic and genetic shifts. ***A****. Such derivatization generates diverse clones of tumor-initiating cells (TICs) or GSCs.* ***B****. TICs expand, adding more heterogeneity to the clonal cell populations as they divide, owing to more genetic and epigenetic alterations. Cells with similar genetic alterations exist nearby, but their invasive properties will cause clonal mixing and invasion into normal brain tissue.* ***C****. Environmental factors add additional heterogeneity at the cellular level. Three niches were identified: the hypoxic niche, the invasive niche, and the perivascular niche from the tumor cell-to-cell communication or tumor cell-to-immune cell communication. Picture reprinted after the publisher approved permission* [272]

e. Epigenetic regulation in GBM

Epigenetic regulation plays a vital role in the development, progression, and prognosis of GBM [162, 276, 312]. A tumor cell's epigenetic and genetic landscape can determine its association with the different cell states denoted by its global chromatin accessibility [276]. The epigenetic modification of enhancer regions drives the aggressive phenotype of the GSCs subtypes in addition to the active promoters being significantly common among GBM patients, as shown by Chromatin Immunoprecipitation followed by sequencing (ChIP-seq) experiments [312]. A recent single-cell multi-omics study unraveled the significant difference in chromatin topography between primary versus recurrent tumors [313]. Relapsed tumors shifted to the more aggressive mesenchymal subtype and increased open chromatin peaks belonging to components of crucial signaling pathways in the GBM [313]. In addition, single-cell assay for transposase-accessible chromatin sequencing (scATAC-seq) experiments revealed three epigenetically distinct populations of GSCs across GBM patients; each population shows a unique signature of epigenetically activated transcription factors [314, 315].

Epigenetic abnormalities are now regarded as prognostic markers and can be used as a means for personalized therapy for matching GBM patients' subgroups and as predictive to patients' survival [314, 316]. In addition, prediction models for specific DNA cytosine methylation patterns provide a high degree of accuracy for the overall survival of GBM patients from TCGA datasets [317]. More comprehensively, the gene expression patterns correlate with epigenetic mark depositions in the transcription start site (TSS) regions in distinct grades of the gliomas [318]. PTM of histones impact chromatin accessibility and have a higher say in activating or repressing gene expression in the GBM [48]. For instance, H3K9me3 and H3K27me3 are hallmarks of condensed heterochromatin and gene silencing in the GBM [133, 155]. In contrast, acetylation of

histone lysine residues, H3K4, H3K79, and H3K36, are typically associated with active chromatin [49]. In addition, Histone H3 acetylation and H3K4me1 marks distant to promoter regions have been related to functional enhancers in different GBM cell types [319]. The interplay between the chromatin organization and various epigenetic mechanisms provides a fine-tuned regulation of gene expression, which has roles in developing or progressing the GBM tumor [312]

*f. T*he histone variant H3.3 in adult and pediatric high-grade gliomas

The human histone H3 family comprises histones: H3.1 and H3.2, known as "canonical histones", H3.3, and the centromere-specific variant CENP-A, known as "histone variants" [120]. The variant H3.3 can operate like its counterpart canonical H3 as a core component of the nucleosome, but in addition it is also deposited into transcriptionally active regions to replace displaced nucleosomes at any point of the cell cycle [320]. Thus, H3.3 is deposited in a replication-independent manner in contrast to the canonical histones, which are deposited in a replication-dependent manner [114]. Moreover, H3.3 is deposited into regions associated with actively transcribed genes in euchromatin in addition to relatively silent regions, such as telomeres and pericentric heterochromatin [121]. Thus, H3.3 is found in the genomic areas enriched for either the euchromatin as H3K4me3 or heterochromatin as H3K27me3 and H3K9me3 [114].

Two major histone chaperone complexes have been identified to be accountable for H3.3 deposition in the nucleosome. Histone regulator A (HIRA), which deposits H3.3 into euchromatic regions in a replication-independent manner, and the death-associated protein (DAXX)/ a-thalassemia X-linked mental retardation protein (ATRX) complex, which deposits H3.3 into pericentromeric and telomeric heterochromatin regions [288, 320]. Consistent with that, the loss

of H3.3 and disruption of the ATRX/DAXX complex was shown to cause the loss of the heterochromatin mark H3K9me3 at some genomic regions [288]. Similarly, the markdown of H3K9me3 was also seen at telomeres in DAXX knockout cells [321]. It was proposed that the ADD domain of ATRX physically interacts with H3K9me3, which presumably induces the chaperoning of ATRX/DAXX/H3.3 [288]. DAXX can then interact with the methyl transferases SETDB1 or SUV39H, both of which catalyze the tri-methylation of H3K9. Subsequently, ATRX/DAXX can target heterochromatin for deposition of H3.3 and recruit more methyltransferases to mediate direct modification of K9me3 on H3.3 [288]. As crucial in the genomic stability as they could be, the loss of ATRX results in chromosomal segregation errors during embryogenesis [322]. Moreover, ATRX and DAXX have been reported to be mutated in cancers, including brain tumors and other cancer types, which makes this complex an appealing target to explore for cancer [286, 323].

On the other hand, HIRA was found to be involved in depositing histone H3.3 into distinct genomic regions, including active promoters, enhancers, and gene bodies[324]. Still, their mechanism of deposition needs to be better understood. One study showed that the single-stranded DNA binding protein (RPA) acts as a regulator that physically interacts with HIRA to form the RPA/HIRA/H3.3 complex [325]. This complex could be driving the deposition of gene regulatory elements [325]. However, how HIRA is recruited to gene regulatory elements to deposit H3.3 in the euchromatin regions of transcriptionally active genes remains elusive.

HIRA chaperoning to H3.3 has a substantial role in oocyte developmental competence and embryogenesis through regulating chromatin condensation and transcriptional quiescence, which is crucial during embryonic development [324]. Likewise, it was reported that loss of HIRA causes

defects in early embryogenesis [326]. Although HIRA plays a crucial role during embryo development, its significance extends beyond this stage. Its reappearance in the transcriptional scene is widely associated with cancer development [327]. HIRA chaperoning and deposition for H3.3 was reported to be related to aggressive tumors and metastatic phenotype, where incorporation of HIRA to H3.3 was found essential for the chromatin remodeling that mediates pro-metastatic transcriptional reprogramming [327]. Taken together, the interplay between HIRA versus ATRX/ DAXX in depositing H3.3 histones may represent a crucial axis in the cellular reprogramming that enables complex cell fate decisions during tumorigenesis; however, the dynamic plasticity between these two complexes still needs to be better understood.

Historically, pediatric patients have been treated the same way adult high-grade gliomas are treated. Moreover, most previous clinical trials on pediatric high-grade glioma tumors were based on studies from adult GBM [328]. It was not until recently that the World Health Organization separated adults from pediatric-type high-grade gliomas, emphasizing the clinical and molecular differences between these different age tumors [268]. High-grade pediatric gliomas account for 10-15% of all brain tumors in children [329]. They are characterized by ominous prognoses with currently no curative therapy available, with the typical survival being less than two years [330]. Around half of the high-grade pediatric gliomas show diffuse growth in the brainstem, mainly in the pons, defining a separate subgroup termed diffuse intrinsic pontine glioma (DIPG) [329, 330]. These tumors are exceptionally challenging to treat owing to their anatomical site, which makes the median survival of these kid patients only nine months [329, 331]. Recent large-scale genomic, epigenomic, and transcriptomic studies of DIPG tumors show that DIPG tumors represent a class by themselves for their unique mutational and gene expression signatures [332].

Histone H3.3 plays a fundamental role in DIPG's tumors. Large-scale genomic studies identified a crucial mutation in histone H3.3 that defines DIPGs, the lysine-27-to-methionine mutation (H3.3K27M), which often co-occurs with a *TP53* mutation (~77%) [333]. While in adult GBM, hypermutation typically arises at the time of GBM recurrence driven by the alkylating agents' dependent therapeutics [314, 334], in children, hypermutation is present at the diagnosis time and what likely impacts the failure response of DIPGs to first-line therapeutic attempts.

The H3.3K27M mutation was found to drive global epigenetic changes in DIPG, such as causing a global reduction in the repressive mark H3K27me3, an increase in the transcriptionally activating mark H3K27ac, as well as a reduction in DNA methylation [126]. H3K27M exhibits a high affinity for the methyltransferase EZH2, the catalytic subunit of the polycomb repressive complex 2 (PRC2), which drives the trimethylation of H3K27, and thereby inhibits the repressive PRC2's enzymatic activity [126, 335]. It was recently proposed that PRC2 recruitment is not majorly impaired in DIPG but that H3K27me3 disrupts spreading across promoter-associated regions, particularly at the extended unmethylated CpG islands related to cell fate and lineage differentiation [336]. It was reported that correcting H3K27M restores the spreading of H3K27me2/me3 and entirely abolishes the tumor formation in mice [336].

After extensive research showed that the standard of care for high-grade gliomas is irrelevant to DIPG, several attempts have been investigated to correct the disrupted epigenetic landscape made by the mutation H3K27M, with some showing possible clinical outcomes. Targeting EZH2, the catalytic subunit of PRC2, was introduced where it was reasoned that since PRC2 activity is indispensable for the proliferation of H3K27M-expressing DIPGs, thus inhibiting EZH2 could be a potential therapeutic strategy for interfering with the transcriptional programs in

these tumors [337, 338]. Another therapeutic approach that was introduced and heavily investigated for its extraordinary potential is using HDACi [339]. The milestone for using the HDACi in DIPGs is that HDACs do not rely on the presence of histone mutations to exert their function. Preclinical work investigating the utility of the pan HDACi Panobinostat showed a positive response against both H3K27M DIPG and the non-mutant DIPG. Currently, HDACi Panobinostat is existing in clinical trials for DIPG, e.g., (NCT02717455).

Nevertheless, pan HDAC inhibition will always have its toxicity toll from the unspecific global HDAC inhibition. In a phase I Panobinostat clinical trial for children with solid tumors, one-third of children experienced severe thrombocytopenia [227]. In light of that, the current attempts are inclined towards isoform-specific HDACi that possess more specificity, better tumor cytotoxicity, and more safety in targeting the highly heterogeneous aggressive high-grade gliomas in children and adults.

g. Current treatment strategies for GBM

The current standard of care for GBM patients is surgery, radiation therapy, and chemotherapy. Depending on the overall health of the patient and disease condition, they may also be enrolled in relevant ongoing clinical trials, Tumor Treating Fields (TTFields), and targeted therapies [340, 341]. Surgery remains the first line to get a biopsy and make an initial diagnosis, ease the pressure from the brain swelling, and safely remove as much tumor as possible [340, 341]. Radiation and chemotherapy often follow surgery to eliminate part of the residual tumor tissues that were not accessible for surgical removal [340, 341]. However, much of the residual tumor that invaded

normal brain tissue remains hidden and inaccessible by therapy, the factor usually behind the relapsed or recurrent GBM.

Temozolomide is a DNA-alkylating agent discovered in the 1970s and approved in 2005 by the FDA to be among the standard of care for newly diagnosed GBM patients. GBM patients who show some initial response towards temozolomide and enhanced survival often have methyl-guanine-methyltransferase (*MGMT*) genes with hypermethylated promoters as compared to patients with hypomethylated *MGMT* genes [342]. Despite its inclusion in the standard chemotherapeutic regimen for GBM, temozolomide exhibits toxicity, fails to eradicate GBM even in combination therapies, and can induce hyper-mutated relapsed GBM. [269, 334].

Tumor Treating Fields (TTFields), generating low-intensity alternating intermediate-frequency electric fields, disrupt the growth and division of tumor cells. This therapy may also be administered in combination with chemotherapy for GBM patients. [343]. TTFields were introduced as an approach to applying intermittent electrical fields to exert biophysical force on charged and polarizable molecules known as dipoles.

Nevertheless, GBM recurrence after first-line therapy is inevitable [265, 285, 344]. Thus far, no standard approach has successfully targeted recurrent highly mutated GBM. Second-line treatments for GBM recurrence encompass various approaches such as surgical resection of the recurrent tumor, reirradiation, temozolomide rechallenge, administration of bevacizumab (an anti-vascular endothelial growth factor monoclonal antibody), or tyrosine kinase inhibitors for GBM patients with mutations in tyrosine kinase receptors [265, 285]. Despite these initiatives, the median overall survival after GBM recurrence is 6.5 months [345], while a longer overall survival (12 months) resulted from bevacizumab and the DNA alkylating chemotherapeutic nitrosourea,

lomustine [346]. Although immunotherapy showed hope with certain types of cancers, it failed its initial battle against GBM. Nevertheless, advanced research that considers the uniqueness of the CNS immune microenvironment provides more hope for opportunities to develop targeted successful immunotherapy for the GBM [285]. Many HDACi are indeed being used in combinational therapy, and many others are being investigated in preclinical settings. Nevertheless, the field desperately needs specific HDACi to match the various pathways and conditions involved in different types of cancers, specifically heterogeneous aggressive tumors like GBM.

Regardless of the chosen therapy and its potential, drug delivery for brain tumors has always been a great challenge. Many cross-talking factors enforce this challenge we face for targeting brain tumors: blood-brain barrier (BBB), blood-brain tumor barrier, the drug distribution hardship from the tightness of the brain parenchymal tissue, the overexpressed efflux pumps, the infiltration, invasion, cancer stem cells' heterogeneity, drug, and immune evasion driven by the collective tumor microenvironment. However, since most of the recurrent GBM bursts are in or near the prior resection cavity, there are recent attempts to locally deliver high doses of therapeutics to the GBM cavity (intraoperatively) that give hope for maximizing local efficiency, minimizing the systemic effect, overcoming constraints from the BBB [347].

Convection-enhanced delivery (CED), a novel modality for local drug delivery currently undergoing clinical trials, operates by applying a positive pressure gradient. The advantage of this modality is that it improves the spatial distribution, with lower concentrations of compounds being necessary to treat a similar area and can remain in situ for a prolonged period [348]. In addition, with the tight brain parenchyma and tumor tissue restricting the diffusion of many therapeutics,

the positive pressure gradient presented by the CED will enhance the diffusion of the therapeutics [347]. Multiple clinical trials with CED (NCT03086616), (NCT02022644), and (NCT03566199) are currently taking place with various therapeutic agents for GBM and DIPG, and advances are also still ongoing with multiple treatment plans and therapeutic agents that present great potential in combatting GBM.

Implanted and injected delivery methods like implanted reservoirs or stereotactic injections with chemo- or immuno-therapeutics are also from the proposed delivery modalities. The advantage of the implanted reservoir is that it is implanted under the skin and can be accessed intermittently, giving more treatment and dosing adjustment flexibility for the patient and clinician during the course of treatment.is A study that used the implanted reservoir to deliver the nitrosourea alkylating agent nimustine into the resection cavity combined with a brain distribution enhancer agent, together with oral temozolomide, showed a slight enhancement in the patients' OS and PFS. However, adjustments to the delivered therapeutics, dose, and implantation techniques might improve the implanted reservoirs' efficacy and safety [347].

In the early days of GBM treatment attempts, the intra-arterial delivery of chemotherapeutics demonstrated significant promise, particularly when other modalities were not feasible [349]. However, concerns regarding neurotoxicity and other unfavorable effects made intra-arterial delivery less appealing in the late 1990s, concurrent with the initial hope given towards temozolomide back then [350]. However, a recent interest in intra-arterial delivery was renewed owing to the improved selective angiographic strategies [350, 351]. An intra-arterial catheter can deliver high dosages of therapeutics directly over the tumor with the help of a brain disruption agent such as mannitol to maximize the route of the compound across the tight brain

parenchyma [351]. At least six various clinical phase I and II trials for primary and recurrent GBM are currently underway using selective intra-arterial delivery of multiple therapeutics (NCT01269853, NCT02285959, NCT01811498, NCT02800486, NCT02861898) [347]. One (NCT03672721) showed a tremendous initial outcome regarding a full or partial response with minor hematological adverse effects and no neurological complications [352].

Furthermore, our group has introduced a novel delivery idea using a biodegradable hydrogel called GliaTrap [353]. GliaTrap is a biodegradable, non-swelling, injectable hydrogel that has sustained release of a chemoattractant. GliaTrap aims to attract and trap the migrating and invading GSCs back to the tumor resection cavity to combat recurrence and improve surgery outcomes. Our team innovated a biodegradable and injectable hyaluronan/collagen II-based (HA/Col) hydrogel that does not swell in vivo. The hydrogel is loaded with a chemoattractant CXCL12-loaded FDA-approved liposomes. However, the GliaTrap concept can expand beyond this application to deliver additional therapeutics.

Local delivery offers promising avenues for enhancing the efficacy of various therapeutics while minimizing systemic side effects. This approach is particularly valuable for therapies with significant antitumorigenic potential but limited benefits when administered systemically due to challenges in crossing the blood-brain barrier (BBB) and accessing the tumor. Ultimately, all these drug delivery modalities have great potential in our battle against GBM.

Taken together, the current focus should be on investigating comparisons between different compounds, drug combinations, doses, and innovative drugs with improved specificity, favoring tumors over normal brain tissue to maximize benefits and minimize adverse effects. The battle against GBM and other forms of cancer necessitates rigorous collaboration among researchers,

clinicians, institutions, and governmental entities. It is crucial to work together to establish environments that foster innovation and development, providing accelerated pathways to translate promising ideas from the bench to the patient.

V. Thesis overview

a) Historical development of the thesis project

This dissertation focuses on HDAC7 as a key epigenetic regulator with therapeutic potential in malignancies. We provide evidence of HDAC7's overexpression in GBM and other cancers and demonstrate that its inhibition significantly affects the self-renewal capability of cancer stem cells, the main driver of GBM pathology.

The last decade witnessed extensive studies on HDACs and their role in cancer, which accelerated the advancement of a new class of cancer therapeutics, HDACi. Indeed, a large number of HDACi compounds have been developed and studied extensively [188-191, 194-199, 237, 239-243]. Many of these compounds were indeed granted FDA approval or under ongoing clinical and preclinical trials [225, 226, 232]. Thus far, the constraints associated with their clinical application stem from their unwanted side effects due to the lack of HDAC-isoform specificity. [354, 355]

Due to the distinctive nature of class IIa HDACs, which have been associated with cancer [77, 84, 85, 213, 250], but with a limited understanding of their regulation in malignancies, we aimed to explore the consequences of their overexpression in GBM. Based on the results from our initial screens, we hypothesized that HDAC7 stands out among class IIa HDACs as a crucial regulator in GBM and could serve as a novel potential druggable target in preclinical settings.

We employed multiple strategies aimed at developing a drug specifically targeting HDAC7 without impacting other HDACs; our approach sought to maximize specificity and minimize unwanted side effects. We also aimed to gain mechanistic insights into the role of HDAC7 in regulating cancer stemness by uncovering the HDAC7 interactome in the nucleus of GSCs. We viewed this comprehensive approach to have the potential to generate valuable insights that may

be translated into therapeutic interventions targeting HDAC7 in GBM, offering new avenues for the treatment of this therapeutically challenging tumor.

b) Overview of the experimental strategic plan for the thesis project

A key experimental system utilized in **Chapter 2** includes investigating the expression of class IIa HDACs in GBM. We utilized various publicly available data sets, through which we compared expression levels of HDAC class IIa members in GBM to those in other malignant gliomas and non-tumorous tissues. Furthermore, we performed survival analyses to test the correlation between individual HDAC isoform expression and overall survival among GBM patients across multiple cohorts. Our results indicated the specific overexpression of HDAC7 in GBM, distinct from the rest of class IIa HDAC.

Next, we collected RNA from paraffin-embedded samples from GBM patients at RIH and performed gene expression analysis using the Nanostring PanCancer progression panel. Data from 84 patients were curated and categorized as high-risk (HR) and low-risk (LR) based on the expression level of genes HDAC7. Subsequently, we performed differential gene expression with the related enrichment analyses. We further conducted a Kaplan-Meier survival analysis based on the HR/LR stratification using patient data based on the risk derived from HDAC7 expression.

Following our findings, we tested HDAC7 expression in various primary stem cells from adult GBM and pediatric Diffuse Intrinsic Pontine Glioma (DIPG) compared to normal brain lysates and human astrocytes to further validate HDAC7's specificity in these tumors.

We then conducted a cell viability assay, comparing GSCs treated with small interfering RNA (siRNA) against HDAC7, and non-targeting siRNA was used as a control. Furthermore, we performed tumorsphere formation on GSCs transfected with siRNA targeting HDAC7. These experiments aimed to identify the potential of HDAC7 to derive phenotypic changes in patient-derived GSCs.

After knocking down HDAC7 in GSCs using siRNA, we performed a transcriptomic analysis using RNA-seq to elucidate the changes in gene expression profiles. We used differential gene expression analysis to identify genes that were significantly changed after HDAC7 inhibition. Next, we utilized various enrichment analyses to gain insights into the biological processes, molecular pathways, and protein domains enriched after the HDAC7 knockdown. Additionally, we tested whether the down-regulated genes have roles in stemness as a way to understand their involvement in GSCs driving the pathogenesis. This comprehensive transcriptomic analysis aimed to provide us with the potential molecular mechanisms HDAC7 inhibition can induce in GSCs, providing valuable insights into its therapeutic potential in GBM treatment.

In **Chapter 3**, our key experimental strategy focused on a drug design pipeline aimed at exploring various methods to specifically target HDAC7. Based on preliminary results indicating that narrowing the spectrum for HDACs could yield a comparable inhibitory effect to pan HDACs while minimizing off-target effects and side effects, we opted to investigate ways to design a drug specifically targeting HDAC7. In collaboration with Fiser's Lab, a structural biology and bioinformatics lab at Albert Einstein University, we conducted a structure-based virtual screening of structurally related compounds of HDAC IIa inhibitors using multiple approaches. This

collaborative effort aimed to identify potential candidate compounds with high specificity for HDAC7, laying the foundation for the development of targeted therapies for GBM.

Our drug design pipeline was meticulously designed to incorporate multiple parallel approaches to mitigate potential challenges and maximize the likelihood of success in developing an effective HDAC7 inhibitor in a timely manner. Recognizing the limitations of computational prediction models, we adopted a comprehensive approach that encompassed both computational and experimental strategies. The first approach involved screening the National Cancer Institute Developmental Therapeutics Program (NCI DTP) library of available compounds to identify potential candidates with binding affinity towards HDAC7. Concurrently, we pursued a second strategy focused on the de novo synthesis of compounds based on structural superimposition computational models, leveraging known HDAC class IIa inhibitors such as TMP269 as templates. Compounds identified through these approaches were then subjected to rigorous analysis to evaluate their specificity towards HDAC7 over other structurally related HDACs, HDAC4, 5, and 9. This involved experimental assays to assess enzymatic activity and binding affinity. Subsequently, we utilized the insights gained from these analyses to refine our structural drug-designing training models and explore innovative approaches, including the use of proteolysis-targeting chimeras (PROTACs) to enhance drug specificity and efficacy.

Ultimately, in our RNA interference (RNAi)-based approach targeting HDAC7, we employed a systematic design process to generate specific siRNAs capable of silencing HDAC7 expression. This strategy aimed to silence HDAC7 expression selectively, offering an alternative therapeutic modality with potential advantages in terms of specificity and mechanism of action. Through BLAST similarity for sequences that target the open reading frame and 3'- untranslated

region of human HDAC7, we filtered and refined the candidate siRNAs to ensure specificity for HDAC7. Ultimately, we selected four individual siRNA sequences for HDAC7 and synthesized them for experimental testing. At the beginning, we utilized a smart pool approach, combining the four designed siRNA variants. Subsequently, we transfected GSCs with the smart pool of siHDAC7 at different concentrations. Following a 72-hour transfection period, we assessed the efficacy of HDAC7 knockdown by analyzing HDAC7 protein expression levels in cell lysates using Western blotting.

To avoid off-targeting effects from the smart pool siRNA, we opted to test the specificity of each siHDAC7 variant in our designed smart pool. Subsequently, we chose the siRNA variant with the highest specific inhibition of HDAC7 protein expression while not affecting the protein expression of HDAC4, HDAC5, and HDAC9.

This comprehensive experimental pipeline allowed us to validate the efficacy and specificity of our siRNA-designed drug in selectively targeting HDAC7 expression in GSCs, paving the way for further investigation of its therapeutic potential in GBM and potentially other cancers.

The key experimental strategy implemented in **Chapter 4** aimed to elucidate the mechanistic insights into HDAC7's role in regulating cancer stemness. Following the knockdown of HDAC7 in GSCs, we conducted Mass Spectrometry analysis (Mod Spec) to examine the global landscape of post-translational histone modifications affected by HDAC7 inhibition. This analysis aimed to provide insights into not only changes in acetylation/deacetylation patterns but also the broader impact of HDAC7 inhibition on the epigenetic landscape of GSCs.

Following this, we conducted rapid immunoprecipitation mass spectrometry of endogenous protein (RIME) experiments to elucidate the protein partners of HDAC7, particularly focusing on transcription factors, chromatin, and DNA binding proteins in close proximity to HDAC7. Our aim from the RIME experiment was to identify the interactome of HDAC7 that could play a role in driving malignancies. We then analyzed the pathways enriched with HDAC7 interactome. To validate our protein-protein interaction findings from the RIME experiment, we performed an array of co-immunoprecipitation followed by western blot experiments.

Next, we tested the potential involvement of HDAC7 in mediating chromatin phenotype changes by examining its coordinated binding with histone H3.3. To test this hypothesis, we performed experiments to validate the protein-protein interaction between HDAC7 and histone H3.3 and its impact on chromatin dynamics. We applied immunofluorescence with antibodies against known chromatin phenotype markers, including H3K9me3 and histone H3.3, following HDAC7 knockdown. Furthermore, we applied western blot for proteins known to have a role in heterochromatin spreading. Additionally, we knocked down HDAC7 and then tested the expression of DAXX, a chromatin assembly protein known to deposit histone H3.3 onto heterochromatin regions. Our findings were further supported with ELISA and western blot to test the expression levels of H3K27me3 and H3K9me3 marks after inhibiting HDAC7 in GSCs. Finally, to provide more rigor to our findings regarding HDAC7's role in mediating chromatin phenotype changes, we utilized electron microscopy to visualize the morphological changes in the chromatin phenotype following HDAC7 inhibition in GSCs.

c) Brief of project impact.

The study presented in this dissertation identifies HDAC7 as a potential epigenetic regulator in GBM. It delves into the biological and molecular consequences of HDAC7 overexpression driving tumorigenesis. Moreover, the study investigates potential strategies to selectively target HDAC7 without impacting other structurally related HDACs. Additionally, it elucidates the mechanistic pathways through which HDAC7 impacts the epigenome and the transcriptome of GSCs. Our ultimate goal is to develop a GBM therapeutic with translational potential in a preclinical setting.

Targeting HDACs for treating human malignancies has rapidly gained momentum in recent years. Four HDACi drugs have already been approved by the FDA: Vorinostat, Romidepsin, Panobinostat, and Belinostat. However, these drugs target the enzymatic activity of HDACs, which HDAC class IIa does not possess. Additionally, pan-HDAC inhibition has been associated with various toxicities and unwanted effects [84, 85, 252].

In this dissertation, we present evidence highlighting the significant genetic and epigenetic implications of a singular HDAC isoform in GSCs, HDAC7, which correlates with the survival of GBM patients. Moreover, we reveal that HDAC7 lacks deacetylase activity but is integrated into a proteome alongside histone H3.3 on the chromatin. Our findings support that HDAC7 functions as a chaperone for the histone variant H3.3, and inhibiting HDAC7 leads to the spreading of heterochromatin in cancer stem cells, thereby silencing tumorigenic transcriptional programs. The data presented in this dissertation strongly supports the hypothesis that HDAC7 represents a promising therapeutic target in GBM and potentially in other cancers as well.

VI. References

[1] R. Holliday, "Epigenetics: a historical overview," *Epigenetics,* vol. 1, no. 2, pp. 76-80, Apr-Jun 2006, doi: 10.4161/epi.1.2.2762.

[2] T. Cheutin, A. J. McNairn, T. Jenuwein, D. M. Gilbert, P. B. Singh, and T. Misteli, "Maintenance of Stable Heterochromatin Domains by Dynamic HP1 Binding," *Science,* vol. 299, no. 5607, pp. 721-725, 2003, doi: 10.1126/science.1078572.

[3] T. Jenuwein and C. D. Allis, "Translating the Histone Code," *Science,* vol. 293, no. 5532, pp. 1074-1080, 2001, doi: 10.1126/science.1063127.

[4] V. Orlando, "Polycomb, Epigenomes, and Control of Cell Identity," *Cell,* vol. 112, no. 5, pp. 599-606, 2003, doi: 10.1016/S0092-8674(03)00157-0.

[5] S. S. Levine, I. F. G. King, and R. E. Kingston, "Division of labor in Polycomb group repression," *Trends in Biochemical Sciences,* vol. 29, no. 9, pp. 478-485, 2004, doi: 10.1016/j.tibs.2004.07.007.

[6] T. Jenuwein, "An RNA-Guided Pathway for the Epigenome," *Science,* vol. 297, no. 5590, pp. 2215-2218, 2002, doi: 10.1126/science.1077903.

[7] M. Lechner, C. Boshoff, and S. Beck, "Cancer Epigenome," 2010, pp. 247-276.

[8] E. G. Toraño, M. G. García, J. L. Fernández-Morera, P. Niño-García, and A. F. Fernández, "The Impact of External Factors on the Epigenome: In Utero and over Lifetime," *BioMed Research International,* vol. 2016, pp. 1-17, 2016, doi: 10.1155/2016/2568635.

[9] G. Almouzni *et al.*, "Relationship between genome and epigenome - challenges and requirements for future research," *BMC Genomics,* vol. 15, no. 1, pp. 487-487, 2014, doi: 10.1186/1471-2164-15-487.

[10] R. Lister *et al.*, "Human DNA methylomes at base resolution show widespread epigenomic differences," *Nature,* vol. 462, no. 7271, pp. 315-322, 2009, doi: 10.1038/nature08514.

[11] A. H. C. Wong, I. I. Gottesman, and A. Petronis, "Phenotypic differences in genetically identical organisms: the epigenetic perspective," *Human Molecular Genetics,* vol. 14, no. suppl_1, pp. R11-R18, 2005, doi: 10.1093/hmg/ddi116.

[12] M. F. Fraga *et al.*, "Epigenetic differences arise during the lifetime of monozygotic twins," *Proceedings of the National Academy of Sciences,* vol. 102, no. 30, pp. 10604-10609, 2005, doi: 10.1073/pnas.0500398102.

[13] G. Egger, G. Liang, A. Aparicio, and P. A. Jones, "Epigenetics in human disease and prospects for epigenetic therapy," *Nature,* vol. 429, no. 6990, pp. 457-463, 2004, doi: 10.1038/nature02625.

[14] M. K. Skinner, "Role of epigenetics in developmental biology and transgenerational inheritance," *Birth Defects Research Part C: Embryo Today: Reviews,* vol. 93, no. 1, pp. 51-55, 2011, doi: 10.1002/bdrc.20199.

[15] H. H. Kazazian, "Mobile Elements: Drivers of Genome Evolution," *Science,* vol. 303, no. 5664, pp. 1626-1632, 2004, doi: 10.1126/science.1089670.

[16] B. M. Turner, "Histone acetylation as an epigenetic determinant of long-term transcriptional competence," *Cellular and Molecular Life Sciences (CMLS),* vol. 54, no. 1, pp. 21-31, 1998, doi: 10.1007/s000180050122.

[17] S. C. Biddie, "Chromatin Architecture and the Regulation of Nuclear Receptor Inducible Transcription," *Journal of Neuroendocrinology,* vol. 23, no. 1, pp. 94-106, 2011, doi: 10.1111/j.1365-2826.2010.02079.x.
[18] L. B. Wan and M. S. Bartolomei, "Chapter 7 Regulation of Imprinting in Clusters: Noncoding RNAs Versus Insulators," 2008, pp. 207-223.
[19] W. Reik, W. Dean, and J. r. Walter, "Epigenetic Reprogramming in Mammalian Development," *Science,* vol. 293, no. 5532, pp. 1089-1093, 2001, doi: 10.1126/science.1063443.
[20] P. Cold Spring Harbor Laboratory, *Epigenetics (eds. Allis, C. D. et al.)*, Second ed. 2015.
[21] F. Perera and J. Herbstman, "Prenatal environmental exposures, epigenetics, and disease," *Reproductive Toxicology,* vol. 31, no. 3, pp. 363-373, 2011, doi: 10.1016/j.reprotox.2010.12.055.
[22] B. Richardson, "Primer: epigenetics of autoimmunity," *Nature Clinical Practice Rheumatology,* vol. 3, no. 9, pp. 521-527, 2007, doi: 10.1038/ncprheum0573.
[23] T. Kawabata *et al.*, "Increased activity and expression of histone deacetylase 1 in relation to tumor necrosis factor-alpha in synovial tissue of rheumatoid arthritis," *Arthritis Research & Therapy,* vol. 12, no. 4, pp. R133-R133, 2010, doi: 10.1186/ar3071.
[24] J. Vojinovic *et al.*, "Safety and efficacy of an oral histone deacetylase inhibitor in systemic-onset juvenile idiopathic arthritis," *Arthritis & Rheumatism,* vol. 63, no. 5, pp. 1452-1458, 2011, doi: 10.1002/art.30238.
[25] Q. Wang *et al.*, "Overexpression of JMJD3 may contribute to demethylation of H3K27me3 in CD4 + T cells from patients with systemic sclerosis," *Clinical Immunology,* vol. 161, no. 2, pp. 396-399, 2015, doi: 10.1016/j.clim.2015.03.006.
[26] H. Hemmatazad *et al.*, "Histone deacetylase 7, a potential target for the antifibrotic treatment of systemic sclerosis," *Arthritis & Rheumatism,* vol. 60, no. 5, pp. 1519-1529, 2009, doi: 10.1002/art.24494.
[27] C. F. Lin *et al.*, "Escape from IFN-gamma-dependent immunosurveillance in tumorigenesis," *J Biomed Sci,* vol. 24, no. 1, p. 10, Feb 1 2017, doi: 10.1186/s12929-017-0317-0.
[28] T. Patel, V. Patel, R. Singh, and S. Jayaraman, "Chromatin remodeling resets the immune system to protect against autoimmune diabetes in mice," *Immunology & Cell Biology,* vol. 89, no. 5, pp. 640-649, 2011, doi: 10.1038/icb.2010.144.
[29] A. P. Feinberg and B. Tycko, "The history of cancer epigenetics," *Nature Reviews Cancer,* vol. 4, no. 2, pp. 143-153, 2004, doi: 10.1038/nrc1279.
[30] M. Wang, B. D. Sunkel, W. C. Ray, and B. Z. Stanton, "Chromatin structure in cancer," *BMC Mol Cell Biol,* vol. 23, no. 1, p. 35, Jul 28 2022, doi: 10.1186/s12860-022-00433-6.
[31] M. L. Suva, N. Riggi, and B. E. Bernstein, "Epigenetic reprogramming in cancer," *Science,* vol. 339, no. 6127, pp. 1567-70, Mar 29 2013, doi: 10.1126/science.1230184.
[32] Y. Lu, Y.-T. Chan, H.-Y. Tan, S. Li, N. Wang, and Y. Feng, "Epigenetic regulation in human cancer: the potential role of epi-drug in cancer therapy," *Molecular Cancer,* vol. 19, no. 1, pp. 79-79, 2020, doi: 10.1186/s12943-020-01197-3.
[33] A. P. Feinberg, R. Ohlsson, and S. Henikoff, "The epigenetic progenitor origin of human cancer," *Nature Reviews Genetics,* vol. 7, no. 1, pp. 21-33, 2006, doi: 10.1038/nrg1748.
[34] C. B. Yoo and P. A. Jones, "Epigenetic therapy of cancer: past, present and future," *Nature Reviews Drug Discovery,* vol. 5, no. 1, pp. 37-50, 2006, doi: 10.1038/nrd1930.

[35] A. D. Riggs and P. A. Jones, "5-Methylcytosine, Gene Regulation, and Cancer," 1983, pp. 1-30.
[36] R. Lakshminarasimhan and G. Liang, "The Role of DNA Methylation in Cancer," *Adv Exp Med Biol,* vol. 945, pp. 151-172, 2016, doi: 10.1007/978-3-319-43624-1_7.
[37] M. F. Fraga *et al.*, "Loss of acetylation at Lys16 and trimethylation at Lys20 of histone H4 is a common hallmark of human cancer," *Nature Genetics,* vol. 37, no. 4, pp. 391-400, 2005, doi: 10.1038/ng1531.
[38] D. B. Seligson *et al.*, "Global histone modification patterns predict risk of prostate cancer recurrence," *Nature,* vol. 435, no. 7046, pp. 1262-1266, 2005, doi: 10.1038/nature03672.
[39] J. Wang, S. T. Lawry, A. L. Cohen, and S. Jia, "Chromosome boundary elements and regulation of heterochromatin spreading," *Cell Mol Life Sci,* vol. 71, no. 24, pp. 4841-52, Dec 2014, doi: 10.1007/s00018-014-1725-x.
[40] B. Schuster-Bockler and B. Lehner, "Chromatin organization is a major influence on regional mutation rates in human cancer cells," *Nature,* vol. 488, no. 7412, pp. 504-7, Aug 23 2012, doi: 10.1038/nature11273.
[41] R. R. Kanherkar, N. Bhatia-Dey, and A. B. Csoka, "Epigenetics across the human lifespan," *Front Cell Dev Biol,* vol. 2, p. 49, 2014, doi: 10.3389/fcell.2014.00049.
[42] T. Jenuwein, "The epigenetic magic of histone lysine methylation," *The FEBS Journal,* vol. 273, no. 14, pp. 3121-3135, 2006, doi: 10.1111/j.1742-4658.2006.05343.x.
[43] P. A. Jones and S. B. Baylin, "The Epigenomics of Cancer," *Cell,* vol. 128, no. 4, pp. 683-692, 2007, doi: 10.1016/j.cell.2007.01.029.
[44] S. B. Baylin and J. E. Ohm, "Epigenetic gene silencing in cancer – a mechanism for early oncogenic pathway addiction?," *Nature Reviews Cancer,* vol. 6, no. 2, pp. 107-116, 2006, doi: 10.1038/nrc1799.
[45] T. Kouzarides, "Chromatin Modifications and Their Function," *Cell,* vol. 128, no. 4, pp. 693-705, 2007, doi: 10.1016/j.cell.2007.02.005.
[46] J. M. Schoelz and N. C. Riddle, "Functions of HP1 proteins in transcriptional regulation," *Epigenetics & Chromatin,* vol. 15, no. 1, pp. 14-14, 2022, doi: 10.1186/s13072-022-00453-8.
[47] V. Mutskov and G. Felsenfeld, "The human insulin gene is part of a large open chromatin domain specific for human islets," *Proceedings of the National Academy of Sciences,* vol. 106, no. 41, pp. 17419-17424, 2009, doi: 10.1073/pnas.0909288106.
[48] A. J. Bannister and T. Kouzarides, "Regulation of chromatin by histone modifications," *Cell Research,* vol. 21, no. 3, pp. 381-395, 2011, doi: 10.1038/cr.2011.22.
[49] N. L. Young, P. A. DiMaggio, and B. A. Garcia, "The significance, development and progress of high-throughput combinatorial histone code analysis," *Cellular and Molecular Life Sciences,* vol. 67, no. 23, pp. 3983-4000, 2010, doi: 10.1007/s00018-010-0475-7.
[50] L. Simó-Riudalbas and M. Esteller, "Targeting the histone orthography of cancer: drugs for writers, erasers and readers," *British Journal of Pharmacology,* vol. 172, no. 11, pp. 2716-2732, 2015, doi: 10.1111/bph.12844.
[51] E. Seto and M. Yoshida, "Erasers of Histone Acetylation: The Histone Deacetylase Enzymes," *Cold Spring Harbor Perspectives in Biology,* vol. 6, no. 4, pp. a018713-a018713, 2014, doi: 10.1101/cshperspect.a018713.
[52] M.-C. Tsai *et al.*, "Long Noncoding RNA as Modular Scaffold of Histone Modification Complexes," *Science,* vol. 329, no. 5992, pp. 689-693, 2010, doi: 10.1126/science.1192002.

[53] S. D. Taverna, H. Li, A. J. Ruthenburg, C. D. Allis, and D. J. Patel, "How chromatin-binding modules interpret histone modifications: lessons from professional pocket pickers," *Nature Structural & Molecular Biology,* vol. 14, no. 11, pp. 1025-1040, 2007, doi: 10.1038/nsmb1338.
[54] A. J. Ruthenburg, H. Li, D. J. Patel, and C. David Allis, "Multivalent engagement of chromatin modifications by linked binding modules," *Nature Reviews Molecular Cell Biology,* vol. 8, no. 12, pp. 983-994, 2007, doi: 10.1038/nrm2298.
[55] E. L. Greer and Y. Shi, "Histone methylation: a dynamic mark in health, disease and inheritance," *Nature Reviews Genetics,* vol. 13, no. 5, pp. 343-357, 2012, doi: 10.1038/nrg3173.
[56] K. D. Robertson, "DNA methylation and human disease," *Nature Reviews Genetics,* vol. 6, no. 8, pp. 597-610, 2005, doi: 10.1038/nrg1655.
[57] A. V. Probst, E. Dunleavy, and G. Almouzni, "Epigenetic inheritance during the cell cycle," *Nature Reviews Molecular Cell Biology,* vol. 10, no. 3, pp. 192-206, 2009, doi: 10.1038/nrm2640.
[58] M. M. Suzuki and A. Bird, "DNA methylation landscapes: provocative insights from epigenomics," *Nature Reviews Genetics,* vol. 9, no. 6, pp. 465-476, 2008, doi: 10.1038/nrg2341.
[59] N. R. Rose and R. J. Klose, "Understanding the relationship between DNA methylation and histone lysine methylation," *Biochim Biophys Acta,* vol. 1839, no. 12, pp. 1362-72, Dec 2014, doi: 10.1016/j.bbagrm.2014.02.007.
[60] B. Jin, Y. Li, and K. D. Robertson, "DNA Methylation: Superior or Subordinate in the Epigenetic Hierarchy?," *Genes & Cancer,* vol. 2, no. 6, pp. 607-617, 2011, doi: 10.1177/1947601910393957.
[61] P. A. Wade, "Methyl CpG-binding proteins and transcriptional repression*," *BioEssays,* vol. 23, no. 12, pp. 1131-1137, 2001, doi: 10.1002/bies.10008.
[62] B. Lehnertz *et al.*, "Suv39h-Mediated Histone H3 Lysine 9 Methylation Directs DNA Methylation to Major Satellite Repeats at Pericentric Heterochromatin," *Current Biology,* vol. 13, no. 14, pp. 1192-1200, 2003, doi: 10.1016/S0960-9822(03)00432-9.
[63] H. Huang, S. Lin, B. A. Garcia, and Y. Zhao, "Quantitative proteomic analysis of histone modifications," *Chem Rev,* vol. 115, no. 6, pp. 2376-418, Mar 25 2015, doi: 10.1021/cr500491u.
[64] C. Lu, M. Coradin, E. G. Porter, and B. A. Garcia, "Accelerating the Field of Epigenetic Histone Modification Through Mass Spectrometry-Based Approaches," *Mol Cell Proteomics,* vol. 20, p. 100006, 2021, doi: 10.1074/mcp.R120.002257.
[65] J. M. Lee, H. M. Hammaren, M. M. Savitski, and S. H. Baek, "Control of protein stability by post-translational modifications," *Nat Commun,* vol. 14, no. 1, p. 201, Jan 13 2023, doi: 10.1038/s41467-023-35795-8.
[66] M. Leutert, S. W. Entwisle, and J. Villen, "Decoding Post-Translational Modification Crosstalk With Proteomics," *Mol Cell Proteomics,* vol. 20, p. 100129, 2021, doi: 10.1016/j.mcpro.2021.100129.
[67] V. G. Allfrey, R. Faulkner, and A. E. Mirsky, "ACETYLATION AND METHYLATION OF HISTONES AND THEIR POSSIBLE ROLE IN THE REGULATION OF RNA SYNTHESIS," *Proceedings of the National Academy of Sciences,* vol. 51, no. 5, pp. 786-794, 1964, doi: 10.1073/pnas.51.5.786.

[68] S. C. Hodawadekar and R. Marmorstein, "Chemistry of acetyl transfer by histone modifying enzymes: structure, mechanism and implications for effector design," *Oncogene,* vol. 26, no. 37, pp. 5528-5540, 2007, doi: 10.1038/sj.onc.1210619.

[69] X. J. Yang and E. Seto, "HATs and HDACs: from structure, function and regulation to novel strategies for therapy and prevention," *Oncogene,* vol. 26, no. 37, pp. 5310-5318, 2007, doi: 10.1038/sj.onc.1210599.

[70] C. Das, M. S. Lucia, K. C. Hansen, and J. K. Tyler, "CBP/p300-mediated acetylation of histone H3 on lysine 56," *Nature,* vol. 459, no. 7243, pp. 113-117, 2009, doi: 10.1038/nature07861.

[71] B. Fierz and M. G. Poirier, "Biophysics of Chromatin Dynamics," *Annu Rev Biophys,* vol. 48, pp. 321-345, May 6 2019, doi: 10.1146/annurev-biophys-070317-032847.

[72] P. A. Grant *et al.*, "Yeast Gcn5 functions in two multisubunit complexes to acetylate nucleosomal histones: characterization of an Ada complex and the SAGA (Spt/Ada) complex," *Genes & Development,* vol. 11, no. 13, pp. 1640-1650, 1997, doi: 10.1101/gad.11.13.1640.

[73] M. Shogren-Knaak, H. Ishii, J.-M. Sun, M. J. Pazin, J. R. Davie, and C. L. Peterson, "Histone H4-K16 Acetylation Controls Chromatin Structure and Protein Interactions," *Science,* vol. 311, no. 5762, pp. 844-847, 2006, doi: 10.1126/science.1124000.

[74] T. Eckschlager, J. Plch, M. Stiborova, and J. Hrabeta, "Histone Deacetylase Inhibitors as Anticancer Drugs," *International Journal of Molecular Sciences,* vol. 18, no. 7, pp. 1414-1414, 2017, doi: 10.3390/ijms18071414.

[75] Q. Yang *et al.*, "Epigenetics in ovarian cancer: premise, properties, and perspectives," *Molecular Cancer,* vol. 17, no. 1, pp. 109-109, 2018, doi: 10.1186/s12943-018-0855-4.

[76] I. Gregoretti, Y.-M. Lee, and H. V. Goodson, "Molecular Evolution of the Histone Deacetylase Family: Functional Implications of Phylogenetic Analysis," *Journal of Molecular Biology,* vol. 338, no. 1, pp. 17-31, 2004, doi: 10.1016/j.jmb.2004.02.006.

[77] Y. Li and E. Seto, "HDACs and HDAC Inhibitors in Cancer Development and Therapy," *Cold Spring Harb Perspect Med,* vol. 6, no. 10, Oct 3 2016, doi: 10.1101/cshperspect.a026831.

[78] A. J. Wilson *et al.*, "Histone Deacetylase 3 (HDAC3) and Other Class I HDACs Regulate Colon Cell Maturation and p21 Expression and Are Deregulated in Human Colon Cancer," *Journal of Biological Chemistry,* vol. 281, no. 19, pp. 13548-13558, 2006, doi: 10.1074/jbc.M510023200.

[79] X.-J. Yang and E. Seto, "Collaborative spirit of histone deacetylases in regulating chromatin structure and gene expression," *Current Opinion in Genetics & Development,* vol. 13, no. 2, pp. 143-153, 2003, doi: 10.1016/S0959-437X(03)00015-7.

[80] X. He, V. Gonzalez, A. Tsang, J. Thompson, T. C. Tsang, and D. T. Harris, "Differential Gene Expression Profiling of CD34 + CD133 + Umbilical Cord Blood Hematopoietic Stem Progenitor Cells," *Stem Cells and Development,* vol. 14, no. 2, pp. 188-198, 2005, doi: 10.1089/scd.2005.14.188.

[81] H. Lee, N. Sengupta, A. Villagra, N. Rezai-Zadeh, and E. Seto, "Histone Deacetylase 8 Safeguards the Human Ever-Shorter Telomeres 1B (hEST1B) Protein from Ubiquitin-Mediated Degradation," *Molecular and Cellular Biology,* vol. 26, no. 14, pp. 5259-5269, 2006, doi: 10.1128/MCB.01971-05.

[82] E. Verdin, F. Dequiedt, and H. G. Kasler, "Class II histone deacetylases: versatile regulators," *Trends in Genetics,* vol. 19, no. 5, pp. 286-293, 2003, doi: 10.1016/S0168-9525(03)00073-8.
[83] A. Muslin, "14-3-3 proteins: regulation of subcellular localization by molecular interference," *Cellular Signalling,* vol. 12, no. 11-12, pp. 703-709, 2000, doi: 10.1016/S0898-6568(00)00131-5.
[84] S.-Y. Park and J.-S. Kim, "A short guide to histone deacetylases including recent progress on class II enzymes," *Experimental & Molecular Medicine,* vol. 52, no. 2, pp. 204-212, 2020, doi: 10.1038/s12276-020-0382-4.
[85] T. C. S. Ho, A. H. Y. Chan, and A. Ganesan, "Thirty Years of HDAC Inhibitors: 2020 Insight and Hindsight," *Journal of Medicinal Chemistry,* vol. 63, no. 21, pp. 12460-12484, 2020, doi: 10.1021/acs.jmedchem.0c00830.
[86] Y. Wang *et al.*, "Histone deacetylase 7: a signalling hub controlling development, inflammation, metabolism and disease," *The FEBS Journal,* vol. 290, no. 11, pp. 2805-2832, 2023, doi: 10.1111/febs.16437.
[87] A. Schuetz *et al.*, "Human HDAC7 Harbors a Class IIa Histone Deacetylase-specific Zinc Binding Motif and Cryptic Deacetylase Activity," *Journal of Biological Chemistry,* vol. 283, no. 17, pp. 11355-11363, 2008, doi: 10.1074/jbc.M707362200.
[88] D. Ramnath *et al.*, "The histone deacetylase Hdac7 supports LPS-inducible glycolysis and Il-1β production in murine macrophages via distinct mechanisms," *Journal of Leukocyte Biology,* vol. 111, no. 2, pp. 327-336, 2022, doi: 10.1002/JLB.2MR1021-260R.
[89] Y. Zhang, R. Andrade, A. A. Hanna, and M. K. H. Pflum, "Evidence that HDAC7 acts as an epigenetic "reader" of AR acetylation through NCoR-HDAC3 dissociation," *Cell Chemical Biology,* vol. 29, no. 7, pp. 1162-1173.e5, 2022, doi: 10.1016/j.chembiol.2022.05.008.
[90] M. Parra, "Class IIa HDACs - new insights into their functions in physiology and pathology," *The FEBS Journal,* vol. 282, no. 9, pp. 1736-1744, 2015, doi: 10.1111/febs.13061.
[91] S.-Y. Park *et al.*, "Structural basis of the specific interaction of SMRT corepressor with histone deacetylase 4," *Nucleic Acids Research,* vol. 46, no. 22, pp. 11776-11788, 2018, doi: 10.1093/nar/gky926.
[92] T. Li *et al.*, "Histone deacetylase 6 in cancer," *J Hematol Oncol,* vol. 11, no. 1, p. 111, Sep 3 2018, doi: 10.1186/s13045-018-0654-9.
[93] L. Gao, M. A. Cueto, F. Asselbergs, and P. Atadja, "Cloning and Functional Characterization of HDAC11, a Novel Member of the Human Histone Deacetylase Family," *Journal of Biological Chemistry,* vol. 277, no. 28, pp. 25748-25755, 2002, doi: 10.1074/jbc.M111871200.
[94] M. A. Glozak and E. Seto, "Acetylation/Deacetylation Modulates the Stability of DNA Replication Licensing Factor Cdt1," *Journal of Biological Chemistry,* vol. 284, no. 17, pp. 11446-11453, 2009, doi: 10.1074/jbc.M809394200.
[95] C. B. Brachmann, J. M. Sherman, S. E. Devine, E. E. Cameron, L. Pillus, and J. D. Boeke, "The SIR2 gene family, conserved from bacteria to humans, functions in silencing, cell cycle progression, and chromosome stability," *Genes & Development,* vol. 9, no. 23, pp. 2888-2902, 1995, doi: 10.1101/gad.9.23.2888.
[96] J. Du *et al.*, "Sirt5 Is a NAD-Dependent Protein Lysine Demalonylase and Desuccinylase," *Science,* vol. 334, no. 6057, pp. 806-809, 2011, doi: 10.1126/science.1207861.

[97] P. Byvoet, G. R. Shepherd, J. M. Hardin, and B. J. Noland, "The distribution and turnover of labeled methyl groups in histone fractions of cultured mammalian cells," *Archives of Biochemistry and Biophysics,* vol. 148, no. 2, pp. 558-567, 1972, doi: 10.1016/0003-9861(72)90174-9.
[98] B. M. Zee, R. S. Levin, B. Xu, G. LeRoy, N. S. Wingreen, and B. A. Garcia, "In Vivo Residue-specific Histone Methylation Dynamics," *Journal of Biological Chemistry,* vol. 285, no. 5, pp. 3341-3350, 2010, doi: 10.1074/jbc.M109.063784.
[99] S. Rea *et al.*, "Regulation of chromatin structure by site-specific histone H3 methyltransferases," *Nature,* vol. 406, no. 6796, pp. 593-599, 2000, doi: 10.1038/35020506.
[100] Q. Feng *et al.*, "Methylation of H3-Lysine 79 Is Mediated by a New Family of HMTases without a SET Domain," *Current Biology,* vol. 12, no. 12, pp. 1052-1058, 2002, doi: 10.1016/S0960-9822(02)00901-6.
[101] R. Magnani, L. M. A. Dirk, R. C. Trievel, and R. L. Houtz, "Calmodulin methyltransferase is an evolutionarily conserved enzyme that trimethylates Lys-115 in calmodulin," *Nature Communications,* vol. 1, no. 1, pp. 43-43, 2010, doi: 10.1038/ncomms1044.
[102] J. Verigos *et al.*, "The Histone Demethylase LSD1/KappaDM1A Mediates Chemoresistance in Breast Cancer via Regulation of a Stem Cell Program," *Cancers (Basel),* vol. 11, no. 10, Oct 17 2019, doi: 10.3390/cancers11101585.
[103] A. Laugesen, J. W. Hojfeldt, and K. Helin, "Molecular Mechanisms Directing PRC2 Recruitment and H3K27 Methylation," *Mol Cell,* vol. 74, no. 1, pp. 8-18, Apr 4 2019, doi: 10.1016/j.molcel.2019.03.011.
[104] M. Tyagi, N. Imam, K. Verma, and A. K. Patel, "Chromatin remodelers: We are the drivers!!," *Nucleus,* vol. 7, no. 4, pp. 388-404, 2016, doi: 10.1080/19491034.2016.1211217.
[105] A. A. Reyes, R. D. Marcum, and Y. He, "Structure and Function of Chromatin Remodelers," *Journal of Molecular Biology,* vol. 433, no. 14, pp. 166929-166929, 2021, doi: 10.1016/j.jmb.2021.166929.
[106] S. Baldi, P. Korber, and P. B. Becker, "Beads on a string—nucleosome array arrangements and folding of the chromatin fiber," *Nature Structural & Molecular Biology,* vol. 27, no. 2, pp. 109-118, 2020, doi: 10.1038/s41594-019-0368-x.
[107] W. K. M. Lai and B. F. Pugh, "Understanding nucleosome dynamics and their links to gene expression and DNA replication," *Nature Reviews Molecular Cell Biology,* vol. 18, no. 9, pp. 548-562, 2017, doi: 10.1038/nrm.2017.47.
[108] S. Eustermann, A. B. Patel, K.-P. Hopfner, Y. He, and P. Korber, "Energy-driven genome regulation by ATP-dependent chromatin remodellers," *Nature Reviews Molecular Cell Biology,* 2023, doi: 10.1038/s41580-023-00683-y.
[109] E. Chacin *et al.*, "Establishment and function of chromatin organization at replication origins," *Nature,* vol. 616, no. 7958, pp. 836-842, 2023, doi: 10.1038/s41586-023-05926-8.
[110] S. L. Klemm, Z. Shipony, and W. J. Greenleaf, "Chromatin accessibility and the regulatory epigenome," *Nature Reviews Genetics,* vol. 20, no. 4, pp. 207-220, 2019, doi: 10.1038/s41576-018-0089-8.
[111] P. Cramer, "Organization and regulation of gene transcription," *Nature,* vol. 573, no. 7772, pp. 45-54, 2019, doi: 10.1038/s41586-019-1517-4.

[112] J. Fei *et al.*, "NDF, a nucleosome-destabilizing factor that facilitates transcription through nucleosomes," *Genes & Development,* vol. 32, no. 9-10, pp. 682-694, 2018, doi: 10.1101/gad.313973.118.
[113] K. N. Schulz *et al.*, "Zelda is differentially required for chromatin accessibility, transcription factor binding, and gene expression in the early Drosophila embryo," *Genome Research,* vol. 25, no. 11, pp. 1715-1726, 2015, doi: 10.1101/gr.192682.115.
[114] C. M. Weber and S. Henikoff, "Histone variants: dynamic punctuation in transcription," *Genes & Development,* vol. 28, no. 7, pp. 672-682, 2014, doi: 10.1101/gad.238873.114.
[115] L. Zheng, R. G. Roeder, and Y. Luo, "S Phase Activation of the Histone H2B Promoter by OCA-S, a Coactivator Complex that Contains GAPDH as a Key Component," *Cell,* vol. 114, no. 2, pp. 255-266, 2003, doi: 10.1016/S0092-8674(03)00552-X.
[116] W. F. Marzluff and K. P. Koreski, "Birth and Death of Histone mRNAs," *Trends in Genetics,* vol. 33, no. 10, pp. 745-759, 2017, doi: 10.1016/j.tig.2017.07.014.
[117] S. Martire and L. A. Banaszynski, "The roles of histone variants in fine-tuning chromatin organization and function," *Nature Reviews Molecular Cell Biology,* vol. 21, no. 9, pp. 522-541, 2020, doi: 10.1038/s41580-020-0262-8.
[118] E. O. N. Phillips and A. Gunjan, "Histone variants: The unsung guardians of the genome," *DNA Repair,* vol. 112, pp. 103301-103301, 2022, doi: 10.1016/j.dnarep.2022.103301.
[119] S. El Kennani *et al.*, "MS_HistoneDB, a manually curated resource for proteomic analysis of human and mouse histones," *Epigenetics & Chromatin,* vol. 10, no. 1, pp. 2-2, 2017, doi: 10.1186/s13072-016-0109-x.
[120] M. Buschbeck and S. B. Hake, "Variants of core histones and their roles in cell fate decisions, development and cancer," *Nature Reviews Molecular Cell Biology,* vol. 18, no. 5, pp. 299-314, 2017, doi: 10.1038/nrm.2016.166.
[121] K. Ahmad and S. Henikoff, "The Histone Variant H3.3 Marks Active Chromatin by Replication-Independent Nucleosome Assembly," *Molecular Cell,* vol. 9, no. 6, pp. 1191-1200, 2002, doi: 10.1016/S1097-2765(02)00542-7.
[122] B. E. Black *et al.*, "Centromere Identity Maintained by Nucleosomes Assembled with Histone H3 Containing the CENP-A Targeting Domain," *Molecular Cell,* vol. 25, no. 2, pp. 309-322, 2007, doi: 10.1016/j.molcel.2006.12.018.
[123] J. Füllgrabe, E. Kavanagh, and B. Joseph, "Histone onco-modifications," *Oncogene,* vol. 30, no. 31, pp. 3391-3403, 2011, doi: 10.1038/onc.2011.121.
[124] J. Schwartzentruber *et al.*, "Driver mutations in histone H3.3 and chromatin remodelling genes in paediatric glioblastoma," *Nature,* vol. 482, no. 7384, pp. 226-231, 2012, doi: 10.1038/nature10833.
[125] K. N. Espinoza Pereira, J. Shan, J. D. Licht, and R. L. Bennett, "Histone mutations in cancer," *Biochemical Society Transactions,* vol. 51, no. 5, pp. 1749-1763, 2023, doi: 10.1042/BST20210567.
[126] S. Bender *et al.*, "Reduced H3K27me3 and DNA Hypomethylation Are Major Drivers of Gene Expression in K27M Mutant Pediatric High-Grade Gliomas," *Cancer Cell,* vol. 24, no. 5, pp. 660-672, 2013, doi: 10.1016/j.ccr.2013.10.006.
[127] A. S. Harutyunyan *et al.*, "H3K27M in Gliomas Causes a One-Step Decrease in H3K27 Methylation and Reduced Spreading within the Constraints of H3K36 Methylation," *Cell Reports,* vol. 33, no. 7, pp. 108390-108390, 2020, doi: 10.1016/j.celrep.2020.108390.

[128] S. Zhao *et al.*, "Mutational landscape of uterine and ovarian carcinosarcomas implicates histone genes in epithelial–mesenchymal transition," *Proceedings of the National Academy of Sciences,* vol. 113, no. 43, pp. 12238-12243, 2016, doi: 10.1073/pnas.1614120113.
[129] R. L. Bennett *et al.*, "A Mutation in Histone H2B Represents a New Class of Oncogenic Driver," *Cancer Discovery,* vol. 9, no. 10, pp. 1438-1451, 2019, doi: 10.1158/2159-8290.CD-19-0393.
[130] J. D. Bagert *et al.*, "Oncohistone mutations enhance chromatin remodeling and alter cell fates," *Nature Chemical Biology,* vol. 17, no. 4, pp. 403-411, 2021, doi: 10.1038/s41589-021-00738-1.
[131] B. A. Nacev *et al.*, "The expanding landscape of 'oncohistone' mutations in human cancers," *Nature,* vol. 567, no. 7749, pp. 473-478, 2019, doi: 10.1038/s41586-019-1038-1.
[132] B. Vogelstein, N. Papadopoulos, V. E. Velculescu, S. Zhou, L. A. Diaz, Jr., and K. W. Kinzler, "Cancer genome landscapes," *Science,* vol. 339, no. 6127, pp. 1546-58, Mar 29 2013, doi: 10.1126/science.1235122.
[133] L. K. Gopi and B. L. Kidder, "Integrative pan cancer analysis reveals epigenomic variation in cancer type and cell specific chromatin domains," *Nat Commun,* vol. 12, no. 1, p. 1419, Mar 3 2021, doi: 10.1038/s41467-021-21707-1.
[134] F. Berger, "Emil Heitz, a true epigenetics pioneer," *Nat Rev Mol Cell Biol,* vol. 20, no. 10, p. 572, Oct 2019, doi: 10.1038/s41580-019-0161-z.
[135] S. W. Brown, "Heterochromatin," *Science,* vol. 151, no. 3709, pp. 417-25, Jan 28 1966, doi: 10.1126/science.151.3709.417.
[136] N. L. van Berkum *et al.*, "Hi-C: a method to study the three-dimensional architecture of genomes," *J Vis Exp,* no. 39, May 6 2010, doi: 10.3791/1869.
[137] M. Simonis *et al.*, "Nuclear organization of active and inactive chromatin domains uncovered by chromosome conformation capture-on-chip (4C)," *Nat Genet,* vol. 38, no. 11, pp. 1348-54, Nov 2006, doi: 10.1038/ng1896.
[138] Q. Wang, Q. Sun, D. M. Czajkowsky, and Z. Shao, "Sub-kb Hi-C in D. melanogaster reveals conserved characteristics of TADs between insect and mammalian cells," *Nat Commun,* vol. 9, no. 1, p. 188, Jan 15 2018, doi: 10.1038/s41467-017-02526-9.
[139] E. P. Nora *et al.*, "Targeted Degradation of CTCF Decouples Local Insulation of Chromosome Domains from Genomic Compartmentalization," *Cell,* vol. 169, no. 5, pp. 930-944 e22, May 18 2017, doi: 10.1016/j.cell.2017.05.004.
[140] K. C. Akdemir *et al.*, "Disruption of chromatin folding domains by somatic genomic rearrangements in human cancer," *Nat Genet,* vol. 52, no. 3, pp. 294-305, Mar 2020, doi: 10.1038/s41588-019-0564-y.
[141] C. Gerner, J. Gotzmann, U. Frohwein, C. Schamberger, A. Ellinger, and G. Sauermann, "Proteome analysis of nuclear matrix proteins during apoptotic chromatin condensation," *Cell Death Differ,* vol. 9, no. 6, pp. 671-81, Jun 2002, doi: 10.1038/sj.cdd.4401010.
[142] J. H. Wilson and T. Hunt, *Molecular biology of the cell, 4th edition : a problems approach*. New York ; London: Garland Science (in English), 2002, pp. xxii, 711 p. : ill.
[143] J. Liu, M. Ali, and Q. Zhou, "Establishment and evolution of heterochromatin," *Ann N Y Acad Sci,* vol. 1476, no. 1, pp. 59-77, Sep 2020, doi: 10.1111/nyas.14303.
[144] Y. C. G. Lee and G. H. Karpen, "Pervasive epigenetic effects of Drosophila euchromatic transposable elements impact their evolution," *Elife,* vol. 6, Jul 11 2017, doi: 10.7554/eLife.25762.

[145] R. Rebollo *et al.*, "Retrotransposon-induced heterochromatin spreading in the mouse revealed by insertional polymorphisms," *PLoS Genet,* vol. 7, no. 9, p. e1002301, Sep 2011, doi: 10.1371/journal.pgen.1002301.
[146] A. Ebert *et al.*, "Su(var) genes regulate the balance between euchromatin and heterochromatin in Drosophila," *Genes Dev,* vol. 18, no. 23, pp. 2973-83, Dec 1 2004, doi: 10.1101/gad.323004.
[147] J. R. Dixon *et al.*, "Topological domains in mammalian genomes identified by analysis of chromatin interactions," *Nature,* vol. 485, no. 7398, pp. 376-80, Apr 11 2012, doi: 10.1038/nature11082.
[148] M. R. Mumbach *et al.*, "HiChIP: efficient and sensitive analysis of protein-directed genome architecture," *Nat Methods,* vol. 13, no. 11, pp. 919-922, Nov 2016, doi: 10.1038/nmeth.3999.
[149] J. M. Dowen *et al.*, "Control of cell identity genes occurs in insulated neighborhoods in mammalian chromosomes," *Cell,* vol. 159, no. 2, pp. 374-387, Oct 9 2014, doi: 10.1016/j.cell.2014.09.030.
[150] B. E. Gryder, J. Khan, and B. Z. Stanton, "Measurement of differential chromatin interactions with absolute quantification of architecture (AQuA-HiChIP)," *Nat Protoc,* vol. 15, no. 3, pp. 1209-1236, Mar 2020, doi: 10.1038/s41596-019-0285-9.
[151] M. M. Adeel *et al.*, "Structural Variations of the 3D Genome Architecture in Cervical Cancer Development," *Front Cell Dev Biol,* vol. 9, p. 706375, 2021, doi: 10.3389/fcell.2021.706375.
[152] R. Vilarrasa-Blasi *et al.*, "Dynamics of genome architecture and chromatin function during human B cell differentiation and neoplastic transformation," *Nat Commun,* vol. 12, no. 1, p. 651, Jan 28 2021, doi: 10.1038/s41467-020-20849-y.
[153] T. Kim *et al.*, "Comparative characterization of 3D chromatin organization in triple-negative breast cancers," *Exp Mol Med,* vol. 54, no. 5, pp. 585-600, May 2022, doi: 10.1038/s12276-022-00768-2.
[154] S. K. Rhie *et al.*, "A high-resolution 3D epigenomic map reveals insights into the creation of the prostate cancer transcriptome," *Nat Commun,* vol. 10, no. 1, p. 4154, Sep 12 2019, doi: 10.1038/s41467-019-12079-8.
[155] C. Gurrion, M. Uriostegui, and M. Zurita, "Heterochromatin Reduction Correlates with the Increase of the KDM4B and KDM6A Demethylases and the Expression of Pericentromeric DNA during the Acquisition of a Transformed Phenotype," *J Cancer,* vol. 8, no. 14, pp. 2866-2875, 2017, doi: 10.7150/jca.19477.
[156] S. Pradhan *et al.*, "Depletion of HP1alpha alters the mechanical properties of MCF7 nuclei," *Biophys J,* vol. 120, no. 13, pp. 2631-2643, Jul 6 2021, doi: 10.1016/j.bpj.2021.05.017.
[157] Y. Chen *et al.*, "Wnt-Induced Stabilization of KDM4C Is Required for Wnt/beta-Catenin Target Gene Expression and Glioblastoma Tumorigenesis," *Cancer Res,* vol. 80, no. 5, pp. 1049-1063, Mar 1 2020, doi: 10.1158/0008-5472.CAN-19-1229.
[158] P. Sehgal and P. Chaturvedi, "Chromatin and Cancer: Implications of Disrupted Chromatin Organization in Tumorigenesis and Its Diversification," *Cancers (Basel),* vol. 15, no. 2, Jan 11 2023, doi: 10.3390/cancers15020466.
[159] N. Wang, T. Ma, and B. Yu, "Targeting epigenetic regulators to overcome drug resistance in cancers," *Signal Transduct Target Ther,* vol. 8, no. 1, p. 69, Feb 17 2023, doi: 10.1038/s41392-023-01341-7.

[160] T. Ugai *et al.*, "Is early-onset cancer an emerging global epidemic? Current evidence and future implications," *Nat Rev Clin Oncol,* vol. 19, no. 10, pp. 656-673, Oct 2022, doi: 10.1038/s41571-022-00672-8.
[161] Y. Cheng *et al.*, "Targeting epigenetic regulators for cancer therapy: mechanisms and advances in clinical trials," *Signal Transduct Target Ther,* vol. 4, p. 62, 2019, doi: 10.1038/s41392-019-0095-0.
[162] S. Feng and D. D. De Carvalho, "Clinical advances in targeting epigenetics for cancer therapy," *FEBS J,* vol. 289, no. 5, pp. 1214-1239, Mar 2022, doi: 10.1111/febs.15750.
[163] N. Ahuja, H. Easwaran, and S. B. Baylin, "Harnessing the potential of epigenetic therapy to target solid tumors," *J Clin Invest,* vol. 124, no. 1, pp. 56-63, Jan 2014, doi: 10.1172/JCI69736.
[164] L. A. Garraway and E. S. Lander, "Lessons from the cancer genome," *Cell,* vol. 153, no. 1, pp. 17-37, Mar 28 2013, doi: 10.1016/j.cell.2013.03.002.
[165] P. A. Jones and S. M. Taylor, "Cellular differentiation, cytidine analogs and DNA methylation," *Cell,* vol. 20, no. 1, pp. 85-93, May 1980, doi: 10.1016/0092-8674(80)90237-8.
[166] E. Kaminskas, A. T. Farrell, Y. C. Wang, R. Sridhara, and R. Pazdur, "FDA drug approval summary: azacitidine (5-azacytidine, Vidaza) for injectable suspension," *Oncologist,* vol. 10, no. 3, pp. 176-82, Mar 2005, doi: 10.1634/theoncologist.10-3-176.
[167] R. W. Robey, K. M. Pluchino, M. D. Hall, A. T. Fojo, S. E. Bates, and M. M. Gottesman, "Revisiting the role of ABC transporters in multidrug-resistant cancer," *Nat Rev Cancer,* vol. 18, no. 7, pp. 452-464, Jul 2018, doi: 10.1038/s41568-018-0005-8.
[168] S. Das, N. Shukla, S. S. Singh, S. Kushwaha, and R. Shrivastava, "Mechanism of interaction between autophagy and apoptosis in cancer," *Apoptosis,* vol. 26, no. 9-10, pp. 512-533, Oct 2021, doi: 10.1007/s10495-021-01687-9.
[169] M. L. Jin and K. W. Jeong, "Histone modifications in drug-resistant cancers: From a cancer stem cell and immune evasion perspective," *Exp Mol Med,* vol. 55, no. 7, pp. 1333-1347, Jul 2023, doi: 10.1038/s12276-023-01014-z.
[170] N. Takebe *et al.*, "Targeting Notch, Hedgehog, and Wnt pathways in cancer stem cells: clinical update," *Nat Rev Clin Oncol,* vol. 12, no. 8, pp. 445-64, Aug 2015, doi: 10.1038/nrclinonc.2015.61.
[171] X. Zhang *et al.*, "Alterations in the Global Proteome and Phosphoproteome in Third Generation EGFR TKI Resistance Reveal Drug Targets to Circumvent Resistance," *Cancer Res,* vol. 81, no. 11, pp. 3051-3066, Jun 1 2021, doi: 10.1158/0008-5472.CAN-20-2435.
[172] N. Wajapeyee and R. Gupta, "Epigenetic Alterations and Mechanisms That Drive Resistance to Targeted Cancer Therapies," *Cancer Res,* vol. 81, no. 22, pp. 5589-5595, Nov 15 2021, doi: 10.1158/0008-5472.CAN-21-1606.
[173] A. J. Sabnis and T. G. Bivona, "Principles of Resistance to Targeted Cancer Therapy: Lessons from Basic and Translational Cancer Biology," *Trends Mol Med,* vol. 25, no. 3, pp. 185-197, Mar 2019, doi: 10.1016/j.molmed.2018.12.009.
[174] D. Bayik and J. D. Lathia, "Cancer stem cell-immune cell crosstalk in tumour progression," *Nat Rev Cancer,* vol. 21, no. 8, pp. 526-536, Aug 2021, doi: 10.1038/s41568-021-00366-w.

[175] Y. Yang and Y. Wang, "Role of Epigenetic Regulation in Plasticity of Tumor Immune Microenvironment," *Front Immunol,* vol. 12, p. 640369, 2021, doi: 10.3389/fimmu.2021.640369.
[176] J. Sun *et al.*, "miR-137 mediates the functional link between c-Myc and EZH2 that regulates cisplatin resistance in ovarian cancer," *Oncogene,* vol. 38, no. 4, pp. 564-580, Jan 2019, doi: 10.1038/s41388-018-0459-x.
[177] X. Liu *et al.*, "LINC00665 Induces Acquired Resistance to Gefitinib through Recruiting EZH2 and Activating PI3K/AKT Pathway in NSCLC," *Mol Ther Nucleic Acids,* vol. 16, pp. 155-161, Jun 7 2019, doi: 10.1016/j.omtn.2019.02.010.
[178] Y. Li *et al.*, "Downregulation of MEIS1 mediated by ELFN1-AS1/EZH2/DNMT3a axis promotes tumorigenesis and oxaliplatin resistance in colorectal cancer," *Signal Transduct Target Ther,* vol. 7, no. 1, p. 87, Mar 30 2022, doi: 10.1038/s41392-022-00902-6.
[179] Z. Liu *et al.*, "SETDB1 interactions with PELP1 contributes to breast cancer endocrine therapy resistance," *Breast Cancer Res,* vol. 24, no. 1, p. 26, Apr 8 2022, doi: 10.1186/s13058-022-01520-4.
[180] M. Zhou *et al.*, "Targeting protein lysine methyltransferase G9A impairs self-renewal of chronic myelogenous leukemia stem cells via upregulation of SOX6," *Oncogene,* vol. 40, no. 20, pp. 3564-3577, May 2021, doi: 10.1038/s41388-021-01799-1.
[181] H. Zhang *et al.*, "MiR-7, inhibited indirectly by lincRNA HOTAIR, directly inhibits SETDB1 and reverses the EMT of breast cancer stem cells by downregulating the STAT3 pathway," *Stem Cells,* vol. 32, no. 11, pp. 2858-68, Nov 2014, doi: 10.1002/stem.1795.
[182] Z. Hou *et al.*, "Blocking histone methyltransferase SETDB1 inhibits tumorigenesis and enhances cetuximab sensitivity in colorectal cancer," *Cancer Lett,* vol. 487, pp. 63-73, Sep 1 2020, doi: 10.1016/j.canlet.2020.05.029.
[183] Z. Wang, P. Hu, F. Tang, and C. Xie, "HDAC6-mediated EGFR stabilization and activation restrict cell response to sorafenib in non-small cell lung cancer cells," *Med Oncol,* vol. 33, no. 5, p. 50, May 2016, doi: 10.1007/s12032-016-0765-5.
[184] W. B. Yang *et al.*, "Increased activation of HDAC1/2/6 and Sp1 underlies therapeutic resistance and tumor growth in glioblastoma," *Neuro Oncol,* vol. 22, no. 10, pp. 1439-1451, Oct 14 2020, doi: 10.1093/neuonc/noaa103.
[185] A. E. Witt *et al.*, "Identification of a cancer stem cell-specific function for the histone deacetylases, HDAC1 and HDAC7, in breast and ovarian cancer," *Oncogene,* vol. 36, no. 12, pp. 1707-1720, Mar 23 2017, doi: 10.1038/onc.2016.337.
[186] M. Yano *et al.*, "Association of histone deacetylase expression with histology and prognosis of ovarian cancer," *Oncol Lett,* vol. 15, no. 3, pp. 3524-3531, Mar 2018, doi: 10.3892/ol.2018.7726.
[187] N. Bora-Singhal *et al.*, "Novel HDAC11 inhibitors suppress lung adenocarcinoma stem cell self-renewal and overcome drug resistance by suppressing Sox2," *Sci Rep,* vol. 10, no. 1, p. 4722, Mar 13 2020, doi: 10.1038/s41598-020-61295-6.
[188] T. Reid *et al.*, "Phase II trial of the histone deacetylase inhibitor pivaloyloxymethyl butyrate (Pivanex, AN-9) in advanced non-small cell lung cancer," *Lung Cancer,* vol. 45, no. 3, pp. 381-6, Sep 2004, doi: 10.1016/j.lungcan.2004.03.002.
[189] L. Santo *et al.*, "Preclinical activity, pharmacodynamic, and pharmacokinetic properties of a selective HDAC6 inhibitor, ACY-1215, in combination with bortezomib in multiple myeloma," *Blood,* vol. 119, no. 11, pp. 2579-89, Mar 15 2012, doi: 10.1182/blood-2011-10-387365.

[190] R. Frye *et al.*, "Romidepsin: a new drug for the treatment of cutaneous T-cell lymphoma," *Clin J Oncol Nurs,* vol. 16, no. 2, pp. 195-204, Apr 2012, doi: 10.1188/12.CJON.195-204.
[191] C. Zwergel, S. Valente, C. Jacob, and A. Mai, "Emerging approaches for histone deacetylase inhibitor drug discovery," *Expert Opin Drug Discov,* vol. 10, no. 6, pp. 599-613, Jun 2015, doi: 10.1517/17460441.2015.1038236.
[192] V. Ribrag *et al.*, "Safety and efficacy of abexinostat, a pan-histone deacetylase inhibitor, in non-Hodgkin lymphoma and chronic lymphocytic leukemia: results of a phase II study," *Haematologica,* vol. 102, no. 5, pp. 903-909, May 2017, doi: 10.3324/haematol.2016.154377.
[193] S. Geurs, D. Clarisse, K. De Bosscher, and M. D'Hooghe, "The Zinc-Binding Group Effect: Lessons from Non-Hydroxamic Acid Vorinostat Analogs," *J Med Chem,* vol. 66, no. 12, pp. 7698-7729, Jun 22 2023, doi: 10.1021/acs.jmedchem.3c00226.
[194] M. L. Guzman *et al.*, "Selective activity of the histone deacetylase inhibitor AR-42 against leukemia stem cells: a novel potential strategy in acute myelogenous leukemia," *Mol Cancer Ther,* vol. 13, no. 8, pp. 1979-90, Aug 2014, doi: 10.1158/1535-7163.MCT-13-0963.
[195] M. A. Bilen *et al.*, "Phase I trial of valproic acid and lenalidomide in patients with advanced cancer," *Cancer Chemother Pharmacol,* vol. 75, no. 4, pp. 869-74, Apr 2015, doi: 10.1007/s00280-015-2695-x.
[196] Y. Shi *et al.*, "Results from a multicenter, open-label, pivotal phase II study of chidamide in relapsed or refractory peripheral T-cell lymphoma," *Ann Oncol,* vol. 26, no. 8, pp. 1766-71, Aug 2015, doi: 10.1093/annonc/mdv237.
[197] M. Dong *et al.*, "Phase I study of chidamide (CS055/HBI-8000), a new histone deacetylase inhibitor, in patients with advanced solid tumors and lymphomas," *Cancer Chemother Pharmacol,* vol. 69, no. 6, pp. 1413-22, Jun 2012, doi: 10.1007/s00280-012-1847-5.
[198] L. R. Pauer *et al.*, "Phase I study of oral CI-994 in combination with carboplatin and paclitaxel in the treatment of patients with advanced solid tumors," *Cancer Invest,* vol. 22, no. 6, pp. 886-96, 2004, doi: 10.1081/cnv-200039852.
[199] J. Knipstein and L. Gore, "Entinostat for treatment of solid tumors and hematologic malignancies," *Expert Opin Investig Drugs,* vol. 20, no. 10, pp. 1455-67, Oct 2011, doi: 10.1517/13543784.2011.613822.
[200] J. H. Lee, M. L. Choy, L. Ngo, S. S. Foster, and P. A. Marks, "Histone deacetylase inhibitor induces DNA damage, which normal but not transformed cells can repair," *Proc Natl Acad Sci U S A,* vol. 107, no. 33, pp. 14639-44, Aug 17 2010, doi: 10.1073/pnas.1008522107.
[201] B. Groselj, N. L. Sharma, F. C. Hamdy, M. Kerr, and A. E. Kiltie, "Histone deacetylase inhibitors as radiosensitisers: effects on DNA damage signalling and repair," *Br J Cancer,* vol. 108, no. 4, pp. 748-54, Mar 5 2013, doi: 10.1038/bjc.2013.21.
[202] L. H. Wright and D. R. Menick, "A class of their own: exploring the nondeacetylase roles of class IIa HDACs in cardiovascular disease," *American Journal of Physiology-Heart and Circulatory Physiology,* vol. 311, no. 1, pp. H199-H206, 2016, doi: 10.1152/ajpheart.00271.2016.
[203] P. Chun, "Histone deacetylase inhibitors in hematological malignancies and solid tumors," *Arch Pharm Res,* vol. 38, no. 6, pp. 933-49, Jun 2015, doi: 10.1007/s12272-015-0571-1.
[204] M. Tomosugi *et al.*, "Retinoblastoma gene-independent G1 phase arrest by flavone, phosphatidylinositol 3-kinase inhibitor, and histone deacetylase inhibitor," *Cancer Sci,* vol. 103, no. 12, pp. 2139-43, Dec 2012, doi: 10.1111/cas.12012.

[205] G. Shanmugam, S. Rakshit, and K. Sarkar, "HDAC inhibitors: Targets for tumor therapy, immune modulation and lung diseases," *Transl Oncol,* vol. 16, p. 101312, Feb 2022, doi: 10.1016/j.tranon.2021.101312.
[206] V. Sandor *et al.*, "P21-dependent g(1)arrest with downregulation of cyclin D1 and upregulation of cyclin E by the histone deacetylase inhibitor FR901228," *Br J Cancer,* vol. 83, no. 6, pp. 817-25, Sep 2000, doi: 10.1054/bjoc.2000.1327.
[207] Z. Dong, Y. Yang, S. Liu, J. Lu, B. Huang, and Y. Zhang, "HDAC inhibitor PAC-320 induces G2/M cell cycle arrest and apoptosis in human prostate cancer," *Oncotarget,* vol. 9, no. 1, pp. 512-523, Jan 2 2018, doi: 10.18632/oncotarget.23070.
[208] H. M. Findeisen *et al.*, "Epigenetic regulation of vascular smooth muscle cell proliferation and neointima formation by histone deacetylase inhibition," *Arterioscler Thromb Vasc Biol,* vol. 31, no. 4, pp. 851-60, Apr 2011, doi: 10.1161/ATVBAHA.110.221952.
[209] E. Batlle and H. Clevers, "Cancer stem cells revisited," *Nat Med,* vol. 23, no. 10, pp. 1124-1134, Oct 6 2017, doi: 10.1038/nm.4409.
[210] A. U. Ahmed, B. Auffinger, and M. S. Lesniak, "Understanding glioma stem cells: rationale, clinical relevance and therapeutic strategies," *Expert review of neurotherapeutics,* vol. 13, no. 5, pp. 545-55, 2013, doi: 10.1586/ern.13.42.
[211] A. Dirkse *et al.*, "Stem cell-associated heterogeneity in Glioblastoma results from intrinsic tumor plasticity shaped by the microenvironment," *Nat Commun,* vol. 10, no. 1, p. 1787, Apr 16 2019, doi: 10.1038/s41467-019-09853-z.
[212] L. Walcher *et al.*, "Cancer Stem Cells-Origins and Biomarkers: Perspectives for Targeted Personalized Therapies," *Front Immunol,* vol. 11, p. 1280, 2020, doi: 10.3389/fimmu.2020.01280.
[213] M. S. Roca, E. Di Gennaro, and A. Budillon, "Implication for Cancer Stem Cells in Solid Cancer Chemo-Resistance: Promising Therapeutic Strategies Based on the Use of HDAC Inhibitors," *J Clin Med,* vol. 8, no. 7, Jun 26 2019, doi: 10.3390/jcm8070912.
[214] A. Pasto *et al.*, "Cancer stem cells from epithelial ovarian cancer patients privilege oxidative phosphorylation, and resist glucose deprivation," *Oncotarget,* vol. 5, no. 12, pp. 4305-19, Jun 30 2014, doi: 10.18632/oncotarget.2010.
[215] M. Y. Wu, J. Fu, X. Xiao, J. Wu, and R. C. Wu, "MiR-34a regulates therapy resistance by targeting HDAC1 and HDAC7 in breast cancer," *Cancer Lett,* vol. 354, no. 2, pp. 311-9, Nov 28 2014, doi: 10.1016/j.canlet.2014.08.031.
[216] M. H. Cai *et al.*, "Depletion of HDAC1, 7 and 8 by Histone Deacetylase Inhibition Confers Elimination of Pancreatic Cancer Stem Cells in Combination with Gemcitabine," *Sci Rep,* vol. 8, no. 1, p. 1621, Jan 26 2018, doi: 10.1038/s41598-018-20004-0.
[217] M. Terranova-Barberio *et al.*, "Synergistic antitumor interaction between valproic acid, capecitabine and radiotherapy in colorectal cancer: critical role of p53," *J Exp Clin Cancer Res,* vol. 36, no. 1, p. 177, Dec 6 2017, doi: 10.1186/s13046-017-0647-5.
[218] M. A. Salvador *et al.*, "The histone deacetylase inhibitor abexinostat induces cancer stem cells differentiation in breast cancer with low Xist expression," *Clin Cancer Res,* vol. 19, no. 23, pp. 6520-31, Dec 1 2013, doi: 10.1158/1078-0432.CCR-13-0877.
[219] M. Wei *et al.*, "Valproic acid sensitizes metformin-resistant human renal cell carcinoma cells by upregulating H3 acetylation and EMT reversal," *BMC Cancer,* vol. 18, no. 1, p. 434, Apr 17 2018, doi: 10.1186/s12885-018-4344-3.
[220] H. Han *et al.*, "Hippo signaling dysfunction induces cancer cell addiction to YAP," *Oncogene,* vol. 37, no. 50, pp. 6414-6424, Dec 2018, doi: 10.1038/s41388-018-0419-5.

[221] B. Deskin, J. Lasky, Y. Zhuang, and B. Shan, "Requirement of HDAC6 for activation of Notch1 by TGF-beta1," *Sci Rep,* vol. 6, p. 31086, Aug 8 2016, doi: 10.1038/srep31086.
[222] G. Qin *et al.*, "Panobinostat (LBH589) inhibits Wnt/beta-catenin signaling pathway via upregulating APCL expression in breast cancer," *Cell Signal,* vol. 59, pp. 62-75, Jul 2019, doi: 10.1016/j.cellsig.2019.03.014.
[223] J. L. Guerriero *et al.*, "Class IIa HDAC inhibition reduces breast tumours and metastases through anti-tumour macrophages," *Nature,* vol. 543, no. 7645, pp. 428-432, 2017, doi: 10.1038/nature21409.
[224] S. Shen and A. P. Kozikowski, "Why Hydroxamates May Not Be the Best Histone Deacetylase Inhibitors--What Some May Have Forgotten or Would Rather Forget?," *ChemMedChem,* vol. 11, no. 1, pp. 15-21, Jan 5 2016, doi: 10.1002/cmdc.201500486.
[225] J. McDermott and A. Jimeno, "Belinostat for the treatment of peripheral T-cell lymphomas," *Drugs Today (Barc),* vol. 50, no. 5, pp. 337-45, May 2014, doi: 10.1358/dot.2014.50.5.2138703.
[226] P. G. Richardson *et al.*, "Panobinostat: a novel pan-deacetylase inhibitor for the treatment of relapsed or relapsed and refractory multiple myeloma," *Expert Rev Anticancer Ther,* vol. 15, no. 7, pp. 737-48, 2015, doi: 10.1586/14737140.2015.1047770.
[227] P. J. Wood *et al.*, "A phase I study of panobinostat in pediatric patients with refractory solid tumors, including CNS tumors," *Cancer Chemother Pharmacol,* vol. 82, no. 3, pp. 493-503, Sep 2018, doi: 10.1007/s00280-018-3634-4.
[228] S. Karthik, R. Sankar, K. Varunkumar, and V. Ravikumar, "Romidepsin induces cell cycle arrest, apoptosis, histone hyperacetylation and reduces matrix metalloproteinases 2 and 9 expression in bortezomib sensitized non-small cell lung cancer cells," *Biomed Pharmacother,* vol. 68, no. 3, pp. 327-34, Apr 2014, doi: 10.1016/j.biopha.2014.01.002.
[229] A. Younes *et al.*, "Mocetinostat for relapsed classical Hodgkin's lymphoma: an open-label, single-arm, phase 2 trial," *Lancet Oncol,* vol. 12, no. 13, pp. 1222-8, Dec 2011, doi: 10.1016/S1470-2045(11)70265-0.
[230] D. T. Gerokonstantis *et al.*, "N-(2-Aminophenyl)-benzamide Inhibitors of Class I HDAC Enzymes with Antiproliferative and Antifibrotic Activity," *J Med Chem,* vol. 66, no. 20, pp. 14357-14376, Oct 26 2023, doi: 10.1021/acs.jmedchem.3c01422.
[231] M. Gottlicher *et al.*, "Valproic acid defines a novel class of HDAC inhibitors inducing differentiation of transformed cells," *EMBO J,* vol. 20, no. 24, pp. 6969-78, Dec 17 2001, doi: 10.1093/emboj/20.24.6969.
[232] B. S. Mann, J. R. Johnson, M. H. Cohen, R. Justice, and R. Pazdur, "FDA approval summary: vorinostat for treatment of advanced primary cutaneous T-cell lymphoma," *Oncologist,* vol. 12, no. 10, pp. 1247-52, Oct 2007, doi: 10.1634/theoncologist.12-10-1247.
[233] A. T. Brunetto *et al.*, "First-in-human, pharmacokinetic and pharmacodynamic phase I study of Resminostat, an oral histone deacetylase inhibitor, in patients with advanced solid tumors," *Clin Cancer Res,* vol. 19, no. 19, pp. 5494-504, Oct 1 2013, doi: 10.1158/1078-0432.CCR-13-0735.
[234] M. G. Fernandez-Barrena, M. Arechederra, L. Colyn, C. Berasain, and M. A. Avila, "Epigenetics in hepatocellular carcinoma development and therapy: The tip of the iceberg," *JHEP Rep,* vol. 2, no. 6, p. 100167, Dec 2020, doi: 10.1016/j.jhepr.2020.100167.
[235] M. Galli *et al.*, "A phase II multiple dose clinical trial of histone deacetylase inhibitor ITF2357 in patients with relapsed or progressive multiple myeloma," *Ann Hematol,* vol. 89, no. 2, pp. 185-90, Feb 2010, doi: 10.1007/s00277-009-0793-8.

[236] S. L. Locatelli *et al.*, "BIM upregulation and ROS-dependent necroptosis mediate the antitumor effects of the HDACi Givinostat and Sorafenib in Hodgkin lymphoma cell line xenografts," *Leukemia,* vol. 28, no. 9, pp. 1861-71, Sep 2014, doi: 10.1038/leu.2014.81.
[237] A. P. Zorzi *et al.*, "A phase I study of histone deacetylase inhibitor, pracinostat (SB939), in pediatric patients with refractory solid tumors: IND203 a trial of the NCIC IND program/C17 pediatric phase I consortium," *Pediatr Blood Cancer,* vol. 60, no. 11, pp. 1868-74, Nov 2013, doi: 10.1002/pbc.24694.
[238] E. Choy *et al.*, "Phase 1 study of oral abexinostat, a histone deacetylase inhibitor, in combination with doxorubicin in patients with metastatic sarcoma," *Cancer,* vol. 121, no. 8, pp. 1223-30, Apr 15 2015, doi: 10.1002/cncr.29175.
[239] B. Venugopal *et al.*, "A phase I study of quisinostat (JNJ-26481585), an oral hydroxamate histone deacetylase inhibitor with evidence of target modulation and antitumor activity, in patients with advanced solid tumors," *Clin Cancer Res,* vol. 19, no. 15, pp. 4262-72, Aug 1 2013, doi: 10.1158/1078-0432.CCR-13-0312.
[240] U. Banerji *et al.*, "A phase I pharmacokinetic and pharmacodynamic study of CHR-3996, an oral class I selective histone deacetylase inhibitor in refractory solid tumors," *Clin Cancer Res,* vol. 18, no. 9, pp. 2687-94, May 1 2012, doi: 10.1158/1078-0432.CCR-11-3165.
[241] T. Shimizu *et al.*, "Phase I first-in-human study of CUDC-101, a multitargeted inhibitor of HDACs, EGFR, and HER2 in patients with advanced solid tumors," *Clin Cancer Res,* vol. 20, no. 19, pp. 5032-40, Oct 1 2014, doi: 10.1158/1078-0432.CCR-14-0570.
[242] C. Qian *et al.*, "Cancer network disruption by a single molecule inhibitor targeting both histone deacetylase activity and phosphatidylinositol 3-kinase signaling," *Clin Cancer Res,* vol. 18, no. 15, pp. 4104-13, Aug 1 2012, doi: 10.1158/1078-0432.CCR-12-0055.
[243] T. Iannitti and B. Palmieri, "Clinical and experimental applications of sodium phenylbutyrate," *Drugs R D,* vol. 11, no. 3, pp. 227-49, Sep 1 2011, doi: 10.2165/11591280-000000000-00000.
[244] S. Kikuchi *et al.*, "Class IIa HDAC inhibition enhances ER stress-mediated cell death in multiple myeloma," *Leukemia,* vol. 29, no. 9, pp. 1918-27, Sep 2015, doi: 10.1038/leu.2015.83.
[245] L. Urwanisch *et al.*, "The Class IIA Histone Deacetylase (HDAC) Inhibitor TMP269 Downregulates Ribosomal Proteins and Has Anti-Proliferative and Pro-Apoptotic Effects on AML Cells," *Cancers (Basel),* vol. 15, no. 4, Feb 7 2023, doi: 10.3390/cancers15041039.
[246] G. Wang *et al.*, "Class I and class II histone deacetylases are potential therapeutic targets for treating pancreatic cancer," *PLoS One,* vol. 7, no. 12, p. e52095, 2012, doi: 10.1371/journal.pone.0052095.
[247] S. Ishikawa *et al.*, "Statins inhibit tumor progression via an enhancer of zeste homolog 2-mediated epigenetic alteration in colorectal cancer," *Int J Cancer,* vol. 135, no. 11, pp. 2528-36, Dec 1 2014, doi: 10.1002/ijc.28672.
[248] L. Colarossi *et al.*, "Inhibition of histone deacetylase 4 increases cytotoxicity of docetaxel in gastric cancer cells," *Proteomics Clin Appl,* vol. 8, no. 11-12, pp. 924-31, Dec 2014, doi: 10.1002/prca.201400058.
[249] M. Bekes, D. R. Langley, and C. M. Crews, "PROTAC targeted protein degraders: the past is prologue," *Nat Rev Drug Discov,* vol. 21, no. 3, pp. 181-200, Mar 2022, doi: 10.1038/s41573-021-00371-6.

[250] Z. Li and W. G. Zhu, "Targeting histone deacetylases for cancer therapy: from molecular mechanisms to clinical implications," *Int J Biol Sci,* vol. 10, no. 7, pp. 757-70, 2014, doi: 10.7150/ijbs.9067.
[251] Y. Xiong *et al.*, "Chemo-proteomics exploration of HDAC degradability by small molecule degraders," *Cell Chem Biol,* vol. 28, no. 10, pp. 1514-1527 e4, Oct 21 2021, doi: 10.1016/j.chembiol.2021.07.002.
[252] F. Fischer, L. A. Alves Avelar, L. Murray, and T. Kurz, "Designing HDAC-PROTACs: lessons learned so far," *Future Med Chem,* vol. 14, no. 3, pp. 143-166, Jan 2022, doi: 10.4155/fmc-2021-0206.
[253] X. M. Anguela and K. A. High, "Entering the Modern Era of Gene Therapy," *Annu Rev Med,* vol. 70, pp. 273-288, Jan 27 2019, doi: 10.1146/annurev-med-012017-043332.
[254] B. Hu *et al.*, "Therapeutic siRNA: state of the art," *Signal Transduct Target Ther,* vol. 5, no. 1, p. 101, Jun 19 2020, doi: 10.1038/s41392-020-0207-x.
[255] H. Li, Y. Yang, W. Hong, M. Huang, M. Wu, and X. Zhao, "Applications of genome editing technology in the targeted therapy of human diseases: mechanisms, advances and prospects," *Signal Transduct Target Ther,* vol. 5, no. 1, p. 1, Jan 3 2020, doi: 10.1038/s41392-019-0089-y.
[256] A. Fire, S. Xu, M. K. Montgomery, S. A. Kostas, S. E. Driver, and C. C. Mello, "Potent and specific genetic interference by double-stranded RNA in Caenorhabditis elegans," *Nature,* vol. 391, no. 6669, pp. 806-11, Feb 19 1998, doi: 10.1038/35888.
[257] A. Wittrup and J. Lieberman, "Knocking down disease: a progress report on siRNA therapeutics," *Nat Rev Genet,* vol. 16, no. 9, pp. 543-52, Sep 2015, doi: 10.1038/nrg3978.
[258] S. A. Dar, A. Thakur, A. Qureshi, and M. Kumar, "siRNAmod: A database of experimentally validated chemically modified siRNAs," *Sci Rep,* vol. 6, p. 20031, Jan 28 2016, doi: 10.1038/srep20031.
[259] D. J. Foster *et al.*, "Advanced siRNA Designs Further Improve In Vivo Performance of GalNAc-siRNA Conjugates," *Mol Ther,* vol. 26, no. 3, pp. 708-717, Mar 7 2018, doi: 10.1016/j.ymthe.2017.12.021.
[260] M. Jayaraman *et al.*, "Maximizing the potency of siRNA lipid nanoparticles for hepatic gene silencing in vivo," *Angew Chem Int Ed Engl,* vol. 51, no. 34, pp. 8529-33, Aug 20 2012, doi: 10.1002/anie.201203263.
[261] K. M. Brown *et al.*, "Expanding RNAi therapeutics to extrahepatic tissues with lipophilic conjugates," *Nat Biotechnol,* vol. 40, no. 10, pp. 1500-1508, Oct 2022, doi: 10.1038/s41587-022-01334-x.
[262] T. Ahmadzada, G. Reid, and D. R. McKenzie, "Fundamentals of siRNA and miRNA therapeutics and a review of targeted nanoparticle delivery systems in breast cancer," *Biophys Rev,* vol. 10, no. 1, pp. 69-86, Feb 2018, doi: 10.1007/s12551-017-0392-1.
[263] C. Qiu *et al.*, "Regulating intracellular fate of siRNA by endoplasmic reticulum membrane-decorated hybrid nanoplexes," *Nat Commun,* vol. 10, no. 1, p. 2702, Jun 20 2019, doi: 10.1038/s41467-019-10562-w.
[264] D. Huang *et al.*, "Continuous Vector-free Gene Transfer with a Novel Microfluidic Chip and Nanoneedle Array," *Curr Drug Deliv,* vol. 16, no. 2, pp. 164-170, 2019, doi: 10.2174/1567201815666181017095044.
[265] A. Tosoni, E. Franceschi, R. Poggi, and A. A. Brandes, "Relapsed Glioblastoma: Treatment Strategies for Initial and Subsequent Recurrences," *Curr Treat Options Oncol,* vol. 17, no. 9, p. 49, Sep 2016, doi: 10.1007/s11864-016-0422-4.

[266] S. T. G *et al.*, "A Review on a Deep Learning Perspective in Brain Cancer Classification," *Cancers (Basel),* vol. 11, no. 1, Jan 18 2019, doi: 10.3390/cancers11010111.
[267] D. N. Louis *et al.*, "Announcing cIMPACT-NOW: the Consortium to Inform Molecular and Practical Approaches to CNS Tumor Taxonomy," *Acta Neuropathol,* vol. 133, no. 1, pp. 1-3, Jan 2017, doi: 10.1007/s00401-016-1646-x.
[268] D. N. Louis *et al.*, "The 2021 WHO Classification of Tumors of the Central Nervous System: a summary," *Neuro Oncol,* vol. 23, no. 8, pp. 1231-1251, Aug 2 2021, doi: 10.1093/neuonc/noab106.
[269] J. Wang *et al.*, "Clonal evolution of glioblastoma under therapy," *Nat Genet,* vol. 48, no. 7, pp. 768-76, Jul 2016, doi: 10.1038/ng.3590.
[270] P. Y. Wen and D. A. Reardon, "Neuro-oncology in 2015: Progress in glioma diagnosis, classification and treatment," *Nat Rev Neurol,* vol. 12, no. 2, pp. 69-70, Feb 2016, doi: 10.1038/nrneurol.2015.242.
[271] I. Paw, R. C. Carpenter, K. Watabe, W. Debinski, and H. W. Lo, "Mechanisms regulating glioma invasion," *Cancer Lett,* vol. 362, no. 1, pp. 1-7, Jun 28 2015, doi: 10.1016/j.canlet.2015.03.015.
[272] S. Osuka and E. G. Van Meir, "Overcoming therapeutic resistance in glioblastoma: the way forward," *J Clin Invest,* vol. 127, no. 2, pp. 415-426, Feb 1 2017, doi: 10.1172/JCI89587.
[273] H. S. Phillips *et al.*, "Molecular subclasses of high-grade glioma predict prognosis, delineate a pattern of disease progression, and resemble stages in neurogenesis," *Cancer Cell,* vol. 9, no. 3, pp. 157-73, Mar 2006, doi: 10.1016/j.ccr.2006.02.019.
[274] R. G. Verhaak *et al.*, "Integrated genomic analysis identifies clinically relevant subtypes of glioblastoma characterized by abnormalities in PDGFRA, IDH1, EGFR, and NF1," *Cancer Cell,* vol. 17, no. 1, pp. 98-110, Jan 19 2010, doi: 10.1016/j.ccr.2009.12.020.
[275] Q. Wang *et al.*, "Tumor Evolution of Glioma-Intrinsic Gene Expression Subtypes Associates with Immunological Changes in the Microenvironment," *Cancer Cell,* vol. 32, no. 1, pp. 42-56 e6, Jul 10 2017, doi: 10.1016/j.ccell.2017.06.003.
[276] D. Eisenbarth and Y. A. Wang, "Glioblastoma heterogeneity at single cell resolution," *Oncogene,* vol. 42, no. 27, pp. 2155-2165, Jun 2023, doi: 10.1038/s41388-023-02738-y.
[277] I. Liu *et al.*, "The landscape of tumor cell states and spatial organization in H3-K27M mutant diffuse midline glioma across age and location," *Nat Genet,* vol. 54, no. 12, pp. 1881-1894, Dec 2022, doi: 10.1038/s41588-022-01236-3.
[278] C. W. Brennan *et al.*, "The somatic genomic landscape of glioblastoma," *Cell,* vol. 155, no. 2, pp. 462-77, Oct 10 2013, doi: 10.1016/j.cell.2013.09.034.
[279] C. M. Jackson, M. Lim, and C. G. Drake, "Immunotherapy for brain cancer: recent progress and future promise," *Clin Cancer Res,* vol. 20, no. 14, pp. 3651-9, Jul 15 2014, doi: 10.1158/1078-0432.CCR-13-2057.
[280] A. Louveau *et al.*, "Structural and functional features of central nervous system lymphatic vessels," *Nature,* vol. 523, no. 7560, pp. 337-41, Jul 16 2015, doi: 10.1038/nature14432.
[281] S. A. Grossman *et al.*, "Immunosuppression in patients with high-grade gliomas treated with radiation and temozolomide," *Clin Cancer Res,* vol. 17, no. 16, pp. 5473-80, Aug 15 2011, doi: 10.1158/1078-0432.CCR-11-0774.
[282] I. Yang *et al.*, "CD8+ T-cell infiltrate in newly diagnosed glioblastoma is associated with long-term survival," *J Clin Neurosci,* vol. 17, no. 11, pp. 1381-5, Nov 2010, doi: 10.1016/j.jocn.2010.03.031.

[283] N. Abdelfattah *et al.*, "Single-cell analysis of human glioma and immune cells identifies S100A4 as an immunotherapy target," *Nat Commun,* vol. 13, no. 1, p. 767, Feb 9 2022, doi: 10.1038/s41467-022-28372-y.
[284] I. Yang, S. J. Han, G. Kaur, C. Crane, and A. T. Parsa, "The role of microglia in central nervous system immunity and glioma immunology," *J Clin Neurosci,* vol. 17, no. 1, pp. 6-10, Jan 2010, doi: 10.1016/j.jocn.2009.05.006.
[285] L. Rong, N. Li, and Z. Zhang, "Emerging therapies for glioblastoma: current state and future directions," *J Exp Clin Cancer Res,* vol. 41, no. 1, p. 142, Apr 15 2022, doi: 10.1186/s13046-022-02349-7.
[286] S. Haase *et al.*, "Mutant ATRX: uncovering a new therapeutic target for glioma," *Expert Opin Ther Targets,* vol. 22, no. 7, pp. 599-613, Jul 2018, doi: 10.1080/14728222.2018.1487953.
[287] J. Schwartzentruber *et al.*, "Driver mutations in histone H3.3 and chromatin remodelling genes in paediatric glioblastoma," *Nature,* vol. 482, no. 7384, pp. 226-31, Jan 29 2012, doi: 10.1038/nature10833.
[288] H. P. Voon and L. H. Wong, "New players in heterochromatin silencing: histone variant H3.3 and the ATRX/DAXX chaperone," *Nucleic Acids Res,* vol. 44, no. 4, pp. 1496-501, Feb 29 2016, doi: 10.1093/nar/gkw012.
[289] B. Wiestler *et al.*, "ATRX loss refines the classification of anaplastic gliomas and identifies a subgroup of IDH mutant astrocytic tumors with better prognosis," *Acta Neuropathol,* vol. 126, no. 3, pp. 443-51, Sep 2013, doi: 10.1007/s00401-013-1156-z.
[290] B. England, T. Huang, and M. Karsy, "Current understanding of the role and targeting of tumor suppressor p53 in glioblastoma multiforme," *Tumour Biol,* vol. 34, no. 4, pp. 2063-74, Aug 2013, doi: 10.1007/s13277-013-0871-3.
[291] X. Wang, J. X. Chen, J. P. Liu, C. You, Y. H. Liu, and Q. Mao, "Gain of function of mutant TP53 in glioblastoma: prognosis and response to temozolomide," *Ann Surg Oncol,* vol. 21, no. 4, pp. 1337-44, Apr 2014, doi: 10.1245/s10434-013-3380-0.
[292] A. Oprita *et al.*, "Updated Insights on EGFR Signaling Pathways in Glioma," *Int J Mol Sci,* vol. 22, no. 2, Jan 8 2021, doi: 10.3390/ijms22020587.
[293] A. B. Heimberger, D. Suki, D. Yang, W. Shi, and K. Aldape, "The natural history of EGFR and EGFRvIII in glioblastoma patients," *J Transl Med,* vol. 3, p. 38, Oct 19 2005, doi: 10.1186/1479-5876-3-38.
[294] G. J. Kitange *et al.*, "Induction of MGMT expression is associated with temozolomide resistance in glioblastoma xenografts," *Neuro Oncol,* vol. 11, no. 3, pp. 281-91, Jun 2009, doi: 10.1215/15228517-2008-090.
[295] M. Butler *et al.*, "MGMT Status as a Clinical Biomarker in Glioblastoma," *Trends Cancer,* vol. 6, no. 5, pp. 380-391, May 2020, doi: 10.1016/j.trecan.2020.02.010.
[296] B. Oldrini *et al.*, "MGMT genomic rearrangements contribute to chemotherapy resistance in gliomas," *Nat Commun,* vol. 11, no. 1, p. 3883, Aug 4 2020, doi: 10.1038/s41467-020-17717-0.
[297] L. Hayflick, "The Limited in Vitro Lifetime of Human Diploid Cell Strains," *Exp Cell Res,* vol. 37, pp. 614-36, Mar 1965, doi: 10.1016/0014-4827(65)90211-9.
[298] L. Roger, F. Tomas, and V. Gire, "Mechanisms and Regulation of Cellular Senescence," *Int J Mol Sci,* vol. 22, no. 23, Dec 6 2021, doi: 10.3390/ijms222313173.

[299] K. Muraki, K. Nyhan, L. Han, and J. P. Murnane, "Mechanisms of telomere loss and their consequences for chromosome instability," *Front Oncol,* vol. 2, p. 135, 2012, doi: 10.3389/fonc.2012.00135.
[300] P. J. Killela *et al.*, "TERT promoter mutations occur frequently in gliomas and a subset of tumors derived from cells with low rates of self-renewal," *Proc Natl Acad Sci U S A,* vol. 110, no. 15, pp. 6021-6, Apr 9 2013, doi: 10.1073/pnas.1303607110.
[301] S. Spiegl-Kreinecker *et al.*, "Prognostic quality of activating TERT promoter mutations in glioblastoma: interaction with the rs2853669 polymorphism and patient age at diagnosis," *Neuro Oncol,* vol. 17, no. 9, pp. 1231-40, Sep 2015, doi: 10.1093/neuonc/nov010.
[302] N. Olympios, V. Gilard, F. Marguet, F. Clatot, F. Di Fiore, and M. Fontanilles, "TERT Promoter Alterations in Glioblastoma: A Systematic Review," *Cancers (Basel),* vol. 13, no. 5, Mar 8 2021, doi: 10.3390/cancers13051147.
[303] S. Jessa *et al.*, "Stalled developmental programs at the root of pediatric brain tumors," *Nat Genet,* vol. 51, no. 12, pp. 1702-1713, Dec 2019, doi: 10.1038/s41588-019-0531-7.
[304] S. R. Alcantara Llaguno and L. F. Parada, "Cell of origin of glioma: biological and clinical implications," *Br J Cancer,* vol. 115, no. 12, pp. 1445-1450, Dec 6 2016, doi: 10.1038/bjc.2016.354.
[305] B. C. Prager, S. Bhargava, V. Mahadev, C. G. Hubert, and J. N. Rich, "Glioblastoma Stem Cells: Driving Resilience through Chaos," *Trends Cancer,* vol. 6, no. 3, pp. 223-235, Mar 2020, doi: 10.1016/j.trecan.2020.01.009.
[306] J. E. Visvader, "Cells of origin in cancer," *Nature,* vol. 469, no. 7330, pp. 314-22, Jan 20 2011, doi: 10.1038/nature09781.
[307] W. A. Flavahan *et al.*, "Insulator dysfunction and oncogene activation in IDH mutant gliomas," *Nature,* vol. 529, no. 7584, pp. 110-4, Jan 7 2016, doi: 10.1038/nature16490.
[308] C. J. Wikstrand, F. C. Grahmann, R. D. McComb, and D. D. Bigner, "Antigenic heterogeneity of human anaplastic gliomas and glioma-derived cell lines defined by monoclonal antibodies," *J Neuropathol Exp Neurol,* vol. 44, no. 3, pp. 229-41, May 1985, doi: 10.1097/00005072-198505000-00002.
[309] G. L. Semenza, "HIF-1 mediates metabolic responses to intratumoral hypoxia and oncogenic mutations," *J Clin Invest,* vol. 123, no. 9, pp. 3664-71, Sep 2013, doi: 10.1172/JCI67230.
[310] N. Charles *et al.*, "Perivascular nitric oxide activates notch signaling and promotes stem-like character in PDGF-induced glioma cells," *Cell Stem Cell,* vol. 6, no. 2, pp. 141-52, Feb 5 2010, doi: 10.1016/j.stem.2010.01.001.
[311] T. S. Zhu *et al.*, "Endothelial cells create a stem cell niche in glioblastoma by providing NOTCH ligands that nurture self-renewal of cancer stem-like cells," *Cancer Res,* vol. 71, no. 18, pp. 6061-72, Sep 15 2011, doi: 10.1158/0008-5472.CAN-10-4269.
[312] A. W. Hall *et al.*, "Bivalent Chromatin Domains in Glioblastoma Reveal a Subtype-Specific Signature of Glioma Stem Cells," *Cancer Res,* vol. 78, no. 10, pp. 2463-2474, May 15 2018, doi: 10.1158/0008-5472.CAN-17-1724.
[313] L. Wang *et al.*, "A single-cell atlas of glioblastoma evolution under therapy reveals cell-intrinsic and cell-extrinsic therapeutic targets," *Nat Cancer,* vol. 3, no. 12, pp. 1534-1552, Dec 2022, doi: 10.1038/s43018-022-00475-x.
[314] P. Guilhamon *et al.*, "Single-cell chromatin accessibility profiling of glioblastoma identifies an invasive cancer stem cell population associated with lower survival," *Elife,* vol. 10, Jan 11 2021, doi: 10.7554/eLife.64090.

[315] X. Lu *et al.*, "Cell-lineage controlled epigenetic regulation in glioblastoma stem cells determines functionally distinct subgroups and predicts patient survival," *Nat Commun,* vol. 13, no. 1, p. 2236, Apr 25 2022, doi: 10.1038/s41467-022-29912-2.
[316] A. L. Rivera *et al.*, "MGMT promoter methylation is predictive of response to radiotherapy and prognostic in the absence of adjuvant alkylating chemotherapy for glioblastoma," *Neuro Oncol,* vol. 12, no. 2, pp. 116-21, Feb 2010, doi: 10.1093/neuonc/nop020.
[317] M. J. Dabrowski *et al.*, "Unveiling new interdependencies between significant DNA methylation sites, gene expression profiles and glioma patients survival," *Sci Rep,* vol. 8, no. 1, p. 4390, Mar 13 2018, doi: 10.1038/s41598-018-22829-1.
[318] K. Stepniak *et al.*, "Mapping chromatin accessibility and active regulatory elements reveals pathological mechanisms in human gliomas," *Nat Commun,* vol. 12, no. 1, p. 3621, Jun 15 2021, doi: 10.1038/s41467-021-23922-2.
[319] O. Bogdanovic *et al.*, "Dynamics of enhancer chromatin signatures mark the transition from pluripotency to cell specification during embryogenesis," *Genome Res,* vol. 22, no. 10, pp. 2043-53, Oct 2012, doi: 10.1101/gr.134833.111.
[320] A. D. Goldberg *et al.*, "Distinct factors control histone variant H3.3 localization at specific genomic regions," *Cell,* vol. 140, no. 5, pp. 678-91, Mar 5 2010, doi: 10.1016/j.cell.2010.01.003.
[321] Q. He *et al.*, "The Daxx/Atrx Complex Protects Tandem Repetitive Elements during DNA Hypomethylation by Promoting H3K9 Trimethylation," *Cell Stem Cell,* vol. 17, no. 3, pp. 273-86, Sep 3 2015, doi: 10.1016/j.stem.2015.07.022.
[322] C. Baumann, M. M. Viveiros, and R. De La Fuente, "Loss of maternal ATRX results in centromere instability and aneuploidy in the mammalian oocyte and pre-implantation embryo," *PLoS Genet,* vol. 6, no. 9, p. e1001137, Sep 23 2010, doi: 10.1371/journal.pgen.1001137.
[323] M. A. Dyer, Z. A. Qadeer, D. Valle-Garcia, and E. Bernstein, "ATRX and DAXX: Mechanisms and Mutations," *Cold Spring Harb Perspect Med,* vol. 7, no. 3, Mar 1 2017, doi: 10.1101/cshperspect.a026567.
[324] R. Smith *et al.*, "The H3.3 chaperone Hira complex orchestrates oocyte developmental competence," *Development,* vol. 149, no. 5, Mar 1 2022, doi: 10.1242/dev.200044.
[325] H. Zhang *et al.*, "RPA Interacts with HIRA and Regulates H3.3 Deposition at Gene Regulatory Elements in Mammalian Cells," *Mol Cell,* vol. 65, no. 2, pp. 272-284, Jan 19 2017, doi: 10.1016/j.molcel.2016.11.030.
[326] E. Szenker, N. Lacoste, and G. Almouzni, "A developmental requirement for HIRA-dependent H3.3 deposition revealed at gastrulation in Xenopus," *Cell Rep,* vol. 1, no. 6, pp. 730-40, Jun 28 2012, doi: 10.1016/j.celrep.2012.05.006.
[327] A. P. Gomes *et al.*, "Dynamic Incorporation of Histone H3 Variants into Chromatin Is Essential for Acquisition of Aggressive Traits and Metastatic Colonization," *Cancer Cell,* vol. 36, no. 4, pp. 402-417 e13, Oct 14 2019, doi: 10.1016/j.ccell.2019.08.006.
[328] D. A. Haas-Kogan *et al.*, "Phase II trial of tipifarnib and radiation in children with newly diagnosed diffuse intrinsic pontine gliomas," *Neuro Oncol,* vol. 13, no. 3, pp. 298-306, Mar 2011, doi: 10.1093/neuonc/noq202.
[329] Q. T. Ostrom *et al.*, "Alex's Lemonade Stand Foundation Infant and Childhood Primary Brain and Central Nervous System Tumors Diagnosed in the United States in 2007-2011," *Neuro Oncol,* vol. 16 Suppl 10, no. Suppl 10, pp. x1-x36, Jan 2015, doi: 10.1093/neuonc/nou327.

[330] T. B. Johung and M. Monje, "Diffuse Intrinsic Pontine Glioma: New Pathophysiological Insights and Emerging Therapeutic Targets," *Curr Neuropharmacol,* vol. 15, no. 1, pp. 88-97, 2017, doi: 10.2174/1570159x14666160509123229.
[331] C. Jones and S. J. Baker, "Unique genetic and epigenetic mechanisms driving paediatric diffuse high-grade glioma," *Nat Rev Cancer,* vol. 14, no. 10, Oct 2014, doi: 10.1038/nrc3811.
[332] A. Mackay *et al.*, "Integrated Molecular Meta-Analysis of 1,000 Pediatric High-Grade and Diffuse Intrinsic Pontine Glioma," *Cancer Cell,* vol. 32, no. 4, pp. 520-537 e5, Oct 9 2017, doi: 10.1016/j.ccell.2017.08.017.
[333] A. Mackay *et al.*, "Integrated Molecular Meta-Analysis of 1,000 Pediatric High-Grade and Diffuse Intrinsic Pontine Glioma," *Cancer Cell,* vol. 32, no. 4, pp. 520-537 e5, Oct 9 2017, doi: 10.1016/j.ccell.2017.08.017.
[334] M. Touat *et al.*, "Mechanisms and therapeutic implications of hypermutation in gliomas," *Nature,* vol. 580, no. 7804, pp. 517-523, Apr 2020, doi: 10.1038/s41586-020-2209-9.
[335] P. W. Lewis *et al.*, "Inhibition of PRC2 activity by a gain-of-function H3 mutation found in pediatric glioblastoma," *Science,* vol. 340, no. 6134, pp. 857-61, May 17 2013, doi: 10.1126/science.1232245.
[336] A. S. Harutyunyan *et al.*, "H3K27M induces defective chromatin spread of PRC2-mediated repressive H3K27me2/me3 and is essential for glioma tumorigenesis," *Nat Commun,* vol. 10, no. 1, p. 1262, Mar 19 2019, doi: 10.1038/s41467-019-09140-x.
[337] M. T. Villanueva, "Anticancer drugs: All roads lead to EZH2 inhibition," *Nat Rev Drug Discov,* vol. 16, no. 4, p. 239, Mar 30 2017, doi: 10.1038/nrd.2017.55.
[338] F. Mohammad *et al.*, "EZH2 is a potential therapeutic target for H3K27M-mutant pediatric gliomas," *Nat Med,* vol. 23, no. 4, pp. 483-492, Apr 2017, doi: 10.1038/nm.4293.
[339] C. S. Grasso *et al.*, "Functionally defined therapeutic targets in diffuse intrinsic pontine glioma," *Nat Med,* vol. 21, no. 6, pp. 555-9, Jun 2015, doi: 10.1038/nm.3855.
[340] C. Fernandes *et al.*, "Current Standards of Care in Glioblastoma Therapy," in *Glioblastoma*, S. De Vleeschouwer Ed. Brisbane (AU), 2017.
[341] M. M. Mrugala, "Advances and challenges in the treatment of glioblastoma: a clinician's perspective," *Discovery medicine,* vol. 15, no. 83, pp. 221-30, 2013. [Online]. Available: http://www.ncbi.nlm.nih.gov/pubmed/23636139.
[342] M. E. Hegi *et al.*, "MGMT gene silencing and benefit from temozolomide in glioblastoma," *N Engl J Med,* vol. 352, no. 10, pp. 997-1003, Mar 10 2005, doi: 10.1056/NEJMoa043331.
[343] O. Rominiyi, A. Vanderlinden, S. J. Clenton, C. Bridgewater, Y. Al-Tamimi, and S. J. Collis, "Tumour treating fields therapy for glioblastoma: current advances and future directions," *Br J Cancer,* vol. 124, no. 4, pp. 697-709, Feb 2021, doi: 10.1038/s41416-020-01136-5.
[344] S. Bahadur, A. K. Sahu, P. Baghel, and S. Saha, "Current promising treatment strategy for glioblastoma multiform: A review," *Oncology reviews,* vol. 13, no. 2, pp. 417-417, 2019, doi: 10.4081/oncol.2019.417.
[345] M. E. van Linde *et al.*, "Treatment outcome of patients with recurrent glioblastoma multiforme: a retrospective multicenter analysis," *J Neurooncol,* vol. 135, no. 1, pp. 183-192, Oct 2017, doi: 10.1007/s11060-017-2564-z.
[346] W. Taal *et al.*, "Single-agent bevacizumab or lomustine versus a combination of bevacizumab plus lomustine in patients with recurrent glioblastoma (BELOB trial): a

randomised controlled phase 2 trial," *Lancet Oncol,* vol. 15, no. 9, pp. 943-53, Aug 2014, doi: 10.1016/S1470-2045(14)70314-6.

[347] T. S. van Solinge, L. Nieland, E. A. Chiocca, and M. L. D. Broekman, "Advances in local therapy for glioblastoma - taking the fight to the tumour," *Nat Rev Neurol,* vol. 18, no. 4, pp. 221-236, Apr 2022, doi: 10.1038/s41582-022-00621-0.

[348] A. Jahangiri, A. T. Chin, P. M. Flanigan, R. Chen, K. Bankiewicz, and M. K. Aghi, "Convection-enhanced delivery in glioblastoma: a review of preclinical and clinical studies," *J Neurosurg,* vol. 126, no. 1, pp. 191-200, Jan 2017, doi: 10.3171/2016.1.JNS151591.

[349] C. B. Wilson, "Chemotherapy of Brain Tumors by Continuous Arterial Infusion," *Surgery,* vol. 55, pp. 640-53, May 1964. [Online]. Available: https://www.ncbi.nlm.nih.gov/pubmed/14146524.

[350] R. S. D'Amico *et al.*, "Super selective intra-arterial cerebral infusion of modern chemotherapeutics after blood-brain barrier disruption: where are we now, and where we are going," *J Neurooncol,* vol. 147, no. 2, pp. 261-278, Apr 2020, doi: 10.1007/s11060-020-03435-6.

[351] B. S. Karmur *et al.*, "Blood-Brain Barrier Disruption in Neuro-Oncology: Strategies, Failures, and Challenges to Overcome," *Front Oncol,* vol. 10, p. 563840, 2020, doi: 10.3389/fonc.2020.563840.

[352] D. Fortin, P. A. Morin, F. Belzile, D. Mathieu, and F. M. Pare, "Intra-arterial carboplatin as a salvage strategy in the treatment of recurrent glioblastoma multiforme," *J Neurooncol,* vol. 119, no. 2, pp. 397-403, Sep 2014, doi: 10.1007/s11060-014-1504-4.

[353] S. M. Yusuke Suita, Deniz Merih-Toruner, Weizhou Yue, Lingxiao Xie, Blessing Akobundu, Nathan Pertsch, Andras Fiser, Eduardo Fajardo, Jie Shen, Nikos Tapinos, "Engineering GliaTrap: a biodegradable non-swelling hydrogel with tuned release of CXCL12 to attract migrating glioblastoma cells," *bioRxiv,* 2023, doi: 10.1101/2023.04.12.536581.

[354] Y. B. Zhou *et al.*, "Pharmacodynamic, pharmacokinetic, and phase 1a study of bisthianostat, a novel histone deacetylase inhibitor, for the treatment of relapsed or refractory multiple myeloma," *Acta Pharmacol Sin,* vol. 43, no. 4, pp. 1091-1099, Apr 2022, doi: 10.1038/s41401-021-00728-y.

[355] A. D. Bondarev, M. M. Attwood, J. Jonsson, V. N. Chubarev, V. V. Tarasov, and H. B. Schioth, "Recent developments of HDAC inhibitors: Emerging indications and novel molecules," *Br J Clin Pharmacol,* vol. 87, no. 12, pp. 4577-4597, Dec 2021, doi: 10.1111/bcp.14889.

CHAPTER 2:

Targeting HDAC7 As a Novel Therapeutic Approach in Glioblastoma Multiforme

Targeting Histone Deacetylase7 as a Novel Therapeutic Strategy for Glioblastoma Multiforme.

Ola Hassan[1], David Karambizi[1], Nikos Tapinos[1,2*]

1: Laboratory of Cancer Epigenetics and Plasticity, Brown University, Rhode Island Hospital, Providence, RI, USA

2: Department of Neurosurgery, Brown University, Rhode Island Hospital, Providence, RI, USA

***: Corresponding Author:**

Nikos Tapinos M.D., Ph.D.
Laboratory of Cancer Epigenetics and Plasticity 593 Eddy Street,
Providence, RI 02903,
Tel: 401-606-4393,
e-mail: nikos_tapinos@brown.edu

DOI: doi.org/10.1096/fasebj.2022.36.S1.R3259

Abstract

Glioblastoma multiforme (GBM) is the most aggressive primary brain tumor. GBM has an ominous prognosis with a survival rate of 14-15 months after diagnosis, and despite worldwide initiatives to optimize therapeutic approaches, GBM is still among the most challenging diseases to treat and the fastest to relapse in clinical oncology. We show that HDAC7, as an epigenetic regulator, plays a crucial role in GBM and constitutes a novel druggable target for this universally fatal disease. Survival analysis of GBM patients from Rhode Island Hospital showed a significant decrease in survival for patients with high HDAC7 mRNA expression as distinct from other members of class IIa HDACs. In addition, analyzing publicly available data revealed that HDAC7 expression is significantly higher in GBM tumors relative to non-tumor samples and correlated with worse survival in these GBM cohorts. Transcriptomic analysis after HDAC7 inhibition in three different primary GSCs (Glioblastoma stem cells) revealed one-third to half differential gene expression of the normally expressed genes. HDAC7 drives the stemness of GSCs to embryonic phenotype and enriches cell cycle and tumorigenic activities, whereas, inhibiting HDAC7 induces stemness phenotype change in GCSs. Taken together, our analysis provides valuable insights into the impact of HDAC7 inhibition on the phenotypic and transcriptomic landscape of GBM, shedding light on the dysregulated expression of HDAC7 and its potential contribution to GBM pathogenesis which holds promise for its targeting as a therapeutic approach in cancer.

I. Introduction

GBM is the most common high-grade primary malignant brain tumor with the worst prognosis among brain tumors [1-3]. The current standard of care for GBM includes surgery, radiotherapy, and pharmacotherapy (typically chemotherapy with temozolomide). Nevertheless, the prognosis for patients remains grim, with a 15-month median survival rate [1, 3-7]. Innovative therapeutic approaches are urgently required that can address the plasticity and diversity characteristics of GBM. [2, 3, 5, 7-11].

With the advancements in global cancer genomic research over the past decade and the enhanced genetic and epigenetic profiling, innovative therapeutics for GBM are now rapidly advancing. This progress is evident through the initiation of numerous active clinical trials with epigenetic-based therapies [12-14].

Given the unique structure and function of class IIa HDACs, with their implications in cancer [15-19], our objective was to investigate whether they have a role in GBM. Examination of GBM data from publicly available genomic atlases revealed elevated expression levels of HDAC7 in GBM compared to other glial tumors, with particularly high expression levels observed in GBM relative to normal brain tissue. This preliminary data built the foundation, elaborated upon in **Chapter 2**, to elucidate our efforts in comprehending the role of HDAC7 in promoting tumor aggressiveness in GBM.

The significant impact of HDACs on tumor regulation and drug resistance, influencing various cellular functions including stemness, proliferation, apoptosis, differentiation, angiogenesis,

migration, and invasion, underscores the considerable potential of HDAC inhibitors (HDACi) as a class of epigenetic-based therapy [15, 20-23]. However, on the functional and mechanistic level, members of the HDAC family are diverse, and some of them act as tumor promotors or suppressors and dually regulate cancer progression [24]. Therefore, broad-spectrum HDAC inhibition for cancer treatment presents challenges, often leading to significant toxicities and adverse effects [25-27]. By delving into the distinct roles played by a specific HDAC isoform and its implication in various cancer types, we aimed to participate in shedding light on how narrow targeted therapy can spare a lot of complications and toxicities during cancer treatment.

Despite its implications in cancer, there remains a limited understanding of HDAC7's involvement in the GBM pathogenesis and the specific transcriptional programs it employs to drive tumorigenesis. Studies have demonstrated that HDAC7 promotes the proliferation and metastasis of many tumors, while its inhibition has been documented in numerous studies to suppress epithelial-to-mesenchymal transition (EMT) and inhibit cancer stem cell (CSC) phenotypes [28-33]. Therefore, we aimed to investigate the tumorigenic phenotypic and genotypic changes following HDAC7 inhibition in our patient-derived GSCs through a variety of functional assays. In addition, we aimed to investigate its overexpression's outcome on GBM local patients from Rhode Island Hospital (RIH) as well as bigger patient cohorts from publicly available data.

A recent study showed that HDAC7 modulated NSCLC proliferation and metastasis via activation of the β-catenin-FGF18 pathway [34]. Another recent study showed that the HDAC7/c-Myc signaling pathway drives the proliferation and metastasis of choroidal melanoma cells [31]. It was also reported that HDAC7 implication in stemness and tumorigenesis is mediated through HDAC7 control over the tumor microenvironment [33]. However, its implications in GBM have

not been extensively characterized before. Expanding upon this knowledge gap, we aimed to elucidate the phenotypic and transcriptomic outcomes of HDAC7 inhibition in primary GSCs. Through this comprehensive analysis, our goal was to uncover the molecular mechanisms underlying the effects of HDAC7 inhibition in GSCs, providing valuable insights into its therapeutic potential for GBM treatment. Lastly, we sought to explore HDAC7's implication in other malignancies as well. The data presented in this **Chapter** supports the high potential of HDAC7 as a promising narrow-spectrum HDACi therapeutic in GBM, as well as other cancers.

II. METHODS

- *Primary GSCs extraction from tumors of RIH GBM patients*

Patient-derived primary GSC (Glioma Stem Cells) samples were GBM tumor tissues obtained from RIH and characterized for patients with a confirmed diagnosis of *IDH* WT GBM. GSCs were obtained directly from the operating room (OR) in the neurosurgical department and then transported to the laboratory as per the Institutional Review Board (IRB) protocols in a sterile 50mL conical tube consisting of 1X Dulbecco's phosphate-buffered saline (DPBS) and 2X Anti-Anti on ice in a sealed biohazard container.

Using BL2 practices, the tissue sample was transferred into a 60mm plate and cut into 1mm3 fragments with sterile microscissors. Digestion was performed by impeding and resuspending in 1mg/mL of collagenase/dispase (Roche, Catalog #: 10 269 638 001), followed by incubation at 37°C for 20-30 minutes or longer as needed. Isolated cells were filtered several times and resuspended in Neurobasal -A only to a final volume of 10mL and span at 110rcf for 10 minutes, removed out of supernatant and cultured in an enrichment growth media and refed two times a week after inspection. GSCs usually start making spheres 3 - 4 weeks after first isolation.

The enrichment complete growth media consists of Neurobasal-A media (Fisher Scientific, Catalog #: 10888022 or 12349015) supplemented with growth factors: 10ug basic fibroblast growth factor (bFGF) and 10ug epidermal growth factor (EGF) (20ng/ml final concentration respectively; Peprotech, Catalog # 100-18B & 100-47 respectively). Heparin is supplemented as a growth co-factor (2ug/ml final concentration; StemCell Tech, Catalog #: 07980). As a serum substitute, B-27 without Vitamin A is used (50X final concentration; Fisher Scientific, Catalog #: 12587010). For energy supplantation, 1X 2mM Glutamax is used (100X final concentration; Fisher Scientific, Catalog #: 35050061). Finally, The GSCs complete media

is supplemented with antibiotics to prevent contaminations during culturing; 1X Antibiotic: Antimycotic (Anti-Anti) (100X final concentration; Fisher Scientific, Catalog #: 1524006.

Following approved guidelines, the freshly isolated GSCs were routinely tested for their stemness through in-vitro and in-vivo techniques by the Tapinos lab team. This was followed by free-of-mycoplasma contamination testing and validation through short tandem repeats (STR) by ATCC. Once the authentication was guaranteed, the cells were either maintained in culture for conducting various experiments or preserved in the liquid nitrogen cryo-freezer for a more extended repository.

A

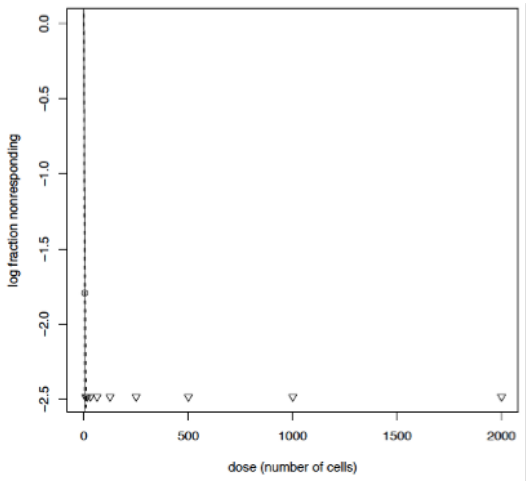

B

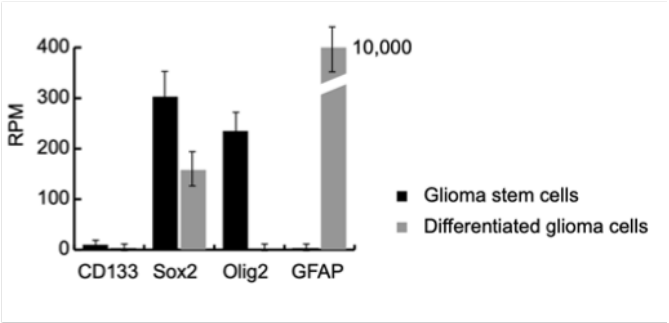

C

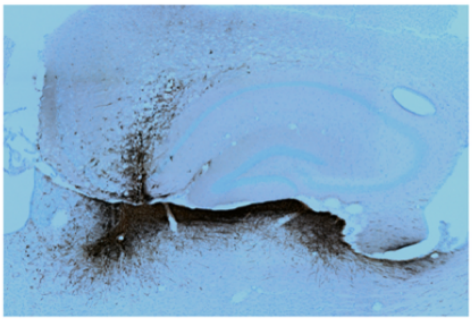

HuNu+ glioblastoma

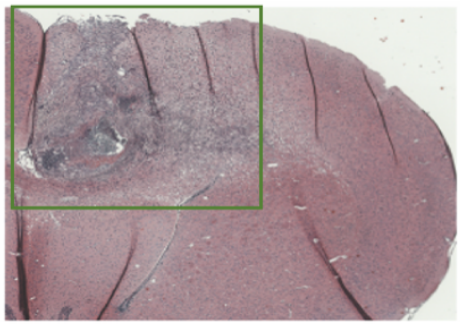

Hematoxylin and Eosin (H & E) stain of glioblastoma

Figure (2.1) ***Characterization of the GSCs used in the study.*** **A.** *In vitro limiting dilution stemness assay showing the self-renewal ability of the GSCs used in this study and other studies in the lab. The experiment was conducted as six technical replicates per cell dose, and significance was calculated with a Chi-square test ($p<0.05$) using the ELDA software.* **B.** *GSCs used in the experiments express stem cell-specific transcripts (CD133, Sox2, Olig2), which they lose entirely (CD133, Olig2) or downregulate (Sox2) after differentiation for seven days by removal of EGF, bFGF, and Heparin and the addition of 10% serum. Moreover, following differentiation, they gain expression of GFAP, which was not expressed in GSCs. The graph presents representative RNA-seq data. The same analysis has been performed for all GSCs that are being used in the lab.* **C.** *An image for a mouse orthotopic xenograft GBM after transplantation of GSCs in nude mice results in the formation of invading glioblastomas (black/dark regions in the HuNu+ image), verifying the tumor-forming ability of the GSC lines. The image shows a HuNu+ glioblastoma (left) and H&E stain (boxed area, right) four weeks after the transplantation of 150,000 GSCs.*

- *GSCs Cell culture maintenance*

Patient-derived GSCs (GSC1, GSC2, GSC3, GSC4, and GSC5) were used in this study. Primary GSCs were cultured in the enrichment complete growth media stated before. Cryopreserved GSCs were passaged twice as neurospheres and then attached for at least one passage to ensure adequate adaptation to culture conditions, which was done routinely for all experiments in this study. According to the experiment in use, neurospheres or attached GSCs were used when ~80% confluency was reached in the culturing medium.

- *DIPG cells maintenance*

The enrichment working tumor stem media (TSM) consists of Neurobasal-A media (Fisher Scientific, Catalog #: 10888022 or 12349015), D-MEM/F-12 (1X), liquid, 1:1 (Invitrogen, Catalog #: 11330-032), HEPES Buffer Solution (1M) 1 (Invitrogen, Catalog #: 15630-080), MEM Sodium Pyruvate Solution (100X) (Invitrogen, Catalog #: 11360-070), MEM Non-Essential Amino Acids solution 10mM (100X) (Invitrogen, Catalog #: 11140-050). TSM media was supplemented with growth factors: 10ug basic fibroblast growth factor (bFGF) and 10ug epidermal growth factor (EGF) (20ng/ml final concentration respectively; Peprotech, Catalog # 100-18B & 100-47

respectively). 10 ug H-PDGF-AA, H-PDGF-BB growth factors were supplemented (10ng/ml final concentration respectively; Peprotech, Catalog # 100-13A & 100-14B respectively). Heparin is supplemented as a growth co-factor (2ug/ml final concentration; StemCell Tech, Catalog #: 07980). As a serum substitute, B-27 without Vitamin A is used (50X final concentration; Fisher Scientific, Catalog #: 12587010). For energy supplantation, 1X 2mM Glutamax is used (100X final concentration; Fisher Scientific, Catalog #: 35050061). Finally, The DIPG complete media is supplemented with antibiotics to prevent contaminations during culturing; 1X Antibiotic: Antimycotic (Anti-Anti) (100X final concentration; Fisher Scientific, Catalog #: 1524006.

- *Cancer cell lines culture maintenance*

Various cancer cell lines were used in this study in addition to the GSCs. Kidney cancer cells (ACHN) were cultured per ATCC recommendations in Eagle's Minimum Essential Medium enriched with 10% fetal bovine serum. Non-small lung cancer cells (A549) were cultured per ATCC recommendations in ATCC-formulated F-12K Medium enriched with 10% fetal bovine serum. Colorectal cancer (HCT116) cells were cultured per ATCC recommendations in TCC-formulated McCoy's 5a Medium Modified enriched with 10% fetal bovine serum. Melanoma (SK-Mel-5) cells were cultured per ATCC recommendations in ATCC-formulated Eagle's Minimum Essential Medium, enriched with 10% fetal bovine serum.

- *Nanostring PanCancer progression panel and related analysis*

We collected RNA from paraffin-embedded samples from GBM patients at RIH and performed gene expression analysis using the Nanostring PanCancer progression panel. The PanCancer Gene Expression Panel is a gene expression panel that comprises the vital components of pathways involved in the complex interplay between the tumor and its microenvironments in

cancer. The Nanostring panel included 48 biological signatures to predict outcomes. Among these signatures was the 18-gene Tumor Inflammation Signature. Data from 84 RIH patients were curated and categorized as high-risk (HR) and low-risk (LR) based on the expression level of the top five GBM epigenetic regulators identified from the vial competition library. Then, we applied differential gene expression analysis on the HR versus LR group on the 770 pan-cancer genes. Then, the same analysis was repeated after filtering the risk from the five top genes to HDAC7 as an expression-level risk factor. Overall survival and progression-free survival were estimated by the Kaplan-Meier method. Gene enrichment and pathway enrichment were performed on the differentially expressed genes via the Gene Ontology Field and the KEGG pathway [35].

- *Analyzing publicly available datasets*

Using the Cancer Genomic Atlas (TCGA) and the Chinese Glioma Genome Atlas (CGGA), we tested the class IIa HDAC expression in GBM tumors across various datasets from these databases and visualized in the Kaplan-Meier Plotter [36], GlioVis [37] web tools and via the R Bioconductor package.

- *siRNA transfection treatment for primary GSCs,*

The following 72-hour transfection protocol was optimized and standardized across the various experiments in this study after testing multiple time points, siRNA concentrations, and transfection conditions. The RNAase-free environment was rigorously maintained in all experiments.

- GSCs were grown over fibronectin/HBSS-treated culture plates in antibiotic-free media supplemented with Neurobasal-A, B-27-A, Glutamax, growth factors (EGF and FGF), and

heparin, and GSCs were incubated at 37ºC with 5 % CO2 overnight. GSCs' readiness for transfection was determined by the optimal confluency of 70 % growth.

- SiRNA (Dharmacon ON-TARGETplus™ siRNA) of 50 nM final concentration was the optimized concentration from the array of various concentrations (25- 100 nM) tested. Stocks of siRNA aliquots were prepared by dissolving in RNase-free water and incubated for 30 minutes on a rotator at room temperature.
- The transfection master mix was prepared by adding 5.5 µL siRNA (equivalent to 50 nM) and 6 µL of TransIT-X2 Dynamic Delivery System (Mirus Bio) to 200 µL of the reduced serum media (Gibco™ Opti-MEM™). Tubes containing the master mix were incubated for 30 minutes at room temperature until the transfection complexes formed.
- Meanwhile, the transfection media of Neurobasal-A, B-27-A, Glutamax, and growth factors (EGF and FGF) were freshly prepared.
- Monolayer GSCs were aspirated from their growth medium and washed with the 1X DPBS (-)(-) (Gibco) to remove any residual heparin that could interfere with the siRNA uptake by cells.
- The formed transfection complex was added dropwise gently while swirling the plate.
- 72 hours after transfection, GSCs were taken down for further downstream experiments.
- After each transfection experiment, an aliquot of the taken-down cells was lysed and inspected by western blot to validate the success of transfection and inhibition of HDAC7.
- Smart pool siRNA used was a pool of 4 siRNA variants against HDAC7 versus non-targeting siRNA, respectively, with the following sequences:

siRNA-1 sense: 5' G.A.C.A.A.G.A.G.C.A.A.G.C.G.A.A.G.U.G 3'

antisense: 5' C.A.C.U.U.C.G.C.U.U.G.C.U.C.U.U.G.U.C 3'

siRNA-2 sense: 5' G.C.A.G.A.U.A.C.C.C.U.C.G.G.C.U.G.A.A 3'

antisense: 5' U.U.C.A.G.C.C.G.A.G.G.G.U.A.U.C.U.G.C 3'

siRNA-3 sense: 5' G.G.U.G.A.G.G.G.C.U.U.C.A.A.U.G.U.C.A 3'

antisense: 5' U.G.A.C.A.U.U.G.A.A.G.C.C.C.U.C.A.C.C 3'

siRNA-4 sense: 5' U.G.G.C.U.G.C.U.U.C.U.C.G.G.G.U.U.A.A 3'

antisense: 5' U.U.A.A.C.C.C.G.A.G.A.A.G.C.A.G.C.C.A 3'

Non-targeting control siRNA- sense: 5' A.G.C.G.A.C.U.A.A.A.C.A.C.A.U.C.A.A 3'

antisense: 5' U.U.G.A.U.G.U.G.U.U.U.A.G.U.C.G.C.U 3'

- siRNA variant two was proven to be the most inhibitory targeting and the most specific. As shown in **Chapter 3**, it was chosen as the inhibitory drug of choice in this study.
- In-vivo siRNA sequences were edited to render stability and escape nuclease cleavage in vivo by the customized siSTABLE form of siRNA with the following sequence in vivo form of variant 2:

In vivo siRNA Sense: 5' G.C.A.G.A.U.A.C.C.C.U.C.G.G.C.U.G.A.A.U.U 3'

Antisense: 5' 5'-P.U.U.C.A.G.C.C.G.A.G.G.G.U.A.U.C.U.G.C.U.U 3'

In vivo non-targeting control siRNA

sense: 5' U.A.G.C.G.A.C.U.A.A.A.C.A.C.A.U.C.A.A.U.U 3'

antisense: 5' P.U.U.G.A.U.G.U.G.U.U.U.A.G.U.C.G.C.U.A.U.U 3'

- *Western blot analysis*

Cells were lysed, and whole lysate protein was extracted using a 1% SDS lysis buffer containing protease inhibitor cocktail and phosphatase inhibitor. After denaturation, samples were

boiled at 95 degrees for 5 minutes, and 40 µg of whole lysates from compared samples were electrophoresed through Bolt™ 4 -12%, Bis-Tris (Invitrogen) or NuPAGE™ 3 to 8%, Tris-Acetate (Invitrogen), 1.0, protein gels. Gels were then transferred to nitrocellulose membranes, followed by blocking with 5% non-fat milk in 1x TBST. Primary antibodies in 5% BSA were incubated with the membrane at 4°C overnight. Anti-rabbit IgG, HRP-linked goat antibody, and anti-mouse IgG, HRP-linked horse antibody were the secondary antibodies against the various primary antibodies, stated below, used in the study.

Antibody	animal	Dilution	M wt	Source
HDAC7 (E7O8V)	Rabbit	1:1000	124 kDa	cell signaling
SMC4 (D14E2)	Rabbit	1:1000	180 kDa	cell signaling
CHD4 (ab72418)	Rabbit	1:2000	280 kDa	Abcam
NCOR2/SMRT (D8D2L)	Rabbit	1:1000	270 kDa	cell signaling
β-Catenin (D10A8)	Rabbit	1:1000	92 kDa	cell signaling
SETDB1 (Me transferase)	Rabbit	1:1000	170 kDA	Proteintech
Ezh2 (D2C9) XP®	Rabbit	1:1000	98 kDA	cell signaling
HIRA (D6O8L)	mouse	2:1000	120 kDA	Active motif
HDAC4 (D8T3Q)	Rabbit	1:1000	140 kDa	cell signaling

HDAC5 (D1J7V)	Rabbit	1:1000	140 kDa	cell signaling
HDAC9	Rabbit	1:1000	145 kDa	Active motif
DAXX	mouse	0.4:1000	90-100 kDA	Proteintech
H3.3	Rabbit	1:1000	15 kDa	Abcam
H3K9me3	Rabbit	1:1000	17 kDa	Active motif
H3K27me3	Rabbit	1:1000	17 kDa	Active motif
H3K9me3	Mouse	1:1000	17 kDa	Active motif
H3K27me3	Mouse	1:1000	17 kDa	Active motif

Table 2.1: List of the antibodies used in the current study

- *Tumor sphere formation assay*

Tumor sphere formation assay was performed as the established protocol [38] with nuance adjustments. Cells were treated with siRNA transfection as described before. After 24 hours, cells were dissociated, and 200 cells in 200 µL (1 cell/µL) were seeded per well into 10 inner wells of a 96-well Clear Flat Bottom Ultra-Low Attachment Microplate. Replicates were given as 10-wells per condition per plate. Singlet cells were left for seven days under standard culture conditions. Sphere formation by visual counting was estimated after seven days in a blinded, unbiased format

by counting the number of spheres in each well by two independent experimenters. Only one of the experimenters knew the condition assignment of the wells. Significance estimation and plotting were tested via Graph-Pad Prism.

- *Cell viability measurement*

Cells were seeded at a density of 5×10^3 cells per well in a 96-well plate in treated fibronectin/HBSS-coated flat bottom plates and left to adhere overnight. After 24 hours, cells were treated accordingly. After the course of treatment, cell viability was estimated using the CellTiter Glo assay (Promega). Cells were combined with 25 µL of CellTiter-Glo reagents in 100 µL of culture non-colored media, and bioluminescence was assessed using the Promega™ GloMax® Plate Reader. Blank (culturing media without cells) was used to normalize the luminescence signals. Cell viability of the treated versus untreated cells was estimated via Graph-Pad Prism.

- *RNA isolation and purification*

RNA isolation and purification for the GSCs was done via the TRIzol method from Invitrogen (Identifier:15596026). Isolated RNA was DNase-treated and concentrated using the Qiagen kit protocol (Identifier:79254 and 74204). At least 500 ng - 1µg of RNA was reverse transcribed following Invitrogen's SuperScript IV (Identifier: 18091050) protocol. RT-qPCR reactions included 1 µl of cDNA per well. RT-qPCR was performed using 500 ng - 1µg of RNA and the PowerUp SYBR Green (Applied Biosystems, Identifier: A25742) protocol. Normalization with GAPDH was used via the Delta Ct method.

- *RNA Sequencing and related transcriptomic analysis*

RNA isolated from siHDAC7-treated versus control-treated for each GSC1, GSC2, and GSC3 were sent to Azenta US, Inc. in duplicates. Samples were shipped on ice-dry and validated via Azenta's quality control assurance for isolated RNA quality and purity to undergo a Standard RNA-seq with ribosomal RNA (rRNA) depletion. Succeeding alignments and other analyses were performed in-house.

RNA-seq differential gene expression was performed in the R Studio platform using DESeq2 for dispersion of RNA seq data and annotated with GENCODE reference annotation for the human hg38 genome. The StemChecker web tool was used to evaluate the stemness of the differentially expressed genes [39]. The ChEA3 web tool was used for the transcription factor enrichment analysis [40]. The GSEA software [41] was used to evaluate the stem cell signature of the GSCs using stemness signature sets for Verhaak *et al.* [42], and Carro *et al.* [43]. Gene enrichment, pathway, and genomic interaction analyses were done via Gene Ontology, KEGG pathway, and InterMine enrichment databases.

- *Statistical analysis*

Kaplan Meier survival analysis based on the same high-risk/low-risk stratification was used with the log-rank test and Gehan-Breslow-Wilcoxon method. For the inhibition analysis, we performed a two-tailed, paired student T-test, or one-way ANOVA for the relations between different groups; the p-value of significance was $P \leq 0.05$, and representation was done as means ± standard deviation (SD) or ± standard error of the mean (SEM). For the tumor sphere formation assay, we performed a two-tailed, unpaired student t-test; the P-value of significance was $P \leq 0.05$. The cutoffs used for the differential expression analysis were adjusted to P-value = 0.05 and Log2FC = 0.5. Statistical significance is represented as follows: $P \leq 0.05$: *, $P \leq 0.01$: **, and $P \leq$

0.001: ***, topped by the number of experiments repetitions as once: *, twice: **, thrice: ***, and quadlet: ****.

R scripts, packages, and related genome-wide tools used in the data analysis are available upon request and have been deposited at GEO.

III. Results

HDAC7 expression is GBM regulator, distinct from other members of class IIa HDAC, from publicly available data.

Previous studies have demonstrated that individual HDACs can play roles in various forms of cancer. However, the expression levels of these HDACs can vary, with some being over-expressed and others under-expressed across different types of cancers [18]. Indeed, the concept of pan HDAC inhibition faced complications, particularly in cancer treatment, due to its nonspecific approach of inhibiting different isoforms. This challenge arose from the fact that these isoforms have been shown to exert distinct mechanisms of epigenetic regulation [15, 19].

By utilizing the Chinese Glioma Genome Atlas (CGGA) and comparing mRNA expression levels of each individual class IIa HDAC in GBM relative to other forms of malignant gliomas, we found that the expression of all class IIa HDACs is elevated across various glial tumors, with HDAC7 showing the highest expression observed in GBM (**Figure 2.2A-D**). Remarkably, survival analysis conducted on GBM patient cohorts from the CGGA revealed that high HDAC7-expressing patients showed a significantly lower probability of survival, while the expression level of other members of Class IIa HDACs has no correlation to worse patient survival (**Figure 2.2E-H**).

Additionally, we utilized the Cancer Genome Atlas (TCGA) to compare expression levels of individual HDAC class IIa members in the GBM TCGA dataset relative to non-tumor samples. Interestingly, our analysis revealed that HDAC7 is the only Class IIa HDAC with significantly higher expression in GBM as compared to the non-tumor samples **(Figure 2.3A-D)**. These findings suggest a potential specificity of HDAC7 as a therapeutic target for tumors over normal cells,

thereby potentially reducing off-target effects. Furthermore, we performed survival analysis on patients, high- and low-expressing Class IIa HDAC. Patients were divided into these two groups based on the maximally ranked statistics using the log-rank test as well as the Gehan-Breslow-Wilcoxon method. High HDAC7-expressing patients showed a significantly lower probability of survival ($p<0.004$), while the expression level of other members of Class IIa HDACs showed no inhibition to patient survival. (**Figure 2.3E-H**).

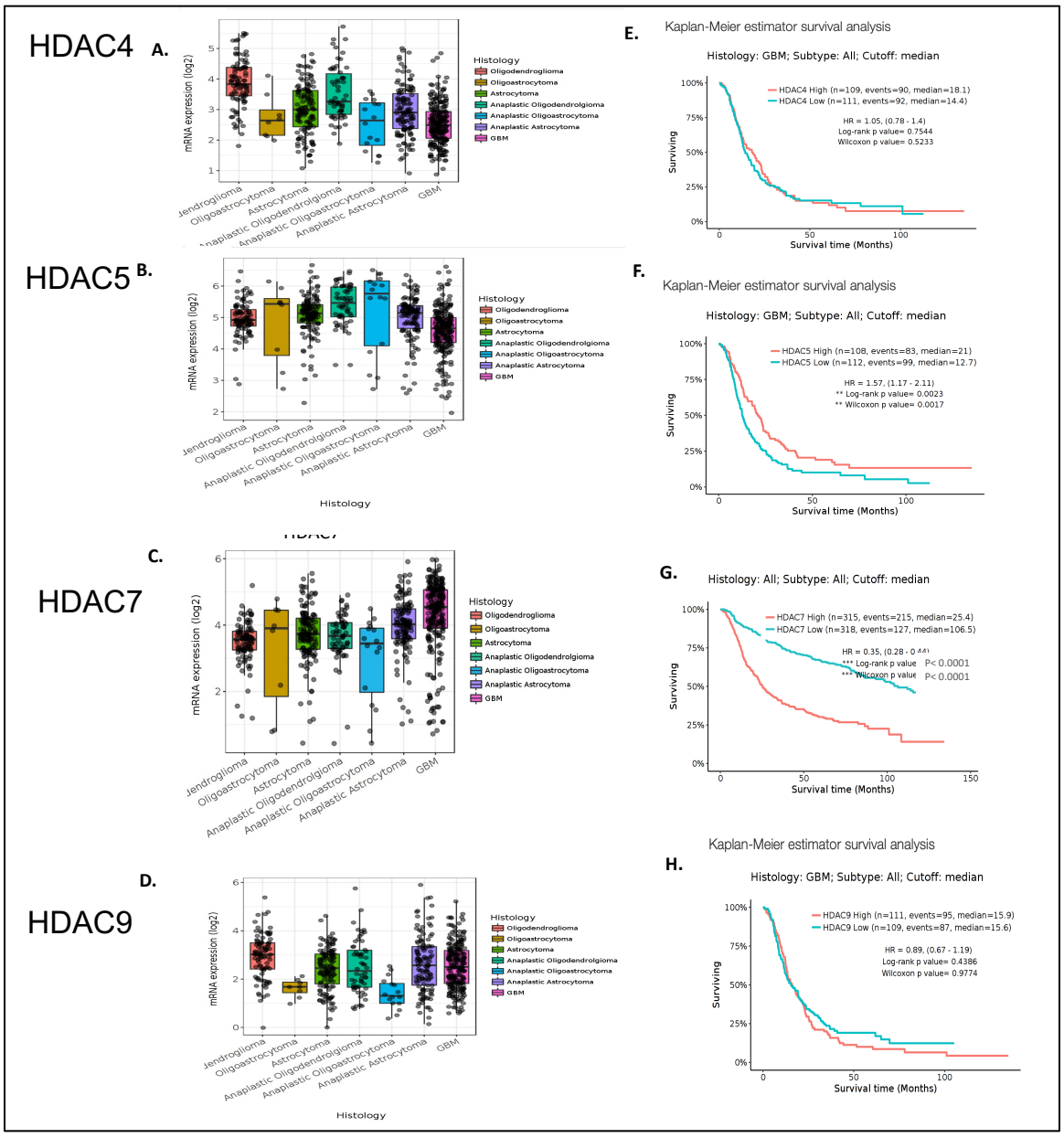

Figure 2.2 Class IIa HDAC is highly expressed in different forms of glioma, where HDAC7 only affects the survival of the GBM patients from the Chinese Glioma Genome Atlas (CGGA). ***A-D.*** *The expression of the individual HDAC class IIa in the different forms of the glial tumors for patients from the CGGA data shows the highest expression for HDAC5 and HDAC7, amongst other gliomas.* ***E-H.*** *Kaplan-Meyer Survival analysis for GBM patients from the CGGA cohort showing the effect of the individual HDAC IIa members on the survival of GBM patients divided into two groups ("high HDAC expression" and "low HDAC expression"), with HDAC7 "low expression" versus "high expression" showing the highest GBM patients survival compared to all other HDAC IIa expressions.*

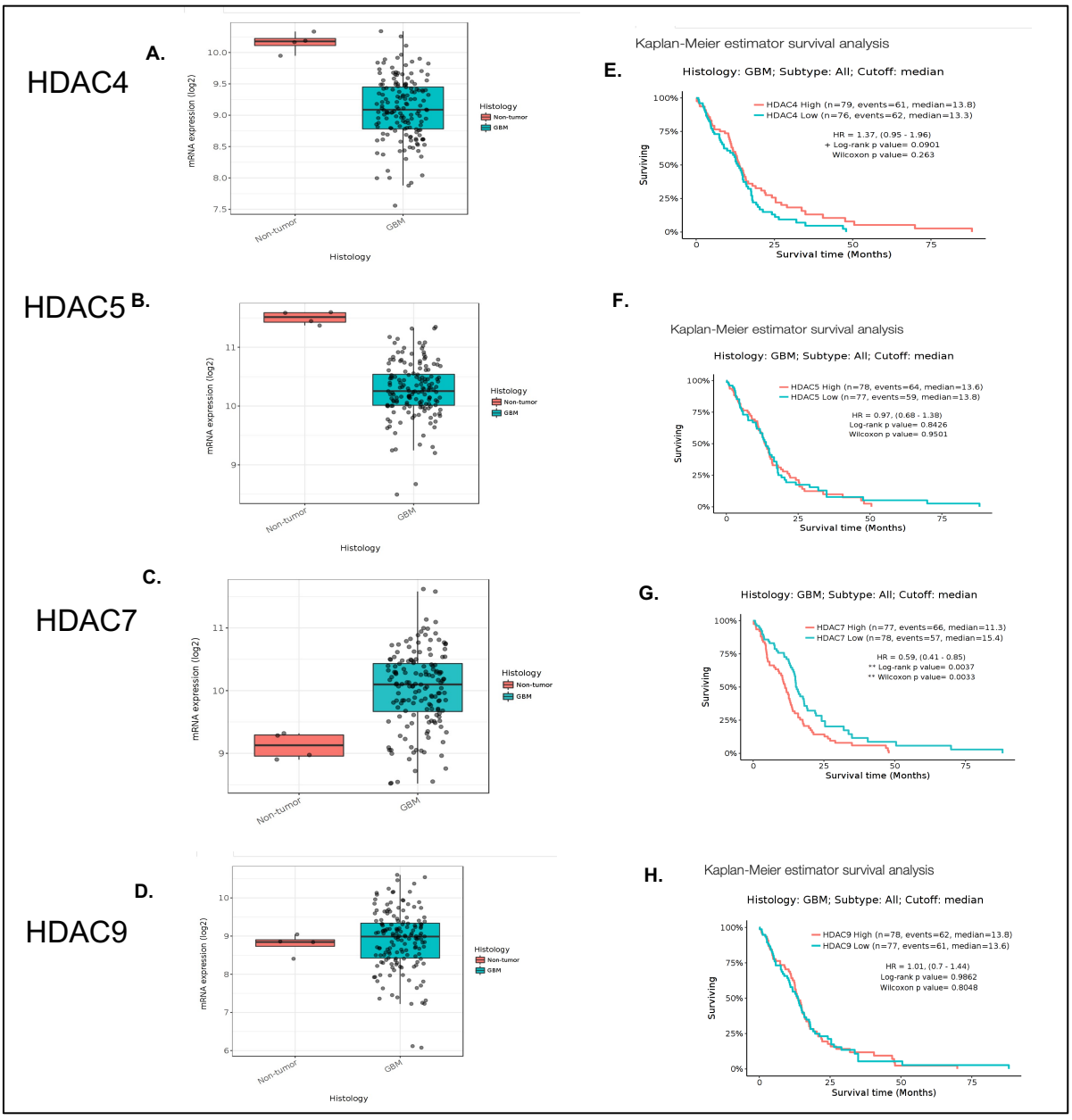

Figure 2.3 HDAC7 is the Class IIa HDAC with the highest expression in GBM from the Cancer Genome Atlas (TCGA). A-D. *The expression of the individual HDAC class IIa in GBM tumors versus non-tumors from the TCGA data with HDAC7 shows the most outstanding exclusivity for GBM over normal brains compared to all other HDAC class IIa.* ***E-H.*** *Kaplan-Meyer Survival analysis for GBM patients from the TCGA cohort showing the effect of the individual HDAC IIa members on the survival of GBM patients divided into two groups ("high HDAC expression" and "low HDAC expression"), with HDAC7 "high expression" group showing the worst survival and HDAC7 "low expression" group showing the highest survival compared to all other HDAC IIa expressions.*

HDAC7's high expression dysregulates the expression of almost half of the genes in the GBM tumors from the TCGA data and enriches metastatic pathways.

From the transcriptomic analysis of RNA-seq data on the GBM cohort downloaded from the TCGA database, we identified 4238 genes that were differentially expressed based on high expression levels of HDAC7 alone with the FDR <0.05 **(Figure 2.4A and B).** Furthermore, Gene Ontology enrichment analysis revealed significant enrichment of biological functions related to angiogenesis and metastasis in GBM **(Figure 2.4C).** The TCGA GBM data cohort consisted of primary, secondary, and recurrent GBM cases. Interestingly, Kaplan-Meier survival analysis indicated that the poorest survival outcomes were observed among patients with primary GBM tumors. This observation suggests that high expression of HDAC7 in GBM tumors at the time of initial diagnosis may contribute to poorer tumor prognosis and reduced survival for patients.

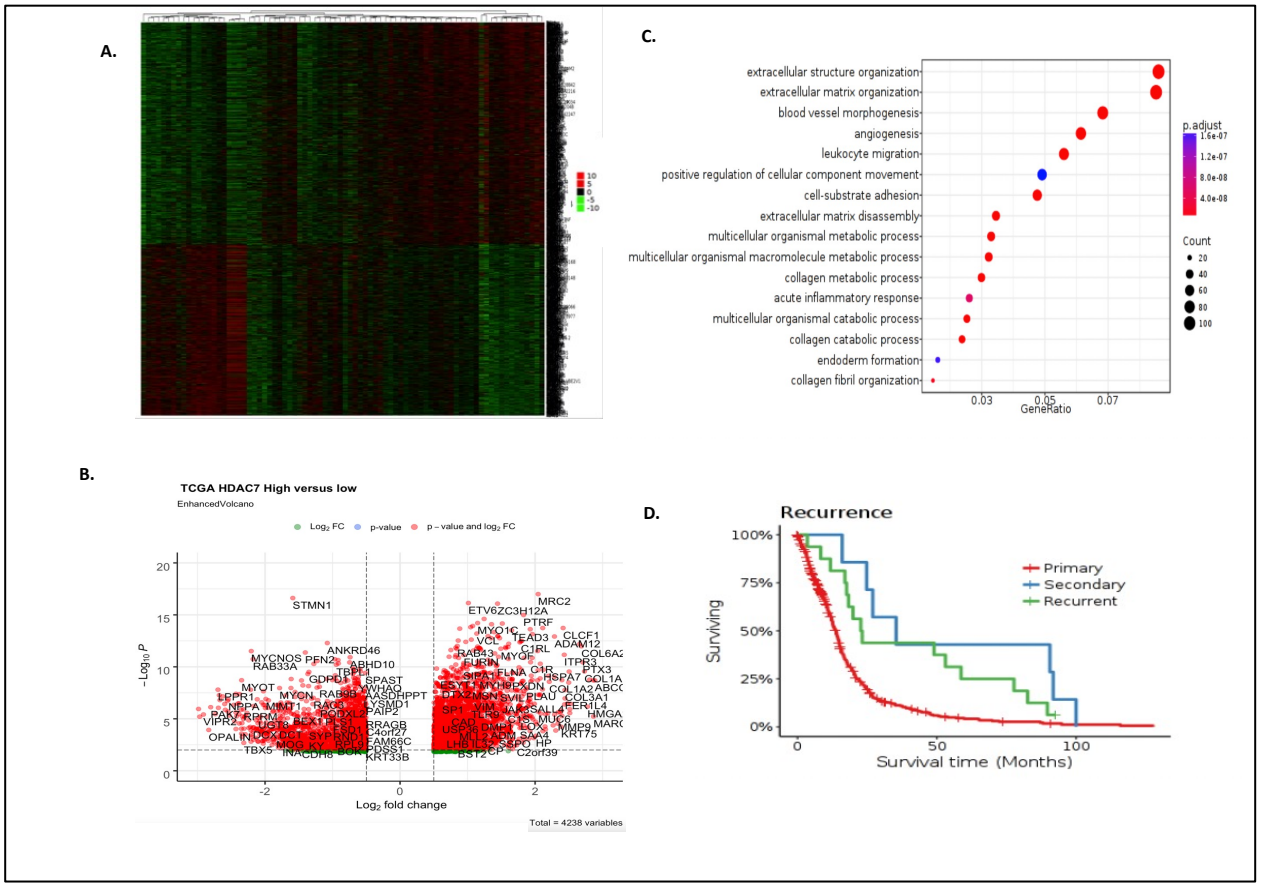

Figure 2.4 HDAC7 expression is a GBM regulation factor in the TCGA RNA-seq data. A. *Heat Map representation of differentially expressed genes in the HDAC7 high expression group versus the HDAC7 low expression group in the GBM cohorts from TCGA data.* ***B.*** *Volcano plot representation showing 4238 differential expressed genes in the HDAC7 high- versus -7 low expression in the TCGA GBM cohorts, FDR<0.05.* ***C****. Gene Ontology enrichment analysis for the RNA-seq from TCGA shows enrichment towards metastatic phenotypes for the HDAC7 high-expression group.* ***D.*** *Kaplan-Meyer Survival Analysis for the three subgroups of the GBM patients from TCGA: primary, secondary, and recurrent GBM.*

The expression of HDAC7 correlates with the progression-free survival and aggressiveness of GBM tumors in RIH's patients.

In collaboration with the Pathology Department at Rhode Island Hospital, we collected 84 PFF tumor samples from patients with a confirmed diagnosis of IDH WT Glioblastoma. We conducted Nanostring gene expression analysis using the Pan-Cancer Panel, comprising 770 genes known to play roles in cancer. We clustered the expression data based on the levels of HDAC expression, where HDAC7 expression was shown to correlate with a significant increase in the expression of 45 genes and inhibition of 2 genes **(Figure 2.5A).** Consistent with findings from the TCGA data, we observed gene enrichment towards pathways involved in migration, metastasis, and cell proliferation **(Figure 2.5C)**. Furthermore, mirroring our previous discoveries from online datasets of GBM patients from TCGA and CGGA, we observed decreased survival in our GBM cohort from RIH patients with high HDAC7 expression. This was determined through Kaplan-Meier survival analysis based on the same low-risk/high-risk stratification using the log-rank test and the Gehan-Breslow-Wilcoxon method **(Figure 2.5B)**.

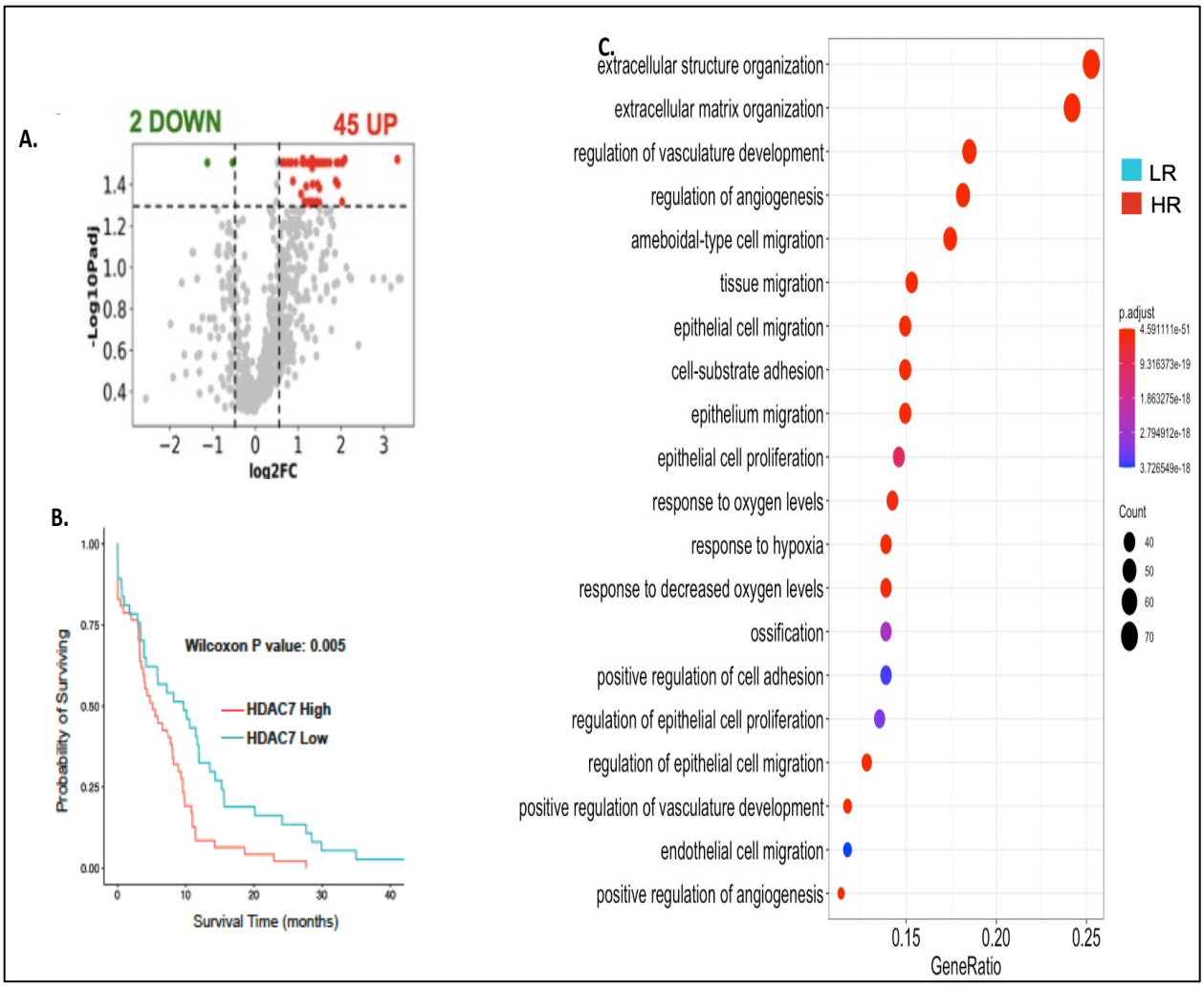

Figure 2.5. HDAC7 is an epigenetic regulator for GBM patients from RIH. A. *Volcano plot representation of differential expression analysis of genes stratified by HDAC7 expression HR/LR tumors, with 10e-5 P adjusted cut-off and Log Fold change cut-off of 0.5.* ***B.*** *Kaplan-Meier Survival Analysis for GBM patients from RIH. Data are divided into two groups, with the HDAC7 "high expression" patient group showing less survival than "low expression" patients. A log-rank test and the Gehan-Breslow-Wilcoxon method are used for the Kaplan-Meier curve estimation.* ***C.*** *Gene Ontology enrichment analysis of the differentially expressed genes. The p-adj (False discovery rate) method is Benjamini & Hochberg with a P-adjusted cut-off of 0.05.*

HDAC7 protein expression is highly expressed in primary GSCs, and DIPGs show minimal expression in human astrocytes.

To validate our hypothesis regarding the specificity of HDAC7 as a potential target for GBM, we conducted protein expression analysis using six primary GSCs and four DIPGs and compared them to normal human astrocytes. We show, through western blot that HDAC7 is highly expressed in GSCs and DIPG cells while minimally expressed in control human astrocyte lysates **(Figure 2.6).** This reaffirms the specificity of HDAC7 as a potential therapeutic target for GBM.

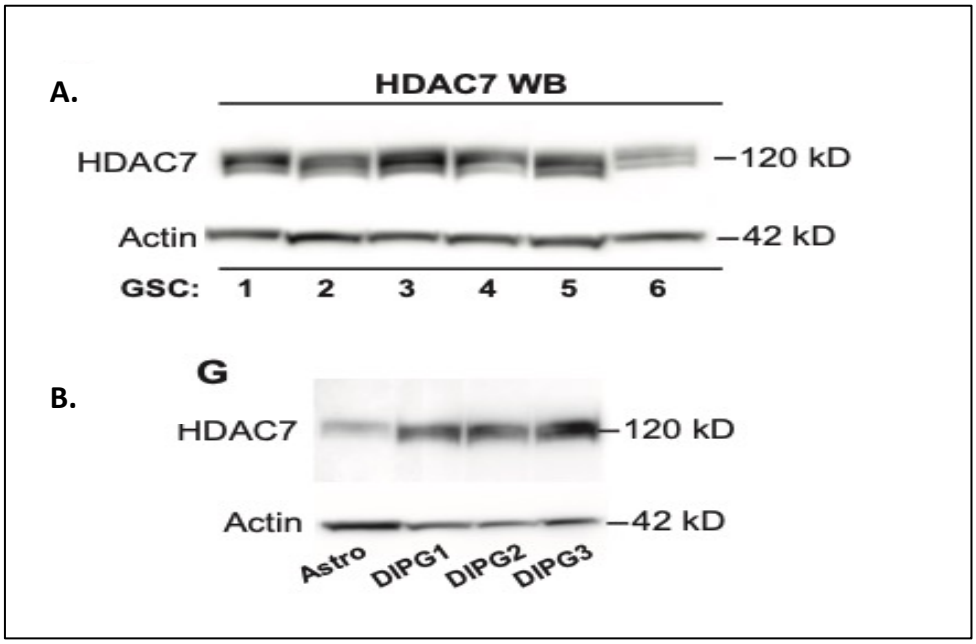

Figure 2.6. HDAC7 protein expression is high in GSCs and DIPGs and is minimally expressed in the human astrocyte lysates. *Relative HDAC7 protein expression in six primary GSCs and four DIPGs versus the normal human astrocytes. Protein levels were done with western blot and normalized with B-actin (n=3). A "Brown-Forsythe ANOVA test" for multiple comparisons was used to calculate statistical significance: $p \leq 0.0001$: ****.*

HDAC7 inhibition suppresses the oncogenic potential for primary GSCs in vitro.

Since increased cell viability and tumorsphere formation capability are crucial for GSCs mediating GBM progression, we conducted experiments to assess these capabilities in patient-derived GSCs after inhibition of HDAC7 using siRNA. We observed that HDAC inhibition significantly suppressed both GSC viability and their ability to form tumorspheres in vitro **(Figure 2.7A and B)**. Furthermore, we transfected two patient-derived GSCs with an expression construct for HDAC7 obtained from Origene and conducted a colony formation assay, comparing HDAC7-transfected GSCs with GSCs transfected with GFP as a control. Our results demonstrated that high expression of HDAC7 significantly increased the number of cell colonies per field at 10X magnification **(Figure 2.7C).**

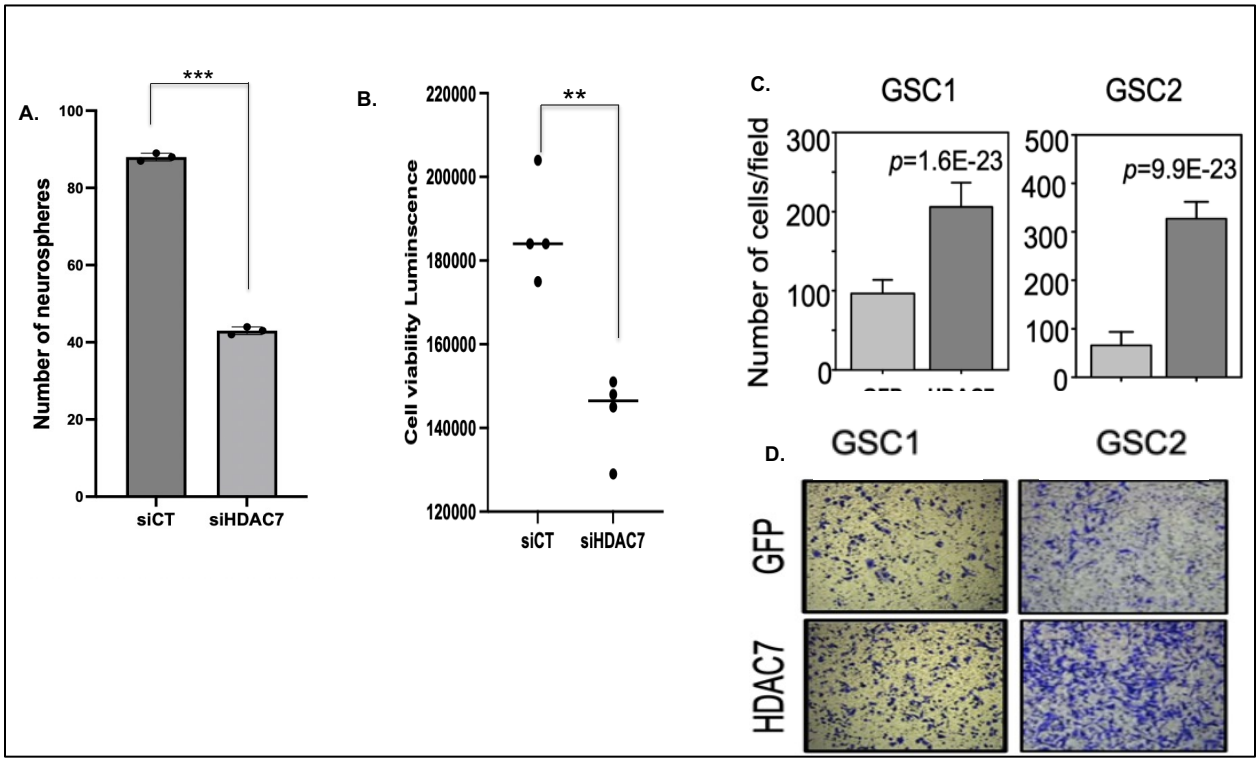

Figure 2.7. HDAC7 alters the phenotypic oncogenic potential of patient-derived GSCs. A. *Quantification of GSCs cell viability with CellTiter Glo shows inhibition of the siHDAC7-treated GSCs compared to siCT-treated.* ***B.*** *Tumor sphere formation assay shows the inhibition of the tumor sphere formation potential for siHDAC7-treated GSCs compared to siCT-treated.* ***C.*** *Representative image of a colony formation assay of two GSCs transfected with GFP or HDAC7.*

Cells were stained with methylene blue, and the images were acquired at 10X magnification (p<1E-22). ***D.*** *Quantification of methylene blue stained colonies following transfection of two patients derived GSCs with HDAC7 or GFP. HDAC7 expression induces a significant increase in the number of cell colonies. (n=3). An unpaired test was used to calculate statistical significance: p ≤ 0.0001: ****, p ≤ 0.001: **.*

Inhibiting HDAC7 disrupts one-third to half of the typically expressed genes in primary GSCs.

Given the known heterogeneity of GSCs, we conducted experiments to assess the effects of specific HDAC7 knockdown in three different patient-derived GSCs using siRNA (n=3), followed by RNA-seq analysis. Transcriptomic analysis revealed differential gene expression, with an FDR<0.05, in 1342, 1870, and 6270 genes across the three primary GSCs after HDAC7 knockdown compared to siRNA negative control. Additionally, distinct significant clustering was observed among the knockdown control samples in the three different GSCs **(Figure 2.8 A-C and Supplementary Figure 1)**, with up to three-fold changes in both upregulated and downregulated genes **(Figure 2.8 D-F).**

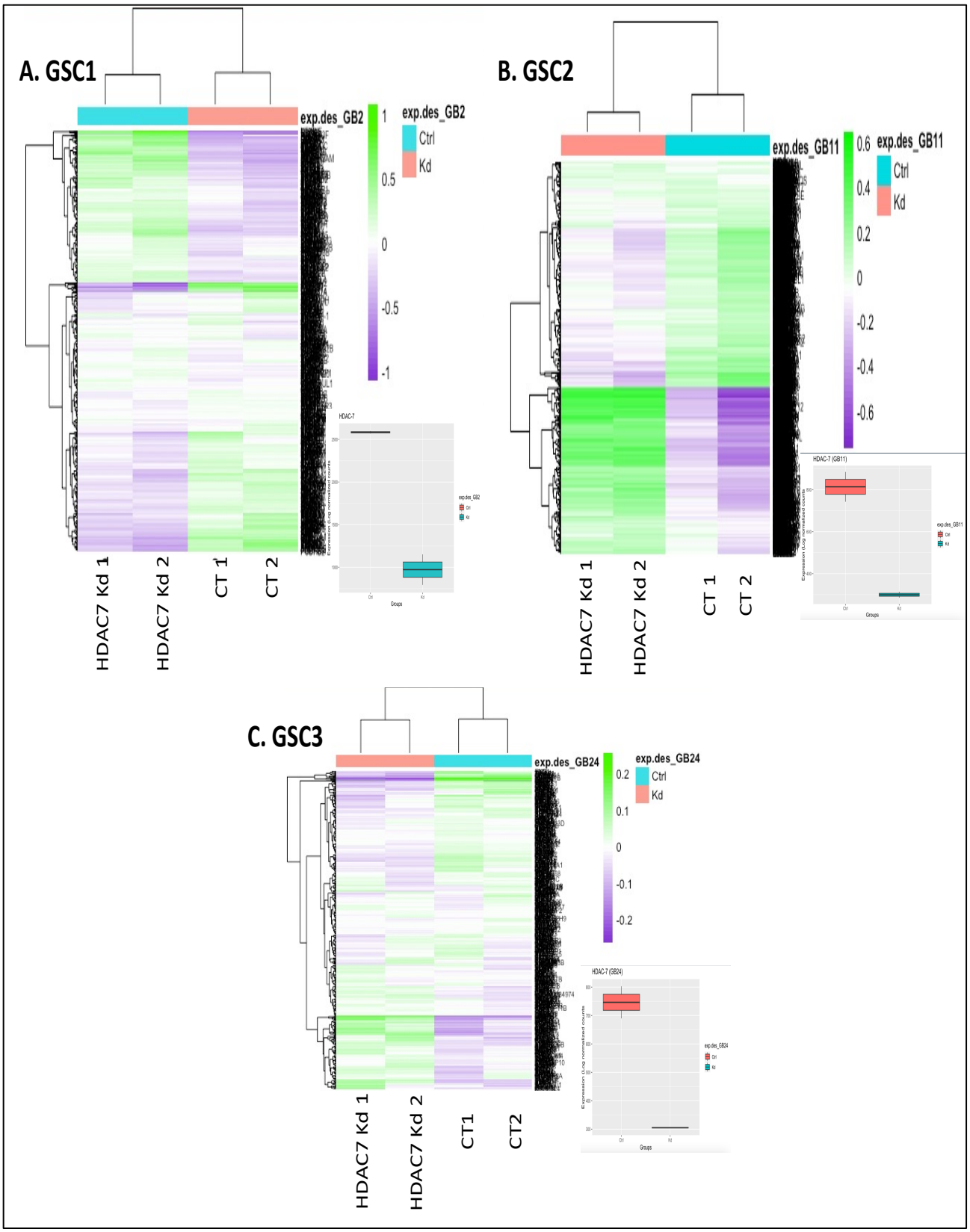
A. GSC1
exp.des_GB2
Ctrl
Kd
1
0.5
0
-0.5
-1
HDAC7 Kd 1
HDAC7 Kd 2
CT 1
CT 2
HDAC-7
B. GSC2
exp.des_GB11
0.6
0.4
0.2
0
-0.2
-0.4
-0.6
HDAC7 Kd 1
HDAC7 Kd 2
CT 1
CT 2
HDAC-7 (GB11)
C. GSC3
exp.des_GB24
0.2
0.1
0
-0.1
-0.2
HDAC7 Kd 1
HDAC7 Kd 2
CT1
CT2
HDAC-7 (GB24)

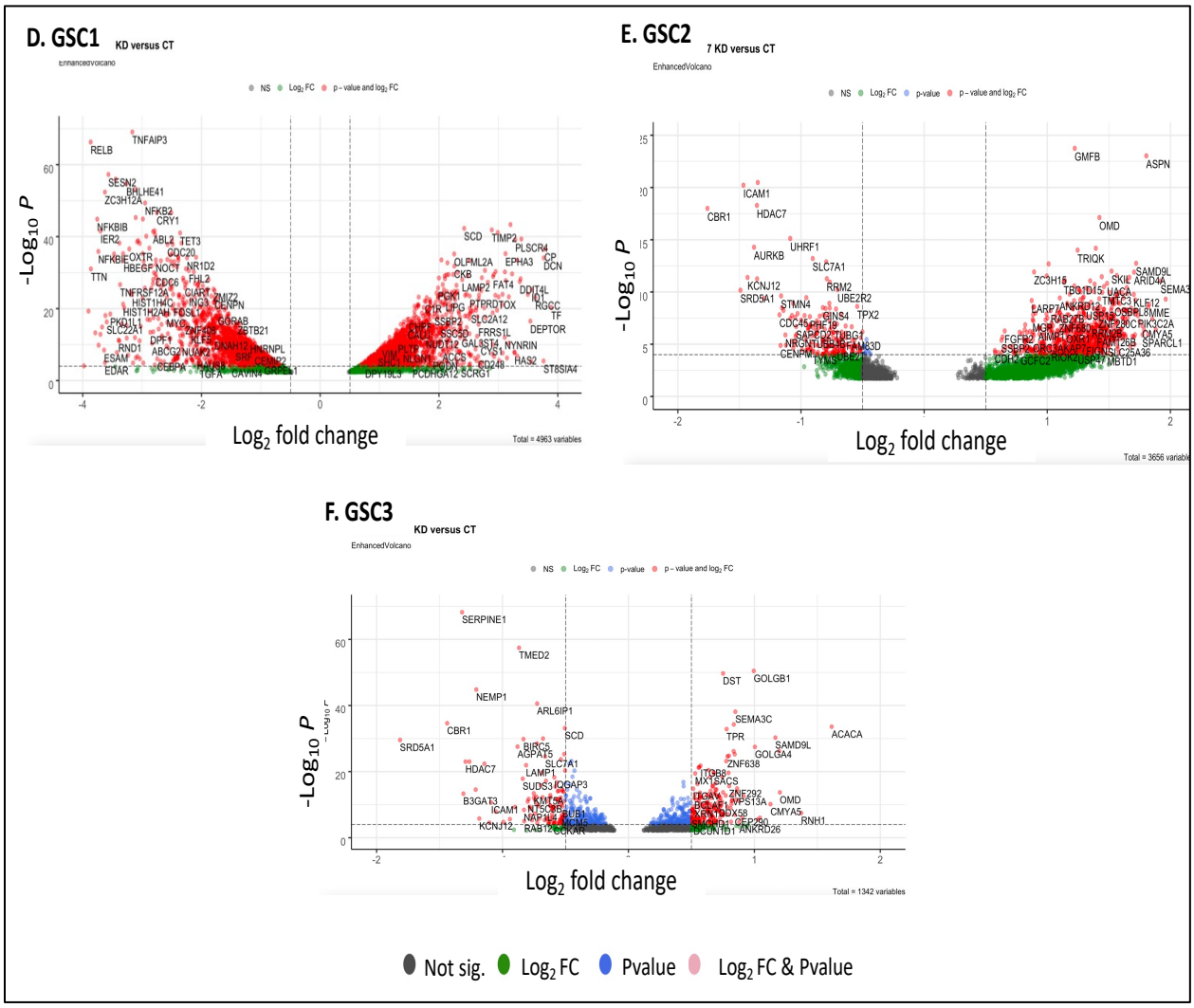

Figure 2.8. HDAC7 inhibition disrupts the transcriptomic profile of patient-derived GSCs. A-C. *Heat Map representation shows inhibition of HDAC7 for the top 500 differentially expressed genes with least P adjusted values, inhibiting HDAC7 causes significant disruption in the gene expression in three different patient-derived GSCs, respectively, compared to control (n=3 per one GSC).* ***D-F.*** *Enhanced Volcano plot representation shows inhibition of HDAC7, causing up to a three-fold decrease or increase in the gene expression in three different patient-derived GSCs, respectively, compared to the control (n=3 per one GSC). The false discovery rate (FDR) is <0.05.*

Inhibiting HDAC7 drives the stemness of GSCs to embryonic phenotype and enriches cell cycle and tumorigenic activities.

We conducted an analysis focused on the downregulated genes after HDAC7 inhibition, revealing that 653, 740, and 394 stemness genes were suppressed by HDAC7 knockdown **(Figure 2.9 A-C)**. Phenotypic assessment of these downregulated stemness genes across 26 stemness gene signatures unraveled that these genes were closely associated with the phenotypes of embryonic stem cells and embryonal carcinoma, with significant adjusted P values < (**Figure 2.9 A-C**).

To understand the functional significance of these genes, we performed gene enrichment analysis on the differentially expressed genes using various tools for gene enrichment, including Gene Ontology and KEGG enrichment pathways. We observed that the enriched pathways primarily suppressed various biological processes related to cell cycle elongation phases, chromatin organization, cellular activities, and cell division (**Figure 2.10 A-C and Supplementary Table 1**). Furthermore, transcriptional factor enrichment analysis on the downregulated genes revealed E2F1, DNMT1, MYBL2, and FOXM1 as hits. These results indicate that HDAC7 enriches the GSCs towards transcriptional programs for cell cycle elongation, chromatin organization, chromosomal segregation, as well as oncogenesis (**Figure 2.10 D-F**).

Figure 2.9. HDAC7 inhibition drives patient-derived GSCs to the embryonic phenotype. A-C. *An overlap radar chart displays the overlap between the downregulated stemness genes across the different stem cell types. HDAC7 inhibition drives the stemness phenotype towards the embryonic stem cell and embryonal carcinoma phenotype with significantly adjusted P values repeated twice in three different patient-derived GSCs, respectively, compared to control (n=3 per one GSC).*

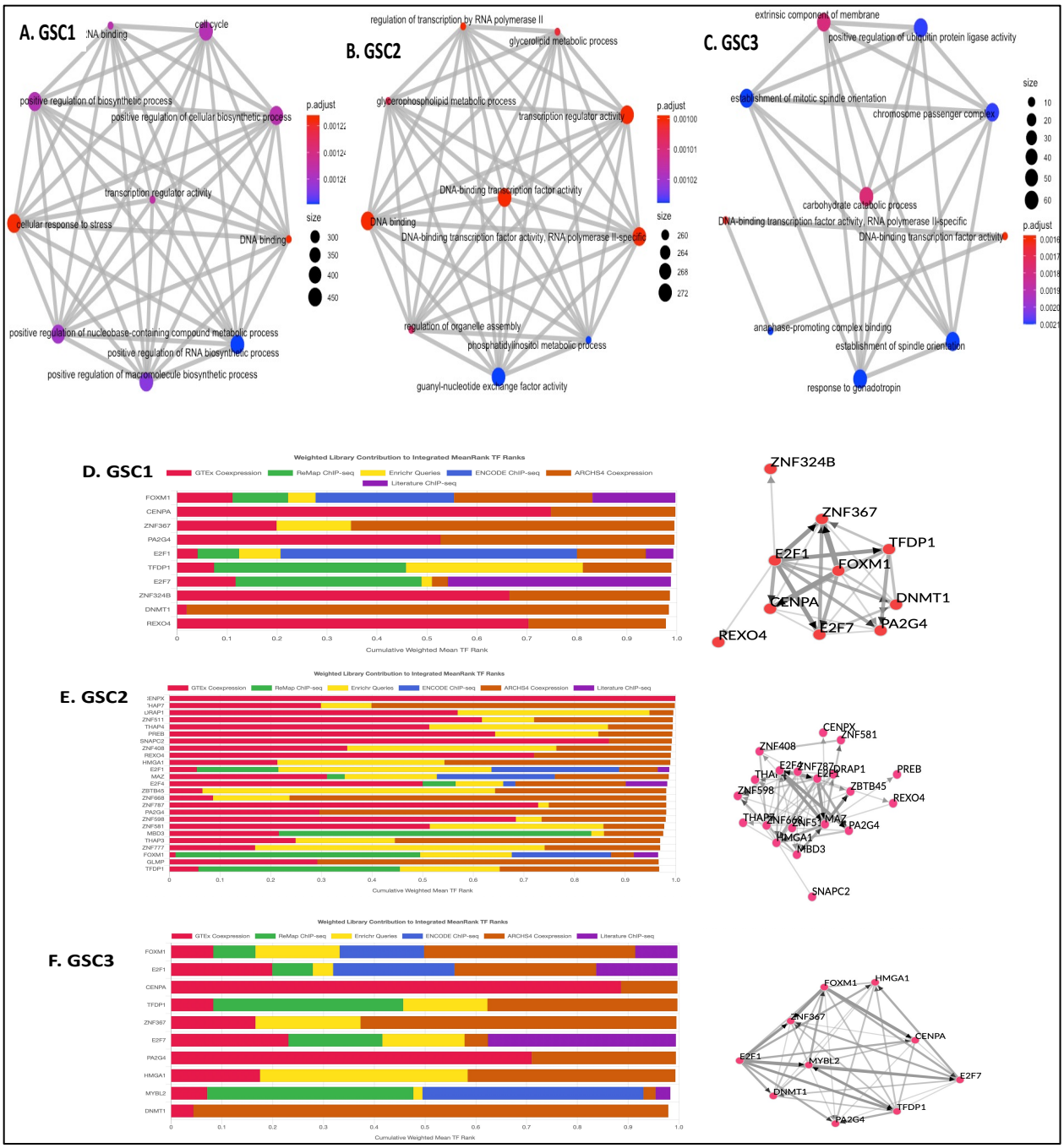

Figure 2.10. HDAC7 is implicated in oncogenic pathways. A-C. *Gene enrichment analysis using Gene Ontology shows the implications of the downregulated genes after HDAC7 inhibition in critical pathways important for oncogenesis and GBM tumor progression.* ***D-C.*** *HDAC7 inhibition drives the enrichment of critical transcription factors implicated in tumor initiation and progression with significantly adjusted P values repeated twice in three different patient-derived GSCs, respectively, compared to control (n=3 per one GSC).*

HDAC7 does not seem to affect the epithelial-to-mesenchymal transition (EMT)

In many human cancers, including GBM, the transition of cancer cells from an epithelial to a mesenchymal phenotype is often associated with more aggressive tumors [44, 45]. We aimed to investigate the involvement of HDAC7 in this phenotypic transition and whether HDAC7 affects the expression of a mesenchymal transcriptome. To achieve this, we utilized GSEA software to identify mesenchymal and proneural (epithelial) expression signatures based on various verified gene signature stratifications [42, 43]. By calculating the enrichment score for each gene set, we observed that HDAC7 inhibition suppresses both the mesenchymal and proneural gene set signatures altogether, which was validated for various GSCs and multiple signature gene sets (**Figure 2.11A**).

To further validate this finding, we examined the expression of subtype signature genes in the TCGA and CGGA GBM databases. Our analysis revealed that HDAC7 expression is relatively evenly distributed among the three GSC subtypes **(Figure 2.11B)**. These findings support the notion that HDAC7 inhibition suppresses transcriptomic signatures across all GSC subtypes without exhibiting specific selectivity towards certain signature profiles.

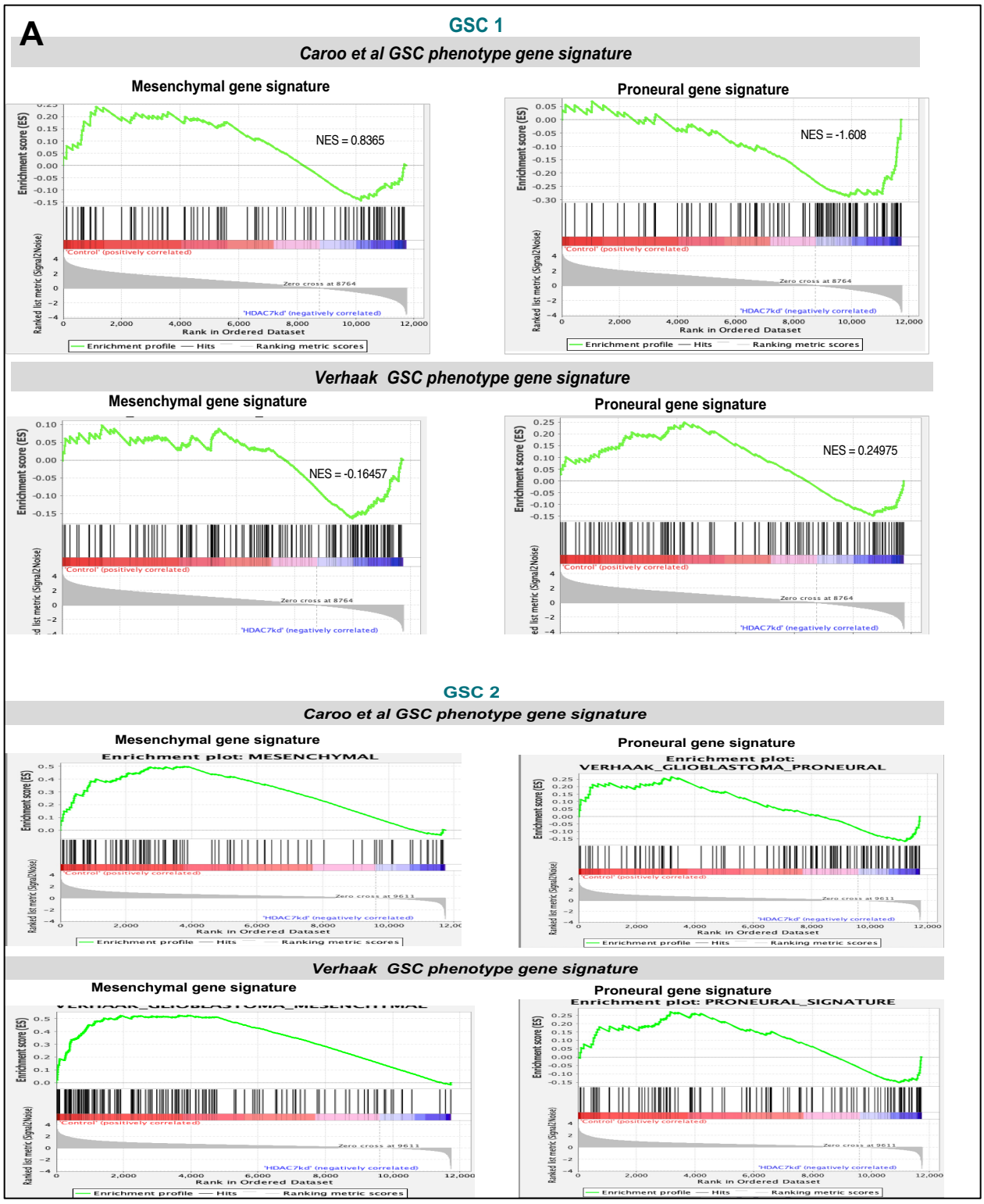
A
GSC 1
Caroo et al GSC phenotype gene signature
Mesenchymal gene signature
NES = 0.8365
Proneural gene signature
NES = -1.608
Verhaak GSC phenotype gene signature
Mesenchymal gene signature
NES = -0.16457
Proneural gene signature
NES = 0.24975
GSC 2
Caroo et al GSC phenotype gene signature
Mesenchymal gene signature
Enrichment plot: MESENCHYMAL
Proneural gene signature
Enrichment plot: VERHAAK_GLIOBLASTOMA_PRONEURAL
Verhaak GSC phenotype gene signature
Mesenchymal gene signature
Proneural gene signature
Enrichment plot: PRONEURAL_SIGNATURE
Enrichment score (ES)
Ranked list metric (Signal2Noise)
'Control' (positively correlated)
'HDAC7kd' (negatively correlated)
Zero cross at 8764
Zero cross at 9611
Rank in Ordered Dataset
Enrichment profile
Hits
Ranking metric scores

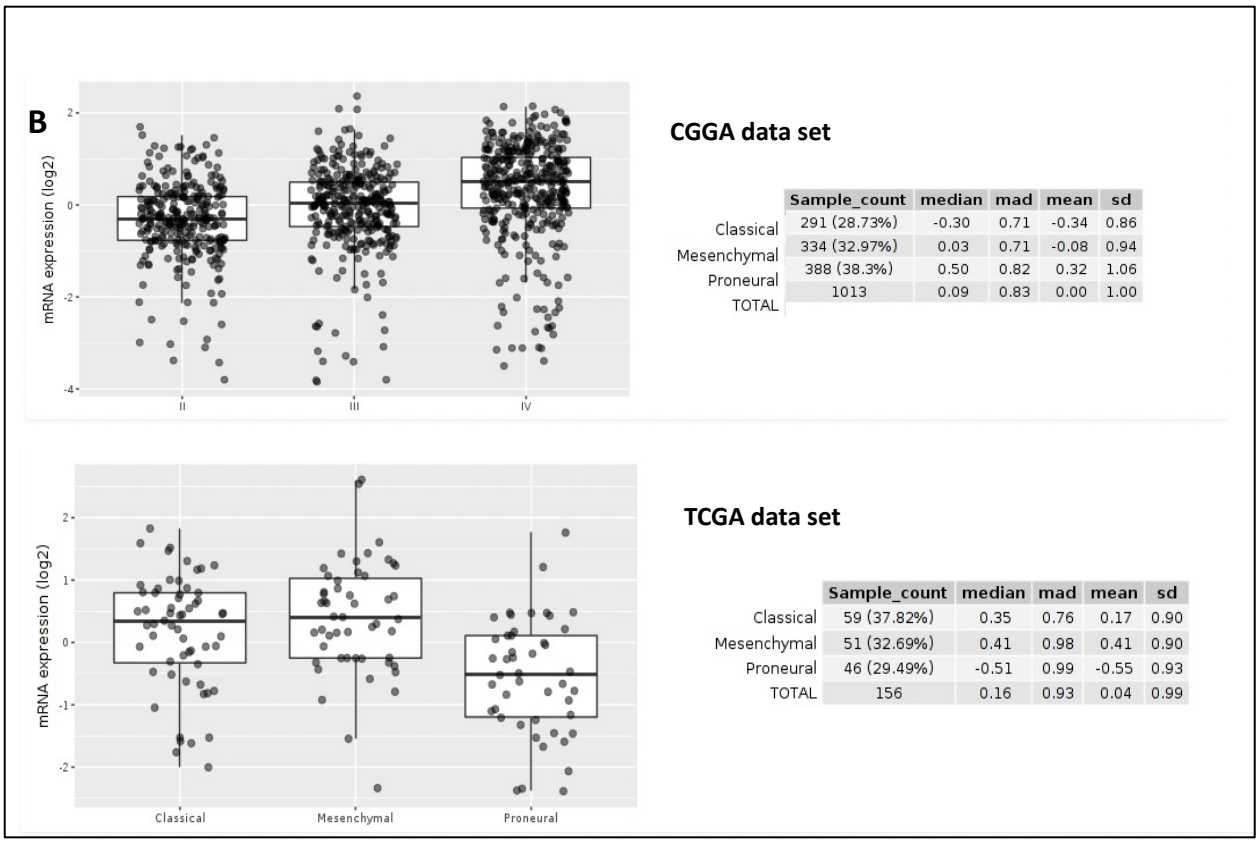

Figure 2.11 HDAC7 expression is implicated in all GSCs subtypes signatures. A*. GSEA enrichment plots of HDAC7-knocked down GSCs versus control using two different signature gene sets showing that HDAC7 inhibition inhibits the signature genes of the mesenchymal and the proneural phenotypes. The normalized enrichment scores (NES) are displayed for each plot. The peak point of the green plot is the ES (enrichment score), which tells how over or under-expressed the gene is with respect to the ranked gene signature list. The second part of the graph (red and blue) shows where the rest of the genes related to the signature feature are located in the ranking. The third part of the graph (gray) shows how the metric is distributed along the list.* ***B.*** *HDAC7 is equally expressed in the three GSCs' subtypes from the publicly available TCGA and CGGA data.*

HDAC7 is highly expressed in other forms of cancers compared to normal counterparts.

Anomalous expression and function of HDAC7 have been associated with various cancers, including colorectal, gastric, renal, pancreatic, melanoma, adenocarcinomas, and brain cancer [31, 46-48]. Additionally, accumulating evidence suggests that HDAC7 may serve as a potential biomarker for the

progression of many cancers [46, 48, 49]. HDAC7 has been shown to play roles in driving tumorigenesis and progression by stimulating oncogenic signaling and evading immune attacks [33, 48, 50-52]. Given the pivotal role we demonstrated for HDAC7 in GBM, we aimed to investigate the potential implications of HDAC7 in other cancers. Utilizing data from the TCGA repository, we performed survival analysis on two patient cohorts (HDAC7 high and low expression patients) in multiple well-known deadly cancers, including cervical squamous cell carcinoma, kidney renal clear cell carcinoma, kidney renal papillary cell carcinoma, liver hepatocellular carcinoma, stomach adenocarcinoma, and uterine corpus endometrial carcinoma. Our analysis revealed a decrease in patients' overall survival proportional to high HDAC7 expression (**Figure 2.12A**).

Furthermore, we assessed HDAC7 protein expression in several known human cancer cell lines from the NCI 60 cell line screen, including A549 (non-small-cell lung cancer carcinoma NSCLC), ACHN (metastatic renal adenocarcinoma), HCT116 (colorectal carcinoma), and SK-Mel-5 (malignant melanoma). Our findings revealed that HDAC7 is expressed in all these cancer cell lines, with the highest expression observed in A549 and ACHN cells (**Figure 2.12B & C**). Additionally, we conducted exploratory transfection experiments on some of these cell lines to evaluate their suitability for HDAC7 siRNA inhibition. Our results demonstrated that HDAC7 siRNA can effectively inhibit the protein expression of HDAC7 in these cells, suggesting the potential applicability of siRNA therapeutics in the corresponding cancers of these cells (**Figure 2.12D & E**). Finally, we investigated the oncogenic changes in cell viability in one of these cell lines (A549) following siRNA inhibition of HDAC7. Our data revealed that HDAC7 inhibition significantly suppresses A549 cancer cell viability (**Figure 2.12F**). Taken together, our findings indicate that HDAC7 is highly expressed in various forms of malignancies. Its association with

tumor aggressiveness and progression suggests that HDAC7 holds promising potential as a therapeutic target in multiple human cancers.

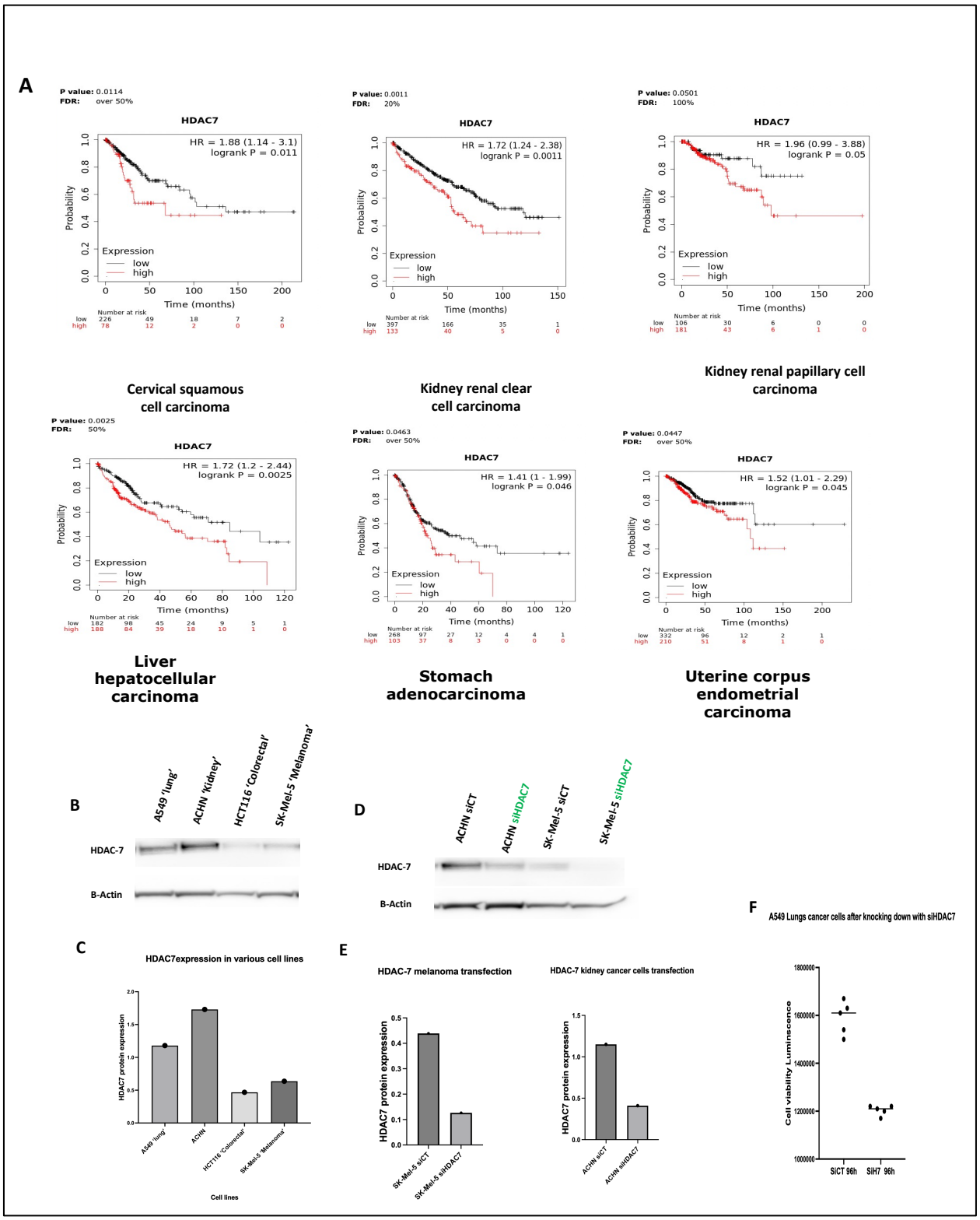
A
P value: 0.0114
FDR: over 50%
HDAC7
HR = 1.88 (1.14 - 3.1)
logrank P = 0.011
Probability
Expression
low
high
Time (months)
Number at risk
low 226 49 18 7 2
high 78 12 2 0 0
Cervical squamous cell carcinoma
P value: 0.0011
FDR: 20%
HDAC7
HR = 1.72 (1.24 - 2.38)
logrank P = 0.0011
Probability
Expression
low
high
Time (months)
Number at risk
low 397 166 35 1
high 133 40 5 0
Kidney renal clear cell carcinoma
P value: 0.0501
FDR: 100%
HDAC7
HR = 1.96 (0.99 - 3.88)
logrank P = 0.05
Probability
Expression
low
high
Time (months)
Number at risk
low 106 30 6 0 0
high 181 43 6 1 0
Kidney renal papillary cell carcinoma
P value: 0.0025
FDR: 50%
HDAC7
HR = 1.72 (1.2 - 2.44)
logrank P = 0.0025
Probability
Expression
low
high
Time (months)
Number at risk
low 182 98 45 24 9 5 1
high 188 84 39 18 10 1 0
Liver hepatocellular carcinoma
P value: 0.0463
FDR: over 50%
HDAC7
HR = 1.41 (1 - 1.99)
logrank P = 0.046
Probability
Expression
low
high
Time (months)
Number at risk
low 268 97 27 12 4 4 1
high 103 37 8 3 0 0 0
Stomach adenocarcinoma
P value: 0.0447
FDR: over 50%
HDAC7
HR = 1.52 (1.01 - 2.29)
logrank P = 0.045
Probability
Expression
low
high
Time (months)
Number at risk
low 332 96 12 2 1
high 210 51 8 1 0
Uterine corpus endometrial carcinoma
B
A549 'lung'
ACHN 'kidney'
HCT116 'Colorectal'
Sk-Mel-5 'Melanoma'
HDAC-7
B-Actin
C
HDAC7expression in various cell lines
HDAC7 protein expression
A549 'lung'
ACHN
HCT116 'Colorectal'
SK-Mel-5 Melanoma
Cell lines
D
ACHN siCT
ACHN siHDAC7
SK-Mel-5 siCT
Sk-Mel-5 siHDAC7
HDAC-7
B-Actin
E
HDAC-7 melanoma transfection
HDAC7 protein expression
Sk-Mel-5 siCT
Sk-Mel-5 siHDAC7
HDAC-7 kidney cancer cells transfection
HDAC7 protein expression
ACHN siCT
ACHN siHDAC7
F
A549 Lungs cancer cells after knocking down with siHDAC7
Cell viability Luminscence
SiCT 96h
SiH7 96h

Figure 2.12 HDAC7 expression could be implicated in other forms of human cancers. A*. Kaplan-Meier Survival Analysis for patients from the TCGA database from various cancers, including A549 (non-small-cell lung cancer carcinoma NSCLC), ACHN (metastatic renal adenocarcinoma), HCT116 (Colorectal carcinoma), and SK-Mel-5 (Malignant Melanoma). Data are divided into two groups, with HDAC7 "high expression" patient group showing less survival than "low expression" patients. A log-rank test and the Gehan-Breslow-Wilcoxon method are used for the Kaplan-Meier curve estimation. Significant corresponding P values are shown on each respective plot* ***B.*** *Western blot analysis for the HDAC7 protein expression of A549, ACHN, HCT-116, and SK-Mel-5 cancer cell lines.* ***C.*** *Quantification of western blot results of HDAC7 protein expression levels in the tested cancer cell lines normalized with B-actin.* ***D.*** *Western blot analysis for the HDAC7 protein expression of each ACHN and SK-Mel-5 cancer cell line with siRNA against HDAC7 versus si-control.* ***E.*** *Quantification of western blot results showing a decrease in the HDAC7 protein expression levels after HDAC7 siRNA transfection in the tested cancer cell lines normalized with B-actin.* ***F.*** *Quantification of A549 NSCLC cell viability with CellTiter Glo. Inhibition of HDAC7 with HDAC7 siRNA induces significant inhibition of A549 cell viability 96 hours after transfection ($p<0.0001$).*

IV. Discussion

Epigenetic modification of gene expression through HDACs has been gripping considerable attention for their significant implications in driving major oncogenic pathways in various hematologic and solid cancers [17, 18, 23, 28, 53, 54]. HDACs influence cellular activities such as stemness, proliferation, apoptosis, differentiation, angiogenesis, migration, and invasion [15, 55].

We demonstrate that HDAC7 is a critical epigenetic regulator in GBM from tumor tissue samples from RIH patients. By analyzing publicly available data from large GBM cohorts, we showed that HDAC7 is distinguished from the other members of HDAC class IIa by demonstrating the highest specificity for GBM tumors versus normal brains. In addition, HDAC7 expression was shown as the most impactful regulator to be inversely correlated with a decrease in the overall survival of the GBM cohort from the public databases. This observation was supported by showing that HDAC7 expression correlated to the progression-free survival and aggressiveness phenotype of GBM patients from RIH. These findings highlight the unique role of HDAC7 in the context of GBM tumorigenesis and suggest its potential as a specific therapeutic target for GBM treatment.

We show that HDAC7 inhibition reduced the oncogenic potential of primary GSCs by inhibiting their cell viability and tumorsphere formation ability. In contrast, GSCs transfected with HDAC7 expression constructs showed increased cell colony formation. Such an observed impact on their phenotype suggests that HDAC7 has the potential to modulate GSCs' tumor pathogenesis.

Through transcriptomic analysis, we reaffirmed HDAC7's significant impact in driving tumor pathogenesis in GSCs at the genomic level. We demonstrated that knocking down HDAC7

disrupts up to half of the gene expression in GSCs derived from RIH patient samples and larger publicly available cohorts.

Our investigation revealed that numerous downregulated genes subsequent to HDAC7 inhibition are associated with stemness, particularly exhibiting an embryonic phenotype rather than neural stem or mesenchymal characteristics distinct from what we anticipated. We reasoned that this suggests that HDAC7 might be involved in fundamental cellular regulation by reactivating cellular activities typically dormant post-embryogenesis. Additionally, gene enrichment analysis indicated that HDAC7 is associated with biological processes and pathways highly active during embryonic development or tumor formation. Furthermore, unsupervised clustering of RNA-seq data post-HDAC7 inhibition, as well as analysis of TCGA data against EMT signature gene sets, demonstrated that HDAC7 inhibition suppressed all GSCs subtypes indiscriminately, further indicating a more fundamental regulatory role for HDAC7 in GBM pathology.

We also show that HDAC7's implication in oncogenesis is beyond GBM and is extended to many other forms of cancer. Indeed, it was shown before that HDAC7 abnormal expression and function have been linked to many forms of cancer [46-49]. We show that HDAC7's high expression is linked to decreased overall survival in patients who were candidates for many types of malignancies. Through assessment of HDAC7 protein expression in various cancer cell lines, we observed significant expression across these cell lines, with particularly high levels detected in cell lines associated with non-small-cell lung carcinoma and metastatic renal adenocarcinoma. Furthermore, employing our HDAC7 siRNA variant and transfection protocol, we successfully inhibited HDAC7 expression in these cell lines, leading to reduced cell viability, which validates the suitability of these cancer cells for our HDAC7 siRNA inhibition strategy.

Our analysis provides valuable insights into the impact of HDAC7 inhibition on the phenotypic and molecular landscape of GBM, shedding light on the dysregulated expression of HDAC7 and its potential contribution to GBM pathogenesis. By elucidating the distinct expression profile of HDAC7 in GBM, we have laid the groundwork for further investigations into its functional roles and therapeutic implications in this aggressive brain tumor. This preclinical study demonstrates the role of HDAC7 as a biomarker for GBM and potentially other cancers and provides new insights for epigenetically driven malignancies, which could significantly improve therapeutic options and outcomes for cancer patients.

Acknowledgment

The authors would like to thank the Department of Pathology at Rhode Island Hospital for providing the glioblastoma tissue samples for Nanostring Analysis. This study was supported by a Warren Alpert Foundation Grant #17775 to N.T., private philanthropic donations to the Laboratory of Cancer Epigenetics and Plasticity and from internal support of the Neurosurgery Department of Brown University to N.T.

V. Supplementary Figures

Supplementary Figure 1. **HDAC7 inhibition disrupts the transcriptomic profile of patient-derived GSCs.** MA plot representation with gold change is computed versus mean expression, considering the magnitude of the P value that is sometimes overlooked in volcano plots. Inhibition of HDAC7 caused up to a three-fold decrease or increase in the gene expression in three different patient-derived GSCs, respectively, compared to control (n=3 per one GSC). The false discovery rate (FDR) is 0.05.

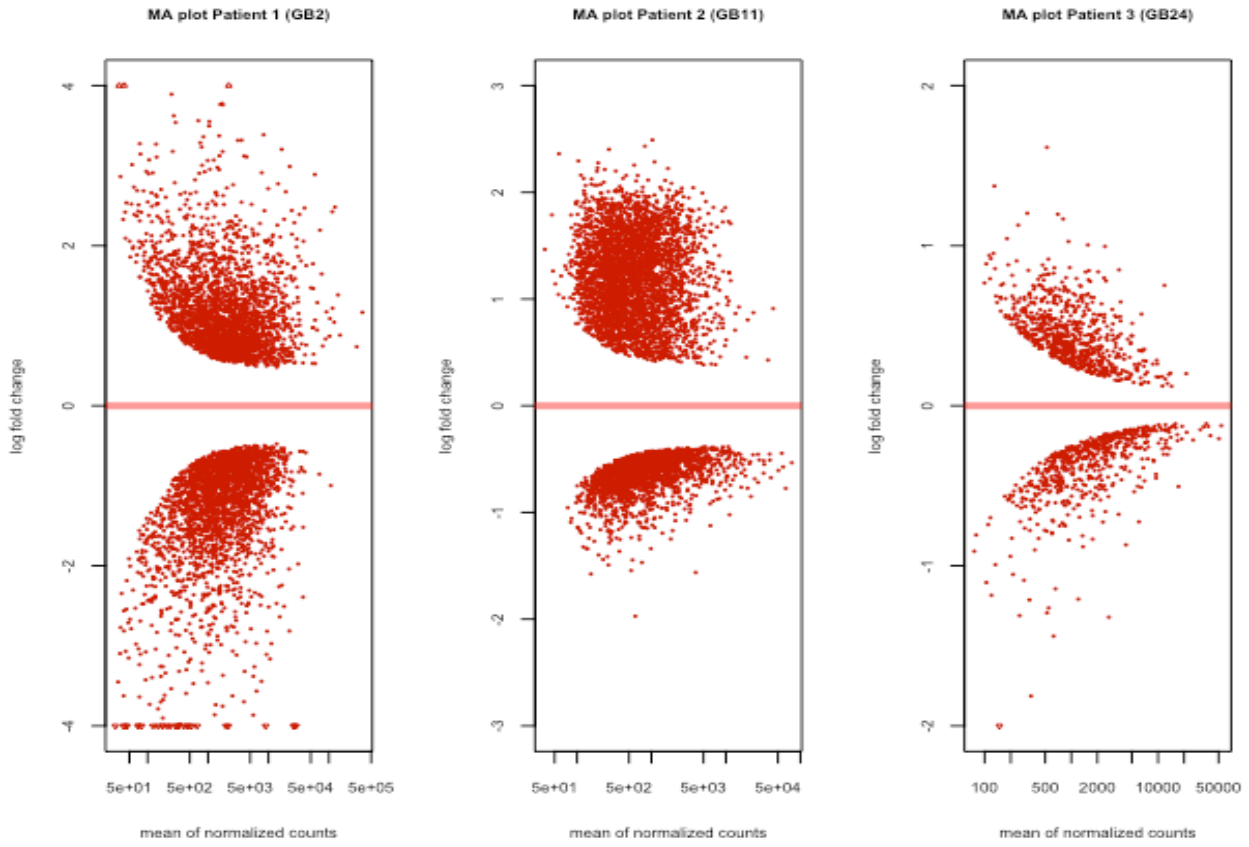

Supplementary Figure 3. Down-regulated genes after HDAC7 suppress many stemness genes verified in various databases. The checkerboard table shows the occurrence of each downregulated stemness gene that is mutual in three different patient-derived GSCs after HDAC7 inhibition and its occurrence across different stemness signature databases. These databases were constructed from TF target genes, expression profiles, RNAi screens, and computationally predicted. Analysis was done using the StemChecker web tool.

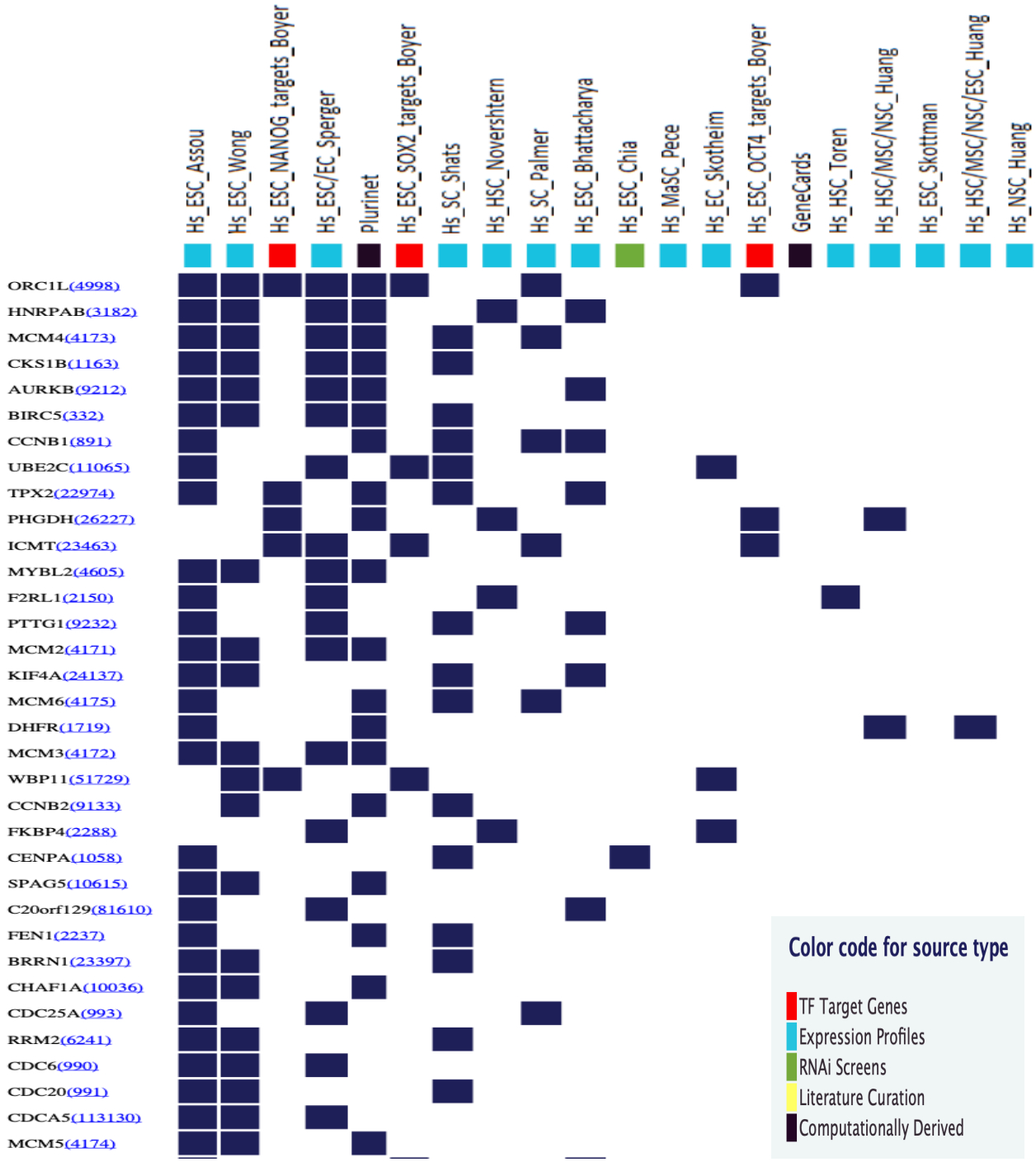

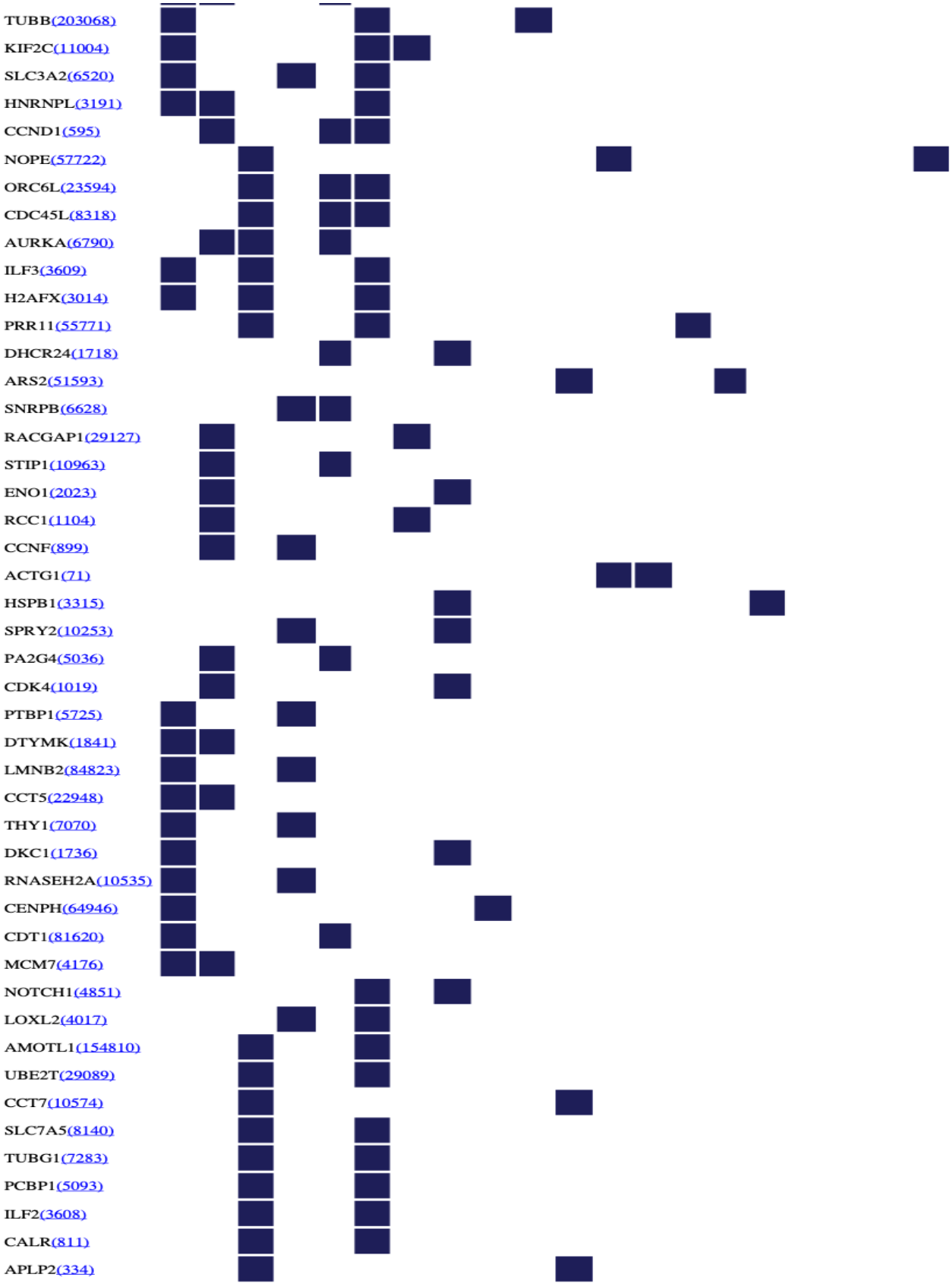
TUBB(203068)
KIF2C(11004)
SLC3A2(6520)
HNRNPL(3191)
CCND1(595)
NOPE(57722)
ORC6L(23594)
CDC45L(8318)
AURKA(6790)
ILF3(3609)
H2AFX(3014)
PRR11(55771)
DHCR24(1718)
ARS2(51593)
SNRPB(6628)
RACGAP1(29127)
STIP1(10963)
ENO1(2023)
RCC1(1104)
CCNF(899)
ACTG1(71)
HSPB1(3315)
SPRY2(10253)
PA2G4(5036)
CDK4(1019)
PTBP1(5725)
DTYMK(1841)
LMNB2(84823)
CCT5(22948)
THY1(7070)
DKC1(1736)
RNASEH2A(10535)
CENPH(64946)
CDT1(81620)
MCM7(4176)
NOTCH1(4851)
LOXL2(4017)
AMOTL1(154810)
UBE2T(29089)
CCT7(10574)
SLC7A5(8140)
TUBG1(7283)
PCBP1(5093)
ILF2(3608)
CALR(811)
APLP2(334)

Supplementary Table 1. Pathways inhibited after HDAC7 inhibition are tumorigenic pathways. Gene enrichment analysis using KEGG pathway databases shows the crucial pathways enriched after HDAC7 inhibition that are important for oncogenesis, GBM tumor progression, and metastasis with the respective P values (n=2 per one GSC repeated in three different patients derives GSCs, respectively).

A. GSC1

Pathway enriched	P value
Generic Transcription Pathway	3.28974662831631E-106
RNA Polymerase II Transcription	3.97623055271196E-103
Gene expression (Transcription)	5.789775949187E-100
HDACs deacetylate histones	2.64524122268871E-42
RNA Polymerase I Promoter Opening	2.78304813431413E-40
DNA methylation	8.58974702769539E-40
Activated PKN1 stimulates transcription of AR (androgen receptor) regulated genes KLK2 and KLK3	2.53291728252377E-39
SIRT1 negatively regulates rRNA expression	4.28009230068003E-39
Assembly of the ORC complex at the origin of replication	7.15980910846623E-39
HCMV Late Events	8.355033758981E-39
PRC2 methylates histones and DNA	5.10820295056192E-38
Defective pyroptosis	5.10820295056192E-38
Condensation of Prophase Chromosomes	8.16621921304687E-38
ERCC6 (CSB) and EHMT2 (G9a) positively regulate rRNA expression	2.03903555984873E-37
B-WICH complex positively regulates rRNA expression	7.51651719578831E-37
RNA Polymerase I Promoter Escape	1.09664330343527E-36
HCMV Early Events	2.88731398890479E-36
Meiotic recombination	1.3045925673562E-35
HATs acetylate histones	1.75955015960117E-35
RMTs methylate histone arginines	2.93713816378342E-35
Transcriptional regulation of granulopoiesis	5.83459990959085E-35
Formation of the beta-catenin:TCF transactivating complex	8.37707357270894E-35
NoRC negatively regulates rRNA expression	9.8167293284156E-35
Positive epigenetic regulation of rRNA expression	1.348155085944E-34
Pre-NOTCH Transcription and Translation	1.70187018743812E-34
RHO GTPases activate PKNs	2.40929697422372E-34
Negative epigenetic regulation of rRNA expression	2.51498050937195E-34

B. GSC2

Pathway enriched	
Cell Cycle	3.58889505988708E-14
Cell Cycle, Mitotic	3.10890933566471E-13
S Phase	1.05491200933268E-12
Synthesis of DNA	2.21935622008388E-12
G1/S Transition	6.36066684679451E-11
Metabolism of RNA	7.12006954136287E-11
Mitotic G1 phase and G1/S transition	1.94335201037295E-10
Mitotic Anaphase	2.98010237563809E-09
Mitotic Metaphase and Anaphase	3.7202680257818E-09
Cellular responses to stimuli	6.27441600376493E-09
The role of GTSE1 in G2/M progression after G2 checkpoint	1.53052685237113E-08
Cellular responses to stress	2.40171175834895E-08
APC/C:Cdh1 mediated degradation of Cdc20 and other APC/C:Cdh1 targeted proteins in late mitosis/early G1	2.1726409863239E-07
Axon guidance	2.52878926449483E-07
Switching of origins to a post-replicative state	3.03991581651475E-07
Orc1 removal from chromatin	3.47701029243999E-07
Separation of Sister Chromatids	8.57309844370356E-07
HIV Infection	0.000001174171114370570 0
APC/C-mediated degradation of cell cycle proteins	0.000001676350303963660
Regulation of mitotic cell cycle	0.000001676350303963660
Nervous system development	0.000019216195210399 8
Cyclin A:Cdk2-associated events at S phase entry	0.000002776462630837 1000
Host Interactions of HIV factors	0.000003261004552642100
SCF(Skp2)-mediated degradation of p27/p21	0.000003422998390300 4300
Cyclin E associated events during G1/S transition	0.000006496099139360690
Translation	0.000006759749867299370
Metabolism of polyamines	0.000008405458478455900

C. GSC3

Pathway enrichment	P value
Cell Cycle, Mitotic	4.07021544645466E-40
Cell Cycle	9.7503756412821E-37
M Phase	5.51410479551253E-19
Cell Cycle Checkpoints	1.21020759567341E-15
Mitotic Anaphase	1.12706213563597E-14
Mitotic Metaphase and Anaphase	1.34622108336118E-14
Mitotic Prometaphase	4.72349050368741E-14
Mitotic G1 phase and G1/S transition	1.85348156612721E-12
Resolution of Sister Chromatid Cohesion	2.00430786799194E-12
G1/S Transition	1.70863381560409E-11
S Phase	4.79664419724917E-11
Separation of Sister Chromatids	5.78977655664552E-11
EML4 and NUDC in mitotic spindle formation	1.14755290663747E-09
RHO GTPases Activate Formins	1.62468838344016E-09
Activation of the pre-replicative complex	2.33568738968273E-09
Unwinding of DNA	2.3977393848987E-09
Mitotic Spindle Checkpoint	4.33257434493814E-09
Synthesis of DNA	6.4504908400489E-09
Activation of ATR in response to replication stress	1.11412389375326E-08
DNA strand elongation	2.60123612414946E-08
RHO GTPase Effectors	2.99942571333847E-08
Amplification of signal from the kinetochores	3.78664150705909E-08
Amplification of signal from unattached kinetochores via a MAD2 inhibitory signal	3.78664150705909E-08
DNA Replication	9.17774704184099E-08
Signaling by Rho GTPases	0.000001854865303697 1400
Signaling by Rho GTPases, Miro GTPases and RHOBTB3	0.000004765325242690 17
G1/S-Specific Transcription	0.000017988689697330900

VI. References

[1] M. E. van Linde *et al.*, "Treatment outcome of patients with recurrent glioblastoma multiforme: a retrospective multicenter analysis," *J Neurooncol,* vol. 135, no. 1, pp. 183-192, Oct 2017, doi: 10.1007/s11060-017-2564-z.

[2] C. Fernandes *et al.*, "Current Standards of Care in Glioblastoma Therapy," in *Glioblastoma*, S. De Vleeschouwer Ed. Brisbane (AU), 2017.

[3] T. S. van Solinge, L. Nieland, E. A. Chiocca, and M. L. D. Broekman, "Advances in local therapy for glioblastoma - taking the fight to the tumour," *Nat Rev Neurol,* vol. 18, no. 4, pp. 221-236, Apr 2022, doi: 10.1038/s41582-022-00621-0.

[4] L. Rong, N. Li, and Z. Zhang, "Emerging therapies for glioblastoma: current state and future directions," *J Exp Clin Cancer Res,* vol. 41, no. 1, p. 142, Apr 15 2022, doi: 10.1186/s13046-022-02349-7.

[5] T. Tykocki and M. Eltayeb, "Ten-year survival in glioblastoma. A systematic review," *Journal of Clinical Neuroscience,* vol. 54, pp. 7-13, 2018, doi: 10.1016/j.jocn.2018.05.002.

[6] A. F. Tamimi and M. Juweid, "Epidemiology and Outcome of Glioblastoma," Codon Publications, 2017, pp. 143-153.

[7] S. Bahadur, A. K. Sahu, P. Baghel, and S. Saha, "Current promising treatment strategy for glioblastoma multiform: A review," *Oncology reviews,* vol. 13, no. 2, pp. 417-417, 2019, doi: 10.4081/oncol.2019.417.

[8] D. Eisenbarth and Y. A. Wang, "Glioblastoma heterogeneity at single cell resolution," *Oncogene,* vol. 42, no. 27, pp. 2155-2165, Jun 2023, doi: 10.1038/s41388-023-02738-y.

[9] S. Osuka and E. G. Van Meir, "Overcoming therapeutic resistance in glioblastoma: the way forward," *J Clin Invest,* vol. 127, no. 2, pp. 415-426, Feb 1 2017, doi: 10.1172/JCI89587.

[10] A. Jahangiri, A. T. Chin, P. M. Flanigan, R. Chen, K. Bankiewicz, and M. K. Aghi, "Convection-enhanced delivery in glioblastoma: a review of preclinical and clinical studies," *J Neurosurg,* vol. 126, no. 1, pp. 191-200, Jan 2017, doi: 10.3171/2016.1.JNS151591.

[11] M. M. Mrugala, "Advances and challenges in the treatment of glioblastoma: a clinician's perspective," *Discovery medicine,* vol. 15, no. 83, pp. 221-30, 2013. [Online]. Available: http://www.ncbi.nlm.nih.gov/pubmed/23636139.

[12] X. Yu *et al.*, "Cancer epigenetics: from laboratory studies and clinical trials to precision medicine," *Cell Death Discov,* vol. 10, no. 1, p. 28, Jan 15 2024, doi: 10.1038/s41420-024-01803-z.

[13] R. Mazzone, C. Zwergel, A. Mai, and S. Valente, "Epi-drugs in combination with immunotherapy: a new avenue to improve anticancer efficacy," *Clin Epigenetics,* vol. 9, p. 59, 2017, doi: 10.1186/s13148-017-0358-y.

[14] T. Feehley, C. W. O'Donnell, J. Mendlein, M. Karande, and T. McCauley, "Drugging the epigenome in the age of precision medicine," *Clin Epigenetics,* vol. 15, no. 1, p. 6, Jan 11 2023, doi: 10.1186/s13148-022-01419-z.

[15] T. C. S. Ho, A. H. Y. Chan, and A. Ganesan, "Thirty Years of HDAC Inhibitors: 2020 Insight and Hindsight," *Journal of Medicinal Chemistry,* vol. 63, no. 21, pp. 12460-12484, 2020, doi: 10.1021/acs.jmedchem.0c00830.

[16] M. S. Roca, E. Di Gennaro, and A. Budillon, "Implication for Cancer Stem Cells in Solid Cancer Chemo-Resistance: Promising Therapeutic Strategies Based on the Use of HDAC Inhibitors," *J Clin Med,* vol. 8, no. 7, Jun 26 2019, doi: 10.3390/jcm8070912.
[17] Z. Li and W. G. Zhu, "Targeting histone deacetylases for cancer therapy: from molecular mechanisms to clinical implications," *Int J Biol Sci,* vol. 10, no. 7, pp. 757-70, 2014, doi: 10.7150/ijbs.9067.
[18] Y. Li and E. Seto, "HDACs and HDAC Inhibitors in Cancer Development and Therapy," *Cold Spring Harb Perspect Med,* vol. 6, no. 10, Oct 3 2016, doi: 10.1101/cshperspect.a026831.
[19] S.-Y. Park and J.-S. Kim, "A short guide to histone deacetylases including recent progress on class II enzymes," *Experimental & Molecular Medicine,* vol. 52, no. 2, pp. 204-212, 2020, doi: 10.1038/s12276-020-0382-4.
[20] B. Deskin, J. Lasky, Y. Zhuang, and B. Shan, "Requirement of HDAC6 for activation of Notch1 by TGF-beta1," *Sci Rep,* vol. 6, p. 31086, Aug 8 2016, doi: 10.1038/srep31086.
[21] H. Han *et al.*, "Hippo signaling dysfunction induces cancer cell addiction to YAP," *Oncogene,* vol. 37, no. 50, pp. 6414-6424, Dec 2018, doi: 10.1038/s41388-018-0419-5.
[22] H. M. Findeisen *et al.*, "Epigenetic regulation of vascular smooth muscle cell proliferation and neointima formation by histone deacetylase inhibition," *Arterioscler Thromb Vasc Biol,* vol. 31, no. 4, pp. 851-60, Apr 2011, doi: 10.1161/ATVBAHA.110.221952.
[23] G. Shanmugam, S. Rakshit, and K. Sarkar, "HDAC inhibitors: Targets for tumor therapy, immune modulation and lung diseases," *Transl Oncol,* vol. 16, p. 101312, Feb 2022, doi: 10.1016/j.tranon.2021.101312.
[24] N. Wang, T. Ma, and B. Yu, "Targeting epigenetic regulators to overcome drug resistance in cancers," *Signal Transduct Target Ther,* vol. 8, no. 1, p. 69, Feb 17 2023, doi: 10.1038/s41392-023-01341-7.
[25] P. J. Wood *et al.*, "A phase I study of panobinostat in pediatric patients with refractory solid tumors, including CNS tumors," *Cancer Chemother Pharmacol,* vol. 82, no. 3, pp. 493-503, Sep 2018, doi: 10.1007/s00280-018-3634-4.
[26] Y. B. Zhou *et al.*, "Pharmacodynamic, pharmacokinetic, and phase 1a study of bisthianostat, a novel histone deacetylase inhibitor, for the treatment of relapsed or refractory multiple myeloma," *Acta Pharmacol Sin,* vol. 43, no. 4, pp. 1091-1099, Apr 2022, doi: 10.1038/s41401-021-00728-y.
[27] A. D. Bondarev, M. M. Attwood, J. Jonsson, V. N. Chubarev, V. V. Tarasov, and H. B. Schioth, "Recent developments of HDAC inhibitors: Emerging indications and novel molecules," *Br J Clin Pharmacol,* vol. 87, no. 12, pp. 4577-4597, Dec 2021, doi: 10.1111/bcp.14889.
[28] M. H. Cai *et al.*, "Depletion of HDAC1, 7 and 8 by Histone Deacetylase Inhibition Confers Elimination of Pancreatic Cancer Stem Cells in Combination with Gemcitabine," *Sci Rep,* vol. 8, no. 1, p. 1621, Jan 26 2018, doi: 10.1038/s41598-018-20004-0.
[29] A. Pasto *et al.*, "Cancer stem cells from epithelial ovarian cancer patients privilege oxidative phosphorylation, and resist glucose deprivation," *Oncotarget,* vol. 5, no. 12, pp. 4305-19, Jun 30 2014, doi: 10.18632/oncotarget.2010.
[30] M. Y. Wu, J. Fu, X. Xiao, J. Wu, and R. C. Wu, "MiR-34a regulates therapy resistance by targeting HDAC1 and HDAC7 in breast cancer," *Cancer Lett,* vol. 354, no. 2, pp. 311-9, Nov 28 2014, doi: 10.1016/j.canlet.2014.08.031.

[31] Y. Zhang *et al.*, "HDAC7/c-Myc signaling pathway promotes the proliferation and metastasis of choroidal melanoma cells," *Cell Death Dis,* vol. 14, no. 1, p. 38, Jan 18 2023, doi: 10.1038/s41419-022-05522-0.
[32] A. E. Witt *et al.*, "Identification of a cancer stem cell-specific function for the histone deacetylases, HDAC1 and HDAC7, in breast and ovarian cancer," *Oncogene,* vol. 36, no. 12, pp. 1707-1720, Mar 23 2017, doi: 10.1038/onc.2016.337.
[33] V. Cutano, E. Di Giorgio, M. Minisini, R. Picco, E. Dalla, and C. Brancolini, "HDAC7-mediated control of tumour microenvironment maintains proliferative and stemness competence of human mammary epithelial cells," *Mol Oncol,* vol. 13, no. 8, pp. 1651-1668, Aug 2019, doi: 10.1002/1878-0261.12503.
[34] K. Guo *et al.*, "HDAC7 promotes NSCLC proliferation and metastasis via stabilization by deubiquitinase USP10 and activation of beta-catenin-FGF18 pathway," *J Exp Clin Cancer Res,* vol. 41, no. 1, p. 91, Mar 11 2022, doi: 10.1186/s13046-022-02266-9.
[35] M. Kanehisa, M. Furumichi, M. Tanabe, Y. Sato, and K. Morishima, "KEGG: new perspectives on genomes, pathways, diseases and drugs," *Nucleic Acids Res,* vol. 45, no. D1, pp. D353-D361, Jan 4 2017, doi: 10.1093/nar/gkw1092.
[36] O. Menyhart, A. Nagy, and B. Gyorffy, "Determining consistent prognostic biomarkers of overall survival and vascular invasion in hepatocellular carcinoma," *R Soc Open Sci,* vol. 5, no. 12, p. 181006, Dec 2018, doi: 10.1098/rsos.181006.
[37] R. L. Bowman, Q. Wang, A. Carro, R. G. W. Verhaak, and M. Squatrito, "GlioVis data portal for visualization and analysis of brain tumor expression datasets," *Neuro-Oncology,* vol. 19, no. 1, pp. 139-141, 2017, doi: 10.1093/neuonc/now247.
[38] S. Johnson, H. Chen, and P. K. Lo, "In vitro Tumorsphere Formation Assays," *Bio Protoc,* vol. 3, no. 3, Feb 5 2013, doi: 10.21769/bioprotoc.325.
[39] J. P. Pinto *et al.*, "StemChecker: a web-based tool to discover and explore stemness signatures in gene sets," *Nucleic Acids Res,* vol. 43, no. W1, pp. W72-7, Jul 1 2015, doi: 10.1093/nar/gkv529.
[40] A. B. Keenan *et al.*, "ChEA3: transcription factor enrichment analysis by orthogonal omics integration," *Nucleic Acids Res,* vol. 47, no. W1, pp. W212-W224, Jul 2 2019, doi: 10.1093/nar/gkz446.
[41] A. Subramanian *et al.*, "Gene set enrichment analysis: a knowledge-based approach for interpreting genome-wide expression profiles," *Proc Natl Acad Sci U S A,* vol. 102, no. 43, pp. 15545-50, Oct 25 2005, doi: 10.1073/pnas.0506580102.
[42] R. G. Verhaak *et al.*, "Integrated genomic analysis identifies clinically relevant subtypes of glioblastoma characterized by abnormalities in PDGFRA, IDH1, EGFR, and NF1," *Cancer Cell,* vol. 17, no. 1, pp. 98-110, Jan 19 2010, doi: 10.1016/j.ccr.2009.12.020.
[43] M. S. Carro *et al.*, "The transcriptional network for mesenchymal transformation of brain tumours," *Nature,* vol. 463, no. 7279, pp. 318-25, Jan 21 2010, doi: 10.1038/nature08712.
[44] X. Lu *et al.*, "Cell-lineage controlled epigenetic regulation in glioblastoma stem cells determines functionally distinct subgroups and predicts patient survival," *Nat Commun,* vol. 13, no. 1, p. 2236, Apr 25 2022, doi: 10.1038/s41467-022-29912-2.
[45] Q. Wang *et al.*, "Tumor Evolution of Glioma-Intrinsic Gene Expression Subtypes Associates with Immunological Changes in the Microenvironment," *Cancer Cell,* vol. 32, no. 1, pp. 42-56 e6, Jul 10 2017, doi: 10.1016/j.ccell.2017.06.003.

[46] Y. Yu *et al.*, "The expression of HDAC7 in cancerous gastric tissues is positively associated with distant metastasis and poor patient prognosis," *Clin Transl Oncol,* vol. 19, no. 8, pp. 1045-1054, Aug 2017, doi: 10.1007/s12094-017-1639-9.
[47] H. Nam *et al.*, "The TGF-beta/HDAC7 axis suppresses TCA cycle metabolism in renal cancer," *JCI Insight,* vol. 6, no. 22, Nov 22 2021, doi: 10.1172/jci.insight.148438.
[48] X. Yu, M. Wang, J. Wu, Q. Han, and X. Zhang, "ZNF326 promotes malignant phenotype of glioma by up-regulating HDAC7 expression and activating Wnt pathway," *J Exp Clin Cancer Res,* vol. 38, no. 1, p. 40, Jan 28 2019, doi: 10.1186/s13046-019-1031-4.
[49] C. Caslini, S. Hong, Y. J. Ban, X. S. Chen, and T. A. Ince, "HDAC7 regulates histone 3 lysine 27 acetylation and transcriptional activity at super-enhancer-associated genes in breast cancer stem cells," *Oncogene,* vol. 38, no. 39, pp. 6599-6614, Sep 2019, doi: 10.1038/s41388-019-0897-0.
[50] X. Li *et al.*, "HDAC inhibition potentiates anti-tumor activity of macrophages and enhances anti-PD-L1-mediated tumor suppression," *Oncogene,* vol. 40, no. 10, pp. 1836-1850, Mar 2021, doi: 10.1038/s41388-020-01636-x.
[51] S. Inoue, M. MacFarlane, N. Harper, L. M. Wheat, M. J. Dyer, and G. M. Cohen, "Histone deacetylase inhibitors potentiate TNF-related apoptosis-inducing ligand (TRAIL)-induced apoptosis in lymphoid malignancies," *Cell Death Differ,* vol. 11 Suppl 2, pp. S193-206, Dec 2004, doi: 10.1038/sj.cdd.4401535.
[52] S. R. Gameiro, A. S. Malamas, K. Y. Tsang, S. Ferrone, and J. W. Hodge, "Inhibitors of histone deacetylase 1 reverse the immune evasion phenotype to enhance T-cell mediated lysis of prostate and breast carcinoma cells," *Oncotarget,* vol. 7, no. 7, pp. 7390-402, Feb 16 2016, doi: 10.18632/oncotarget.7180.
[53] M. Yano *et al.*, "Association of histone deacetylase expression with histology and prognosis of ovarian cancer," *Oncol Lett,* vol. 15, no. 3, pp. 3524-3531, Mar 2018, doi: 10.3892/ol.2018.7726.
[54] G. Qin *et al.*, "Panobinostat (LBH589) inhibits Wnt/beta-catenin signaling pathway via upregulating APCL expression in breast cancer," *Cell Signal,* vol. 59, pp. 62-75, Jul 2019, doi: 10.1016/j.cellsig.2019.03.014.
[55] A. Suraweera, K. J. O'Byrne, and D. J. Richard, "Combination Therapy With Histone Deacetylase Inhibitors (HDACi) for the Treatment of Cancer: Achieving the Full Therapeutic Potential of HDACi," *Front Oncol,* vol. 8, p. 92, 2018, doi: 10.3389/fonc.2018.00092.

CHAPTER 3:

Drug Design Pipeline to Identify Novel Isoform-Selective HDAC Inhibitor

I. Introduction

The potential of HDAC inhibitors (HDACi) as a therapeutic for diseases, specifically cancers, is superb. HDACs have been implicated in regulating the cell cycle, angiogenesis, and potentiating stemness in various cancer stem cells [1-4]. Conversely, HDAC inhibition was shown to disrupt the G1/S and G2/M cell cycle transition [4-6]. In addition, it was demonstrated that HDACi induced selective death of the CSC subpopulation in several cancer models [7-9]. However, most limitations accompanying their clinical usage are tied to many unwanted side effects from the lack of HDAC-isoform specificity [10, 11]. In a phase I Panobinostat clinical trial for children with solid tumors, one-third of children experienced severe thrombocytopenia [12]. Given these findings, current efforts are directed toward developing isoform-specific HDACi that offer increased specificity, enhanced tumor cytotoxicity, and improved safety profiles.

Recently, a high-throughput screen study discovered the trifluoromethyl oxadiazole (TMFO) derivatives as inhibitors selective for class IIa HDACs [13]. TMP269, a TMFO derivative, was shown to stimulate apoptosis by activating endoplasmic reticulum stress signaling and enhancing the tumor response to the chemotherapeutics, tunicamycin, or carfilzomib in multiple myeloma [13]. Furthermore, recent studies have shown that TMP269 treatment exhibited anti-tumor proliferative effects and enhanced apoptotic effects when combined with the chemotherapy Venetoclax in acute myeloid leukemia [14]. Another class IIa HDAC-specific, MC1568, significantly enhanced apoptosis and drove G2/M arrest in pancreatic cancer cells [15]. It was also shown that the combination treatment of MC1568 with simvastatin led to synergistic induction of p27 expression and increased the antiproliferative effect in colorectal cancer cells [16] and potentiated cytotoxicity in gastric cancer cells when combined with docetaxel [17]. Based on these

previous findings, in **Chapter 3**, we tested the potentiality of the class IIa HDACi in changing the GSCs' phenotype. We demonstrate how the inhibitory effect of class IIa HDACi (TMP269) is comparable to an FDA-approved pan HDACi.

We layered pieces of evidence from **Chapter 2** showing how HDAC7, distinguished from its peers from the same class IIa HDAC, significantly impacts the genetic expression and phenotype change in patient-derived GSCs. In addition, HDAC7 was reported in many studies to suppress the epithelial-to-mesenchymal transition (EMT) and inhibit CSC phenotypes, decrease therapy resistance, and inhibit the likelihood of metastasis in multiple malignancies [18-23].

Given the encouraging outcomes observed with class IIa HDACi, we pursued several strategies to formulate a specific drug tailored to target HDAC7 while distinguishing it from closely related class IIa HDAC members. Our primary goal from the design was to achieve an innovative design of novel, potent, isoform-specific HDAC7i that would possess maximum efficacy and minimal side effects as a translational therapy.

Our drug design pipeline included several parallel and backup scenarios that overcome being stuck by one unwanted outcome; we understood from the beginning that computational prediction models are not fault-free by the end, and we preplanned accordingly. Since members of HDAC class IIa are structurally similar and different from other members of HDAC superfamily, we built our model based on a known and previously crystallized class IIa HDACi, TMP269. Our pipeline employed three outline approaches: first, screening the NCI DTP library of available compounds. The second is an utterly new synthesis based on structural superimposition computational models. The output compounds from both approaches were courtesy ordered from the NIH or were outsourced for chemical synthesis, respectively. We analyzed the received compounds to

determine their specificity towards HDAC7 over HDAC4, 5, and 9. Accordingly, we improved the structural drug-designing training models and introduced the PROTAC approaches to improved designs.

PROTACs are heterobifunctional small molecules composed of two ligands connected by a linker. One ligand is designed to recruit and bind the target protein of interest, such as HDAC7, while the other ligand recruits and binds an E3 ubiquitin ligase. Upon binding both proteins, the PROTAC induces ubiquitylation of the target protein, leading to its degradation by the ubiquitin-proteasome complex. Once the targeted HDAC7 protein is degraded, the PROTAC complex can recycle to target another copy of the HDAC7 protein. Studies have shown that HDAC-PROTACs offer sustained inhibition compared to their parent HDAC inhibitors [24]. Furthermore, HDAC-PROTACs designed to target members of class IIa HDAC can be engineered to bind to the regulatory N-terminal domain. This approach is advantageous because it can target regions independent of the deacetylase activity of HDACs, which HDAC class IIa are known to lack.

However, the main challenge in PROTAC technology lies in finding the optimal combination of the three key components: the linker moiety that best matches the E3 ligase and the ligand moiety for the target protein. Achieving this precise match is crucial for the successful design and function of PROTAC molecules.

Our last approach in our drug design was RNAi-based HDACi using siRNA specific against HDAC7. RNAi therapeutics have emerged as class of drugs with high potential in various diseases, including cancer. In our study, siRNA presented a promising approach to target HDAC7 with high degree of specificity and efficacy.

By employing several specificity assays and through evaluations to assess the efficacy and selectivity of our tested modalities from different approaches in our drug design pipeline, we reached a consensus that the siRNA targeting HDAC7 was the most effective and selective drug in this study.

II. Methods

- *Cell culture maintenance.*

Patient-derived GSCs were used in this study. Primary GSCs were cultured in the Neurobasal-A media enriched with Glutamax, FGF, EGF growth factors, heparin, and antimicrobials. Cryopreserved GSCs were passaged twice as neurospheres and then attached for at least one passage to ensure adequate adaptation to culture conditions. According to the experiment, neurospheres or attached GSCs were used when ~80% confluency was reached in the culturing medium. GSCs were incubated at 37°C in a humidified environment containing 6% CO2. The GSC was authenticated and tested to ensure the culture was free from mycoplasma infection.

- *Primary GSCs HDAC inhibitor treatment*

At 80% confluency, GSCs were counted, and a corresponding volume of 5,000 cells was added to each well of a treated fibronectin/HBSS-coated 96-well microtiter plate. 100 µL of culture noncolored complete growth media was added to each well. GSCs were left 24 hours at normal culturing conditions for complete attachment. After an overnight attachment period, GSCs were treated with the designated concentrations of the new compounds, positive controls (known HDACi), or negative control (DMSO). 5 and 25 µM concentrations from the different compounds were used for the initial screening. The compounds that were tested are listed below:

  - Pan HDACi used: Vorinostat (SAHA), Trichostatin A (TSA)
  - Class IIa inhibitor used: TMP269.
  - The number of NCI-DTP compounds: 11 compounds

- The number of computational hit compounds: 114 compounds
- The number of synthesized compounds: 63 compounds
- The number of the actual tested compounds after filtering out those with molecular weight< 400 kDA: 54 compounds
- The number of PROTAC-HDACi tested: seven compounds.

For all the compounds in this study, stocks of 5 mM, 2.5 mM, 1 mM, and 0.5 mM were prepared by dissolving in DMSO. The final concentration of DMSO in all experiments was kept below 0.8%.

- *Cell viability measurement*

After the course of treatment, cell viability was estimated using the CellTiter Glo assay (Promega™). Cells were combined with 25 µL of CellTiter-Glo reagents in the 100 µL of media, and bioluminescence was assessed using the Promega™ GloMax® Plate Reader. Blank (culturing media without cells) was used to normalize the luminescence signals. Cell viability of the treated versus untreated cells was estimated via Graph-Pad Prism.

- *Limiting dilution assay*

Extreme Limiting dilution assay (ELDA) is used to characterize the frequency of self-renewing cells in a population [25]. Upon harvesting, dissociating, and briefly culturing, primary GSCs were plated in 6 replicates into the inner 60 wells of 96-well plates in GSC growth media. A ten-serial dilution of GSCs (ranging from 2,000 cells/well down to 4 cells/well) was generally used in two-fold dilutions, as illustrated in (**Table 3.1)**. GSCs were observed microscopically to ensure the singleness of the seeding of GSCs. The GSCs were maintained under standard culturing conditions

of incubation at a 37ºC 6% CO2 incubator. After 1-week, the cells were examined to ensure healthy growth, and GSCs were fed by topping 50 µL of freshly prepared media/well. The cells were then allowed to grow for an additional week. By the end of the second week, the cells were examined and scored for neurosphere formation using binary identification where "1" denotes the presence of neurospheres and "0" indicates the lack of neurospheres; all the "1s" were summed up for each cell dose and used for the score sheet. After that, the score sheet was used to conclude self-renewability through a logarithmic software, "Extreme Limiting Dilution Analysis (ELDA) Software" [26]. In the score sheet, "Tested" refers to the number of replicates used, and "Response" refers to the sum of "1s" found for each cell dose. An example of a sphere formation setup, score sheet, and an example of LDA scoring, and ELDA analysis is shown in (**Table 3.1 A and B**).

A.

Column #	**# of GSCs**	**Initial conc./ml**	**Final conc./ml**	**Cell suspension volume (µl)**	**Media volume (µl)**	**Final volume (µl)/ well**
2	2000	**100,000**	**20,000**	100	0	100
3	1000	100,000	20,000	50	50	100
4	500	100,000	20,000	25	75	100
5	250	100,000	20,000	12.5	87.5	100
6	125	100,000	20,000	6.25	93.75	100
7	63	**10,000**	**2,000**	31.5	68.5	100
8	31	10,000	2,000	15.5	84.5	100
9	16	10,000	2,000	8	92	100
10	8	10,000	2,000	4	96	100
11	4	10,000	2,000	3	98	100

B.

Limiting Dilution Data entered.

Counter	Dose	Tested	Response
1	4	6	0
2	8	6	0
3	16	6	0
4	32	6	0
5	63	6	0
6	125	6	0
7	250	6	0
8	500	6	6
9	1000	6	6
10	2000	6	6

Table (3.1) A. *Limiting dilution assay setup.* ***B.*** *Limiting dilution analysis score entry in the ELDA software.*

- *Drug design pipeline*

Using multiple approaches, our pipeline started with a structure-based virtual screening of HDAC IIa inhibitor TMP269 with HDAC7 versus TMP269 with each HDAC4, 5, and 9.

Initially, we conducted a screening of library compounds sourced from the National Cancer Institute Therapeutics (NCI DTP) library. Positive hits specific to HDAC7 were identified among the small molecules in the library. Subsequently, we narrowed down the positive-hit compounds based on their ability to dock successfully inside the HDAC7 pocket using a comprehensive pipeline for virtual ligand screening facilitated by Schrödinger ligand designer software. The top-performing structures were then requested from the National Institutes of Health (NIH) and, upon approval, granted to us for further research.

The second approach involved designing a de novo HDAC7 selective inhibitor compound using the crystal structure of HDAC7 complexed with the HDAC class IIa inhibitor (TMP269) as positive design input and the crystal structures of HDAC4, HDAC5, and HDAC9 as negative design inputs. We utilized Schrödinger computational ligand designer software, which integrates

predictive physics-based methods with machine learning techniques, for combinatorial chemical binding, docking, and affinity calculations to model potential ligand compounds specific to HDAC7 versus HDAC4, HDAC5, and HDAC9. By leveraging the software, we obtained more reliable predictions than manual prediction methods for sites tolerating the extension of binding groups similar to TMP269. We explored numerous binding groups in these predicted sites until we identified potential compounds successfully docked with higher affinity towards HDAC7 and lower affinity towards other HDAC class IIa members.

Furthermore, to evaluate physical interactions and affinity calculations for the potential compounds towards HDAC7, we employed dynamic simulations and interactions with water molecules, neighboring ions, and necessary cofactors. This approach aimed to simulate druggable compounds with improved pharmacokinetics and pharmacodynamics when utilized biologically. Ultimately, the designed winning compounds were outsourced to a chemical biology facility for small compound synthesis.

We worked on refining the most promising synthesized compounds from approach two through more rigorous computational superimposition techniques. Subsequently, we leveraged PROTAC (proteolysis-targeting chimera) technology to advance our efforts [27].

RNAi-dependent HDACi was the last and winning approach for us. We tried various HDAC7 siRNA variants with multiple concentrations. SiRNA against HDAC7 (Dharmacon ON-TARGETplus™ siRNA) of 50 nM final concentration was the optimized concentration from the array of the concentrations (25- 100 nM) tested. The transfection protocol was applied according to the optimization protocol described in **Chapter 2**. Initially, a smart pool siRNA used was a pool of four siRNA variants against HDAC7 versus non-targeting siRNA. Shortly, we tested the

transfection specificity of each siHDAC7 variant. siRNA variant 2 (highlighted) was proven to be the most inhibitory targeting and the most specific (shown in the results section of this Chapter).

The siHDAC7 smart pool was a pool of the following sequences:

siRNA-1 sense: 5' G.A.C.A.A.G.A.G.C.A.A.G.C.G.A.A.G.U.G 3'

antisense: 5' C.A.C.U.U.C.G.C.U.U.G.C.U.C.U.U.G.U.C 3'

siRNA-2 sense: 5' G.C.A.G.A.U.A.C.C.C.U.C.G.G.C.U.G.A.A 3'

antisense: 5' U.U.C.A.G.C.C.G.A.G.G.G.U.A.U.C.U.G.C 3'

siRNA-3 sense: 5' G.G.U.G.A.G.G.G.C.U.U.C.A.A.U.G.U.C.A 3'

antisense: 5' U.G.A.C.A.U.U.G.A.A.G.C.C.C.U.C.A.C.C 3'

siRNA-4 sense: 5' U.G.G.C.U.G.C.U.U.C.U.C.G.G.G.U.U.A.A 3'

antisense: 5' U.U.A.A.C.C.C.G.A.G.A.A.G.C.A.G.C.C.A 3'

Non-targeting control siRNA- sense: 5' A.G.C.G.A.C.U.A.A.A.C.A.C.A.U.C.A.A

antisense: 5' U.U.G.A.U.G.U.G.U.U.U.A.G.U.C.G.C.U 3'

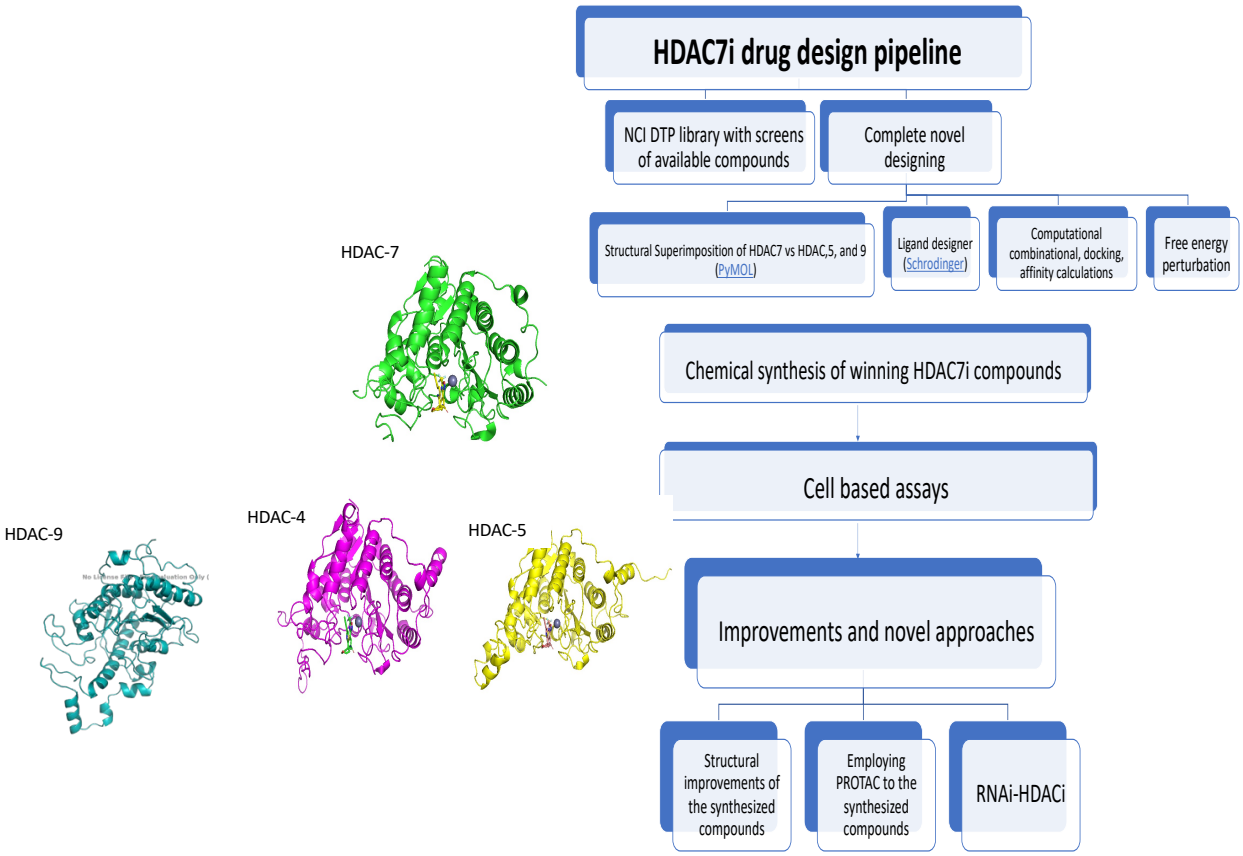

Figure (3.1) Outline for our drug design pipeline. *Overview of the hierarchal routes we employed while looking for a novel compound specific for HDAC7 inhibition.*

- *HDAC fluorogenic enzymatic assays*

All dilutions for HDAC substrates and HDAC7 enzymes were prepared immediately prior to the HDAC fluorogenic assay, following the protocols provided by BPS Bioscience. A master mix for the N number of wells was freshly prepared by the addition of diluted HDAC substrate (20 µM) to an equal volume of 5 µl of 1 mg/ml of BSA and completed with 30 µl of HDAC assay buffer to bring a total of 40 µl master mix, prepared for N wells. Various concentrations of the

compounds were prepared from stocks so that each well received an equal volume of 5 µl of the tested compound. Positive controls (TSA, SAHA, and TMP269) were prepared and added similarly to their designated wells. Blank wells were designated by adding 5 µl of HDAC assay buffer. Enzymatic reactions were initiated using a multi-channel pipette by adding 5 µl of HDAC7 enzyme to all wells (with tested compounds, positive control, and Blank). 50 µl of undiluted HDAC Assay Developer (2x) was added to each well, and plates were incubated at room temperature. After 15 minutes, the plate was imaged in a microtiter plate-reading fluorimeter using the Promega™ GloMax® Plate Reader with excitation at a wavelength in the range of 350-380 nm and detection of emitted light in the range of 440-460 nm. Blank was used to normalize the fluorescence signals. Enzymatic activity was estimated via Graph-Pad Prism.

- *Timepoint treatment of GSCs with the designed PROTAC HDAC7 inhibitor*

Seven synthesized PROTAC-HDACi were prepared as stocks in DMSO. Upon harvesting, dissociating, and briefly culturing, primary GSCs are seeded into a 6-well culturing treated and coated plate with 2 ml of enrichment standard growth media. 1 µM of each PROTAC compound was treated per well of the 6-well plate. Time 0-hour is initiated by maintaining GSCs under standard culturing conditions of incubation at a 37^{o}C 6% CO2 incubator. Cell lysis and harvesting of cells were done at the time points: 1-hour, 4-hour, and 24 hours. Cells were lysed, and whole lysate protein was extracted using a 1% SDS lysis buffer containing protease inhibitor cocktail and phosphatase inhibitor. After denaturation, samples were boiled at 95 degrees for 5 minutes, and 40 µg of whole lysate from compared samples were analyzed using the same western blot protocol described in **Chapter 2**.

- *Statistical analysis*

For the various analyses, we performed a two-tailed, paired student T-test, or one-way ANOVA for the relations between different groups; the p-value of significance was $P \leq 0.05$, and representation was done as means ± standard deviation (SD) or ± standard error of the mean (SEM). For the tumor sphere formation assay, we performed a two-tailed, unpaired student t-test; the P-value of significance was $P \leq 0.05$. GraphPad Prism was used for statistical analyses and graphical representation. Statistical significance is represented as follows: $P \leq 0.05$: *, $P \leq 0.01$: **, and $P \leq 0.001$: ***, topped by the number of experiments repetitions as once: *, twice: **, thrice: ***, and quadlet: ****.

III. Results

A class IIa HDAC inhibitor suppresses the cell viability of the GSCs in a manner comparable to that of the pan HDAC inhibitors.

Since specific HDACi targeting HDAC7 do not currently exist, we tested our hypothesis using an HDACi targeting class IIa HDACs, TMP269. We compared its effect on GSCs' viability with the FDA-approved pan HDACi, Vorinostat (SAHA), and Trichostatin-A (TSA) (**Figure 3.2)**. Interestingly, we observed that the TMP269 reduced GSCs' viability to a similar extent as the pan HDAC inhibitor SAHA, which is FDA-approved under the brand name ZOLINZA® and is currently used clinically in combination therapies for multiple types of cancers [28, 29]. This data supports our hypothesis that targeting a narrower spectrum of HDAC inhibition can yield a comparable inhibitory effect to pan HDACi, potentially leading to fewer off-target effects and side effects.

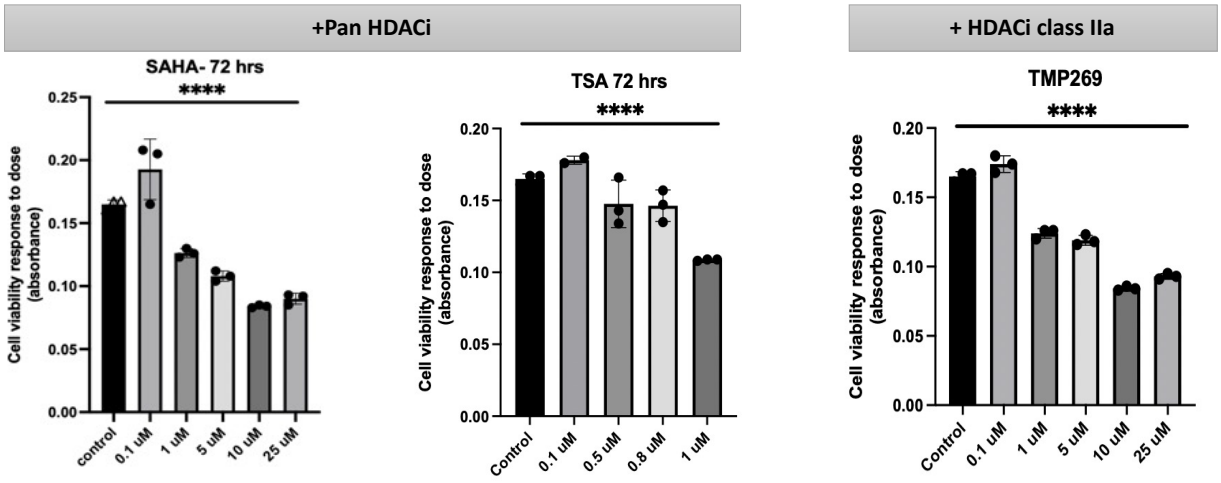

Figure (3.2) Class IIa HDACi inhibits GSCs cell viability by a comparable trend to Pan HDACi. *Dose-response curve for GSCs cell viability inhibition after treatment with HDAC class IIa inhibitor (TMP269) compared to pan HDACi Trichostatin A (TSA) and Vorinostat (SAHA). A "Brown-Forsythe ANOVA test" for multiple comparisons was used to calculate statistical significance: $p \leq 0.0001$: ****.*

HDAC class IIa inhibition hinders the self-renewal capability of primary GSC from different RIH patients.

Upon testing the stemness capability of our GSCs following treatment with the class IIa HDACi compared to control-treated GSCs, we observed a significant inhibition in the ability of the TMP269-treated GSCs to self-renew. This was assessed using the established LDA to characterize the frequency of self-renewing cells [25]. Importantly, we replicated the experiment several times using various patient-derived GSCs, consistently obtaining significant results (**Figure 3.3)**.

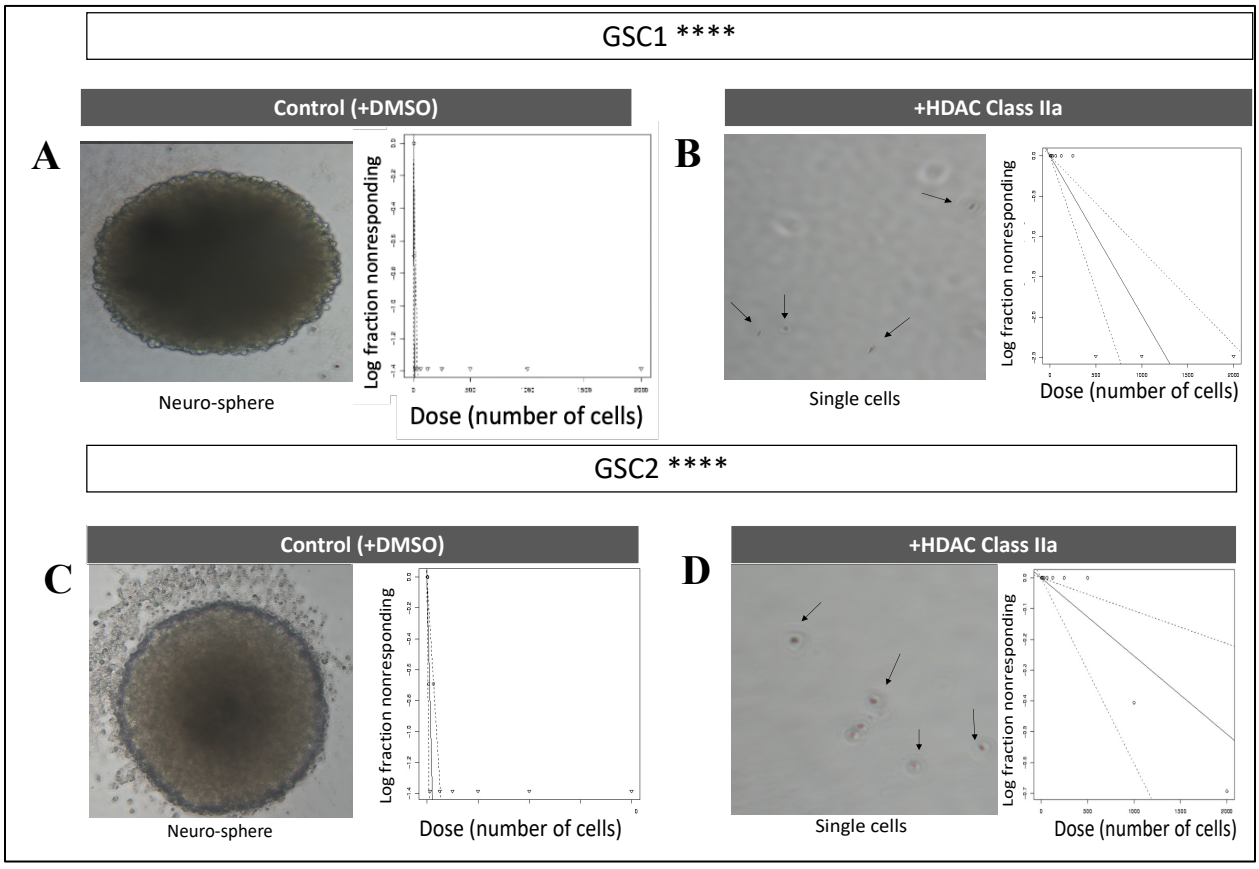

Figure (3.3) Class IIa HDACi blocks GSCs' stemness capability*. Microscopic images for GSC1 and GSC2 from cultures treated with 0.8% DMSO (control)* ***A. and C*** *and class IIa HDACi.* ***B. and D.*** *with the respective graph using an online algorism to score and assess the self-renew ability of*

*each GSC treated with DMSO, respectively, in a limiting dilution assay, where GSCs treated with the HDAC class IIa inhibitor show an inability to form neuro-spheres in a 2-week LDA compared to the control GSCs that showed neurosphere-forming ability at a very early time point. A "Likelihood ratio test of single-hit mode test" for whether the log-dose slope equals one was used to calculate statistical significance: $p \leq 0.0001$: ****.*

Small molecule screened compounds from NCI-DTP screens did not show efficacy towards HDAC7.

After screening library compounds from the NCI-DTP library and filtering the positive hits specific to HDAC7 for small molecules, we tested the compounds the NIH granted for their HDAC activity towards HDAC7. This assessment was conducted in the presence of HDAC substrates using HDAC7 enzymatic fluorogenic assays. However, despite our efforts, we did not observe any significant affinity of HDAC7 for the tested compounds compared to positive and negative controls **(Figure 3.4).**

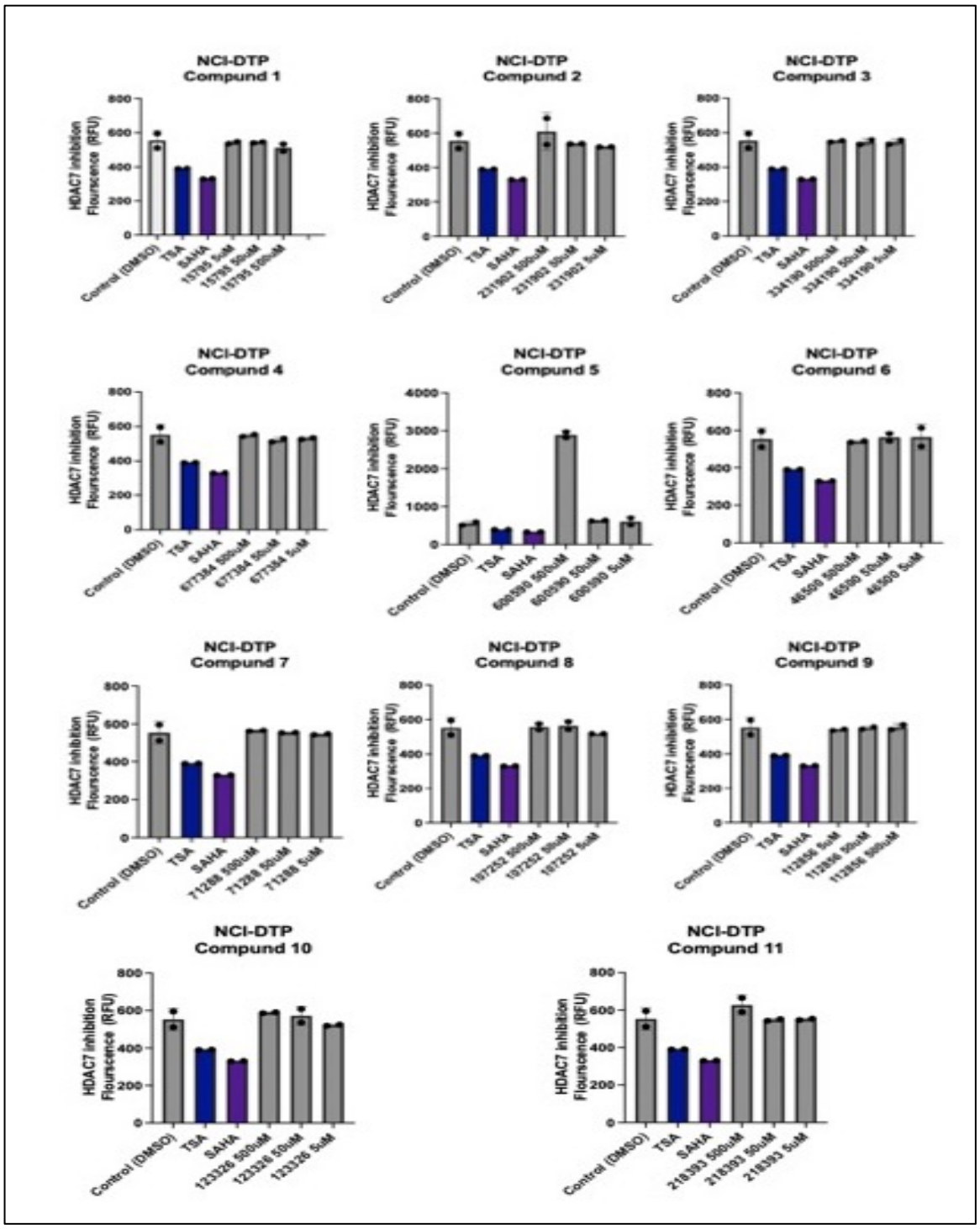

Figure (3.4) NCI- DTP screen compounds do not display HDAC7 affinity. *Graph plots for compounds (1-11) from NCI-DTP screens showing no affinity towards HDAC7 in an HDAC7 fluorogenic assay. Results were estimated in GraphPad Prism and represented as mean of+/- SD (n=2)*

Pharmacophore differences among the class IIa HDAC members shed light on structural differences between members of HDAC class IIa.

After shifting our focus to the alternative strategy in the drug design pipeline, we began exploring potential modifications to the class IIa HDACi TMP269 that could enhance its affinity for HDAC7 while reducing its affinity for other class IIa members. To achieve this, we visualized the interaction between the parent compound TMP269 and the class IIa HDAC binding pocket using molecular modeling techniques (**Figure 3.5 and Supplementary Figures 1 and 2)**. By superimposing the molecular structures of the class IIa HDAC members using Schrodinger software, we identified several potential sites within the TMP269 structure that could be modified to confer greater specificity towards HDAC7.

Among these sites, we found that HDAC4, in contrast to other class IIa HDACs, has a tyrosine amino acid instead of histidine at position 843. This difference presented an interesting opportunity for enhancing selectivity towards HDAC7. By selecting an appropriate R binding group at positions C35 and C36, we hypothesized that we could increase selectivity towards HDAC7. Additionally, the added group presented a potential to hinder accessibility to C34, which interacts with the tyrosine residue at position 843 in HDAC4. This strategic modification could help to tailor the inhibitor towards HDAC7 while reducing its affinity for HDAC4.

Another site that caught our attention as a potential differentiator between HDAC5 and HDAC7 was the presence of aspartate at position 146. In HDAC5, this residue is located at a distance greater than 8 angstroms from position C13. However, in HDAC4 and HDAC7, it is approximately half this distance from C13. Additionally, at position C13, the added R-group forms an interaction bridge between the aspartate at position 146 and the phenylalanine at position 258,

specifically in HDAC7. This interaction bridge was not observed in HDAC4 and HDAC5 **(Figure 3.5C)**. This unique interaction pattern suggests that modifications at this site could enhance the selectivity of inhibitors towards HDAC7 over HDAC5.

In addition, at HDAC4, an NH3 group at position C36 was not observed; instead, an OH group clashes with tyrosine at position 363. This distinction in interaction patterns highlights another potential site for modifying inhibitors to enhance selectivity towards HDAC7 over HDAC4 and HDAC5 **(Figure 3.5D)**.

Together, we decided with the Fiser lab that by designing a class IIa HDACi derivate through trying several possible binding groups at positions C34, C35, C36 & C13 in the parent compound TMP269, we can generate potential HDACi with more specificity towards HDAC7 over the rest of class IIa HDAC.

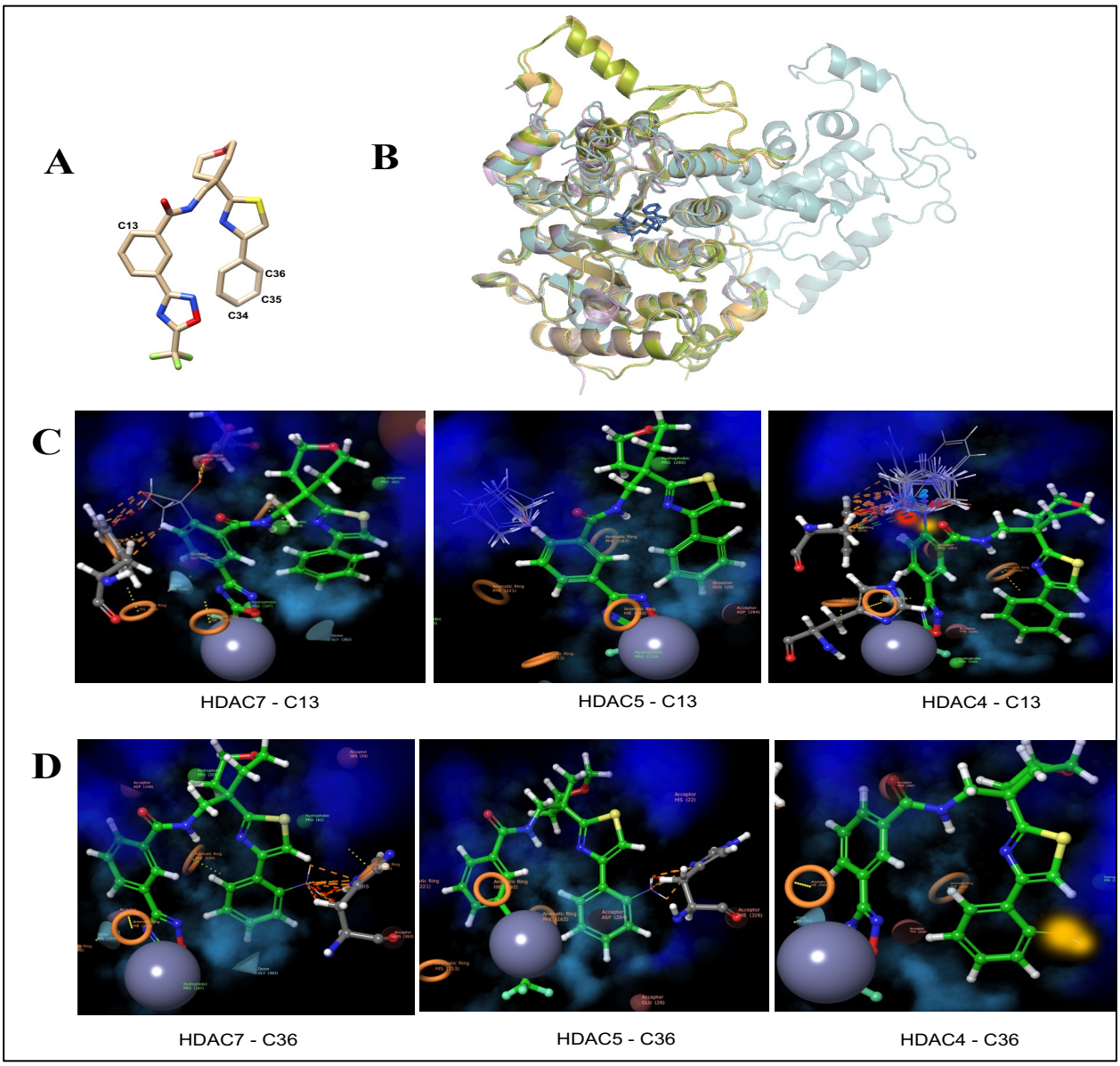

Figure (3.5) Structural differences were found among the closely related HDAC class IIa members. *Snapshots from the Schrodinger designer software for* ***A.*** *The molecular structure for the parent HDAC class IIa compound with enumeration for the potential sites identified to guide differences between members of class IIa.* ***B.*** *Superimposition for the three-dimensional protein structures for HDAC7 (violet-colored) with HDAC4 (green-colored), HDAC5 (teal-colored), and HDAC9 (orange-colored) having the parent compound TMP269 in the binding pocket with all the possible binding strands. Protein-ligand interaction for* ***C.*** *Position C13 and* ***D.*** *Position C36 for the parent TMP269 in the binding pocket of each of HDAC7, 5, and 4.*

Some designed and synthesized small molecule compounds showed affinity towards HDAC7 inhibition comparable to the pan HDACi and the parent class IIa HDACi compound.

After the designed compounds were outsourced for chemical synthesis, we tested the designed synthesized compounds in-house. From all the 72 screened compounds, three showed an inhibitory effect towards inhibiting HDAC7 in the presence of HDAC substrates using HDAC7 specificity assays in a trend comparable to the pan HDACi (TSA) and the parent compound (TMP269) **(Figure 3.6).**

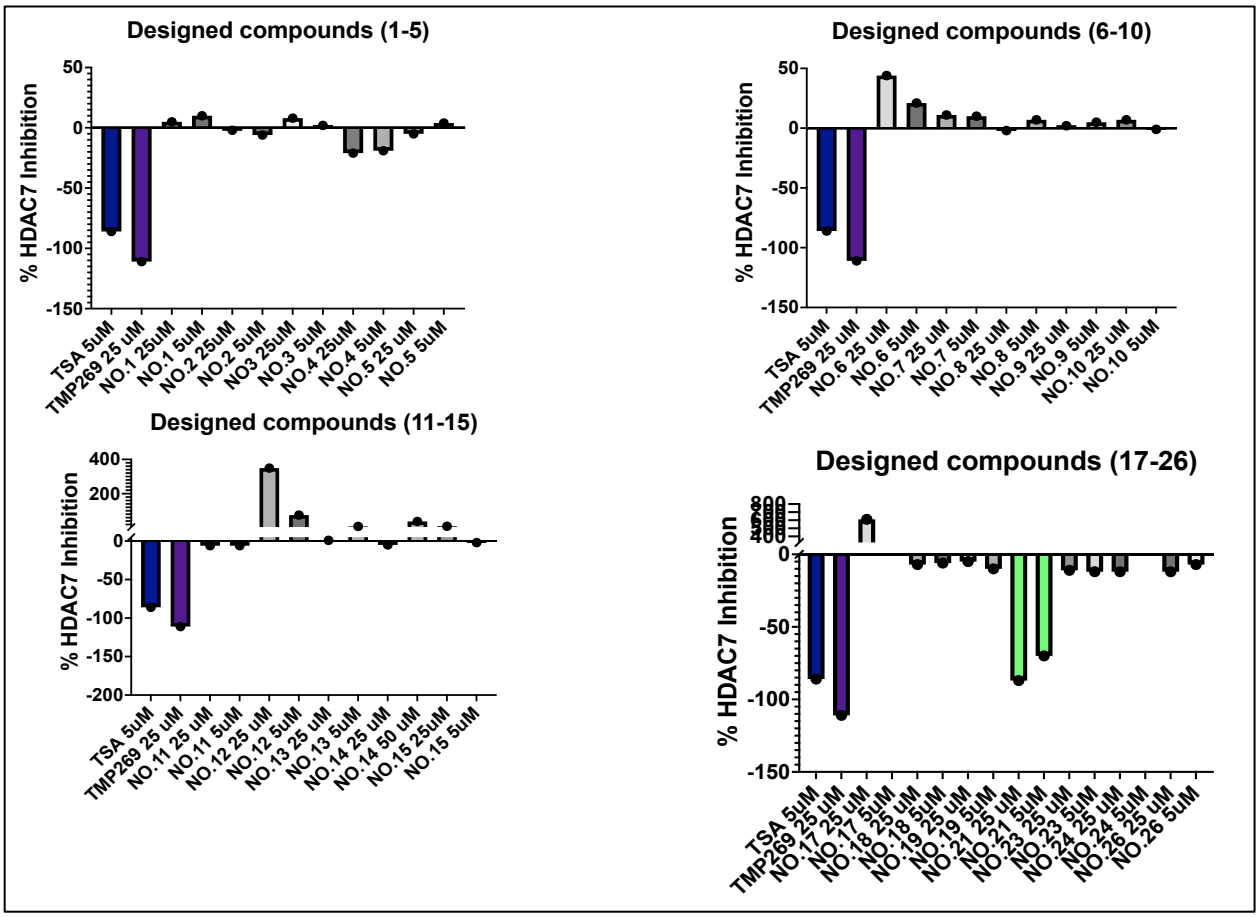

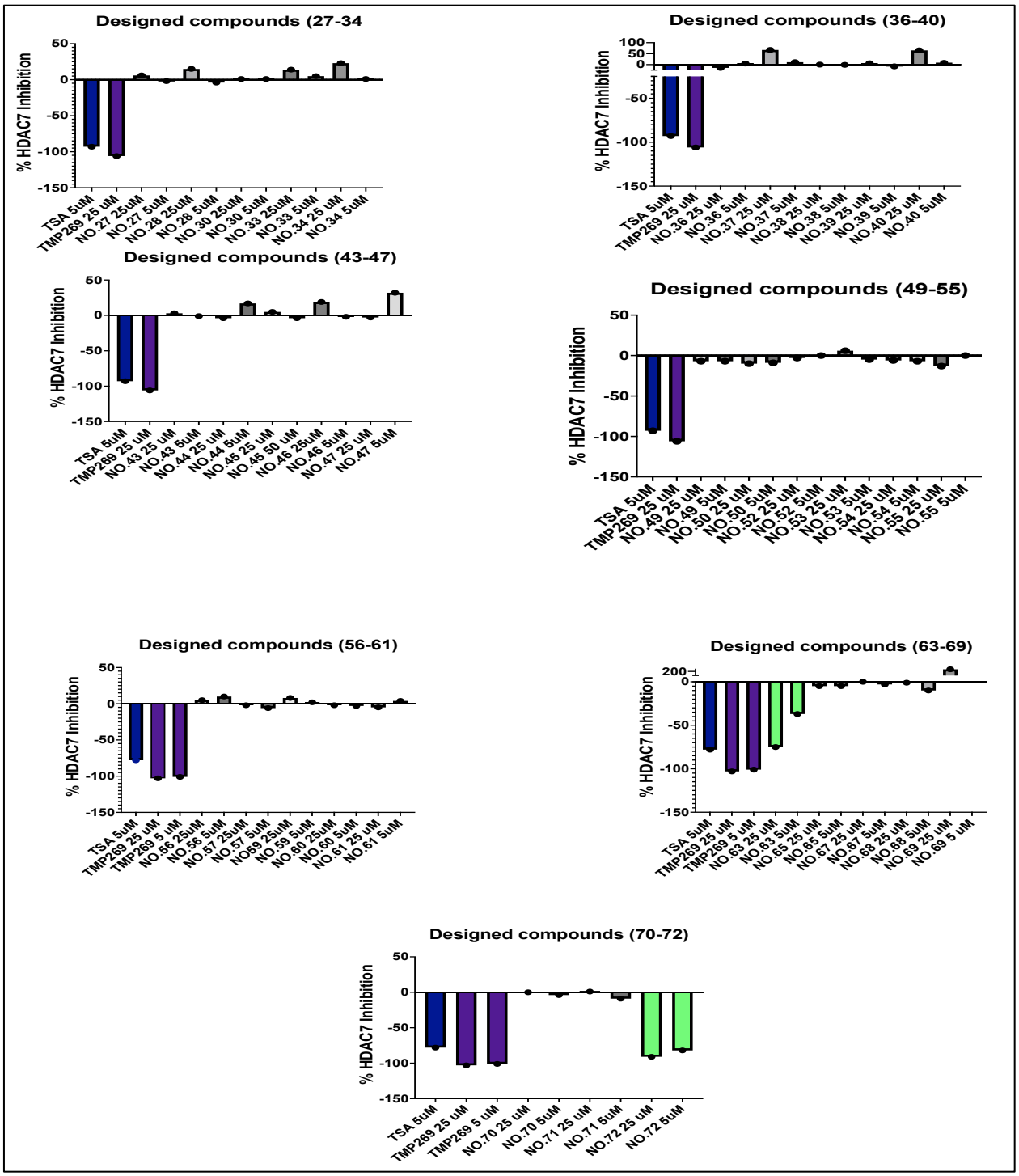

Figure (3.6) Novel small molecule compounds inhibit HDAC7 enzymatic activity. *Graph plots for small molecule newly designed small molecule compounds (1-72), some of which show affinity towards HDAC7 inhibition in an HDAC7 fluorogenic assay (Fluorescent green-colored) as compared to TSA as pan HDACi (Dark blue-colored) and the class IIa HDACi Purple-colored). Results were estimated in GraphPad Prism.*

Novel small molecule HDACi exhibits promising specificity towards HDAC7, demonstrating higher affinity than other class IIa HDACs.

To assess the specificity of compounds demonstrating HDAC7 inhibitory effects over the other class IIa HDACs, we conducted HDAC4, HDAC5, and HDAC9 affinity assays. These assays were compared against the pan HDAC inhibitor TSA and the parent class IIa HDAC inhibitor TMP269. This screening identified three compounds showing promising potential relative to the others **(Figure 3.7)**. One specific compound exhibited the highest affinity towards HDAC7. Consequently, compound 21 emerged as the most promising candidate and warranted further optimization.

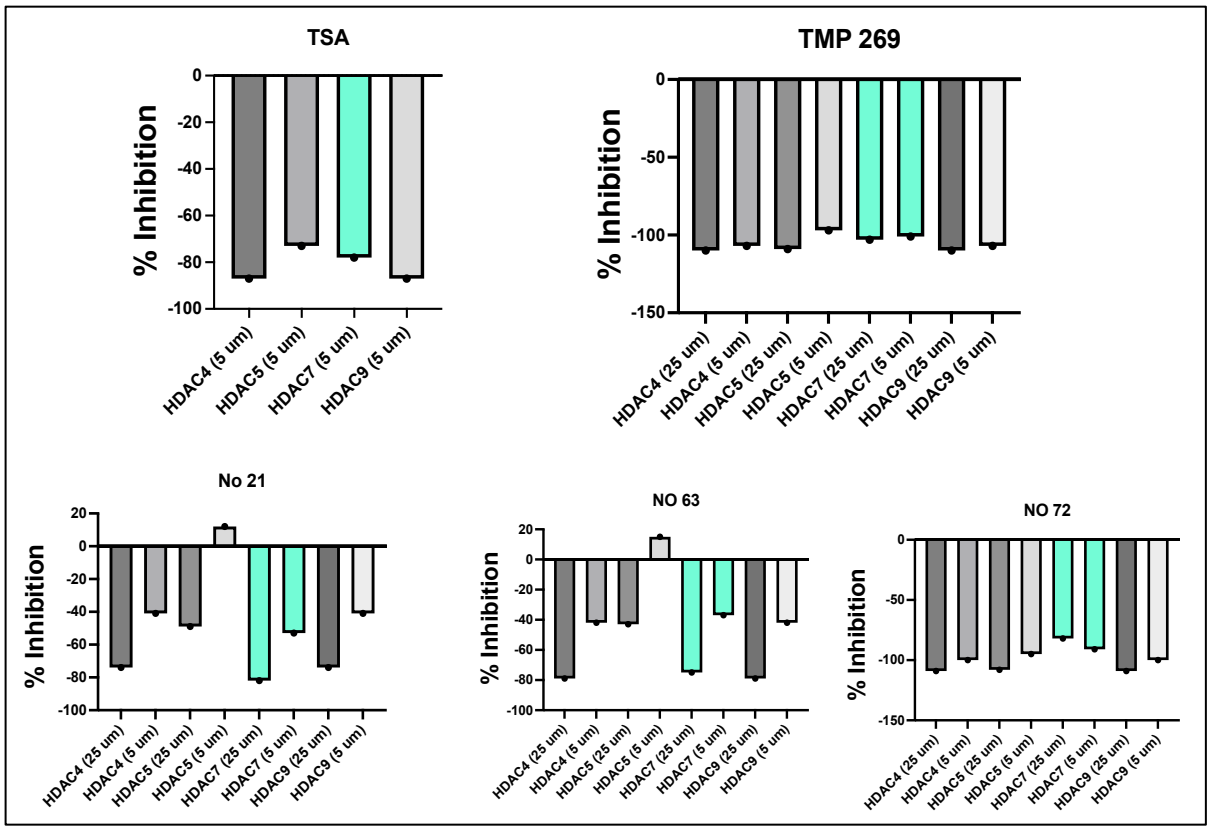

Figure (3.7) Novel small molecule compounds affinity towards class IIa HDACs. *Graph plots for three small molecule newly synthesized compounds, pan HDACi and class IIa HDACi, with their relative affinities towards HDAC7 as compared to their affinities towards HDAC4, 5, and 9 in an HDAC4, 5,7, and 9 fluorogenic assays. The teal green color is for the HDAC7 affinity of the tested compounds). Results were estimated in GraphPad Prism.*

Protein proteolysis-targeting chimera (PROTAC) is a promising and appealing approach to overcome the low enzymatic activity of HDAC class IIa.

With advances in novel drug design technology, PROTACs have introduced a good solution for targets with low structural similarity. We sought to introduce PROTAC to the newly synthesized HDACi small molecule compound, which showed good potential from our test screens. With the help of the chemical biology lab at Albert Einstein University, Dr. Sidoli and his team helped us develop heterobifunctional small molecules comprised of two ligands joined by a linker; one ligand is compound 21 from our screens that recruits and binds HDAC7, while other recruits and binds an E3 ubiquitin ligase.

We synthesized seven de novo PROTAC-HDACi compounds from a comprehensive ligand-linker screen. However, despite treating GSCs with these compounds at different time points (one, four, and 24 hours), analysis of the whole lysate revealed that none of the engineered compounds demonstrated the ability to induce proteolysis of HDAC7.

Nonetheless, we are actively pursuing further investigation of this approach through collaboration involving our group, Dr. Sidoli's team, and Dr. Fiser's team. Conducting larger screens and exploring various combinations of linkers and ligands for PROTACs holds tremendous potential for success. This concerted effort could ultimately result in discovering novel and effective PROTAC-HDAC inhibitors specifically targeting HDAC7.

RNA interference (RNAi) targeting HDAC7 represents a successful approach with a high level of specificity.

We designed and screened sequences through BLAST similarity to target the open reading frame and 3'- untranslated region of human HDAC7, where we ended up with four individual siRNAs for HDAC7. We used a smart pool of the four designed and synthesized siRNA variants to transfect our patients' derived GSCs using different concentrations. We tested the expression of HDAC7 in the lysates of the 72-hours-transfected GSCs using Western blot, and Beta Actin was used as a loading control. Accordingly, we chose the 50 nM concentration for giving 70-90% HDAC7 inhibition relative to the non-targeting siRNA-treated control **(Figure 3.8A & B).**

Next, we decided to test the specificity of our designed siHDAC7 across all members of class IIa HDACs in the transfected GSCs using Western blotting 72 hours after transfection. Control cells were transfected with non-targeting siRNA, and Actin was used as a loading control. Our designed siHDAC7 showed high selectivity towards inhibiting HDAC7 and minimally affects the rest of class IIa HDACs **(Figure 3.8C & D)**.

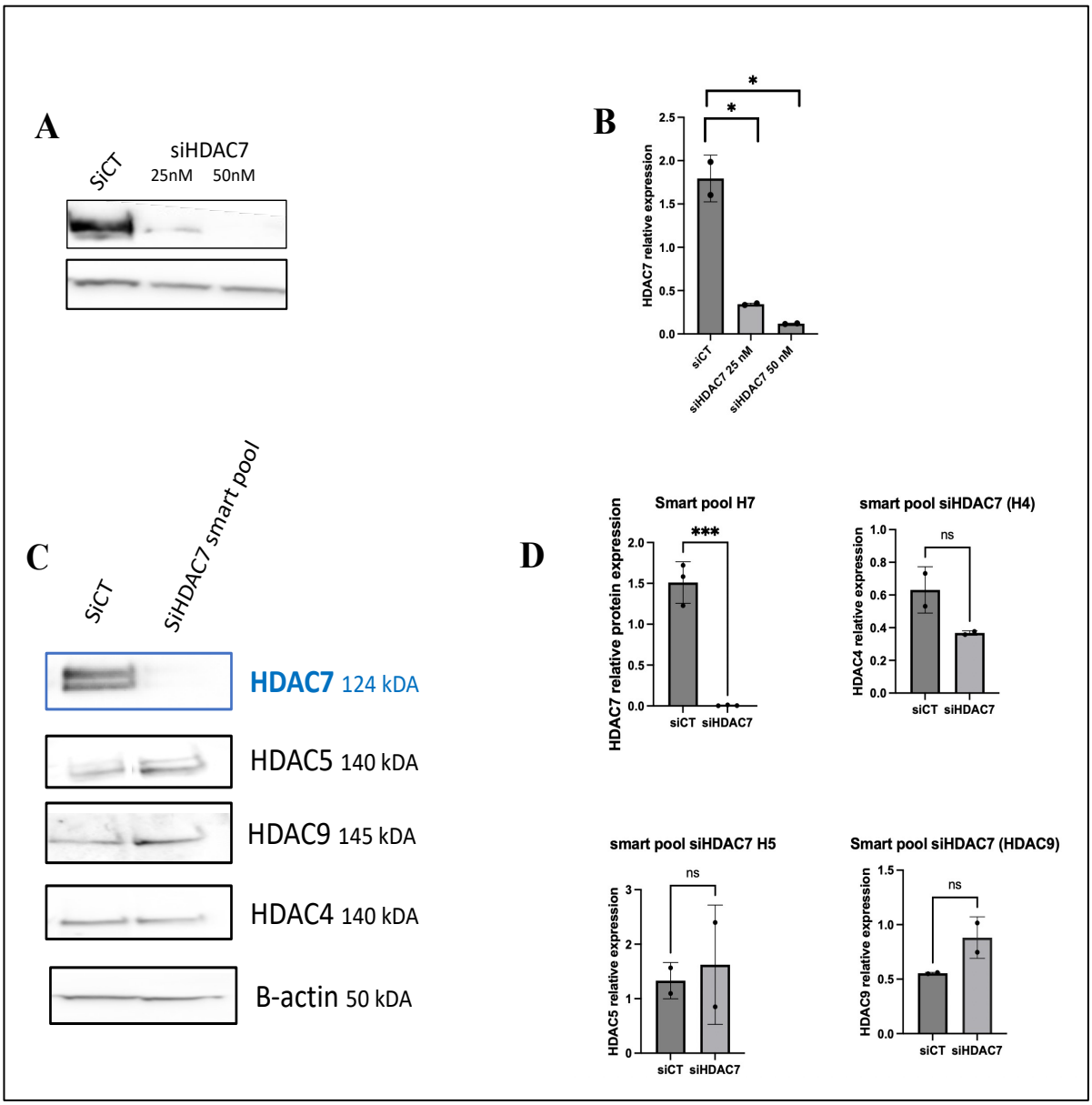

Figure (3.8) Designed siRNA shows significant specificity toward HDAC7. A & B. *Western blot detection images and its plotted quantification graph respectively for HDAC7 following transfection of GSCs with our designed siHDAC7 comparing two concentrations where 50nM showed more inhibition.* ***C. & D.*** *Western blot detection images and its corresponding plotted quantification graph for all class IIa HDACs following transfection of GSCs with our designed siHDAC7. HDAC4, HDAC5, and HDAC9 expression show minimal changes between the siHDAC7 and si-control GSCs, while HDAC7 expression is abolished. Results were estimated in GraphPad Prism. Error bars represent the mean +/- standard deviation. Statistical test: unpaired t-test with P-values, *** $p < 0.001$. ns: nonsignificant.*

Individual variant HDAC7 siRNA shows great specificity in inhibiting HDAC7 with minimal to no effect on other class HDAC IIa members.

To avoid off-targeting effects from the smart pool siRNA, we decided to test the specificity of each siHDAC7 variant in our designed smart pool. One variant (siHDAC7 variant-2) showed the highest specific inhibition of HDAC7 protein expression and did not significantly affect the expression of HDAC4, HDAC5, and HDAC9 **(Figure 3.9A- Q)**. In addition, our designed siRNA introduced phenotypic morphological stress to GSCs 72-hour post-transfection **(Figure 3.10A- D)**.

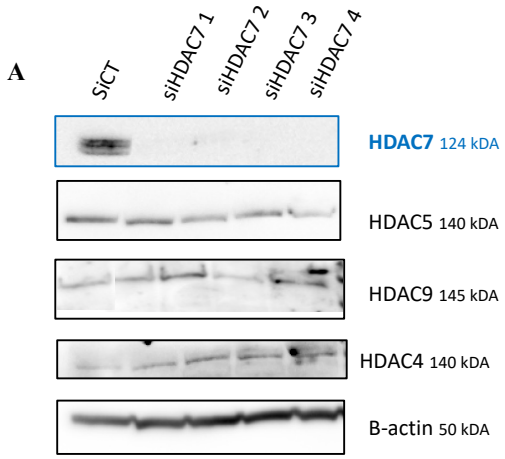

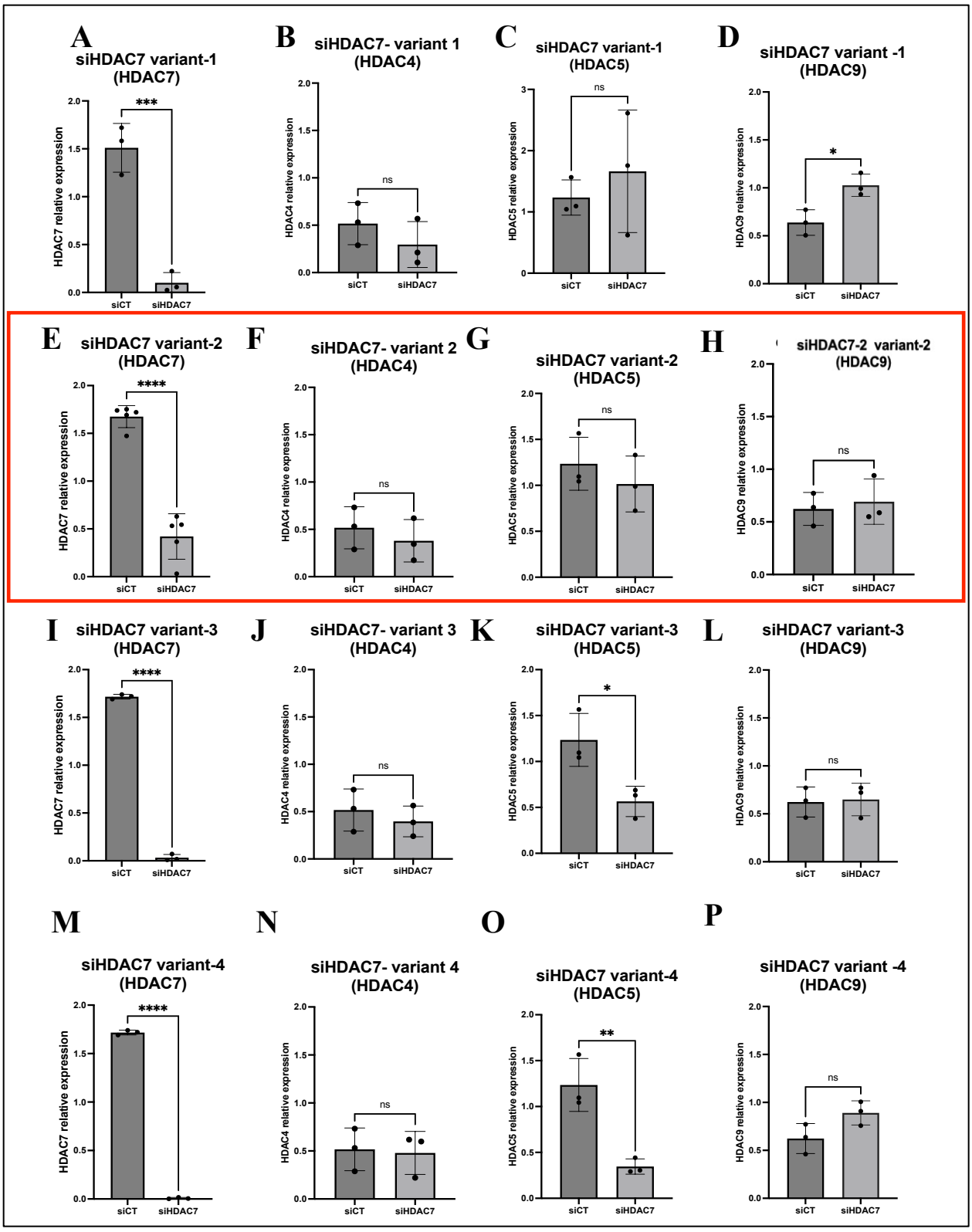

Figure (3.9) Designed specific variant for siRNA shows significant specificity toward HDAC7. A. *Western blot detection images for all class IIa HDACs following transfection of*

GSCs with our designed siHDAC7.HDAC4, HDAC5, and HDAC9 expression show minimal changes between the siHDAC7 and si-control GSCs, while HDAC7 expression is abolished. ***B-Q****. Corresponding plotted graphs for the relative class IIa HDAC expression for each siRNA variant, where siRNA variant 2 (F-I) shows the greatest HDAC7 inhibition with the highest HDAC7 specificity. Results were estimated in GraphPad Prism. Error bars represent the mean +/- standard deviation. Statistical test: unpaired t-test with P-values, *** p < 0.001. ns: nonsignificant.*

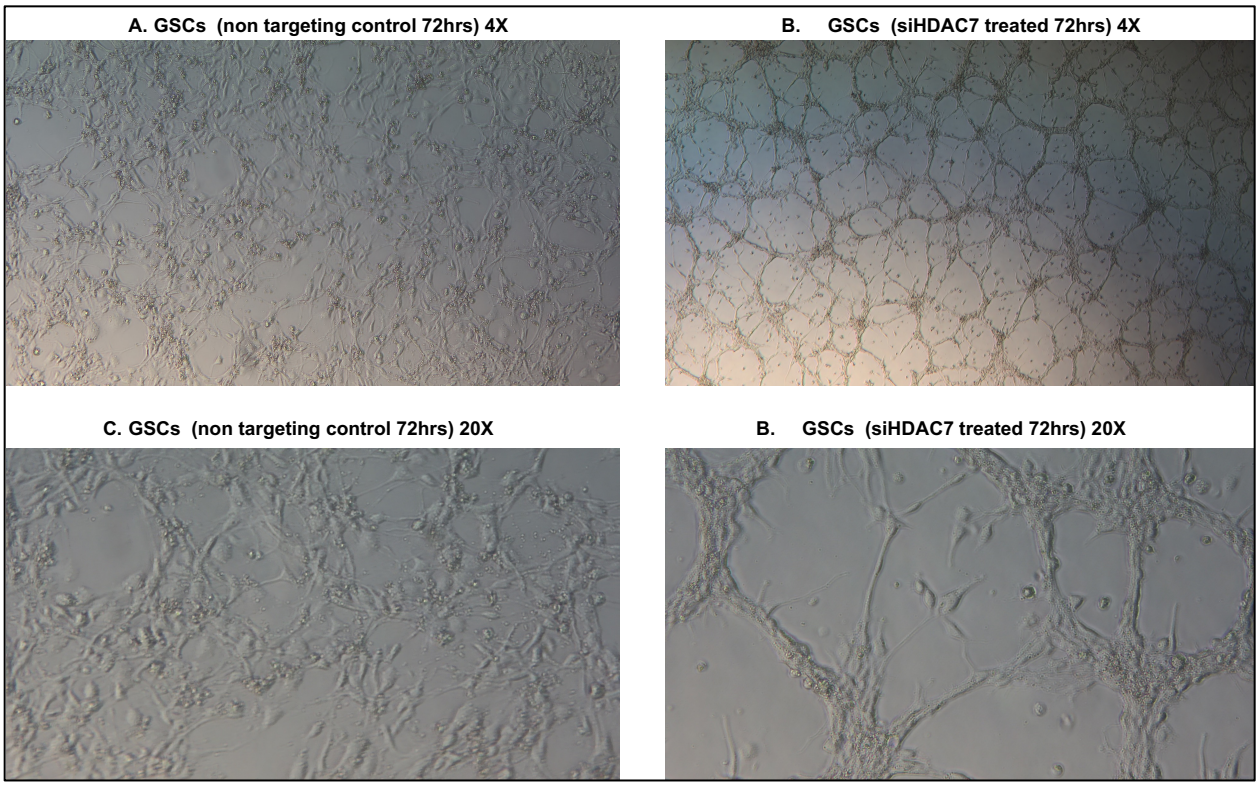

Figure (3.10) SiRNA against HDAC7 causes morphological changes to GSCs after 72 hours of transfection. *Microscopic images for control GSCs (non-targeting siRNA) with 4X* ***A.*** *and 20X* ***C.*** *magnification lens compared to siHDAC7 treated-GSCs with 4X* ***B.*** *and 20X* ***D.*** *magnification lens. The images show how siHDAC7 induces morphological stress to the GSCs compared to their control counterparts.*

IV. Discussion

We demonstrate that using class IIa HDACi exhibits comparable potential in changing the phenotype of patient-derived GSCs like pan HDACi, which are clinically used to treat some cancers. Despite the recognized side effects linked with pan HDACi, their inclusion in cancer regimens underscores their high potential to induce significant therapeutic impact, thus highlighting their promising role in cancer treatment.

Therefore, we contend that comparable results could be achieved with even fewer off-target effects by further narrowing the spectrum towards an HDACi specific for HDAC7. Indeed, in **Chapters 2 and 3**, we showed that the HDAC7 inhibition in GSCs and NSCLC cells changed the phenotype of these patient-derived and cancer cell lines. Together with our previous findings from **Chapter 2** that HDAC7 exhibits high expression in the GBM and is minimally expressed in the normal cells, we contend that HDAC7 is a promising druggable target for GBM with less off-target effects from the narrowed spectrum of HDAC inhibition.

HDACi drug discovery demonstrates much interest in the field; at least four are currently FDA-approved. We designed an innovative pipeline with several approaches that led to a promising design for siRNA against HDAC7 that does not significantly affect other HDACs.

RNAi discovery has opened a new arena for developing relatively fast approaches toward cancer drug design. Furthermore, the abundance of FDA-approved nanoparticles derived from polymers and lipids, specifically designed for RNAi drug delivery, holds significant promise for the effective and safe treatment of human cancers.

Although the BBB has long posed a challenge for drug delivery to the brain, there are now several advanced drug delivery modalities emerging to overcome this obstacle. These include implanted reservoirs and stereotactic injections, among others [30]. Furthermore, the concept of intra-arterial delivery, once proposed in earlier days, has been revitalized and reintroduced as a modality for delivering high dosages of therapeutics directly to the tumor site. Currently, there are six clinical trials underway involving intrathecal delivery, highlighting the renewed interest and potential of this method. Also, among the promising novel modalities for local brain delivery existing in clinical trials is convection-enhanced delivery (CED), which works by applying a positive pressure gradient that demonstrates improved spatial drug distribution, with lower concentrations of compounds being necessary to treat a similar area and can remain in situ for a prolonged time [31].

To date, four RNAi therapeutics, including GIVLAARI™ (givosiran), ONPATTRO® (patisiran), OXLUMO® (lumasiran), and LEQVIO® (inclisiran), have received approval for commercial therapeutic use. Additionally, at least seven siRNA-dependent therapeutics are undergoing phase-3 clinical studies, with numerous candidates in preclinical settings targeting various diseases, including cancer [32].

Ultimately, with our proposed HDAC7 siRNA drug design model, we believe we have the nourishing environment to take this innovative drug to more advanced preclinical settings, with the goal of changing the trajectory of this deadly disease, cancer.

Acknowledgment

We extend our appreciation to Dr. Andras Fiser and the Fiser team, Eduardo, Rehan, and Raj at Albert Einstein University, for their valuable assistance in the computational library screening and drug design pipeline. Our gratitude also goes to the NIH for providing the compounds granted from their library of small-molecule compounds. Additionally, we acknowledge Dr. Sidoli and his team for their contributions to PROTAC-HDAC engineering. Collaborative efforts between experts from diverse fields are vital and have the potential to greatly influence the development of cancer therapeutics.

V. Supplementary Figures

Supplementary Figure 1. **The protein-Ligand interaction profiler for class IIa HDACi (TMP269) within the virtual binding pocket of class IIa HDAC.** Snapshots from the Schrodinger designer software show how class IIa HDAC members possess different bindings and interactions with this parent compound.

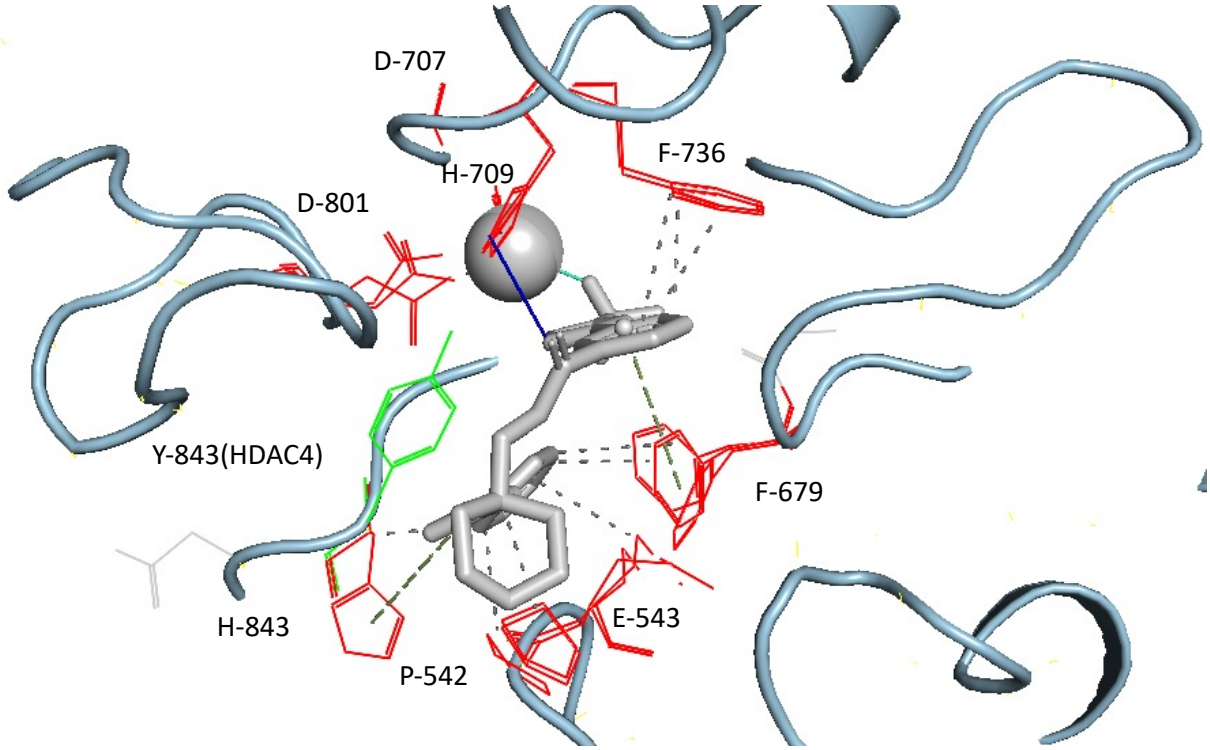

Supplementary Figure 2. **TMP269 within the virtual binding pocket of HDAC7.** Snapshots from the Schrodinger designer software show the binding of TMP269 within HDAC7, with the blue clouds referring to the areas that tolerate modification in this parent compound to render it more HDAC7-specific.

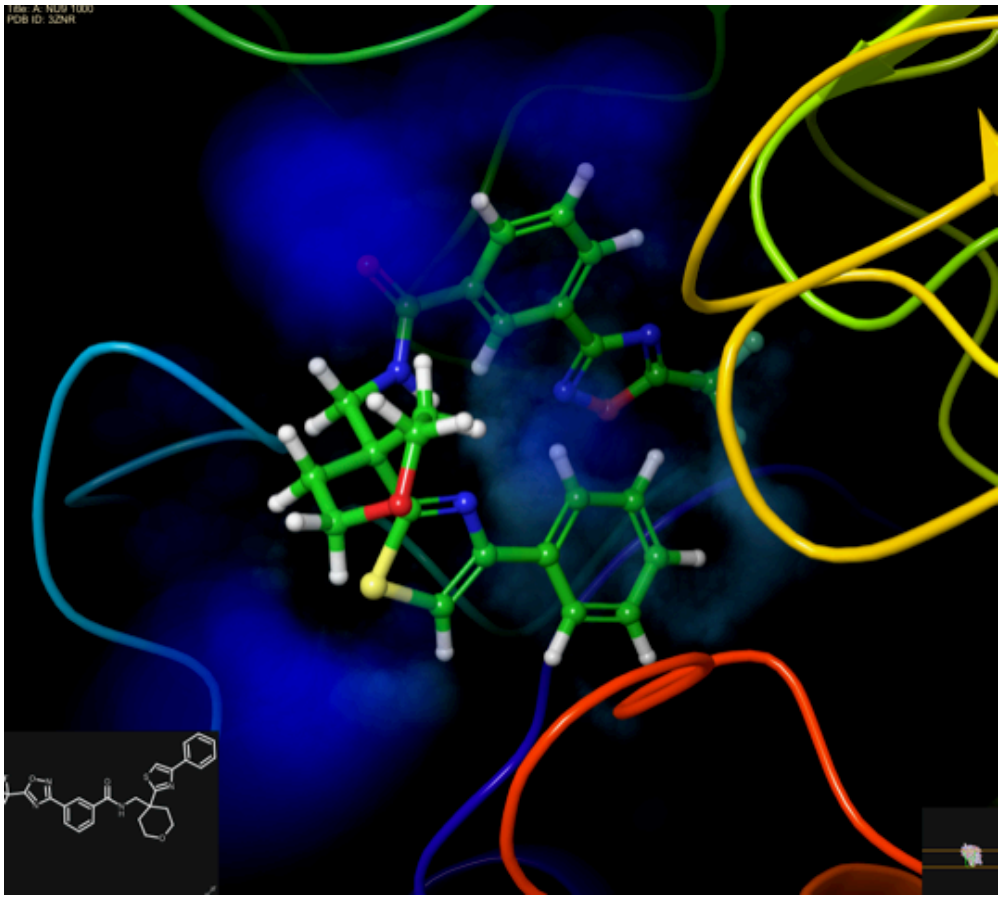

VI. References

[1] B. Deskin, J. Lasky, Y. Zhuang, and B. Shan, "Requirement of HDAC6 for activation of Notch1 by TGF-beta1," *Sci Rep,* vol. 6, p. 31086, Aug 8 2016, doi: 10.1038/srep31086.

[2] H. Han *et al.*, "Hippo signaling dysfunction induces cancer cell addiction to YAP," *Oncogene,* vol. 37, no. 50, pp. 6414-6424, Dec 2018, doi: 10.1038/s41388-018-0419-5.

[3] H. M. Findeisen *et al.*, "Epigenetic regulation of vascular smooth muscle cell proliferation and neointima formation by histone deacetylase inhibition," *Arterioscler Thromb Vasc Biol,* vol. 31, no. 4, pp. 851-60, Apr 2011, doi: 10.1161/ATVBAHA.110.221952.

[4] G. Shanmugam, S. Rakshit, and K. Sarkar, "HDAC inhibitors: Targets for tumor therapy, immune modulation and lung diseases," *Transl Oncol,* vol. 16, p. 101312, Feb 2022, doi: 10.1016/j.tranon.2021.101312.

[5] Y. Li and E. Seto, "HDACs and HDAC Inhibitors in Cancer Development and Therapy," *Cold Spring Harb Perspect Med,* vol. 6, no. 10, Oct 3 2016, doi: 10.1101/cshperspect.a026831.

[6] Z. Dong, Y. Yang, S. Liu, J. Lu, B. Huang, and Y. Zhang, "HDAC inhibitor PAC-320 induces G2/M cell cycle arrest and apoptosis in human prostate cancer," *Oncotarget,* vol. 9, no. 1, pp. 512-523, Jan 2 2018, doi: 10.18632/oncotarget.23070.

[7] Z. Wang, P. Hu, F. Tang, and C. Xie, "HDAC6-mediated EGFR stabilization and activation restrict cell response to sorafenib in non-small cell lung cancer cells," *Med Oncol,* vol. 33, no. 5, p. 50, May 2016, doi: 10.1007/s12032-016-0765-5.

[8] M. Terranova-Barberio *et al.*, "Synergistic antitumor interaction between valproic acid, capecitabine and radiotherapy in colorectal cancer: critical role of p53," *J Exp Clin Cancer Res,* vol. 36, no. 1, p. 177, Dec 6 2017, doi: 10.1186/s13046-017-0647-5.

[9] M. A. Salvador *et al.*, "The histone deacetylase inhibitor abexinostat induces cancer stem cells differentiation in breast cancer with low Xist expression," *Clin Cancer Res,* vol. 19, no. 23, pp. 6520-31, Dec 1 2013, doi: 10.1158/1078-0432.CCR-13-0877.

[10] Y. B. Zhou *et al.*, "Pharmacodynamic, pharmacokinetic, and phase 1a study of bisthianostat, a novel histone deacetylase inhibitor, for the treatment of relapsed or refractory multiple myeloma," *Acta Pharmacol Sin,* vol. 43, no. 4, pp. 1091-1099, Apr 2022, doi: 10.1038/s41401-021-00728-y.

[11] A. D. Bondarev, M. M. Attwood, J. Jonsson, V. N. Chubarev, V. V. Tarasov, and H. B. Schioth, "Recent developments of HDAC inhibitors: Emerging indications and novel molecules," *Br J Clin Pharmacol,* vol. 87, no. 12, pp. 4577-4597, Dec 2021, doi: 10.1111/bcp.14889.

[12] P. J. Wood *et al.*, "A phase I study of panobinostat in pediatric patients with refractory solid tumors, including CNS tumors," *Cancer Chemother Pharmacol,* vol. 82, no. 3, pp. 493-503, Sep 2018, doi: 10.1007/s00280-018-3634-4.

[13] S. Kikuchi *et al.*, "Class IIa HDAC inhibition enhances ER stress-mediated cell death in multiple myeloma," *Leukemia,* vol. 29, no. 9, pp. 1918-27, Sep 2015, doi: 10.1038/leu.2015.83.

[14] L. Urwanisch *et al.*, "The Class IIA Histone Deacetylase (HDAC) Inhibitor TMP269 Downregulates Ribosomal Proteins and Has Anti-Proliferative and Pro-Apoptotic Effects

on AML Cells," *Cancers (Basel),* vol. 15, no. 4, Feb 7 2023, doi: 10.3390/cancers15041039.
[15] G. Wang *et al.*, "Class I and class II histone deacetylases are potential therapeutic targets for treating pancreatic cancer," *PLoS One,* vol. 7, no. 12, p. e52095, 2012, doi: 10.1371/journal.pone.0052095.
[16] S. Ishikawa *et al.*, "Statins inhibit tumor progression via an enhancer of zeste homolog 2-mediated epigenetic alteration in colorectal cancer," *Int J Cancer,* vol. 135, no. 11, pp. 2528-36, Dec 1 2014, doi: 10.1002/ijc.28672.
[17] L. Colarossi *et al.*, "Inhibition of histone deacetylase 4 increases cytotoxicity of docetaxel in gastric cancer cells," *Proteomics Clin Appl,* vol. 8, no. 11-12, pp. 924-31, Dec 2014, doi: 10.1002/prca.201400058.
[18] M. H. Cai *et al.*, "Depletion of HDAC1, 7 and 8 by Histone Deacetylase Inhibition Confers Elimination of Pancreatic Cancer Stem Cells in Combination with Gemcitabine," *Sci Rep,* vol. 8, no. 1, p. 1621, Jan 26 2018, doi: 10.1038/s41598-018-20004-0.
[19] A. Pasto *et al.*, "Cancer stem cells from epithelial ovarian cancer patients privilege oxidative phosphorylation, and resist glucose deprivation," *Oncotarget,* vol. 5, no. 12, pp. 4305-19, Jun 30 2014, doi: 10.18632/oncotarget.2010.
[20] M. Y. Wu, J. Fu, X. Xiao, J. Wu, and R. C. Wu, "MiR-34a regulates therapy resistance by targeting HDAC1 and HDAC7 in breast cancer," *Cancer Lett,* vol. 354, no. 2, pp. 311-9, Nov 28 2014, doi: 10.1016/j.canlet.2014.08.031.
[21] Y. Zhang *et al.*, "HDAC7/c-Myc signaling pathway promotes the proliferation and metastasis of choroidal melanoma cells," *Cell Death Dis,* vol. 14, no. 1, p. 38, Jan 18 2023, doi: 10.1038/s41419-022-05522-0.
[22] A. E. Witt *et al.*, "Identification of a cancer stem cell-specific function for the histone deacetylases, HDAC1 and HDAC7, in breast and ovarian cancer," *Oncogene,* vol. 36, no. 12, pp. 1707-1720, Mar 23 2017, doi: 10.1038/onc.2016.337.
[23] V. Cutano, E. Di Giorgio, M. Minisini, R. Picco, E. Dalla, and C. Brancolini, "HDAC7-mediated control of tumour microenvironment maintains proliferative and stemness competence of human mammary epithelial cells," *Mol Oncol,* vol. 13, no. 8, pp. 1651-1668, Aug 2019, doi: 10.1002/1878-0261.12503.
[24] Y. Xiong *et al.*, "Chemo-proteomics exploration of HDAC degradability by small molecule degraders," *Cell Chem Biol,* vol. 28, no. 10, pp. 1514-1527 e4, Oct 21 2021, doi: 10.1016/j.chembiol.2021.07.002.
[25] N. Abdelfattah *et al.*, "Single-cell analysis of human glioma and immune cells identifies S100A4 as an immunotherapy target," *Nat Commun,* vol. 13, no. 1, p. 767, Feb 9 2022, doi: 10.1038/s41467-022-28372-y.
[26] Y. Hu and G. K. Smyth, "ELDA: extreme limiting dilution analysis for comparing depleted and enriched populations in stem cell and other assays," *J Immunol Methods,* vol. 347, no. 1-2, pp. 70-8, Aug 15 2009, doi: 10.1016/j.jim.2009.06.008.
[27] M. Bekes, D. R. Langley, and C. M. Crews, "PROTAC targeted protein degraders: the past is prologue," *Nat Rev Drug Discov,* vol. 21, no. 3, pp. 181-200, Mar 2022, doi: 10.1038/s41573-021-00371-6.
[28] B. S. Mann, J. R. Johnson, M. H. Cohen, R. Justice, and R. Pazdur, "FDA approval summary: vorinostat for treatment of advanced primary cutaneous T-cell lymphoma," *Oncologist,* vol. 12, no. 10, pp. 1247-52, Oct 2007, doi: 10.1634/theoncologist.12-10-1247.

[29] S. R. Gameiro, A. S. Malamas, K. Y. Tsang, S. Ferrone, and J. W. Hodge, "Inhibitors of histone deacetylase 1 reverse the immune evasion phenotype to enhance T-cell mediated lysis of prostate and breast carcinoma cells," *Oncotarget,* vol. 7, no. 7, pp. 7390-402, Feb 16 2016, doi: 10.18632/oncotarget.7180.

[30] T. S. van Solinge, L. Nieland, E. A. Chiocca, and M. L. D. Broekman, "Advances in local therapy for glioblastoma - taking the fight to the tumour," *Nat Rev Neurol,* vol. 18, no. 4, pp. 221-236, Apr 2022, doi: 10.1038/s41582-022-00621-0.

[31] A. Jahangiri, A. T. Chin, P. M. Flanigan, R. Chen, K. Bankiewicz, and M. K. Aghi, "Convection-enhanced delivery in glioblastoma: a review of preclinical and clinical studies," *J Neurosurg,* vol. 126, no. 1, pp. 191-200, Jan 2017, doi: 10.3171/2016.1.JNS151591.

[32] B. Hu *et al.*, "Therapeutic siRNA: state of the art," *Signal Transduct Target Ther,* vol. 5, no. 1, p. 101, Jun 19 2020, doi: 10.1038/s41392-020-0207-x.

CHAPTER 4:

Heterochromatin Spreading in Cancer Cells Through HDAC7-Mediated Histone H3.3 Landscape Reprogramming

Heterochromatin spreading in cancer cells through HDAC7 mediated histone H3.3 landscape reprogramming.

Ola Hassan[1], Mattia Pizzagalli[1], Laura Jinxuan Wu[1], David Karambizi[1], John P. Zepecki[1], Eduardo Fajardo[2], Andras Fiser[2], Nikos Tapinos[1,3*]

1: Laboratory of Cancer Epigenetics and Plasticity, Brown University, Rhode Island Hospital, Providence, RI, USA

2: Department of Computational and Systems Biology, Albert Einstein College of Medicine, Bronx, NY

3: Department of Neurosurgery, Brown University, Rhode Island Hospital, Providence, RI, USA

***: Corresponding Author:**

Nikos Tapinos M.D., Ph.D.
Laboratory of Cancer Epigenetics and Plasticity 593 Eddy Street,
Providence, RI 02903,
Tel: 401-606-4393,
e-mail: nikos_tapinos@brown.edu

Conflict of Interest Disclosure

The authors declare no conflict of interest.

Preprint

DOI: 10.1101/2024.03.12.584656v1

Abstract

Class IIa histone deacetylases (HDACs) are a family of enzymes that, despite their name, do not have any measurable histone deacetylase activity, but they function as multi-protein interaction hubs due to the presence of a prolonged N-terminal domain. Here, we show that HDAC7, a member of the Class IIa HDAC family, is a chaperone for Histone H3.3 and interacts with H3.3 and HIRA on chromatin. Specific inhibition of HDAC7 expression with subtype-specific siRNAs results in inhibition of the interaction of H3.3 with HIRA, while the association of H3.3 with DAXX and H3K9me3 is significantly increased, resulting in H3.3 being deposited on H3K9me3+/DAPI+ heterochromatin nuclear foci. Inhibition of HDAC7 triggers a significant increase of heterochromatin marks H3K9me3 and H3K27me3, global heterochromatin spreading in cancer cells, and reprogramming of the H3.3 chromatin landscape. This drives substantial alteration of cancer cell gene expression as well as inhibition of the stemness phenotype for cancer cells. Our work demonstrates the involvement of HDAC7 in the euchromatic H3.3 chaperone network and shows that inhibiting HDAC7 induces H3.3 landscape reprogramming, heterochromatin spreading, and epigenetic restriction in cancer cells.

Highlights:

- Inhibiting HDAC7 induces an increase in heterochromatin histone marks H3K9me3 and H3K27me3
- Inhibiting HDAC7 inhibits CSC stemness phenotype
- Inhibiting HDAC7 drives H3.3 chromatin deposition switch from HIRA to DAXX
- HDAC7 induces global heterochromatin spreading in cancer stem cells

Graphical Abstract

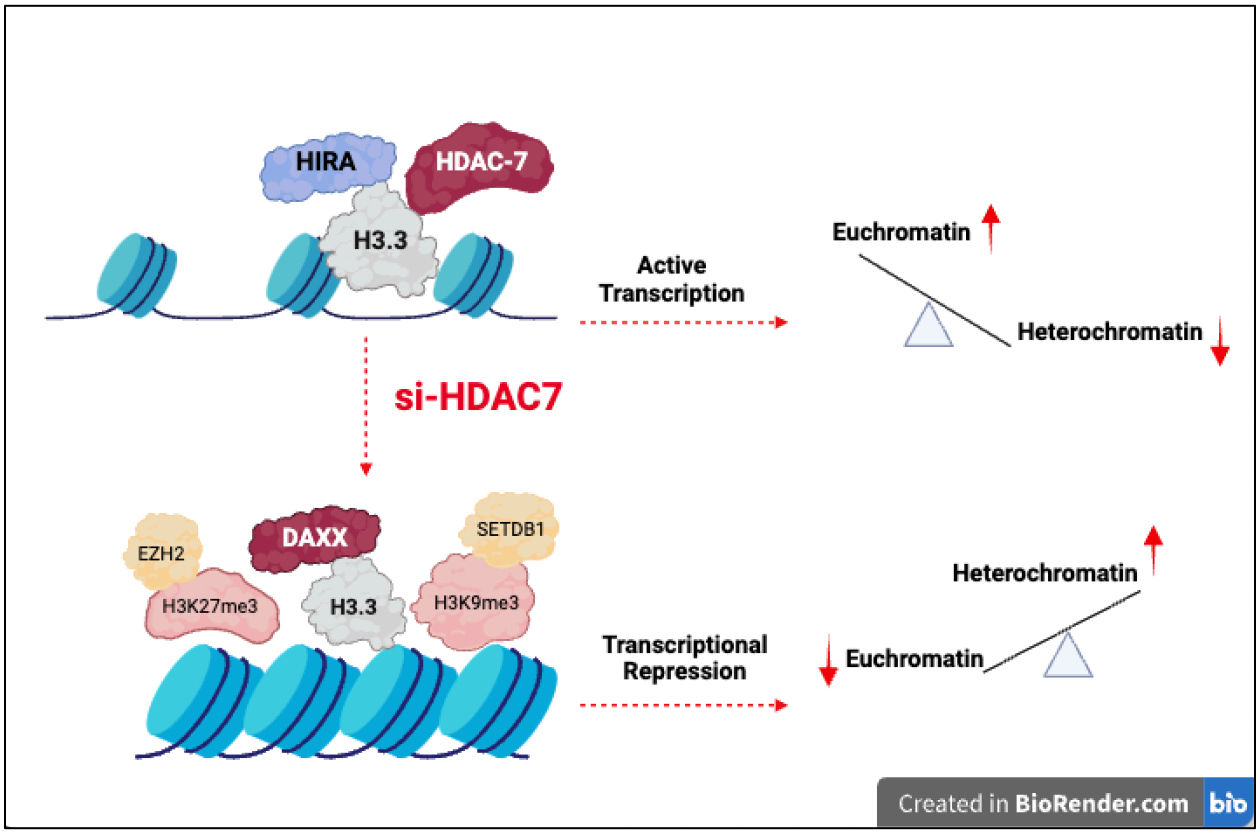

II. Introduction

Epigenetic mechanisms have emerged as key players in cancer development. Alterations in chromatin mediate cell reprogramming and oncogenesis, while epigenetic changes triggered by the tumor microenvironment regulate cancer cell phenotypic transitions and tumor architecture [1, 2]. Chromatin exists in two higher-order states: euchromatin refers to loosely packed chromatin that is easily accessible to transcriptional regulators and RNA polymerase, while heterochromatin is densely packed and not accessible [3, 4]. Alteration of the state of chromatin impacts global gene expression by making genes either more or less accessible for transcription. Interconversion between these two chromatin states occurs through the function of several regulators that affect levels of DNA methylation or posttranslational modification of histones (acetylation, methylation, phosphorylation, SUMOylating, etc.). This dynamic regulatory system is commonly referred to as the epigenetic control of gene transcription [5].

Histone deacetylases (HDACs) remove acetyl- groups from histone molecules, hence regulating posttranslational modification of histone marks. Expression of HDACs is elevated in several tumors, resulting in transcriptional activation of oncogenes, increased transcriptional rates, and chromosomal translocations [4, 6, 7]. HDACs can be divided into class I (HDAC1, 2, 3, and 8), class II (HDAC4, 5, 6, 7, 9, and 10), and class IV (HDAC11) based on sequence similarity. The class II HDACs are further divided into class IIa (HDAC4, 5, 7, and 9) and class IIb (HDAC6 and 10) according to their domain compositions. However, Class IIa HDACs lack any measurable enzymatic activity and their deacetylase activity is minimal towards acetylated histones [5]. Class IIa HDACs exhibit a prolonged N-terminal region compared to Class I HDACs that harbor a nuclear localization signal and a nuclear export signal, so they are found both in the nucleus and the cytoplasm [5]. The presence of this unique N-terminal region suggests that Class IIa HDACs

may participate in multi-protein complexes to exert their biological function. In human malignancies, Class I and II HDACs are considered oncoproteins that regulate gene expression to promote tumorigenesis and cancer development [5-7]. Specifically, HDAC7 has been implicated in the pathogenesis of colorectal [8, 9], pancreatic [10, 11], liver [12], gastric [13], lung [14], breast [15] and brain cancer [16, 17].

Canonical histone proteins are incorporated into chromatin in a DNA replication-dependent manner, while Histone H3.3 is incorporated in a DNA replication-independent manner [18-20]. In Drosophila melanogaster and Arabidopsis thaliana, H3.3 is enriched in replication origins [21-26], while in human cells, it is associated with early replication and recruited on sites of DNA repair [26-28]. Although H3.3 is mainly associated with euchromatin and regulation of active transcription [20, 29], recently, it was shown that it was also associated with heterochromatin on telomeres, pericentric heterochromatin, and heterochromatin marks on gene regulatory regions[29, 30]. Association of H3.3 with euchromatin or heterochromatin is largely dependent on a group of proteins with chaperone activity that interact with H3.3 and deposit it on chromatin regions. Euchromatin deposition is regulated by a HIRA/UBN1/CABIN1 chaperone complex, while heterochromatin deposition of H3.3 depends on interaction with DAXX/ATRX [31, 32]. The balance between HIRA/UBN1/CABIN1 versus DAXX/ATRX deposition of H3.3 on euchromatin or heterochromatin, respectively, may represent a crucial node in histone landscape reprogramming that enables complex cell fate decisions during tumorigenesis. Involvement of HDACs on these Histone chaperone complexes has only been suggested for the MIER1 complex but not for individual HDACs [33] and the participation of Class IIa HDACs in the regulation of the Histone H3.3 chromatin landscape has not been studied to date.

Here, we show high expression of HDAC7 in glioblastoma tumors, patients-derived glioma stem cells (GSCs), and patient-derived pediatric DIPG cells. HDAC7 shows minimal histone deacetylase activity but forms protein-protein interactions with Histone H3.3 on chromatin. Specific inhibition of HDAC7 expression with an in vivo stable siRNA results in an increase of heterochromatin marks H3K9me3 and H3K27me3, global heterochromatin spreading in cancer cells, and rebalancing of the H3.3 chromatin landscape. Following HDAC7 inhibition, the interaction of H3.3 with HIRA is reduced, the association of H3.3 with DAXX and H3K9me3 is significantly increased, and H3.3 is deposited on $H3K9me3^{+}/DAPI^{+}$ heterochromatin nuclear foci. This results in significant alteration of cancer cell gene expression, and inhibition of GSC growth and self-renewal. Our work demonstrates the involvement of HDAC7 in euchromatic H3.3 chaperone complexes and shows that inhibition of HDAC7 results in H3.3 landscape reprogramming, heterochromatin spreading, and epigenetic restriction in cancer cells.

III. Methods

- *GSCs culture maintenance.*

Patient-derived GSCs (GSC1, GSC2, GSC3) were used in this study. Primary GSCs were cultured in the enrichment complete growth media described before. Cryopreserved GSCs were passaged twice as neurospheres and then attached for at least one passage to ensure adequate adaptation to culture conditions, which was done routinely for all experiments in this study. All cultures were routinely tested for mycoplasma contamination using the LookOut Mycoplasma PCR Detection kit (Sigma). According to the experiment in use, neurospheres or attached GSCs are used when ~80% confluency is reached in the culturing medium.

- *DIPG cells maintenance*

The enrichment working tumor stem media (TSM) consists of Neurobasal-A media (Fisher Scientific, Catalog #: 10888022 or 12349015), D-MEM/F-12 (1X), liquid, 1:1 (Invitrogen, Catalog #: 11330-032), HEPES Buffer Solution (1M) 1 (Invitrogen, Catalog #: 15630-080), MEM Sodium Pyruvate Solution (100X) (Invitrogen, Catalog #: 11360-070), MEM Non-Essential Amino Acids solution 10mM (100X) (Invitrogen, Catalog #: 11140-050). TSM media was supplemented with growth factors: 10ug basic fibroblast growth factor (bFGF) and 10ug epidermal growth factor (EGF) (20ng/ml final concentration respectively; Peprotech, Catalog # 100-18B & 100-47 respectively). 10 ug H-PDGF-AA, H-PDGF-BB growth factors were supplemented (10ng/ml final concentration respectively; Peprotech, Catalog # 100-13A & 100-14B respectively). Heparin is supplemented as a growth co-factor (2ug/ml final concentration; StemCell Tech, Catalog #: 07980). As a serum substitute, B-27 without Vitamin A is used (50X final concentration; Fisher Scientific, Catalog #: 12587010). For energy supplantation, 1X 2mM Glutamax is used (100X

final concentration; Fisher Scientific, Catalog #: 35050061). Finally, The DIPG complete media is supplemented with antibiotics to prevent contaminations during culturing; 1X Antibiotic: Antimycotic (Anti-Anti) (100X final concentration; Fisher Scientific, Catalog #: 1524006.

Cryopreserved DIPGs underwent two passages as neurospheres before being attached for at least one passage to ensure proper adaptation to the culture conditions. This protocol was consistently followed for all experiments conducted in this study. Regular testing for mycoplasma contamination was performed on all cultures using the LookOut Mycoplasma PCR Detection kit (Sigma). Depending on the specific experiment, neurospheres or attached DIPGs were employed when they reached approximately 80% confluency in the culture medium.

- *siRNA transfection treatment*

The transfection protocol was applied according to the optimization done in **Chapter 2,** and the HDAC7 siRNA variant.2 from the validation study done in **Chapter 3** was the selected transfection treatment in this study.

HDAC7 siRNA sense: 5' G.C.A.G.A.U.A.C.C.C.U.C.G.G.C.U.G.A.A 3'

antisense: 5' U.U.C.A.G.C.C.G.A.G.G.G.U.A.U.C.U.G.C 3'

Non-targeting control siRNA- sense: 5' A.G.C.G.A.C.U.A.A.A.C.A.C.A.U.C.A.A 3'

antisense: 5' U.U.G.A.U.G.U.G.U.U.U.A.G.U.C.G.C.U 3'

All transfection experiments were followed by western blot analysis to validate the knocking-down efficiency, which was maintained at 70-90% inhibition as compared to non-targeting control.

- *LC-MS for histone PTM Mass Spectrometry (Mod-Spec)*

a- Histone extraction and preparation for mass spectrometry

Five million GSCs were counted per condition per replicate and seeded in coated cell culture plates. Three biological replicates for siHDAC7-treated versus si-control treated GSCs were verified for HDAC7 inhibition by Western blot. Bulk histones from each sample were acid-extracted from cell pellets, propionylated, and subjected to trypsin digestion as described previously [34]. Briefly, histones were extracted by incubating samples at room temperature for 1 hour in 0.2M sulfuric acid with intermittent vortexing. Histones were then precipitated by the addition of trichloroacetic acid (TCA) on ice, and recovered by centrifugation at 10,000 x g for 5 minutes at 4°C. The pellet was then washed once with 1mL cold acetone/0.1% HCl and twice with 100% acetone, and then air dried in a clean hood. The histones were propionylated by adding 1:3 v/v propionic anhydride/2-propanol and incrementally adding ammonium hydroxide to keep the pH around 8, and subsequently dried in a SpeedVac concentrator. The pellet was then resuspended in 100mM ammonium bicarbonate and adjusted to pH 7-8 with ammonium hydroxide. The histones were then digested with trypsin resuspended in 100 mM ammonium bicarbonate overnight at 37°C and dried in a SpeedVac concentrator. The pellet was resuspended in 100mM ammonium bicarbonate and propionylated a second time by adding 1:3 v/v propionic anhydride/2-propanol and incrementally adding ammonium hydroxide to keep the pH around 8, and subsequently dried in a SpeedVac concentrator. Histone peptides were resuspended in 0.1% TFA in H_2O for mass spectrometry analysis

b- Mass spectrometry

Samples were analyzed on a triple quadrupole (QqQ) mass spectrometer (Thermo Fisher Scientific Quantum Ultra mass spectrometer TSQ) directly coupled with an UltiMate 3000 Dionex nano-liquid chromatography system. Peptides were first loaded onto a packed trapping column (3cm×150µm) and then separated on a New Objectives PicoChip analytical column (10 cm×75 µm). Both columns were packed with New Objectives ProntoSIL C18-AQ, 3µm, 200Å resin. The chromatography gradient was achieved by increasing the percentage of buffer B from 0 to 35% at a flow rate of 0.30 µl/min over 45 minutes. Solvent A: 0.1% formic acid in water, and B: 0.1% formic acid in 95% acetonitrile. The QqQ settings were as follows: collision gas pressure of 1.5 mTorr; Q1 peak width of 0.7 (FWHM); cycle time of 2 s; skimmer offset of 10 V; electrospray voltage of 2.5 kV. Targeted analysis of unmodified and various modified histone peptides was performed. This entire process was repeated three separate times for each sample. The data was quantified using Skyline [35] and represents the percent of each modification within the total pool of that tryptic peptide.

- *Rapid-immunoprecipitation-mass-spectrometry-of-endogenous-protein (RIME)*

Two biological replicates of GSCs (5 x 10^8 cells per replicate) were fixed for 8 minutes with a formaldehyde solution of 11% Methanol Free Formaldehyde, 0.1M NaCl (Invitrogen™), 1 mM EDTA, pH 8 (Invitrogen™), and 50mM HEPES, pH 7.9 (Fisher BioReagents™). Fixation was stopped using 2.5 M Glycine solution in water (Sigma). Fixed cells were washed with chilled PBS-Igepal (0.5% Igepal CA-630 in PBS) and PMSF (Active Motif). Washed cells were centrifuged, pelleted, and snap-frozen on dry ice and sent to Active Motif for RIME® service [36]. PEAKS

Studio was used for visualization and analysis, and the "Decoy Fused Method" was applied for calculating FDR where the default cutoff is set to -10logP > 20 to ensure high-quality peptide spectrum matches and increase confidence in the proteins list obtained.

- *Co-immunoprecipitation followed by western blot experiment.*

After the respective course of treatment, GSCs (8-10 million cells) were collected and prepared for nuclear extraction and purification using a nuclear extraction kit (Active Motif). Nuclear extracts were treated with enzymatic Shearing. Cocktail for DNA digestion to release undissociated protein complexes, including histone proteins and DNA binding proteins from the DNA. 500 µg of extracted and purified nuclear lysate was used per IP per condition after pre-clearing with normal IgG for 1 hour on a rotator at 4°C. Pre-cleared nuclear lysates were then combined with 25 µl of Protein G beads and incubated for 1 hour on a rotator at 4°C to clear away any IgG nonspecific binding. After separating the magnetic beads on a magnetic stand, the collected nuclear supernatant was then combined with the IP antibody (Table below) and incubated for 4 hours on a rotator at 4°C. The immunoprecipitated samples were then combined with 25 µl of Protein G beads and incubated for 1 hour on a rotator at 4°C. After separating the magnetic beads on a magnetic stand, the immunoprecipitated samples (now bound to the beads) were washed four times with Co-IP wash buffer (Active Motif). The washed immunoprecipitated samples bound to beads were then resuspended in 20 µl of 2X Reducing Loading Buffer (130 mM Tris pH 6.8, 4% SDS, 0.02% Bromophenol blue, 20% glycerol, 100 mM DTT) and boiled at 95C for 5 minutes. Magnetic beads were then separated from desaturated samples using a magnetic stand. All extraction and IP steps were performed in buffers supplemented with Protease and Phosphatase and Inhibitors to limit further protein modifications (expression, proteolysis,

dephosphorylation, etc.). Immunoprecipitated samples were analyzed for pulling down capacity using Western blot. Western blot was applied as described earlier in Chapter 2.

Antibody	animal	Amount of antibody used in IP	Concentration	Source
HDAC7	Rabbit	1 µg	10 µl (1 ug) in the 500 µl	Cell signaling (E7O8V)
H3.3	Rabbit	4 µg	6.55 µl (4 ug) in the 500 µl	Abcam ChIP Grade (ab176840)
Pre-clearing Normal IgG	Rabbit	1 µg or 4 µg	Same concentration as the respective IP antibody	Cell signaling (2729)

- *Histone lysates extraction and purification*

Histone acid precipitation technique was used to extract pure crude histones from GSCs following the respective treatment needed in any experiment. After the course of treatment, GSCs were detached using the detaching enzyme StemPro Accutase (Gibco) and spun-down pellets were collected. Pellets were then resuspended in the appropriate volume of ice-cold histone extraction buffer and incubated overnight at 4°C on a rotator. On the next day, cell suspensions were centrifuged to collect core histone extracts. Acid extractions were pH measured and neutralized with the needed volume of 5X neutralization buffer until it reached complete neutralization. Core histones were then purified with column elution, and purified histone lysates were stored at -80°C for downstream experiments.

- *Histone lysate western blot*

Purified histone lysates were boiled at 95°C for 5 minutes, and 5 ug of pure histones from compared samples were electrophoresed through NuPAGE™ 16 %, Tris-Glycine, 1.5, Mini

Protein Gels. The gels were then transferred to nitrocellulose membranes, followed by blocking with 5% BSA in 1x TBST. Primary antibodies (reported in Chapter 2) in 5% BSA were incubated with the membrane at 4°C overnight.

- *Histone H3 methylated Lys27 and Histone H3 methylated Lys27 ELISA*

Purified core histone extracts prepared as described above were quantified for histone lysine trimethylation at lysine 9 and lysine 27 using ELISA kits from Active motif (Catalogue # 53109 and 53106, respectively). Briefly, 500 ng of pure histones from each sample was added to a histone H3 antibody-coated plate and incubated for 1 hour at room temperature with agitation on an orbital shaker. The 96 well plates were set up in a way that, in addition to the wells having the samples replicates; the standard curve was obtained from a serial dilution of the positive controls: recombinant histone H3 trimethyl Lys27 and recombinant histone H3 trimethyl Lys9, for the two assays H3K9me3 and H3K27me3, respectively. The H3 antibody-coated plates with the samples and standards were washed three times, after which diluted 1:1000 of each of H3K9me3 and H3K27me3 primary antibodies were added to the respective assays having samples and standards and incubated for 1 hour at room temperature with agitation on an orbital shaker. Secondary HRP-conjugated anti-rabbit IgG antibody 1:1000 was then mixed thoroughly in each assay and incubated for 1 hour at room temperature. Plates were washed five times, and then 100 µl of room temperature Developing Solution was added and incubated away from light; after exactly 2.5 minutes, 100 µl of Stop solution was added to stop the reactions. Absorbance at 450nm with a reference wavelength of 655 nm was read on Promega™ GloMax® Plate Reader. Absorbance was normalized after subtracting blank wells. The quantification for the amount of methyl Lys9 and methyl Lys2 from histone H3 in the samples in both assays was obtained using a standard curve plotted in GraphPad prism.

- *Immunofluorescence*

Primary glioblastoma stem cells were seeded in complete media without heparin on cell-culture treated chamber slides (Ibidi) overnight and transfected after 24 hours with x2 lipid (Mirus Bio) and either 25 nM control (Horizon) or HDAC7 (Horizon) siRNA. All immunofluorescence staining was performed 48 hours post-transfection. For H3.3, cells were fixed/permeabilized with 100% ice-cold methanol for 5 min and incubated in blocking buffer (1% BSA, 10% donkey serum, 22.52 mg/mL glycine in PBST (PBS+ 0.1% Tween 20)) for 1 hour at room temperature. Primary antibody (Abcam) was applied 1:1000 in primary antibody buffer (1% BSA in PBST) overnight at 4^{o}C. Cells were washed with DPBS and incubated with secondary antibody (Jackson) 1:100 in DPBS for 1 hour and mounted with DAPI (Vector Labs). For H3k9me3, cells were fixed with 4% paraformaldehyde (methanol-free) for 10 min, and permeabilized with .1% Triton in DPBS for 5 min. Blocking, primary antibody (Active Motif), secondary antibody, and mounting was applied as described above. Images were taken using a Zeiss Axiovert Inverted Microscope with Apotome II.

- *Electron microscopy (TEM)*

Treated GSCs were harvested as usual, and pellets were resuspended in a 5 ml volume of fixative master mix of Paraformaldehyde-Glutaraldehyde Solution Karnovsky's Fixative (Electron Microscopy Sciences (Catalogue # 15720, Mixture 2). Fixative solution was prepared with 16% paraformaldehyde solution, 5% Glutaraldehyde EM Grade, and 0.2 M Sodium phosphate buffer. Fixed samples were outsourced to Charles River laboratories for EM imaging service (Frederick PAI Project No. 20354508). Each sample was examined on a transmission electron microscope (TEM), and up to 10 representative digital images per sample were taken with an AMT camera.

- *Quantification and Statistical analysis*

For Mod Spec, raw MS files were imported and analyzed in Skyline with Savitzky-Golay smoothing [35]. All Skyline peak area assignments for monitored peptide transitions were manually confirmed. Multiple peptide transitions were quantified for each modification. For each monitored amino acid residue, each modified (and unmodified) form was quantified by first calculating the sum of peak areas of corresponding peptide transitions; the sum of all modified forms was then calculated for each amino acid to represent the total pool of modifications for that residue. Finally, each modification is then represented as a percentage of the total pool of modifications. This process was carried out for each of the three separate mass spec runs (technical replicates), and the raw data was estimated as the mean ± standard deviation of the resulting three values from this analysis for each modified and unmodified form of the corresponding amino acid residue.

For RIME, PEAKS Studio was used, and the "Decoy Fused Method" was applied for calculating FDR, with the default cutoff set to -10logP > 20 to ensure high-quality peptide spectrum matches and increase confidence in the proteins list obtained.

For the Differential expression analysis, the cutoffs used were adjusted P-value = 0.05 and Log2FC = 0.5

To determine the significance among the means of two independent groups, we perform an unpaired two-tailed t-test. To verify the Gaussian distribution of data before applying the t-test, we perform the D'Agostino and Pearson and Shapiro-Wilk normality tests.
To calculate the sample size, we assume the following:

Input: Tails= two**,** Effect size Delta= 2.5**,** α error probe= 0.05**,** Power (1-β err probe) = 0.90**,** Allocation ration N2/N1= 1

Output: Noncentrality parameter δ= 3.9528471**,** Critical t= 2.3**,** Df=8

Actual Power= 0.9

Significance is stated as follows: (ns), $p < 0.05$ (*), $p < 0.01$ (**), $p < 0.001$ (***), $p < 0.0001$ (****).

R scripts, packages, and related genome-wide tools used in the data analysis are available and were deposited at the GEO.

IV. Results

HDAC7 is highly expressed in glioblastoma tumors and correlates with decreased patient survival.

Using data from The Cancer Genome Atlas (TCGA), we compared the expression of all Class IIa HDACs in glioblastoma. HDAC7 is the only Class IIa HDAC with significantly higher expression in glioblastoma as compared to the non-tumor samples (**Figure 4.1A**). Also, to show a clinical correlation of HDAC7 expression in glioblastoma, we performed survival analysis on Class IIa high- and low-expressing patients. Patients were divided into these two groups based on the maximally ranked statistics using the log-rank test as well as the Gehan-Breslow-Wilcoxon method. High HDAC7-expressing patients show a significantly lower probability of survival ($p<0.004$) (**Figure 4.1B**), while the expression level of other members of Class IIa HDACs has no correlation to patient survival.

In collaboration with the Pathology Department at Rhode Island Hospital, we collected 84 PFF tumor samples from patients with a confirmed diagnosis of IDH WT Glioblastoma. We performed Nanostring gene expression analysis using the Pan-Cancer Panel, which contains 770 genes with confirmed roles in cancer. The expression data were clustered based on high versus low expression of HDACs. Classification of gene expression in HDAC7 "high" versus HDAC7 "low" expressing patients showed that high HDAC7 expression correlates with a significant increase in the expression of 45 genes and inhibition of 2 genes (**Figure 4.1C**). Functional classification of the significantly increased genes shows that they have significant pro-tumorigenic roles like Vimentin, Lox, SERPINH1, TGFb, etc. (**Figure 4.1D**). Then we performed Kaplan Meier survival analysis on the 84 patients based on high (n=37) or low expression (n=47) of

HDAC7 and showed that patients with high HDAC7 expression had significantly lower disease-free survival (Wilcoxon p<0.005) (**Figure 4.1E**).

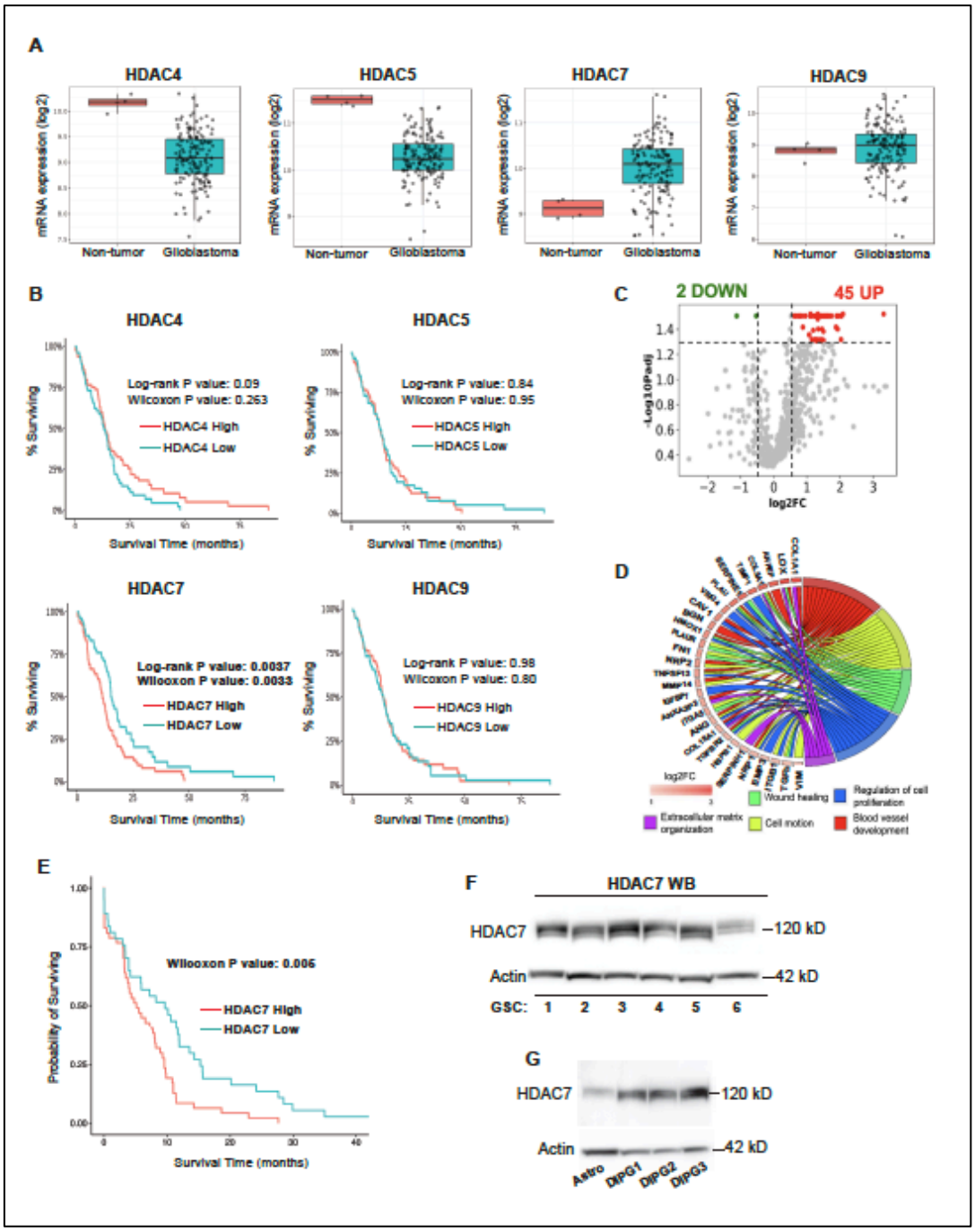

Figure (4.1) HDAC7 is highly expressed in glioblastoma tissue, GSCs, and DIPG cells and correlates with a significant decrease in patient survival. ***A)*** *Transcript expression of Class IIa HDACs in glioblastoma compared to non-tumor control tissue using TCGA data. HDAC7 is the only Class IIa HDAC that is expressed significantly higher*

in glioblastoma compared to control tissue. ***B)*** *Kaplan Meier survival analysis from the TCGA data, shows that high expression of HDAC7 is significantly (p<0.003) correlated with decreased patient survival.).* ***C)*** *Clustering of transcript expression in 84 tissue samples from glioblastoma patients based on high versus low expression of HDAC7 reveals high expression of 45 transcripts (log2FC>0.5) in patient tumors that express high HDAC7.* ***D)*** *Functional classification of the significantly increased genes shows that they have significant pro-tumorigenic roles like Vimentin, Lox, SERPINH1, and TGFb.* ***E)*** *Functional classification of the significantly increased genes shows that they have significant pro-tumorigenic roles like Vimentin, Lox, SERPINH1, and TGFb. E) Kaplan Meier survival analysis in 84 patients with glioblastoma from Rhode.* ***F)*** *Expression of HDAC7 in 6 patients derived GSCs as detected by Western blot.* ***G)*** *Expression of HDAC7 in 3 patients derived from pediatric DIPG cells compared to normal human astrocytes*.

Expression of HDAC7 in cancer cells.

To determine the expression levels of HDAC7 in various human cancer cells, we performed Western blotting on lysates from six patients' derived GSCs with IDH WT glioblastoma and 4 pediatric primary DIPG cells and compared their expression to that of control human astrocytes. We show that HDAC7 is highly expressed in GSCs and DIPG cells while minimally expressed in control human astrocyte lysates (**Figure 4.1F-G**).

The presence of nuclear localization and nuclear export signals makes HDAC7 capable of nuclear and cytoplasmic expression, depending on the cell type [37, 38]. To determine the topology of HDAC7 expression in patients-derived GSCs, we performed immunofluorescent staining of HDAC7 expression (red) and Vimentin (green) as cytoplasmic markers. Nuclei were visualized with DAPI (blue) and z-stack images were acquired with a Zeiss Axiovert inverted microscope equipped with Apotome II. We show that HDAC7 is highly expressed in the nucleus of GSCs with minimal expression in the cytoplasm (**Figure 4.2A**).

Class specificity of HDAC7 siRNA.

To determine the target specificity of the HDAC7 siRNA, we designed, filtered through BLAST similarity search, and finally synthesized 4 individual siRNAs that target the open reading frame and 3'- untranslated region of human HDAC7. 50nM of each siRNA was separately

transfected into patients-derived GSCs, and the expression of Class IIa HDACs was determined by Western blotting 72 hours after transfection. Control cells were transfected with non-targeting siRNA and Actin was used as loading control. The selected siRNA shows specific inhibition of HDAC7 protein expression and does not affect the expression of HDAC4, HDAC5, and HDAC9 (**Figure 4.2B**).

MS profiling of histone marks following inhibition of HDAC7 expression.

To determine if HDAC7 has any effect on levels of histone modifications, we performed histone modification Mass Spectrometry (ModSpec-Active Motif) after inhibition of HDAC7 expression with our specific siRNA. Individual histone modifications were quantified by ModSpec and expressed as a proportion of all modified and unmodified residues (% of the peptide pool). At baseline (siControl GSCs), we found histones H3 and H4 to be highly modified. In contrast, H1 and H2 showed minor to no modifications (**Figure 4.2C**). The most modified histone sites were H3K9, H3.1K27, H3.3K27, and H4K20. On aggregate, dimethylation of histone marks shows the highest abundance in comparison to other modifications in GSCs. To determine significant changes in levels of histone modifications following inhibition of HDAC7, we used a cut-off of 3% change and a $P<0.05$. Differences in the total enrichment of all marks (as a proportion of all modified and unmodified peptides) at each of the different histone sites are shown in (**Figure 4.2D**). We show that inhibition of HDAC7 expression does not affect levels of histone acetylation, suggesting minimal histone deacetylase activity, but induces a significant increase in H3K9me1 and reduction at levels of unmodified H3K9UN, which implies major chromatin landscape restructuring and increase of heterochromatin. In addition, we detect a significant increase in H3.3K27me1 and H3.1K27me1, which is a mark that has been associated mainly with heterochromatin [39, 40] but also with active transcription in embryonic stem cells [41].

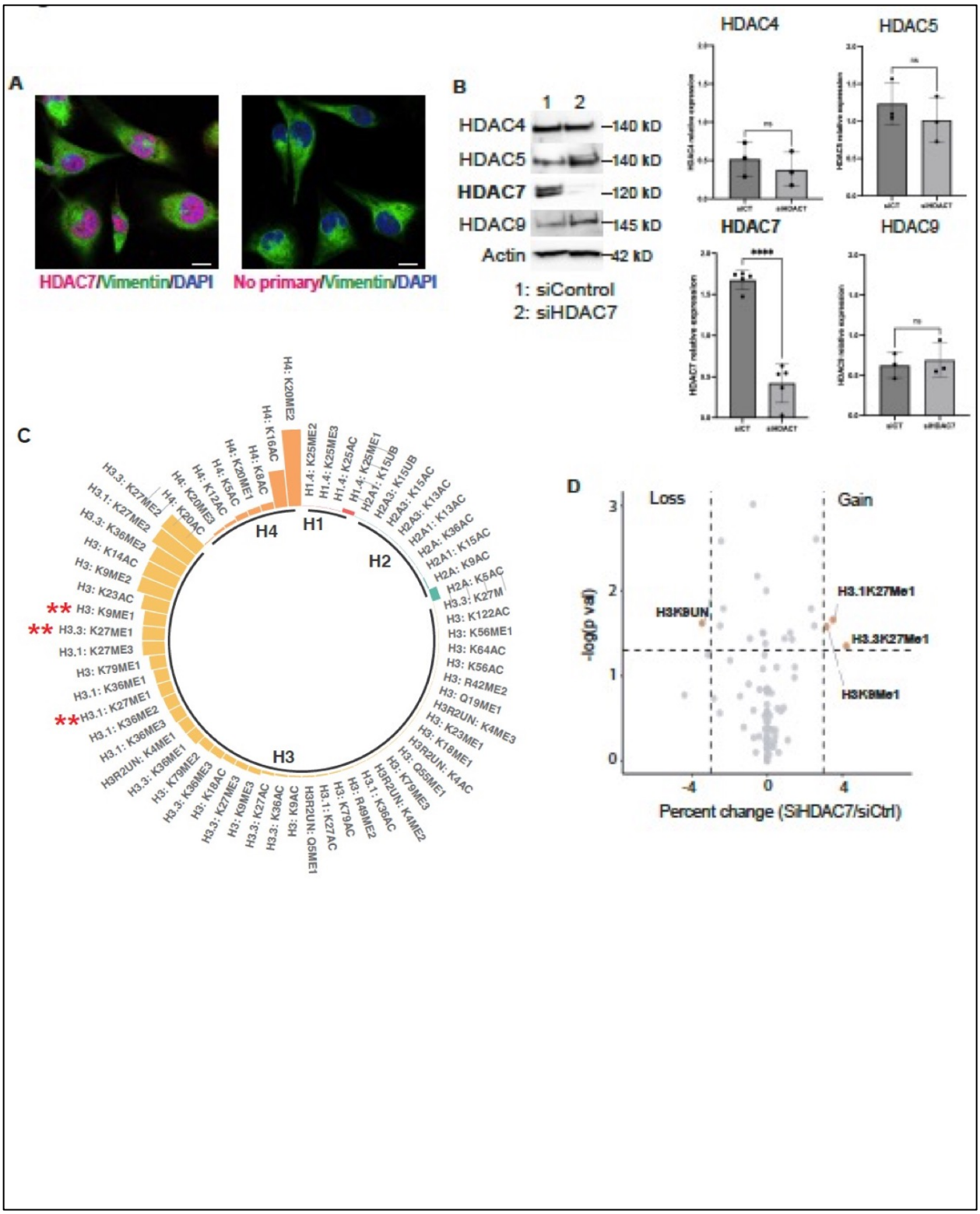
A
HDAC7/Vimentin/DAPI
No primary/Vimentin/DAPI
B
1 2
HDAC4 —140 kD
HDAC5 —140 kD
HDAC7 —120 kD
HDAC9 —145 kD
Actin —42 kD
1: siControl
2: siHDAC7
HDAC4
HDAC5
HDAC7
HDAC9
C
H1
H2
H3
H4
D
Loss
Gain
H3K8UN
H3.1K27Me1
H3.3K27Me1
H3K8Me1
-log(p val)
Percent change (SiHDAC7/siCtrl)

Figure (4.2) HDAC7 specific knock-down does not alter histone acetylation status but increases heterochromatin marks in GSCs. ***A)*** *Nuclear expression of HDAC7 in patient-derived GSCs stained with an HDAC7 antibody (magenta) and vimentin (green) as a cytoplasmic marker. No primary antibody control shows a lack of non-specific staining.* ***B)*** *Class specificity of the HDAC7 in vivo stable siRNA. siHDAC7 induces significant knockdown of HDAC7 protein expression ($p<0.0001$, $n=5$) whole does not affect the expression of the other members of the Class IIa HDAC family ($n=3$, n.s.).* ***C)*** *Circular plot shows percent abundance of histone modifications in GSCs. Asterisks are used to indicate histone sites undergoing significant alterations following HDAC7 knockdown.* ***D)*** *Volcano plot of differentially modified histone marks in control versus siHDAC7 samples (cut-off of 3% change and $P<0.05$. Multiple peptide transitions were quantified for peptide transitions*[42]*; the sum of all modified forms was then calculated for each amino acid to represent the total pool of modifications for that residue. Finally, each modification is then represented as a percentage of the total pool of modifications. This process was carried out for each of the three separate mass spec runs, and the results correspond to the mean and standard deviation of the resulting three values from this analysis.*

Rapid Immunoprecipitation Mass Spectrometry of Endogenous Proteins (RIME) to identify the HDAC7 interactome on chromatin.

To determine how inhibition of HDAC7 results in an increase of heterochromatin marks, we hypothesized that HDAC7 forms multiprotein interactions on euchromatin to participate in the regulation of active transcription. We employed Rapid Immunoprecipitation Mass Spectrometry of Endogenous Proteins (RIME) to discover the HDAC7 protein-protein interaction network on the chromatin of GSCs. GSCs (n=3) were fixed with formaldehyde to crosslink proteins and DNA that are in very close proximity, nuclei were isolated, and HDAC7 immunoprecipitation was performed. The HDAC7 precipitated protein complex was subjected to Mass Spectrometry (RIME) which revealed 247 proteins constituting the HDAC7 interactome. The proteins were entered into STRING for network analysis using default settings and exported into Cytoscape for network construction. 229 from the 247 proteins formed a highly interconnected network **(Figure 4.3A**). To focus the analysis, we extracted the HDAC7 1st degree interactome (**Figure 4.3B**). This refers to the complete set of nodes and edges of proteins directly linked to HDAC7 (**Figure 4.3B**). There were 10 proteins/genes directly connected with HDAC7, these were NCOR2, H3.3, H3.4, H3C13, H3C12, CTNNB1, CHD4, TBLX1XR1 and HSPA4. The nodes in the resulting network

were highly interconnected (PPI p val = 5.28E-18). The HDAC7 1st degree interactome/network was enriched for transcription regulation pathways, notch signaling, chromatin modeling, and Beta-catenin signaling (**Figure 4.3B**). Next, we extended the analysis to include nodes connecting directly to the HDAC7 1st degree interactome, thus generating the 1st and 2nd degree interactome (**Figure 4.3C**). The 1st and 2nd degree interactome was composed of 84 nodes that were significantly enriched for mitotic activity and cell cycle pathways (**Figure 4.3C**).

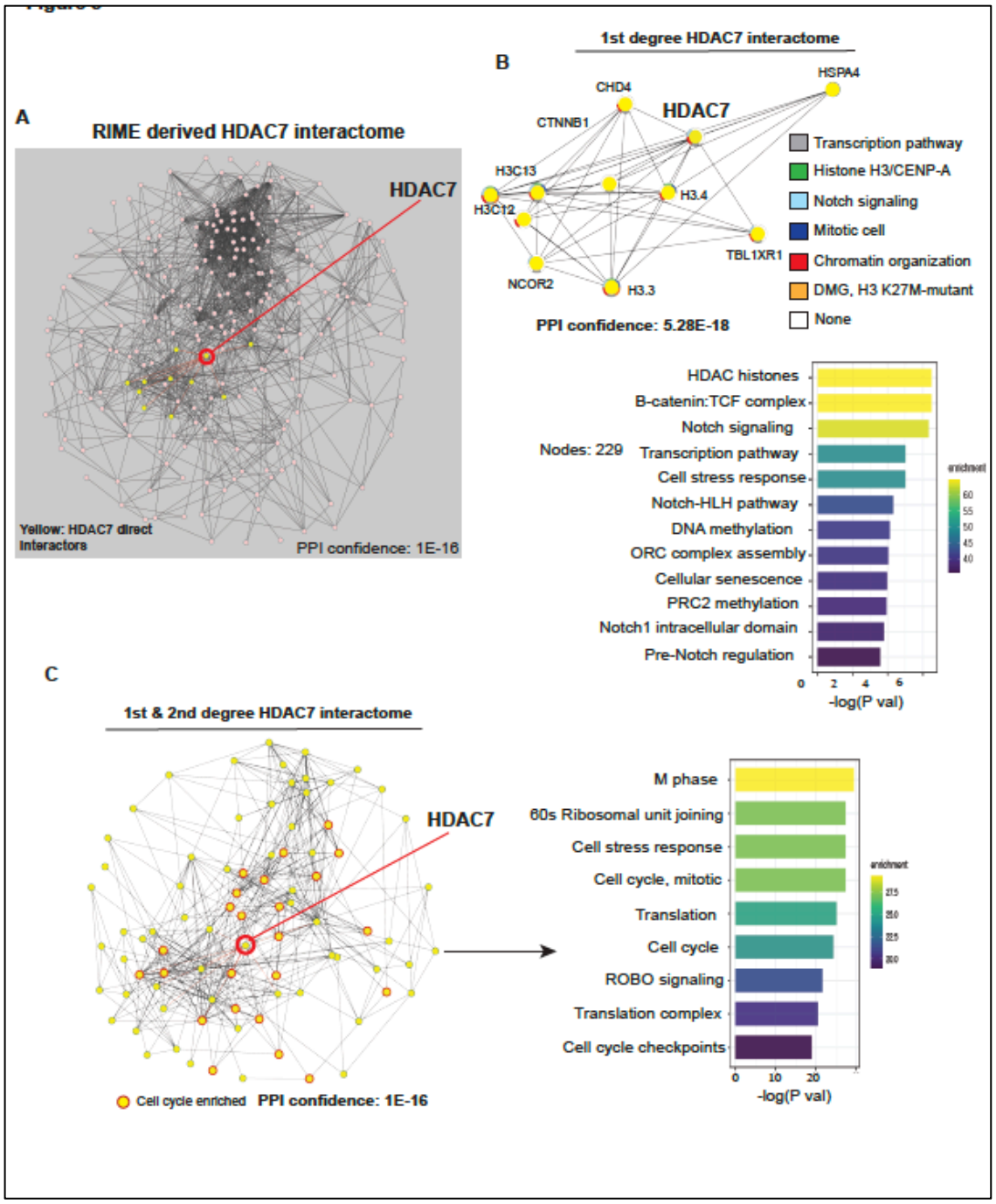

Figure (4.3) HDAC7 interactome on chromatin of patient-derived GSCs. ***A)*** *Network of HDAC7 interactome: the proteins directly interacting with HDAC7 (1E-16) derived from RIME-identified proteins interacting with HDAC7. Each protein/gene is color-coded based on functional enrichment. A corresponding enrichment analysis is shown. HDAC7 is shown near the center of the network.* ***B)*** *1st-degree interactome: the proteins directly interacting with HDAC7(5.2E-18). Each protein/gene is color-coded based on functional enrichment. A corresponding enrichment analysis is shown.* ***C)*** *Heatmap representation for the protein interactors with HDAC7 from nuclear lysates of GSCs. Representative example of 3 independent experiments.*

HDAC7 interacts with Histone H3.3 and the H3.3 mutant variant H3K27M.

To validate the interaction between HDAC7 and H3.3, we performed co-immunoprecipitation (co-IP) experiments using protein lysates from patients-derived GSCs (n=3). Immunoprecipitation was performed with an HDAC7-validated antibody (Abcam), and the presence of H3.3 was detected with an H3.3 specific antibody (Active Motif). We show that HDAC7 co-precipitates with H3.3 (**Figure 4.4A**), validating the RIME interactome results. Since the H3.3 mutant variant H3K27M has been implicated in pediatric brain tumors, we performed co-IPs using lysates from patient-derived pediatric diffuse pontine glioma (DIPG) cells (kind gift of Dr. Michelle Monje) and showed that HDAC7 interacts and co-precipitates with H3K27M (**Figure 4.4B**) suggesting a role for HDAC7 in these pediatric tumors.

Inhibition of HDAC7 reduces the interaction of H3.3 with HIRA and increases interaction with DAXX and H3K9me3.

To determine how HDAC7 affects the H3.3 landscape in cancer cells, we inhibited the expression of HDAC7 with siHDAC7 and determined the effects of HDAC7 inhibition on the interaction of H3.3 with its euchromatin chaperone HIRA, or its heterochromatin chaperone DAXX/ATRX. We show that inhibition of HDAC7 results in a reduction of the interaction of H3.3 with HIRA in GSCs, an increase of the interaction of H3.3 with the heterochromatin chaperone DAXX (**Figure 4.4C**), and a significant increase in total levels of DAXX (**Figure 4.4D**). These results suggest that inhibition of HDAC7 expression results in rebalancing of the H3.3 landscape and reduction of H3.3 association with euchromatin chaperones and increased association of H3.3 with heterochromatin. To verify that inhibition of HDAC7 results in an increased association of H3.3 with heterochromatin, we performed co-IP of H3.3 with H3K9me3. This shows that

following inhibition of HDAC7 expression, the interaction of H3.3 with heterochromatin mark H3K9me3 is increased significantly (**Figure 4.4E**).

HDAC7 inhibition results in increased levels of SETDB1, EZH2, H3K9me3, and H3K27me3.

Since inhibition of HDAC7 results in increased association of H3.3. with heterochromatin, we examined if siHDAC7 induces a global increase of heterochromatin marks in cancer cells. We performed Western blot detection of H3K9me3 and H3K27me3 in patients derived GSCs (n=3) and showed a significant increase of both H3K9me3 and H3K27me3 (**Figure 4.4F**). In addition, protein levels of SETDB1 and EZH2, the histone methyltransferases that mediate the trimethylation of H3K9 and H3K27, respectively, were both significantly elevated following inhibition of HDAC7 (**Figure 4.4F**). To verify these results, we performed quantitative ELISA (Active Motif) to detect levels of H3K9me3 and H3K27me3 in 5 patient-derived GSCs. The results show a significant increase in both heterochromatin marks following the inhibition of HDAC7 (**Figure 4.4G**).

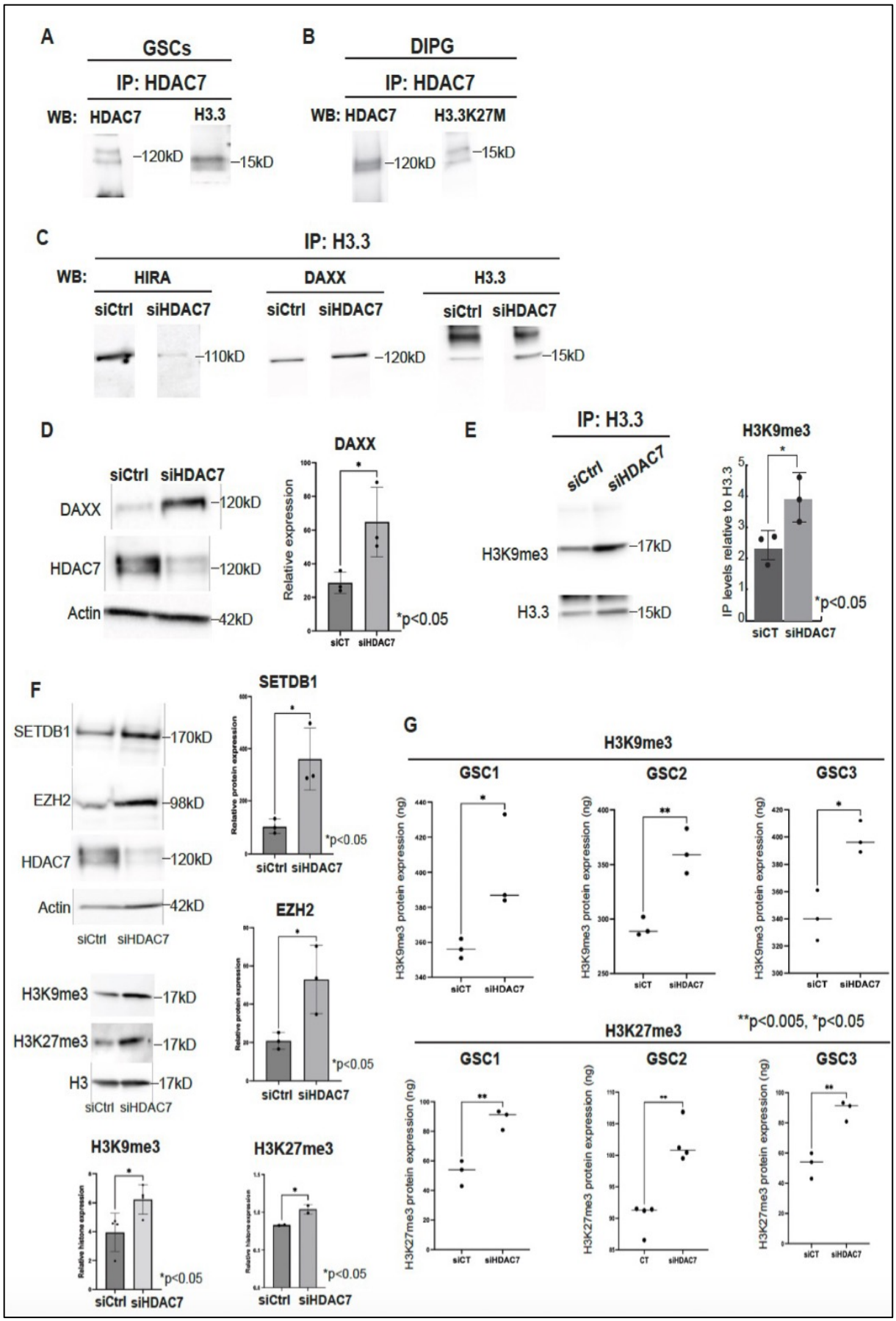
A
GSCs
IP: HDAC7
WB: HDAC7
H3.3
~120kD
~15kD
B
DIPG
IP: HDAC7
WB: HDAC7
H3.3K27M
~120kD
~15kD
C
IP: H3.3
WB:
HIRA
DAXX
H3.3
siCtrl siHDAC7
~110kD
~120kD
~15kD
D
siCtrl siHDAC7
DAXX
HDAC7
Actin
~120kD
~120kD
~42kD
DAXX
Relative expression
*p<0.05
siCT siHDAC7
E
IP: H3.3
siCtrl siHDAC7
H3K9me3
H3.3
~17kD
~15kD
H3K9me3
IP levels relative to H3.3
*p<0.05
siCT siHDAC7
F
SETDB1
EZH2
HDAC7
Actin
~170kD
~98kD
~120kD
~42kD
siCtrl siHDAC7
H3K9me3
H3K27me3
H3
~17kD
~17kD
~17kD
siCtrl siHDAC7
SETDB1
Relative protein expression
*p<0.05
siCtrl siHDAC7
EZH2
Relative protein expression
*p<0.05
siCtrl siHDAC7
H3K9me3
Relative histone expression
*p<0.05
siCtrl siHDAC7
H3K27me3
Relative histone expression
*p<0.05
siCtrl siHDAC7
G
H3K9me3
GSC1
GSC2
GSC3
H3K9me3 protein expression (ng)
siCT siHDAC7
**p<0.005, *p<0.05
H3K27me3
GSC1
GSC2
GSC3
H3K27me3 protein expression (ng)
siCT siHDAC7
CT siHDAC7

Figure (4.4) HDAC7 interacts with H3.3 and HIRA, and inhibition of HDAC7 increases DAXX and deposits H3.3 on H3K9me3 and H3K27me3 heterochromatin. ***A)*** *complexInhibition of HDAC7 results in loss of H3.3 interaction with HIRA and increase in interaction of H3.3 with DAXX. Co-immunoprecipitations were repeated 3 independent times.* ***D)*** *Inhibition of HDAc7 results in a significant increase of DAXX in the nucleus of GSCs ($p<0.05$, n=3).* ***E)*** *HDAC7 knockdown results in a significant increase in the direct association of histone H3.3 with the heterochromatin mark H3K9me3 ($p<0.05$, n=3). F) Inhibition of HDAC7 expression in GSCs results in a significant increase in levels of SETDB1, EZH2, H3K9me3, and H3K27me3 ($p<0.05$, n=3, n=4). HDAC7 knockdown results in a significant increase in the direct association of histone H3.3 with the heterochromatin mark H3K9me3 ($p<0.05$, n=3).* ***F)*** *Inhibition of HDAC7 expression in GSCs results in a significant increase in levels of SETDB1, EZH2, H3K9me3, and H3K27me3 ($p<0.05$, n=3, n=4).* ***G)*** *H3K9me3 and H3K27me3 ELISA on nuclear lysates from three independent patients derived GSCs shows a significant increase of both heterochromatin marks (*$p<0.05$, **$p<0.01$, n=3, n=4).*

Inhibition of HDAC7 induces heterochromatin spreading in cancer cells.

To visualize and quantify the increased association of H3.3 with heterochromatin and the global increase of heterochromatin marks in cancer cell nuclei, we performed immunofluorescence localization of H3.3 and H3K9me3 with and without inhibition of HDAC7 with siRNAs. Quantification of the number of H3.3 containing heterochromatin foci per nucleus from 30 individual cell nuclei shows that siHDAC7 induces a significant increase in the localization of H3.3 within heterochromatin foci (**Figure 4.5A-B**). In addition, siHDAC7 induces a significant increase in H3K9me3 expression in the nucleus of cancer cells (**Figure 4.5C-D**). To better visualize the spreading of heterochromatin within the cancer cell nucleus, we performed transmission electron microscopy (TEM) on patient-derived GSC nuclei before and after inhibition of HDAC7 with siRNAs. We show that inhibition of HDAC7 results in the spreading of electron-dense pericentric heterochromatin and an increase of heterochromatin chromobodies (**Figure 4.5F**, arrows).

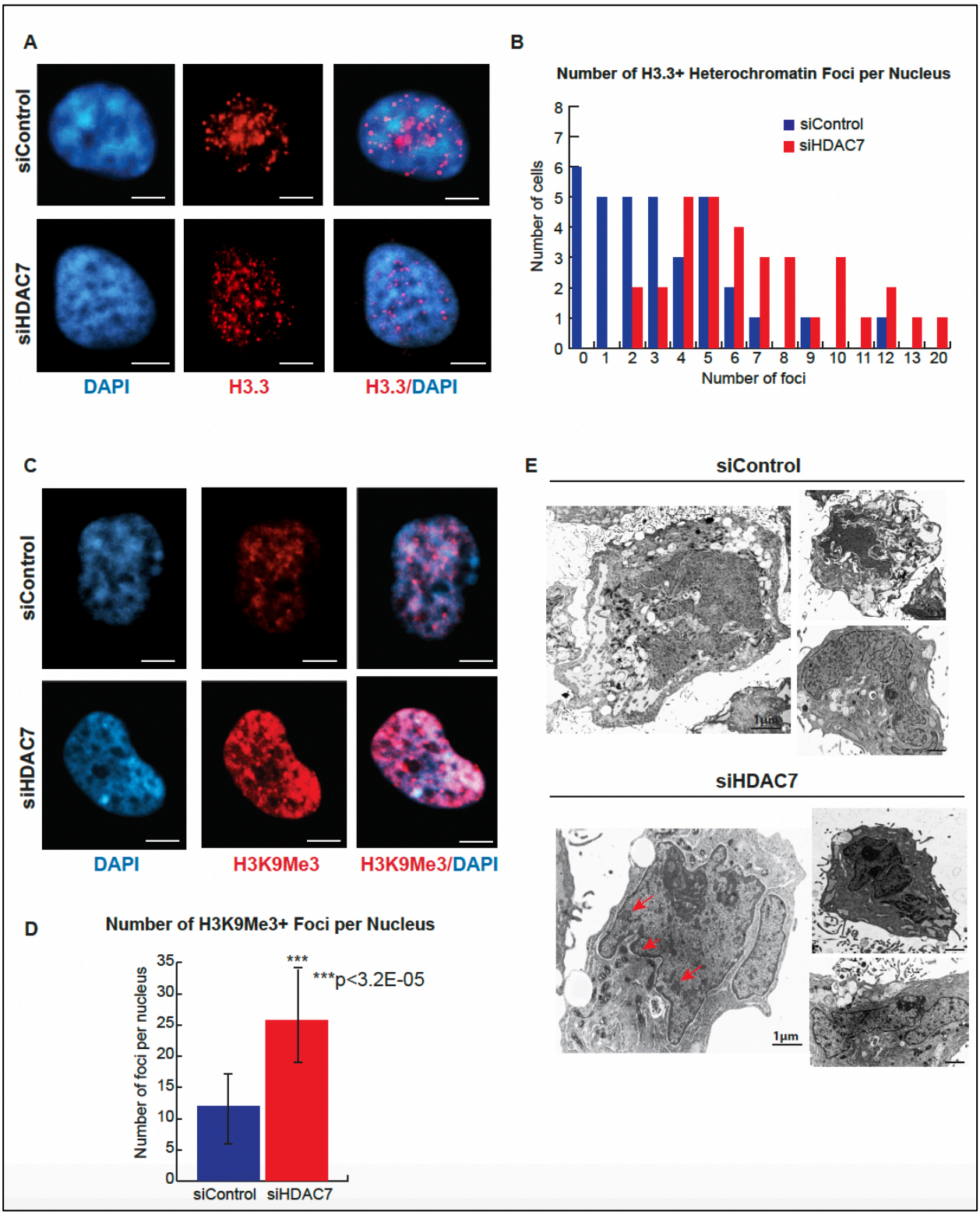
A
siControl
siHDAC7
DAPI
H3.3
H3.3/DAPI
B
Number of H3.3+ Heterochromatin Foci per Nucleus
siControl
siHDAC7
Number of cells
Number of foci
C
siControl
siHDAC7
DAPI
H3K9Me3
H3K9Me3/DAPI
D
Number of H3K9Me3+ Foci per Nucleus
***p<3.2E-05
Number of foci per nucleus
siControl
siHDAC7
E
siControl
siHDAC7
1µm

Figure (4.5) Inhibition of HDAC7 results in H3.3 landscape rebalancing and heterochromatin spreading in cancer cells. ***A)*** *Immunofluorescence staining of H3.3 (red) and DAPI (blue) in GSCs before and after knock-down of HDAC7 shows that inhibition of HDAC7 expression results in redistribution of H3.3 from DAPI(-) euchromatin nuclear domains to DAPI(+) heterochromatin foci.* ***B)*** *Quantification of the number of H3.3+ heterochromatin foci per nucleus from 30 GSC nuclei per condition (siControl vs siHDAC7). There is a significant increase in the average number of H3.3+ heterochromatin foci following HDAC7 inhibition. Control average number of H3.3+ foci: 3.14 +/- 2.5, siHDAC7 average number of H3.3+ heterochromatin foci: 7 +/- 3.5. P<1.3E-05.* ***C)*** *Immunofluorescence staining of H3K9me3 (red) and DAPI (blue) in GSCs before and after the knock-down of HDAC7 shows that inhibition of HDAC7 expression results in an increase of the heterochromatin mark in the nucleus of GSCs.* ***D)*** *Quantification of the number of H3K9me3+ foci in the nucleus of 20 GSCs with and without inhibition of HDAC7 shows a significant increase in the number of H3K9me3+ foci following inhibition of HDAC7 (p<3.2E-05).* ***E)*** *Transmission electron microscopy of patient-derived GSCs before (siControl) and after (siHDAC7) inhibition of HDAC7 expression shows the spreading of electron-dense heterochromatin in pericentric nuclear domains (arrowhead) and nuclear chromobodies (arrows).*

Inhibition of HDAC7 results in broad transcriptomic changes in cancer cells and inhibition of GSC self-renewal.

To assess the effect of HDAC7 inhibition at the transcript expression level, we performed RNA-seq with and without inhibition of HDAC7 expression in GSCs (n=2). PCA demonstrated appropriate segregation across conditions, suggesting that the siRNA targeting of HDAC7 induced reproducible changes across patients (**Figure 4.6A**). We identified 194 downregulated and 432 upregulated genes (adj. p val < 0.001, FC>2) (**Figure 4.6B**). A downregulated set of genes showed significant enrichment for cell cycle, chromosomal organization/segregation, and DNA damage/ replication (**Figure 4.6E**). There was a notable decrease in major regulators of cell cycling (CDC6, E2F1, E4F1), genome stability (H2AX, MCM3/5/7), and replication fork progression (ORC1) (**Figure 4.6D**), as well as the notable inhibition of crucial stemness marker genes (**Figure 4.6C**). To determine the functional significance of the effect of HDAC7 inhibition in transcript expression and since transcripts of major regulators of cell cycle and DNA replication were affected, we

performed tumor-sphere formation assay with and without inhibition of HDAC7 in GSCs (n=3). Tumor-sphere formation provides a direct link to cancer stem cell self-renewal and division. We show that inhibition of HDAC7 results in significant inhibition of tumor sphere formation capabilities of human GSCs ($p<0.0001$) (**Figure 4.6F**).

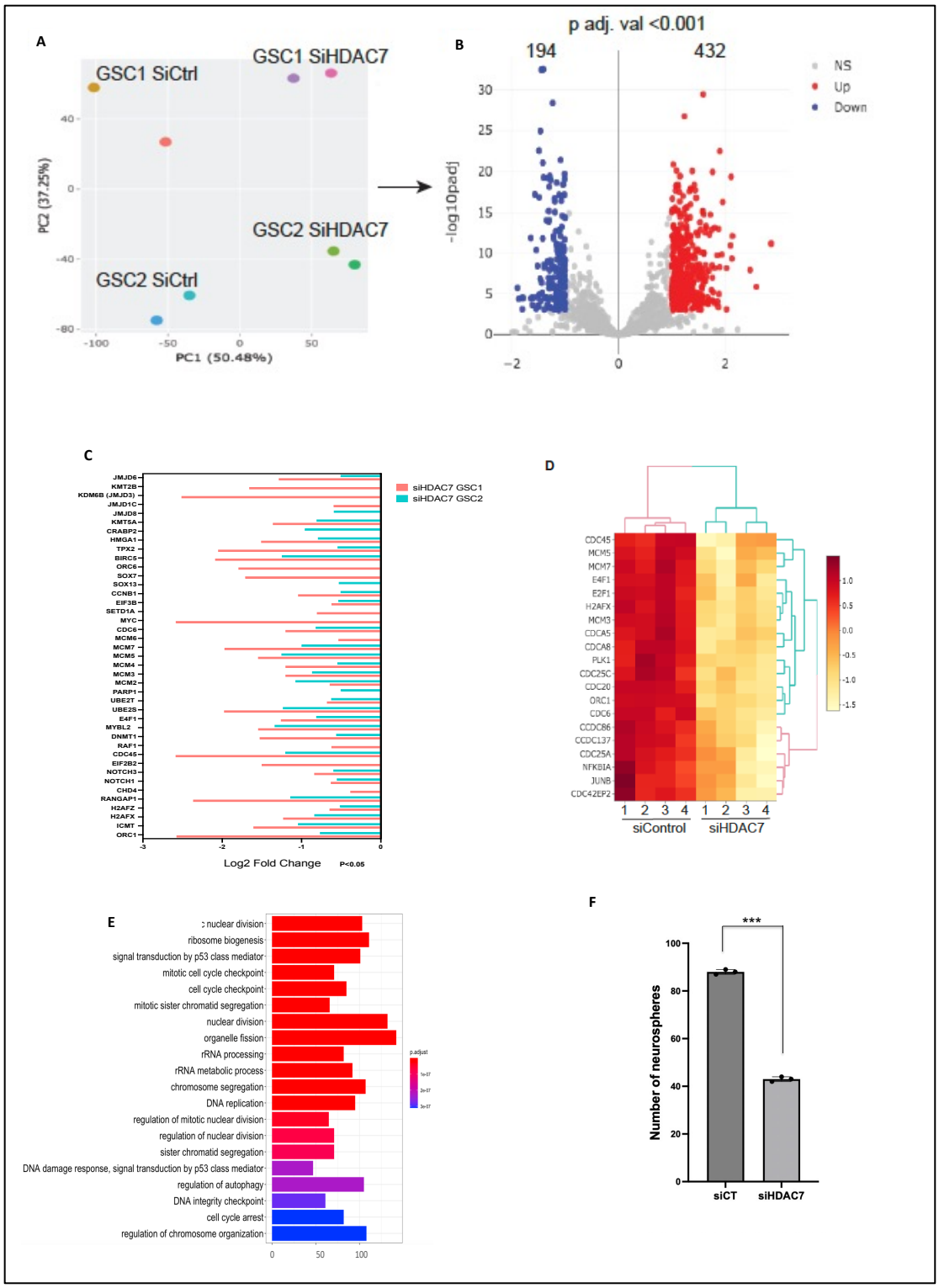

Figure (4.6) Transcript expression analysis and tumor sphere formation assay in GSCs following inhibition of HDAC7 expression. ***A)*** *PCA plot of GSCs in control versus siHDAC7 samples* ***B)*** *Volcano plot of differentially expressed genes following HDAC7 knockdown (adj. p*

val < 0.001, FC>2). ***C)*** *A graph displays the inhibition of stemness genes following HDAC7 inhibition (n=2).* ***D)*** *Heat Map representation following HDAC7 showing differential expression of major regulators of cell cycling (CDC6, E2F1, E4F1), genome stability (H2AX, MCM3/5/7), and replication fork progression (ORC1).* ***E)*** *Pathway enrichment of downregulated genes.* ***F)*** *Tumor sphere formation assay shows significant (p<0.0001) inhibition of GSC self-renewal following inhibition of HDAC7.*

IV . Discussion

Class IIa HDACs have limited catalytic activity in eukaryotic cells mainly due to a substitution of tyrosine with histidine within the enzymatic pocket of these molecules [43]. Although Class IIa HDACs can bind to acetylated lysine, they don't exert deacetylase activity, and it has been proposed that they function to attract other HDAC subtypes to deacetylate the substrates [44, 45]. Several studies have shown the role of class IIa HDACs in cancer, but the exact function of each member of the class varies depending on the type of cancer [46]. HDAC7 has been implicated in the regulation of cancer stem cell fate, specifically in breast and ovarian tumors, where it was shown that overexpression of HDAC7 can increase the cancer stem cell phenotype [47]. HDAC7 binds near transcription start sites (TSS) and super-enhancers (SEs) of oncogenes in breast cancer stem cells and contributes to their transcriptional regulation. Although it was shown that HDAC7 is required to maintain levels of H3K27Ac at TSS and SEs, how this is achieved has not been determined to date [46, 48].

Our findings provide robust evidence supporting the interaction between HDAC7 and Histone H3.3 in glioblastoma stem cells. Through RIME and co-immunoprecipitation, we demonstrated a direct physical association between these molecules. This adds to the growing body of literature elucidating the complex interplay between histone molecules and their regulatory enzymes. The interaction between HDAC7 and Histone H3.3 suggests a potential role for HDAC7 in chromatin remodeling and gene regulation.

The specific interaction with H3.3, a histone variant associated mainly with active chromatin states, underscores the importance of HDAC7 in maintaining chromatin homeostasis. Histone H3.3 is deposited into euchromatin in a DNA replication-independent manner. Specifically, H3.3

forms complexes with the histone chaperone HIRA to mediate DNA synthesis-independent nucleosome assembly [49]. We show here, that HDAC7 participates in these euchromatin complexes by interacting with H3.3 and HIRA. HDAC7 regulates the deposition of H3.3 into euchromatin, and inhibition of HDAC7 results in a reduction of the association of H3.3 with HIRA and an increased association of H3.3 with DAXX and H3K9me3. This results in remodeling of the H3.3 landscape in cancer cells resulting in heterochromatin spreading and association of H3.3 with heterochromatin foci. Our study unveils a novel aspect of HDAC7 biology in cancer. The observed increase in heterochromatin upon HDAC7 inhibition suggests a role for HDAC7 in maintaining the balance between euchromatin and heterochromatin, which is often dysregulated in cancer cells. Dysfunctional chromatin remodeling is a hallmark of cancer, and our findings shed light on the potential contribution of HDAC7 to this process.

The identification of HDAC7 as a regulator of heterochromatin dynamics provides a rationale for exploring the inhibition of HDAC7 as a potential therapeutic strategy in cancer. By promoting heterochromatin formation, HDAC7 inhibition may suppress oncogenic transcriptional programs and impede tumor progression. This is supported by our RNA-seq data showing significant inhibition of pro-tumorigenic transcription factors and transcripts that promote cancer cell division and DNA replication following loss of HDAC7. In addition, inhibition of HDAC7 results in a significant reduction of GSC self-renewal, which is a hallmark of cancer stem cell propagation and growth. Despite the significant findings presented in this study, there are certain limitations that warrant consideration. Although our siRNA is subtype-specific and does not affect the expression of other members of the Class IIa HDAC family, delivery of the siRNA in solid tumors as an effective therapeutic in human cancers is challenging. Although following the mRNA vaccines for

COVID, the use of lipid nanoparticles (LNP) for delivery of mRNA payloads has been streamlined, there is still no example of a siRNA therapeutic showing effective pharmacokinetic profile and distribution within solid tumors, suggesting that more research and development efforts need to focus on effective LNP delivery of anti-cancer siRNA therapeutics. In addition, the development of class and subtype-specific small molecule inhibitors for HDACs has also been problematic due to the sequence similarity between subtypes. These limitations are important to overcome to develop an effective anti-HDAC7 therapeutic for human use. Future investigations should aim to address these limitations and further elucidate the molecular mechanisms underlying the role of HDAC7 in chromatin dynamics and cancer pathogenesis. Additionally, exploring the crosstalk between HDAC7 and other chromatin modifiers will deepen our understanding of the regulatory networks governing chromatin organization. A specific HDAC7 interaction that requires further investigation is the reported interaction with HDAC3 [50] to determine if specific inhibition of HDAC7 results in alteration of HDAC3 functions in cancer cells.

In summary, our study identifies HDAC7 as a critical regulator of chromatin dynamics and heterochromatin formation in cancer. These findings not only expand our knowledge of HDAC biology but also highlight the therapeutic potential of targeting HDAC7 in cancer treatment. Further research in this area promises to uncover new avenues for precision medicine and improve patient outcomes in oncology.

Acknowledgments

The authors would like to thank the Department of Pathology at Rhode Island Hospital for providing the glioblastoma tissue samples. We also thank Charles River for Electron Microscopy services. This study was supported by a Warren Alpert Foundation Grant #17775 to N.T., private philanthropic donations to the Laboratory of Cancer Epigenetics and Plasticity and from internal support of the Neurosurgery Department of Brown University to N.T.

V. Supplementary Figures

Supplementary Figure 1. False discovery rate (FDR) curve. X axis is the number of peptide-spectrum matches (PSM) being kept. Y axis is the corresponding FDR

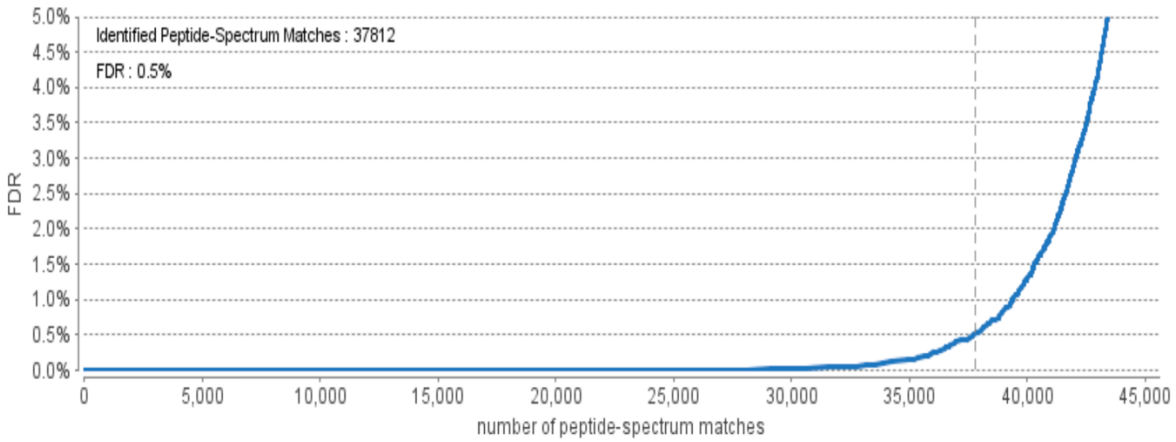

Supplementary Figure 4. PSM score distribution (a) Distribution of PEAKS peptide score; (b) Scattered plot of PEAKS peptide score versus precursor mass error. PEAKS Studio uses the "Decoy Fused Method" when calculating FDR where the default cutoff is set to -10logP > 20 to ensure high-quality peptide spectrum matches and increase confidence in the proteins list obtained. Figure 2b shows the accuracy and resolution of the instrument, as higher scoring points should be centered around a mass error of 0. Three layers of filtration were done:

- All proteins exported from the MS run are filtered to proteins with at least 2 unique peptides
- Upon filtering the experimental reaction data against the negative control IgG reaction data, a number of unique proteins were pulled down, along with HDAC7.
- Filtration removed other proteins considered as background (below the spectral count of 5).

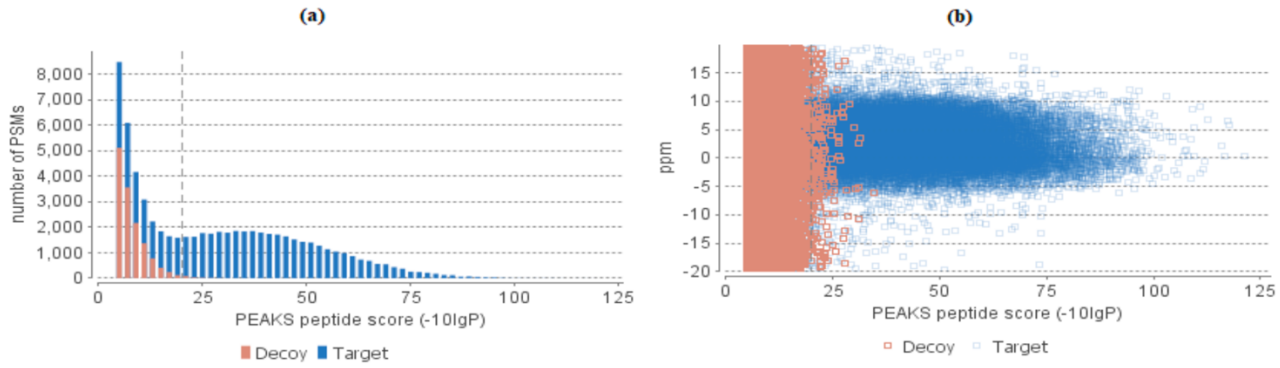

Supplementary Figure 2. Quality control assessment for the RIME experiment

Mass spectrometry of the RIME resulted in good coverage (30%-39%) of the bait protein (HDAC7) and has met the minimum requirement of 10% coverage needed for a passing experiment according to the guidelines below.

• >40% coverage =great

• 20%-39% coverage =good

• 10%-19% coverage = fair

• <10% coverage = failed.

HDAC7 coverage

Accession	Description	Coverage	#Spec	Samples
Q8WUI4	Histone deacetylase 7 OS=Homo sapiens GN=HDAC...	30%	35	1.GB2_R3
Q8WUI4	Histone deacetylase 7 OS=Homo sapiens GN=HDAC...	39%	41	1.GB2_R1

H3.3 peptide coverage from RIME

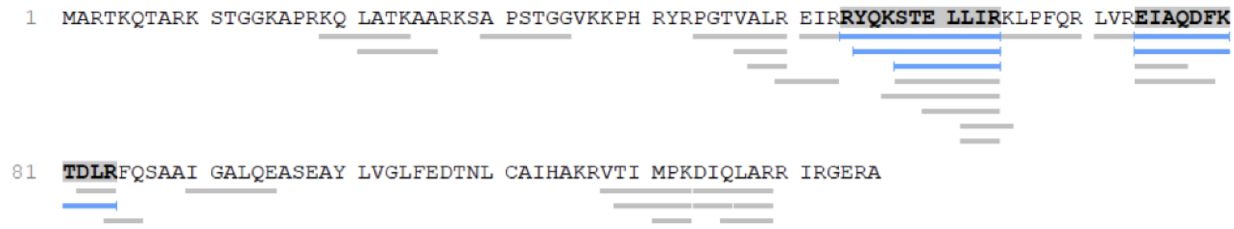

SMC4 peptide coverage from RIME

CHD4 peptide coverage from RIME

β-Catenin peptide coverage from RIME

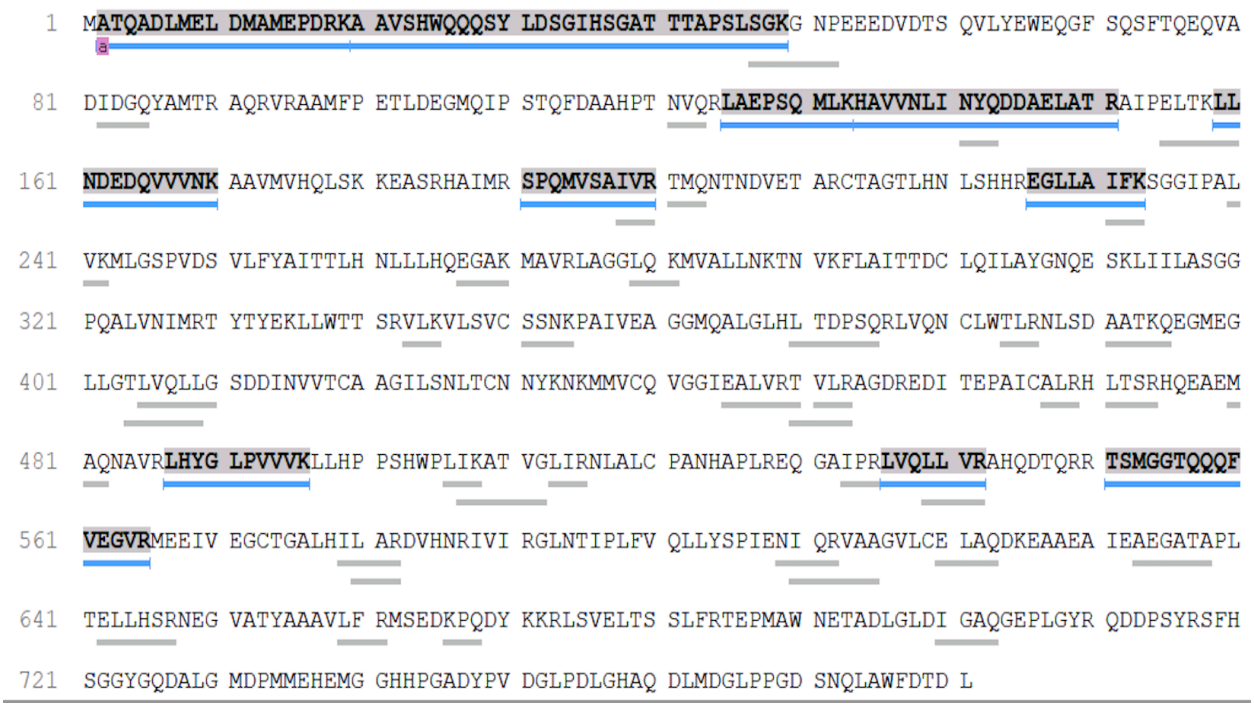

VI . References

[1] E. N. Wainwright and P. Scaffidi, "Epigenetics and Cancer Stem Cells: Unleashing, Hijacking, and Restricting Cellular Plasticity," *Trends Cancer,* vol. 3, no. 5, pp. 372-386, May 2017, doi: 10.1016/j.trecan.2017.04.004.

[2] C. Guetta-Terrier *et al.*, "Chi3l1 Is a Modulator of Glioma Stem Cell States and a Therapeutic Target in Glioblastoma," *Cancer Res,* vol. 83, no. 12, pp. 1984-1999, Jun 15 2023, doi: 10.1158/0008-5472.CAN-21-3629.

[3] V. G. Allfrey, R. Faulkner, and A. E. Mirsky, "Acetylation and Methylation of Histones and Their Possible Role in the Regulation of Rna Synthesis," *Proc Natl Acad Sci U S A,* vol. 51, no. 5, pp. 786-94, May 1964, doi: 10.1073/pnas.51.5.786.

[4] G. Li, Y. Tian, and W. G. Zhu, "The Roles of Histone Deacetylases and Their Inhibitors in Cancer Therapy," *Front Cell Dev Biol,* vol. 8, p. 576946, 2020, doi: 10.3389/fcell.2020.576946.

[5] S. Y. Park and J. S. Kim, "A short guide to histone deacetylases including recent progress on class II enzymes," *Exp Mol Med,* vol. 52, no. 2, pp. 204-212, Feb 2020, doi: 10.1038/s12276-020-0382-4.

[6] K. J. Falkenberg and R. W. Johnstone, "Histone deacetylases and their inhibitors in cancer, neurological diseases and immune disorders," *Nat Rev Drug Discov,* vol. 13, no. 9, pp. 673-91, Sep 2014, doi: 10.1038/nrd4360.

[7] A. C. West and R. W. Johnstone, "New and emerging HDAC inhibitors for cancer treatment," *J Clin Invest,* vol. 124, no. 1, pp. 30-9, Jan 2014, doi: 10.1172/JCI69738.

[8] Y. Stypula-Cyrus *et al.*, "HDAC up-regulation in early colon field carcinogenesis is involved in cell tumorigenicity through regulation of chromatin structure," *PLoS One,* vol. 8, no. 5, p. e64600, 2013, doi: 10.1371/journal.pone.0064600.

[9] S. Gao *et al.*, "MiR-489 suppresses tumor growth and invasion by targeting HDAC7 in colorectal cancer," *Clin Transl Oncol,* vol. 20, no. 6, pp. 703-712, Jun 2018, doi: 10.1007/s12094-017-1770-7.

[10] M. Ouaissi *et al.*, "High histone deacetylase 7 (HDAC7) expression is significantly associated with adenocarcinomas of the pancreas," *Ann Surg Oncol,* vol. 15, no. 8, pp. 2318-28, Aug 2008, doi: 10.1245/s10434-008-9940-z.

[11] M. Ouaissi *et al.*, "Further characterization of HDAC and SIRT gene expression patterns in pancreatic cancer and their relation to disease outcome," *PLoS One,* vol. 9, no. 9, p. e108520, 2014, doi: 10.1371/journal.pone.0108520.

[12] K. Freese *et al.*, "Histone Deacetylase Expressions in Hepatocellular Carcinoma and Functional Effects of Histone Deacetylase Inhibitors on Liver Cancer Cells In Vitro," *Cancers (Basel),* vol. 11, no. 10, Oct 18 2019, doi: 10.3390/cancers11101587.

[13] Y. Yu *et al.*, "The expression of HDAC7 in cancerous gastric tissues is positively associated with distant metastasis and poor patient prognosis," *Clin Transl Oncol,* vol. 19, no. 8, pp. 1045-1054, Aug 2017, doi: 10.1007/s12094-017-1639-9.

[14] Y. Wei, F. Zhou, H. Zhou, J. Huang, D. Yu, and G. Wu, "Endothelial progenitor cells contribute to neovascularization of non-small cell lung cancer via histone deacetylase 7-mediated cytoskeleton regulation and angiogenic genes transcription," *Int J Cancer,* vol. 143, no. 3, pp. 657-667, Aug 1 2018, doi: 10.1002/ijc.31349.

[15] M. Y. Wu, J. Fu, X. Xiao, J. Wu, and R. C. Wu, "MiR-34a regulates therapy resistance by targeting HDAC1 and HDAC7 in breast cancer," *Cancer Lett,* vol. 354, no. 2, pp. 311-9, Nov 28 2014, doi: 10.1016/j.canlet.2014.08.031.

[16] X. Yu, M. Wang, J. Wu, Q. Han, and X. Zhang, "ZNF326 promotes malignant phenotype of glioma by up-regulating HDAC7 expression and activating Wnt pathway," *J Exp Clin Cancer Res,* vol. 38, no. 1, p. 40, Jan 28 2019, doi: 10.1186/s13046-019-1031-4.

[17] P. Peixoto *et al.*, "HDAC7 inhibition resets STAT3 tumorigenic activity in human glioblastoma independently of EGFR and PTEN: new opportunities for selected targeted therapies," *Oncogene,* vol. 35, no. 34, pp. 4481-94, Aug 25 2016, doi: 10.1038/onc.2015.506.

[18] K. Ahmad and S. Henikoff, "The histone variant H3.3 marks active chromatin by replication-independent nucleosome assembly," *Mol Cell,* vol. 9, no. 6, pp. 1191-200, Jun 2002, doi: 10.1016/s1097-2765(02)00542-7.

[19] B. E. Schwartz and K. Ahmad, "Transcriptional activation triggers deposition and removal of the histone variant H3.3," *Genes Dev,* vol. 19, no. 7, pp. 804-14, Apr 1 2005, doi: 10.1101/gad.1259805.

[20] E. Szenker, D. Ray-Gallet, and G. Almouzni, "The double face of the histone variant H3.3," *Cell Res,* vol. 21, no. 3, pp. 421-34, Mar 2011, doi: 10.1038/cr.2011.14.

[21] R. B. Deal, J. G. Henikoff, and S. Henikoff, "Genome-wide kinetics of nucleosome turnover determined by metabolic labeling of histones," *Science,* vol. 328, no. 5982, pp. 1161-4, May 28 2010, doi: 10.1126/science.1186777.

[22] H. K. MacAlpine, R. Gordan, S. K. Powell, A. J. Hartemink, and D. M. MacAlpine, "Drosophila ORC localizes to open chromatin and marks sites of cohesin complex loading," *Genome Res,* vol. 20, no. 2, pp. 201-11, Feb 2010, doi: 10.1101/gr.097873.109.

[23] M. L. Eaton, J. A. Prinz, H. K. MacAlpine, G. Tretyakov, P. V. Kharchenko, and D. M. MacAlpine, "Chromatin signatures of the Drosophila replication program," *Genome Res,* vol. 21, no. 2, pp. 164-74, Feb 2011, doi: 10.1101/gr.116038.110.

[24] H. Stroud, S. Otero, B. Desvoyes, E. Ramirez-Parra, S. E. Jacobsen, and C. Gutierrez, "Genome-wide analysis of histone H3.1 and H3.3 variants in Arabidopsis thaliana," *Proc Natl Acad Sci U S A,* vol. 109, no. 14, pp. 5370-5, Apr 3 2012, doi: 10.1073/pnas.1203145109.

[25] N. P. Paranjape and B. R. Calvi, "The Histone Variant H3.3 Is Enriched at Drosophila Amplicon Origins but Does Not Mark Them for Activation," *G3 (Bethesda),* vol. 6, no. 6, pp. 1661-71, Jun 1 2016, doi: 10.1534/g3.116.028068.

[26] M. Strobino, J. M. Wenda, L. Padayachy, and F. A. Steiner, "Loss of histone H3.3 results in DNA replication defects and altered origin dynamics in C. elegans," *Genome Res,* vol. 30, no. 12, pp. 1740-1751, Dec 2020, doi: 10.1101/gr.260794.120.

[27] S. Adam, S. E. Polo, and G. Almouzni, "Transcription recovery after DNA damage requires chromatin priming by the H3.3 histone chaperone HIRA," *Cell,* vol. 155, no. 1, pp. 94-106, Sep 26 2013, doi: 10.1016/j.cell.2013.08.029.

[28] C. Clement *et al.*, "High-resolution visualization of H3 variants during replication reveals their controlled recycling," *Nat Commun,* vol. 9, no. 1, p. 3181, Aug 9 2018, doi: 10.1038/s41467-018-05697-1.

[29] L. Shi, H. Wen, and X. Shi, "The Histone Variant H3.3 in Transcriptional Regulation and Human Disease," *J Mol Biol,* vol. 429, no. 13, pp. 1934-1945, Jun 30 2017, doi: 10.1016/j.jmb.2016.11.019.

[30] A. D. Goldberg *et al.*, "Distinct factors control histone variant H3.3 localization at specific genomic regions," *Cell,* vol. 140, no. 5, pp. 678-91, Mar 5 2010, doi: 10.1016/j.cell.2010.01.003.
[31] P. Drane, K. Ouararhni, A. Depaux, M. Shuaib, and A. Hamiche, "The death-associated protein DAXX is a novel histone chaperone involved in the replication-independent deposition of H3.3," *Genes Dev,* vol. 24, no. 12, pp. 1253-65, Jun 15 2010, doi: 10.1101/gad.566910.
[32] P. W. Lewis, S. J. Elsaesser, K. M. Noh, S. C. Stadler, and C. D. Allis, "Daxx is an H3.3-specific histone chaperone and cooperates with ATRX in replication-independent chromatin assembly at telomeres," *Proc Natl Acad Sci U S A,* vol. 107, no. 32, pp. 14075-80, Aug 10 2010, doi: 10.1073/pnas.1008850107.
[33] S. Wang *et al.*, "A potential histone-chaperone activity for the MIER1 histone deacetylase complex," *Nucleic Acids Res,* vol. 51, no. 12, pp. 6006-6019, Jul 7 2023, doi: 10.1093/nar/gkad294.
[34] Y. Zheng, P. M. Thomas, and N. L. Kelleher, "Measurement of acetylation turnover at distinct lysines in human histones identifies long-lived acetylation sites," *Nat Commun,* vol. 4, p. 2203, 2013, doi: 10.1038/ncomms3203.
[35] B. MacLean *et al.*, "Skyline: an open source document editor for creating and analyzing targeted proteomics experiments," *Bioinformatics,* vol. 26, no. 7, pp. 966-8, Apr 1 2010, doi: 10.1093/bioinformatics/btq054.
[36] H. Mohammed, C. Taylor, G. D. Brown, E. K. Papachristou, J. S. Carroll, and C. S. D'Santos, "Rapid immunoprecipitation mass spectrometry of endogenous proteins (RIME) for analysis of chromatin complexes," *Nat Protoc,* vol. 11, no. 2, pp. 316-26, Feb 2016, doi: 10.1038/nprot.2016.020.
[37] M. Martin, R. Kettmann, and F. Dequiedt, "Class IIa histone deacetylases: regulating the regulators," *Oncogene,* vol. 26, no. 37, pp. 5450-67, Aug 13 2007, doi: 10.1038/sj.onc.1210613.
[38] H. Y. Kao, A. Verdel, C. C. Tsai, C. Simon, H. Juguilon, and S. Khochbin, "Mechanism for nucleocytoplasmic shuttling of histone deacetylase 7," *J Biol Chem,* vol. 276, no. 50, pp. 47496-507, Dec 14 2001, doi: 10.1074/jbc.M107631200.
[39] A. Loyola *et al.*, "The HP1alpha-CAF1-SetDB1-containing complex provides H3K9me1 for Suv39-mediated K9me3 in pericentric heterochromatin," *EMBO Rep,* vol. 10, no. 7, pp. 769-75, Jul 2009, doi: 10.1038/embor.2009.90.
[40] J. Dong *et al.*, "H3.1K27me1 maintains transcriptional silencing and genome stability by preventing GCN5-mediated histone acetylation," *Plant Cell,* vol. 33, no. 4, pp. 961-979, May 31 2021, doi: 10.1093/plcell/koaa027.
[41] K. J. Ferrari *et al.*, "Polycomb-dependent H3K27me1 and H3K27me2 regulate active transcription and enhancer fidelity," *Mol Cell,* vol. 53, no. 1, pp. 49-62, Jan 9 2014, doi: 10.1016/j.molcel.2013.10.030.
[42] N. R. Rose and R. J. Klose, "Understanding the relationship between DNA methylation and histone lysine methylation," *Biochim Biophys Acta,* vol. 1839, no. 12, pp. 1362-72, Dec 2014, doi: 10.1016/j.bbagrm.2014.02.007.
[43] A. Lahm *et al.*, "Unraveling the hidden catalytic activity of vertebrate class IIa histone deacetylases," *Proc Natl Acad Sci U S A,* vol. 104, no. 44, pp. 17335-40, Oct 30 2007, doi: 10.1073/pnas.0706487104.

[44] C. Brancolini, E. Di Giorgio, L. Formisano, and T. Gagliano, "Quis Custodiet Ipsos Custodes (Who Controls the Controllers)? Two Decades of Studies on HDAC9," *Life (Basel),* vol. 11, no. 2, Jan 27 2021, doi: 10.3390/life11020090.

[45] E. Di Giorgio and C. Brancolini, "Regulation of class IIa HDAC activities: it is not only matter of subcellular localization," *Epigenomics,* vol. 8, no. 2, pp. 251-69, Feb 2016, doi: 10.2217/epi.15.106.

[46] C. Brancolini, T. Gagliano, and M. Minisini, "HDACs and the epigenetic plasticity of cancer cells: Target the complexity," *Pharmacol Ther,* vol. 238, p. 108190, Oct 2022, doi: 10.1016/j.pharmthera.2022.108190.

[47] A. E. Witt *et al.*, "Identification of a cancer stem cell-specific function for the histone deacetylases, HDAC1 and HDAC7, in breast and ovarian cancer," *Oncogene,* vol. 36, no. 12, pp. 1707-1720, Mar 23 2017, doi: 10.1038/onc.2016.337.

[48] C. Caslini, S. Hong, Y. J. Ban, X. S. Chen, and T. A. Ince, "HDAC7 regulates histone 3 lysine 27 acetylation and transcriptional activity at super-enhancer-associated genes in breast cancer stem cells," *Oncogene,* vol. 38, no. 39, pp. 6599-6614, Sep 2019, doi: 10.1038/s41388-019-0897-0.

[49] H. Tagami, D. Ray-Gallet, G. Almouzni, and Y. Nakatani, "Histone H3.1 and H3.3 complexes mediate nucleosome assembly pathways dependent or independent of DNA synthesis," *Cell,* vol. 116, no. 1, pp. 51-61, Jan 9 2004, doi: 10.1016/s0092-8674(03)01064-x.

[50] W. Fischle, F. Dequiedt, M. Fillion, M. J. Hendzel, W. Voelter, and E. Verdin, "Human HDAC7 histone deacetylase activity is associated with HDAC3 in vivo," *J Biol Chem,* vol. 276, no. 38, pp. 35826-35, Sep 21 2001, doi: 10.1074/jbc.M104935200.

CHAPTER 5:

Discussion and Future Directions

IV. Overview

This study demonstrates HDAC7 inhibition (HDAC7i) as a promising novel therapeutic strategy for GBM as well as other cancers. It delves into the biological and molecular consequences of HDAC7 overexpression in driving tumorigenesis. Furthermore, it investigates novel strategies to target HDAC7 specifically without affecting other structurally related HDACs. This study also examines the mechanistic pathways through which HDAC7 modulates the epigenome and the transcriptome of cancer stem cells to allow sustained tumorigenic transcription activation.

We here provide insights into one mechanism HDAC7i employs to reprogram the epigenome and restore normal gene expression patterns. By specifically targeting HDAC7, we aim to modulate the epigenetic landscape and potentially reverse the aberrant gene expression associated with cancer. Our ultimate objective is to develop a potential translational therapy to treat human malignancies effectively while minimizing off-target effects. This approach highlights the importance of epigenetic regulation in cancer and the promise targeted epigenetic-based therapies hold to restore normal cellular function and combat cancer.

Epigenetic regulation of gene expression via HDAC inhibition presents a promising avenue with therapeutic potential for various conditions, including cancer. PTMs play a crucial role in many pathways that are fundamental to the initiation and advancement of tumorigenesis, including gene transcription, chromatin remodeling, and nuclear organization [1, 2].

In recent years, targeting HDACs for the treatment of human malignancies grew as an area of research focus, evidenced by the four HDACi FDA-approved drugs: Vorinostat, Romidepsin, Panobinostat, and Belinostat. However, these drugs primarily target the enzymatic activity of

HDACs, which HDAC class IIa isoforms barely have. Additionally, the clinical usage of the pan-HDAC inhibition presented major reported toxicities, owing to the lack of specificity and the disregard for the individual HDAC tissue expression [3-7]. These limitations underscore the need for further initiatives to develop more selective HDACi that can target specific HDAC isoforms implicated in a particular type of cancer while minimizing off-target effects and adverse reactions to normal tissues. Thus, this study sheds light on a novel isoform-specific HDACi with promising therapeutic potential in specific types of cancers.

V. Summary, Limitations, and Future Directions

We show that HDAC7, a class IIa HDAC group member, is a crucial epigenetic regulator in GBM. This insight stems from a comprehensive screening of HDAC7 conducted on RNA samples collected from 84 RIH patients with recurrent invasive GBM. HDAC7 overexpression elicited significant phenotypic changes for GSCs in vitro. Through an analysis of publicly accessible data from large GBM cohorts, we delineated HDAC7 as distinct from other class IIa HDAC members due to its notably high specificity for GBM tumors compared to normal brain tissues. Moreover, HDAC7 expression exhibited inversely correlated with overall survival in the GBM cohort documented in public databases as well from RIH.

We demonstrate that inhibiting HDAC7 reduced the oncogenic capabilities of primary GSCs by suppressing their cell viability and ability to form tumorspheres. Conversely, GSCs transfected with HDAC7 expression constructs exhibited increased cell colony formation significantly. Moreover, we show through transcriptomic analysis that targeted reduction of HDAC7 significantly disrupts the expression of nearly half of the genes in primary GSCs from RIH patients. Many of the genes that are downregulated following HDAC7 inhibition are known to be associated with stemness, particularly exhibiting an embryonic phenotype. We hypothesized that HDAC7 plays a role in fundamental cellular regulation by reactivating transcriptional programs typically active during embryonic development, which are supposed to be silenced beyond this stage of life. Consistent with this, our gene enrichment analysis from GSCs and analyzing public data indicated that HDAC7 is involved in biological processes related to cell cycle activities as well as chromatin reorganization.

We additionally show preliminary data that HDAC7's involvement in oncogenesis extends beyond GBM to encompass various other cancer types. Previous studies have demonstrated the increased expression of HDAC7 in several cancers, such as colorectal, gastric, breast, renal, melanoma, and brain cancer [8-11]. Hence, a potential avenue for future research could delve deeper into the role of HDAC7 in these types of cancers and assess whether they are good candidates for HDAC7-targeted therapy.

Our investigation proposes a mechanistic model of HDAC7's role in promoting tumor aggressiveness. We demonstrate how HDAC7 epigenetically influences GSCs by modulating the chromatin structure and gene transcription. Our findings suggest that targeting HDAC7 can induce a phenotypic shift from euchromatin to heterochromatin in cancer stem cells, resulting in gene silencing and potentially inhibiting oncogenesis.

- **Future Direction for Studying the Involvement of HDAC7 in DNA Repair Mechanisms**

Our observation of the presence of crucial DNA repair proteins within the HDAC7 interacting network suggests a potential connection between HDAC7 and DNA repair mechanisms, which could further explain HDAC7's role in driving tumorigenesis. DNA repair is the body's built-in machinery for correcting DNA damage. However, when mistakes happen during DNA repair mechanisms, they can drive mutations or chromosomal abnormalities that can affect oncogenes or tumor suppressor genes, which could cause normal cells to undergo malignant transformation [12-14]. Maintaining genomic stability and effective DNA repair mechanisms are highly crucial for

preventing the initiation and progression of cancers. This opens up a new avenue for future research to expand our understanding of the mechanisms underlying HDAC7-mediated tumorigenesis and its potential as a therapeutic target in cancer.

- **Future Directions for Investigating HDAC7 expression in various Normal and Malignant Tissues**

A notable limitation of targeting HDAC7 is its expression in various other normal body tissues. Our understanding of the precise role of individual HDACs in a particular type of cancer remains incomplete. Hence, more research is necessary to determine the role of specific HDACs and ascertain whether they are over-expressed or under-expressed in specific tissues and the respective cancers. Such efforts will enable the design and development of HDAC isoform-specific inhibitors or other compounds capable of regulating the expression of a particular HDAC.

- **Future Directions for Understanding the Role of HDAC7 Expression in Stemness.**

Our transcriptomic investigation revealed the downregulation of huge number of stemness genes after inhibiting HDAC7. Phenotypic assessment of these downregulated stemness genes across 26 stemness gene signatures unraveled that these genes were closely associated with the embryonic phenotype. Therefore, a prospective avenue for research in this area could involve delving deeper into how HDAC7 modulates the activity of these stemness genes through various

immunohistochemistry studies and experiments employing colocalization with various stem markers.

- **Prospective Direction for Investigating the Involvement of HDAC7 Expression in Tumor Cell Migration.**

Our functional enrichment analyses indicates that HDAC7 is implicated in diverse migration and metastasis pathways. Hence, a promising direction for further research could involve exploring the mechanisms through which HDAC7 influences tumor cells' migration capacity, and assessing whether targeting HDAC7 could affect the migratory potential of CSCs in GBM and other cancer types.

- **Exploring the Role of HDAC7 in Histone H3.3 Deposition: Implications for Basic Biology and Pathobiology**

Our novel finding regarding the role of HDAC7 in histone H3.3 deposition over the heterochromatin is opening a multitude of investigations in both the basic biology and pathobiology. Delving into the significance of HDAC7-H3.3 interaction during H3.3 deposition, particularly in the replication-independent manner throughout the cell cycle, holds the potential to deepen our comprehension of the programmed cell division during embryogenesis and fetal development. Additionally, it raises questions about whether targeting HDAC7 could offer promise for addressing some congenital abnormalities. Furthermore, it sheds light on the

dysregulated cell division during tumorigenesis, offering insights into potential therapeutic strategies.

- **Future Avenues for Investigating the Impact of HDAC7 Targeting on the Immune System**

A noteworthy constraint of targeting HDAC7 is its expression in the thymus, where it was reported to be involved in T-cell development, similar to other HDACs [16, 17]. However, the reported effects of HDACi drugs on tumor immune response remain inconsistent [18, 19]. Numerous studies have reported the induction of anti-tumor T cell immune reactions subsequent to HDACi treatment. This encompasses regulating the expression of tumor antigens [20-22], amplification of antigen-presenting machinery such as MHC-I/II [23, 24], the augmentation of the secretion of T cell-recruiting chemokines [25], making tumors susceptible to death receptor killing [20, 26], and regulating the balance between the suppressive versus inflammatory myeloid cells [27, 28].

On the contrary, other studies have shown that HDAC7 deletion affects thymocyte maturation, particularly during positive selection [17]. However, research with lck-cre transgenic mice has indicated that introducing a T cell receptor (TCR) transgene could mitigate the negative effects of HDAC7 deficiency on thymocyte development. [17]. This finding suggests that combining therapies targeting HDAC7 with strategies like CAR-T immunotherapy could potentially enhance the effectiveness of T cell-based cancer treatments while synergistically targeting cancer. Further investigation into the effect of each HDAC isoform, including HDAC7 inhibition, on TCR

development in GBM and the potential combination with immunotherapy could elucidate its efficacy and safety in clinical settings.

GBM is known to have a weak immune response due to the unique immunosuppressive microenvironment of the brain. There are various factors behind this immune evasion, including the BBB, which restricts immune cells and therapeutics from accessing the brain parenchyma. Besides, the brain has limited lymphatic drainage and a low expression of MHC class II molecules, that's why proper antigen presentation to T cells is lacking in the brain. Furthermore, the brain TME secretes immunosuppressive cytokines like TGF-β, which further dampens immune responses within the TME. [29]. It has been proposed that the recruitment of regulatory T cells (Tregs) up to fourfold antagonizes the infiltration of CD8+ T cells in the GBM TME, which could explain the severe immunosuppressive TME in the GBM. [30-32]. In addition, HDAC7 has been implicated in hematological malignancies in numerous reports, and pan HDACi are being utilized in their combinational therapy [33-36]. In line with that, we observed from our RNA sequencing data that inhibiting HDAC7 in GSCs caused significant changes in the mRNA expression of key inflammatory cytokines fostering tumorigenesis. We observed an upregulation in the mRNA expression levels of anti-tumorigenic inflammatory cytokines, including IFN-γ and TNF-α, after HDAC7 inhibition. These cytokines are known to promote anti-tumor immune responses and inhibit tumor growth [32, 37-39]. Conversely, we observed a downregulation in the mRNA expression of pro-tumorigenic cytokines such as TGF-β, IL13RA2, NF-κB, IL-10, and IL-1 from RNA seq data following HDAC7 inhibition. These cytokines have been implicated in enriching a pro-tumor TME and promoting tumor cell proliferation, invasion, and immune evasion [40-43].

In this context, the negative impact of HDAC7 on T cell differentiation could potentially yield positive outcomes by selectively inhibiting the immunosuppressive Tregs. This suggests that targeting HDAC7 may be a promising approach to disrupt the immunosuppression in the TME and enhance antitumor immune responses in GBM and potentially other cancers where Tregs predominate. However, further investigation and rigorous testing are essential to validate the efficacy and safety of HDAC7i and the effects it has on Tregs within the total population of CD4+CD8+ cells.

Although some investigations have been carried out on the direct impact of HDACi on the immune system, specifically T cells, the findings in existing literature are incomplete and conflicting. These disparities may be due to the utilization of different models in these studies or the lack of specificity profiles of different HDACi towards individual HDACs. As a future aspect, it's crucial to further investigate the precise mechanisms by which HDAC7 inhibition affects immune system components, overall immune homeostasis, and antitumor responses. Additionally, exploring the combination therapies targeting HDAC7 with immunotherapy and evaluating the effect of HDAC7 inhibition on the endogenous T cell pool versus immunotherapy is an interesting research area to expand. Indeed, synergistic effects of HDACi have been observed when combined with immunotherapies targeting T cells [44-46], such as checkpoint blockade with αPD-1 [44, 45], adoptive cell therapy models [20], and other immunotherapy modalities, [47]. Extensive preclinical studies and clinical trials are necessary to evaluate the specificity, efficacy, and safety profile of HDAC7 inhibition in modulating the TME alone and in combination therapies and to address its therapeutic potential in cancer treatment and its impact on immune modulation.

- **Potential Modalities for Therapeutically Targeting HDAC7 in the Future**

Our combined efforts in HDAC7 drug design pipeline have achieved a significant milestone in targeting HDAC7. We've explored various strategies, including small molecule inhibitor, PROTACs and siRNA approaches. Currently our focus is on refining the specificity of our designed small molecule inhibitors by redesigning and reassessing their physical interactions and affinity towards HDAC7 compared to the rest of class IIa HDACi.

On a parallel route, we engineered seven de novo PROTAC-HDACi compounds from a comprehensive ligand-linker screen that none of them engineered compounds demonstrated the ability to induce proteolysis of HDAC. Nonetheless, we are actively pursuing further investigation of this approach through collaboration involving our group, Dr. Sidoli's team, and Dr. Fiser's team. Conducting larger screens and exploring various combinations of linkers and ligands for PROTACs holds tremendous potential for success. This concerted effort could ultimately result in discovering novel and effective PROTAC-HDAC inhibitors specifically targeting HDAC7.

Furthermore, we are exploring additional avenues to target HDAC7 by focusing on its protein-protein interaction with histone H3.3. Our current study has established and validated the physical interaction between histone H3.3 and HDAC7. Crystalizing the interface between these two proteins has the potential to open up new opportunities for targeting HDAC7 through peptide inhibitors that selectively disrupt its mechanism. This approach holds promise for the development of more precise and effective therapeutic interventions aimed at specifically modulating HDAC7 activity.

- **Prospects for Future drug Delivery Methods for HDAC Inhibitor Therapeutic**

Overcoming the BBB has been a persistent challenge in drug delivery to the brain. However, there are now several advanced drug delivery methods emerging to address this obstacle. These include implanted reservoirs and stereotactic injections, which offer precise delivery of therapeutics to targeted areas within the brain [48-51]. Additionally, intra-arterial delivery allows for the direct delivery of high doses of therapeutics to the tumor site facilitated by a brain disruption agent like mannitol. Intra-arterial delivery was proposed in earlier days and is now revitalized with numerous ongoing clinical trials showing promising outcome [48, 52]. Convection-enhanced delivery (CED) is a novel modality for local brain delivery currently being evaluated in clinical trials. By optimizing drug distribution, CED has the potential to enable the use of lower concentrations of drugs to achieve therapeutic effects over a similar area [49].

Our proposed siRNA targeting HDAC7 represents an innovative approach that harnesses the power of RNAi, which has emerged as a groundbreaking discovery in therapeutics. RNAi-based therapeutics have garnered considerable attention in the pharmaceutical field, particularly in the wake of the COVID-19 vaccine development, paving the way for a new class of drugs capable of specifically silencing target genes and offering immense potential for treating various diseases, including cancer. Additionally, given the relatively low expression of HDAC7 in the brain, advanced novel local brain delivery modalities offer the potential to reduce unwanted toxicities associated with systemic administration substantially. Moreover, the availability of numerous FDA-approved lipid nanoparticles (LNP) designed for RNAi drug delivery further enhances the promise of siRNA-based therapeutics. These nanoparticles provide the efficient and targeted delivery promise of our HDAC7 siRNA to the desired cancer cells while minimizing off-target

effects and enhancing therapeutic efficacy. However, there remains a lack of examples of siRNA therapeutics showing an effective pharmacokinetic profile and distribution within solid tumors. Numerous developmental efforts are being conducted globally, with the goal of achieving effective LNP delivery of anti-cancer siRNA therapeutics [53-55].

The innovation of the ligand–siRNA conjugation strategy has enabled enhanced tissue-specific targeting. This approach introduces tissue specificity and facilitates the accumulation of siRNA in target tissues, thereby mitigating undesired side effects and toxicity while achieving potent gene silencing at low dosages [56-58]. The specific recognition of the ligand–siRNA conjugation strategy is accomplished by various ligands, such as carbohydrates, peptides, antibodies, aptamers, and small molecules, which can recognize and bind to surface receptors on the target tissue [56-58]. Incorporating the ligand–siRNA approach into our proposed HDAC7 siRNA therapy could enable targeted treatment of solid cancers where HDAC7 is involved, while reducing off-target effects in other normal tissues. This strategy would leverage specific ligands capable of recognizing and binding to surface receptors on the target cancer cells, thereby enhancing the delivery of HDAC7-targeted siRNA to the intended sites and minimizing potential side effects elsewhere. Indeed, further investigation and rigorous testing are necessary to validate the effectiveness and safety of combining HDAC7 siRNA with specific ligands and assess their efficacy across various types of cancers. This process will ensure a thorough evaluation of the potential benefits and risks associated with this therapeutic approach before clinical implementation.

By leveraging RNAi technology and utilizing FDA-approved nanoparticles for delivery, our HDAC7-targeting siRNA holds significant promise as an effective therapeutic for treating

particular human cancers. The combination of innovative science and advanced drug delivery strategies underscores the potential of RNAi-based therapies in revolutionizing cancer treatment.

VI. References

[1] R. A. Mathias, A. J. Guise, and I. M. Cristea, "Post-translational Modifications Regulate Class IIa Histone Deacetylase (HDAC) Function in Health and Disease," *Molecular & Cellular Proteomics,* vol. 14, no. 3, pp. 456-470, 2015, doi: 10.1074/mcp.O114.046565.

[2] M. H. Cai *et al.*, "Depletion of HDAC1, 7 and 8 by Histone Deacetylase Inhibition Confers Elimination of Pancreatic Cancer Stem Cells in Combination with Gemcitabine," *Sci Rep,* vol. 8, no. 1, p. 1621, Jan 26 2018, doi: 10.1038/s41598-018-20004-0.

[3] S.-Y. Park and J.-S. Kim, "A short guide to histone deacetylases including recent progress on class II enzymes," *Experimental & Molecular Medicine,* vol. 52, no. 2, pp. 204-212, 2020, doi: 10.1038/s12276-020-0382-4.

[4] F. Fischer, L. A. Alves Avelar, L. Murray, and T. Kurz, "Designing HDAC-PROTACs: lessons learned so far," *Future Med Chem,* vol. 14, no. 3, pp. 143-166, Jan 2022, doi: 10.4155/fmc-2021-0206.

[5] T. C. S. Ho, A. H. Y. Chan, and A. Ganesan, "Thirty Years of HDAC Inhibitors: 2020 Insight and Hindsight," *Journal of Medicinal Chemistry,* vol. 63, no. 21, pp. 12460-12484, 2020, doi: 10.1021/acs.jmedchem.0c00830.

[6] Y. B. Zhou *et al.*, "Pharmacodynamic, pharmacokinetic, and phase 1a study of bisthianostat, a novel histone deacetylase inhibitor, for the treatment of relapsed or refractory multiple myeloma," *Acta Pharmacol Sin,* vol. 43, no. 4, pp. 1091-1099, Apr 2022, doi: 10.1038/s41401-021-00728-y.

[7] A. D. Bondarev, M. M. Attwood, J. Jonsson, V. N. Chubarev, V. V. Tarasov, and H. B. Schioth, "Recent developments of HDAC inhibitors: Emerging indications and novel molecules," *Br J Clin Pharmacol,* vol. 87, no. 12, pp. 4577-4597, Dec 2021, doi: 10.1111/bcp.14889.

[8] Y. Yu *et al.*, "The expression of HDAC7 in cancerous gastric tissues is positively associated with distant metastasis and poor patient prognosis," *Clin Transl Oncol,* vol. 19, no. 8, pp. 1045-1054, Aug 2017, doi: 10.1007/s12094-017-1639-9.

[9] X. Yu, M. Wang, J. Wu, Q. Han, and X. Zhang, "ZNF326 promotes malignant phenotype of glioma by up-regulating HDAC7 expression and activating Wnt pathway," *J Exp Clin Cancer Res,* vol. 38, no. 1, p. 40, Jan 28 2019, doi: 10.1186/s13046-019-1031-4.

[10] C. Caslini, S. Hong, Y. J. Ban, X. S. Chen, and T. A. Ince, "HDAC7 regulates histone 3 lysine 27 acetylation and transcriptional activity at super-enhancer-associated genes in breast cancer stem cells," *Oncogene,* vol. 38, no. 39, pp. 6599-6614, Sep 2019, doi: 10.1038/s41388-019-0897-0.

[11] H. Nam *et al.*, "The TGF-beta/HDAC7 axis suppresses TCA cycle metabolism in renal cancer," *JCI Insight,* vol. 6, no. 22, Nov 22 2021, doi: 10.1172/jci.insight.148438.

[12] L. Y. Li, Y. D. Guan, X. S. Chen, J. M. Yang, and Y. Cheng, "DNA Repair Pathways in Cancer Therapy and Resistance," *Front Pharmacol,* vol. 11, p. 629266, 2020, doi: 10.3389/fphar.2020.629266.

[13] R. Huang and P. K. Zhou, "DNA damage repair: historical perspectives, mechanistic pathways and clinical translation for targeted cancer therapy," *Signal Transduct Target Ther,* vol. 6, no. 1, p. 254, Jul 9 2021, doi: 10.1038/s41392-021-00648-7.

[14] A. Torgovnick and B. Schumacher, "DNA repair mechanisms in cancer development and therapy," *Front Genet,* vol. 6, p. 157, 2015, doi: 10.3389/fgene.2015.00157.

[15] W. Fischle, F. Dequiedt, M. Fillion, M. J. Hendzel, W. Voelter, and E. Verdin, "Human HDAC7 histone deacetylase activity is associated with HDAC3 in vivo," *J Biol Chem,* vol. 276, no. 38, pp. 35826-35, Sep 21 2001, doi: 10.1074/jbc.M104935200.
[16] F. Dequiedt *et al.*, "HDAC7, a thymus-specific class II histone deacetylase, regulates Nur77 transcription and TCR-mediated apoptosis," *Immunity,* vol. 18, no. 5, pp. 687-98, May 2003, doi: 10.1016/s1074-7613(03)00109-2.
[17] H. G. Kasler *et al.*, "Histone deacetylase 7 regulates cell survival and TCR signaling in CD4/CD8 double-positive thymocytes," *J Immunol,* vol. 186, no. 8, pp. 4782-93, Apr 15 2011, doi: 10.4049/jimmunol.1001179.
[18] B. Moran, M. Davern, J. V. Reynolds, N. E. Donlon, and J. Lysaght, "The impact of histone deacetylase inhibitors on immune cells and implications for cancer therapy," *Cancer Lett,* vol. 559, p. 216121, Apr 10 2023, doi: 10.1016/j.canlet.2023.216121.
[19] N. Holay *et al.*, "Elucidating the direct effects of the novel HDAC inhibitor bocodepsin (OKI-179) on T cells to rationally design regimens for combining with immunotherapy," *Front Immunol,* vol. 14, p. 1260545, 2023, doi: 10.3389/fimmu.2023.1260545.
[20] T. Murakami *et al.*, "Transcriptional modulation using HDACi depsipeptide promotes immune cell-mediated tumor destruction of murine B16 melanoma," *J Invest Dermatol,* vol. 128, no. 6, pp. 1506-16, Jun 2008, doi: 10.1038/sj.jid.5701216.
[21] A. S. Truong *et al.*, "Entinostat induces antitumor immune responses through immune editing of tumor neoantigens," *J Clin Invest,* vol. 131, no. 16, Aug 16 2021, doi: 10.1172/JCI138560.
[22] S. R. Gameiro, A. S. Malamas, K. Y. Tsang, S. Ferrone, and J. W. Hodge, "Inhibitors of histone deacetylase 1 reverse the immune evasion phenotype to enhance T-cell mediated lysis of prostate and breast carcinoma cells," *Oncotarget,* vol. 7, no. 7, pp. 7390-402, Feb 16 2016, doi: 10.18632/oncotarget.7180.
[23] K. A. Cycon, K. Mulvaney, L. M. Rimsza, D. Persky, and S. P. Murphy, "Histone deacetylase inhibitors activate CIITA and MHC class II antigen expression in diffuse large B-cell lymphoma," *Immunology,* vol. 140, no. 2, pp. 259-72, Oct 2013, doi: 10.1111/imm.12136.
[24] X. Wang *et al.*, "Histone Deacetylase Inhibition Sensitizes PD1 Blockade-Resistant B-cell Lymphomas," *Cancer Immunol Res,* vol. 7, no. 8, pp. 1318-1331, Aug 2019, doi: 10.1158/2326-6066.CIR-18-0875.
[25] H. Zheng *et al.*, "HDAC Inhibitors Enhance T-Cell Chemokine Expression and Augment Response to PD-1 Immunotherapy in Lung Adenocarcinoma," *Clin Cancer Res,* vol. 22, no. 16, pp. 4119-32, Aug 15 2016, doi: 10.1158/1078-0432.CCR-15-2584.
[26] S. Inoue, M. MacFarlane, N. Harper, L. M. Wheat, M. J. Dyer, and G. M. Cohen, "Histone deacetylase inhibitors potentiate TNF-related apoptosis-inducing ligand (TRAIL)-induced apoptosis in lymphoid malignancies," *Cell Death Differ,* vol. 11 Suppl 2, pp. S193-206, Dec 2004, doi: 10.1038/sj.cdd.4401535.
[27] A. O. Adeshakin *et al.*, "Blockade of myeloid-derived suppressor cell function by valproic acid enhanced anti-PD-L1 tumor immunotherapy," *Biochem Biophys Res Commun,* vol. 522, no. 3, pp. 604-611, Feb 12 2020, doi: 10.1016/j.bbrc.2019.11.155.
[28] X. Li *et al.*, "HDAC inhibition potentiates anti-tumor activity of macrophages and enhances anti-PD-L1-mediated tumor suppression," *Oncogene,* vol. 40, no. 10, pp. 1836-1850, Mar 2021, doi: 10.1038/s41388-020-01636-x.

[29] C. M. Jackson, M. Lim, and C. G. Drake, "Immunotherapy for brain cancer: recent progress and future promise," *Clin Cancer Res,* vol. 20, no. 14, pp. 3651-9, Jul 15 2014, doi: 10.1158/1078-0432.CCR-13-2057.
[30] D. A. Wainwright, S. Sengupta, Y. Han, and M. S. Lesniak, "Thymus-derived rather than tumor-induced regulatory T cells predominate in brain tumors," *Neuro Oncol,* vol. 13, no. 12, pp. 1308-23, Dec 2011, doi: 10.1093/neuonc/nor134.
[31] J. F. Jacobs *et al.*, "Regulatory T cells and the PD-L1/PD-1 pathway mediate immune suppression in malignant human brain tumors," *Neuro Oncol,* vol. 11, no. 4, pp. 394-402, Aug 2009, doi: 10.1215/15228517-2008-104.
[32] N. F. Brown, T. J. Carter, D. Ottaviani, and P. Mulholland, "Harnessing the immune system in glioblastoma," *Br J Cancer,* vol. 119, no. 10, pp. 1171-1181, Nov 2018, doi: 10.1038/s41416-018-0258-8.
[33] J. C. Wang *et al.*, "Histone deacetylase in chronic lymphocytic leukemia," *Oncology,* vol. 81, no. 5-6, pp. 325-9, 2011, doi: 10.1159/000334577.
[34] M. Van Damme *et al.*, "HDAC isoenzyme expression is deregulated in chronic lymphocytic leukemia B-cells and has a complex prognostic significance," *Epigenetics,* vol. 7, no. 12, pp. 1403-12, Dec 1 2012, doi: 10.4161/epi.22674.
[35] D. A. Moreno *et al.*, "Differential expression of HDAC3, HDAC7 and HDAC9 is associated with prognosis and survival in childhood acute lymphoblastic leukaemia," *Br J Haematol,* vol. 150, no. 6, pp. 665-73, Sep 2010, doi: 10.1111/j.1365-2141.2010.08301.x.
[36] B. S. Mann, J. R. Johnson, M. H. Cohen, R. Justice, and R. Pazdur, "FDA approval summary: vorinostat for treatment of advanced primary cutaneous T-cell lymphoma," *Oncologist,* vol. 12, no. 10, pp. 1247-52, Oct 2007, doi: 10.1634/theoncologist.12-10-1247.
[37] C. F. Lin *et al.*, "Escape from IFN-gamma-dependent immunosurveillance in tumorigenesis," *J Biomed Sci,* vol. 24, no. 1, p. 10, Feb 1 2017, doi: 10.1186/s12929-017-0317-0.
[38] M. F. Mercogliano, S. Bruni, F. Mauro, P. V. Elizalde, and R. Schillaci, "Harnessing Tumor Necrosis Factor Alpha to Achieve Effective Cancer Immunotherapy," *Cancers (Basel),* vol. 13, no. 3, Feb 2 2021, doi: 10.3390/cancers13030564.
[39] S. F. Josephs *et al.*, "Unleashing endogenous TNF-alpha as a cancer immunotherapeutic," *J Transl Med,* vol. 16, no. 1, p. 242, Aug 31 2018, doi: 10.1186/s12967-018-1611-7.
[40] S. S. Widodo, M. Dinevska, L. M. Furst, S. S. Stylli, and T. Mantamadiotis, "IL-10 in glioma," *Br J Cancer,* vol. 125, no. 11, pp. 1466-1476, Nov 2021, doi: 10.1038/s41416-021-01515-6.
[41] T. Yan *et al.*, "TGF-beta induces GBM mesenchymal transition through upregulation of CLDN4 and nuclear translocation to activate TNF-alpha/NF-kappaB signal pathway," *Cell Death Dis,* vol. 13, no. 4, p. 339, Apr 13 2022, doi: 10.1038/s41419-022-04788-8.
[42] R. Liang, C. Wu, S. Liu, and W. Zhao, "Targeting interleukin-13 receptor alpha2 (IL-13Ralpha2) for glioblastoma therapy with surface functionalized nanocarriers," *Drug Deliv,* vol. 29, no. 1, pp. 1620-1630, Dec 2022, doi: 10.1080/10717544.2022.2075986.
[43] N. G. Avci *et al.*, "NF-kappaB inhibitor with Temozolomide results in significant apoptosis in glioblastoma via the NF-kappaB(p65) and actin cytoskeleton regulatory pathways," *Sci Rep,* vol. 10, no. 1, p. 13352, Aug 7 2020, doi: 10.1038/s41598-020-70392-5.
[44] A. Orillion *et al.*, "Entinostat Neutralizes Myeloid-Derived Suppressor Cells and Enhances the Antitumor Effect of PD-1 Inhibition in Murine Models of Lung and Renal Cell

Carcinoma," *Clin Cancer Res,* vol. 23, no. 17, pp. 5187-5201, Sep 1 2017, doi: 10.1158/1078-0432.CCR-17-0741.
[45] B. Burke *et al.*, "Inhibition of Histone Deacetylase (HDAC) Enhances Checkpoint Blockade Efficacy by Rendering Bladder Cancer Cells Visible for T Cell-Mediated Destruction," *Front Oncol,* vol. 10, p. 699, 2020, doi: 10.3389/fonc.2020.00699.
[46] A. S. Harutyunyan *et al.*, "H3K27M in Gliomas Causes a One-Step Decrease in H3K27 Methylation and Reduced Spreading within the Constraints of H3K36 Methylation," *Cell Reports,* vol. 33, no. 7, pp. 108390-108390, 2020, doi: 10.1016/j.celrep.2020.108390.
[47] L. Booth, J. L. Roberts, A. Poklepovic, J. Kirkwood, and P. Dent, "HDAC inhibitors enhance the immunotherapy response of melanoma cells," *Oncotarget,* vol. 8, no. 47, pp. 83155-83170, Oct 10 2017, doi: 10.18632/oncotarget.17950.
[48] B. S. Karmur *et al.*, "Blood-Brain Barrier Disruption in Neuro-Oncology: Strategies, Failures, and Challenges to Overcome," *Front Oncol,* vol. 10, p. 563840, 2020, doi: 10.3389/fonc.2020.563840.
[49] A. Jahangiri, A. T. Chin, P. M. Flanigan, R. Chen, K. Bankiewicz, and M. K. Aghi, "Convection-enhanced delivery in glioblastoma: a review of preclinical and clinical studies," *J Neurosurg,* vol. 126, no. 1, pp. 191-200, Jan 2017, doi: 10.3171/2016.1.JNS151591.
[50] D. Huang *et al.*, "Continuous Vector-free Gene Transfer with a Novel Microfluidic Chip and Nanoneedle Array," *Curr Drug Deliv,* vol. 16, no. 2, pp. 164-170, 2019, doi: 10.2174/1567201815666181017095044.
[51] R. S. D'Amico *et al.*, "Super selective intra-arterial cerebral infusion of modern chemotherapeutics after blood-brain barrier disruption: where are we now, and where we are going," *J Neurooncol,* vol. 147, no. 2, pp. 261-278, Apr 2020, doi: 10.1007/s11060-020-03435-6.
[52] D. Fortin, P. A. Morin, F. Belzile, D. Mathieu, and F. M. Pare, "Intra-arterial carboplatin as a salvage strategy in the treatment of recurrent glioblastoma multiforme," *J Neurooncol,* vol. 119, no. 2, pp. 397-403, Sep 2014, doi: 10.1007/s11060-014-1504-4.
[53] K. Paunovska, D. Loughrey, and J. E. Dahlman, "Drug delivery systems for RNA therapeutics," *Nat Rev Genet,* vol. 23, no. 5, pp. 265-280, May 2022, doi: 10.1038/s41576-021-00439-4.
[54] M. A. Subhan, N. Filipczak, and V. P. Torchilin, "Advances with Lipid-Based Nanosystems for siRNA Delivery to Breast Cancers," *Pharmaceuticals (Basel),* vol. 16, no. 7, Jul 6 2023, doi: 10.3390/ph16070970.
[55] D. Hattab, A. M. Gazzali, and A. Bakhtiar, "Clinical Advances of siRNA-Based Nanotherapeutics for Cancer Treatment," *Pharmaceutics,* vol. 13, no. 7, Jul 2 2021, doi: 10.3390/pharmaceutics13071009.
[56] K. M. Brown *et al.*, "Expanding RNAi therapeutics to extrahepatic tissues with lipophilic conjugates," *Nat Biotechnol,* vol. 40, no. 10, pp. 1500-1508, Oct 2022, doi: 10.1038/s41587-022-01334-x.
[57] R. J. Holland *et al.*, "Ligand conjugate SAR and enhanced delivery in NHP," *Mol Ther,* vol. 29, no. 10, pp. 2910-2919, Oct 6 2021, doi: 10.1016/j.ymthe.2021.06.002.
[58] I. V. Chernikov, V. V. Vlassov, and E. L. Chernolovskaya, "Current Development of siRNA Bioconjugates: From Research to the Clinic," *Front Pharmacol,* vol. 10, p. 444, 2019, doi: 10.3389/fphar.2019.00444.